INTERNATIONAL HYDROLOGICAL PROGRAMME

Environmental isotopes in the hydrological cycle

Principles and applications

Edited by
W.G. Mook

Volume I

Introduction

Theory Methods Review

by
Willem G. Mook
Centre for Isotope Research
Groningen

IHP-V | Technical Documents in Hydrology | No. 39, Vol. I
UNESCO, Paris, 2000

United Nations Educational,
Scientific and Cultural Organization

International Atomic Energy Agency

SC-2000/WS/58

UNESCO/IAEA Series on

Environmental Isotopes in the Hydrological Cycle
Principles and Applications

÷

Volume I	**Introduction: Theory, Methods, Review**
Volume II	**Atmospheric Water**
Volume III	**Surface Water**
Volume IV	**Groundwater: Saturated and Unsaturated Zone**
Volume V	**Man's Impact on Groundwater Systems**
Volume VI	**Modelling**

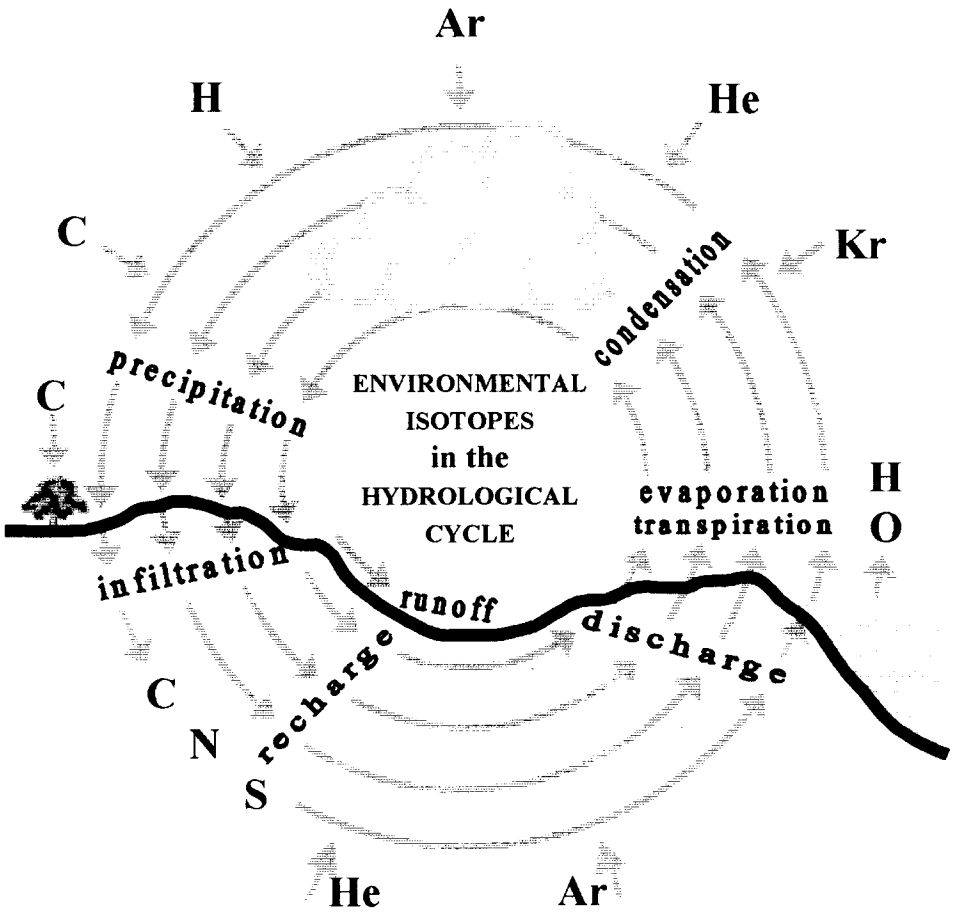

Contributing Author

J.J.de Vries, Free University, Amsterdam

PREFACE

The availability of freshwater is one of the great issues facing mankind today - in some ways the greatest, because problems associated with it affect the lives of many millions of people. It has consequently attracted a wide scale international attention of UN Agencies and related international/regional governmental and non-governmental organisations. The rapid growth of population coupled to steady increase in water requirements for agricultural and industrial development have imposed severe stress on the available freshwater resources in terms of both the quantity and quality, requiring consistent and careful assessment and management of water resources for their sustainable development.

More and better water can not be acquired without the continuation and extension of hydrological research. In this respect has the development and practical implementation of isotope methodologies in water resources assessment and management been part of the IAEA's programme in nuclear applications over the last four decades. Isotope studies applied to a wide spectrum of hydrological problems related to both surface and groundwater resources as well as environmental studies in hydro-ecological systems are presently an established scientific discipline, often referred to as "Isotope Hydrology". The IAEA contributed to this development through direct support to research and training, and to the verification of isotope methodologies through field projects implemented in Member States.

The world-wide programme of the International Hydrological Decade (1965-1974) and the subsequent long-term International Hydrological Programme (IHP) of UNESCO have been an essential part of the well recognised international frameworks for scientific research, education and training in the field of hydrology. The International Atomic Energy Agency (IAEA) and UNESCO have established a close co-operation within the framework of both the earlier IHD and the ongoing IHP in the specific aspects of scientific and methodological developments related to water resources that are of mutual interest to the programmes of both organisations.

The first benchmark publication on isotope hydrology entitled "Guidebook on Nuclear Techniques in Hydrology" was realised in 1983 through the activity of the joint IAEA/UNESCO Working Group on Nuclear Techniques established within the framework of IHP, and it has been widely used as practical guidance material in this specific field.

In view of the fact that the IHP's objectives include also a multi-disciplinary approach to the assessment and rational management of water resources and taking note of the advances made

in isotope hydrology, the IAEA and UNESCO have initiated a joint activity in preparation of a series of six up-to-date textbooks, covering the entire field of hydrological applications of natural isotopes (environmental isotopes) to the overall domain of water resources and related environmental studies.

The main aim of this series is to provide a comprehensive review of basic theoretical concepts and principles of isotope hydrology methodologies and their practical applications with some illustrative examples. The volumes are designed to be self-sufficient reference material for scientists and engineers involved in research and/or practical applications of isotope hydrology as an integral part of the investigations related to water resources assessment, development and management. Furthermore, they are also expected to serve as "Teaching Material" or text books to be used in universities and teaching institutions for incorporating the study of "isotopes in water" in general into the curriculum of the earth sciences. Additionally the contents can fulfil the need for basic knowledge in other disciplines of the Earth Sciences dealing with water in general.

These six volumes have been prepared through efforts and contributions of a number of scientists involved in this specific field as cited in each volume, under the guidance and co-ordination of the main author/co-ordinating editor designated for each volume. W.G.Mook (Netherlands), J.Gat (Israel), K.Rozanski (Poland), W.Stichler (Germany), M.Geyh (Germany), K.P.Seiler (Germany) and Y.Yurtsever (IAEA, Vienna) were involved as the main author/co-ordinating editors in preparation of these six volumes, respectively. Final editorial work on all volumes aiming to achieve consistency in the contents and layout throughout the whole series was undertaken by W.G.Mook (Netherlands).

Mr.Y. Yurtsever, Staff Member of the Isotope Hydrology Section of the IAEA; and Ms. A. Aureli, Programme Specialist, Division of Water Sciences of UNESCO, were the Scientific Officers in charge of co-ordination and providing scientific secretariat to the various meetings and activities that were undertaken throughout the preparation of these publications.

The IAEA and UNESCO thank all those who have contributed to the preparation of these volumes and fully acknowledge the efforts and achievements of the main authors and co-ordinating editors.

It is hoped that these six volumes will contribute to wider scale applications of isotope methodologies for improved assessment and management of water resources, facilitate incorporation of isotope hydrology into the curricula of teaching and education in water sciences and also foster further developments in this specific field.

Paris / Vienna, March 2000

PREFACE TO VOLUME I

The first volume in the series of textbooks on the environmental isotopes in the hydrological cycle is the result of a re-orientation and in part extension of the lecture notes I used during the years I was teaching the hydrology students of the Free University of Amsterdam an annual course in Isotope Hydrology. During these years my colleague and friend, Joe Pearson, and I set ourselves to publish the lecture notes, but did not find the time for the accomplishment of this task. Now I have come to realise how much he taught me and I gratefully acknowledge those days.

The need for international agreement on definitions and the use of symbols can not be sufficiently emphasised. In this introductory volume I have aimed at consistency as well as mathematical and physical correctness. However, it is unavoidable that, for historical reasons, the same consistency could not be continued in all subsequent volumes.

The second important aim of this volume has been to present no equations dealing with isotopes without the proper and understandable mathematical derivation.

After an introductory chapter on the hydrological cycle, this volume contains the principles of radioactivity and of the isotope effects for stable isotopes. The elements of hydrogen, carbon and oxygen are being treated in detail, as they form the "heart" of isotopic applications in the water cycle. The contribution of the other isotopes is discussed less extensively in this volume. Concrete isotopic applications in hydrology, here only touched at in an illustrative manner, have become greatly expanded by my colleagues in the next volumes.

We felt that it is preferable that subjects of more general interest to the other volumes, such as the aqueous chemistry of inorganic carbon, the treatment of water samples in the field and in the laboratory, the techniques of isotopic analyses, the statistical treatment of data, should be treated in the first volume.

This series of 6 volumes are meant to be textbooks. This leads to certain requirements different from the existing handbooks. Especially in this introductory volume I have kept the number of references to literature minimal, in favour of the readability of the text.

I owe much gratitude to the "former" co-workers of "my lab" for their assistance in reading the manuscript, making many corrections, pointing out subjects that were failing and explanations that could not well be understood, in short for their continuing hospitality.

To my colleagues co-authors of this series I want to express my appreciation for our highly stimulating and pleasant co-operation.

Groningen, 29 February 2000

Willem G Mook

CONTENTS

1 THE GLOBAL CYCLE OF WATER *)

1.1 INTRODUCTION

The global hydrological cycle together with its driving force, solar radiation, forms the basic resource for primary biological production. It provides the water that is required for the assimilation of carbon and plays an important role in the supply of nutrients and their transport. Moreover, the hydrological cycle is responsible for the moderate and favourable temperature conditions prevailing on Earth through its linkage with the global atmospheric cycle.

The hydrosphere is the interconnection between the biosphere, the atmosphere and the lithosphere, notably integrating the fluxes of water, energy and geochemical compounds.

Water is able to execute these tasks because of a number of exceptional properties:

1) high and universal **dissolving power**, essential for distributing geochemical material and to transport nutrients and to remove waste substances from living organisms
2) high **surface tension**, causing high capillary forces; together with osmotic forces, this enables water and solute transport within organisms and maintaining a high cellular tension.
3) large **heat capacity** and **heat of vaporisation**, inherent to its role as energy transporter
4) maximum **density** above freezing point, at 4^0C; this anomaly causes freezing to proceed from the surface downward, slowing down both the heat release and the advancement of the freezing process, thus protecting living organisms
5) high **freezing** and **boiling point** relative to its molecular weight, in comparison with similarly structured compounds, such as H_2S and H_2Se; compared to these compounds, these temperatures would be between -50 and -100^0C.

All these properties are related to the high cohesion and pseudo-crystalline structure of water. This structure is caused by the eccentricity of the positive hydrogen nuclei with respect to the electrons and the oxygen nucleus, which gives the H_2O molecule an electrical polarity or dipole character.

In this chapter we will discuss the composition of the hydrosphere and the basic concepts of the hydrological cycle and its interaction with atmospheric circulation. Subsequently, we will consider the individual elements of the hydrological cycle, and their mutual interaction. Finally, attention

---

*) Original version by J.J.de Vries, professor of hydrology, Free University, Amsterdam

is paid to the impact of climatic change and man's interference with the hydrological cycle.

1.2 THE HYDROSPHERE

1.2.1 ORIGIN OF WATER ON EARTH

Most probably water has been in our solar system from the beginning and was formed by the thermonuclear fusion process that produced the elements of the periodic system and their compounds. The total amount of water contained on Earth is estimated at some 0.4% by volume, sufficient to form a sphere of ice with a diameter of almost 2500 km and a volume of 8.2×10^9 km^3. Most of this water is chemically and physically bound in rocks and minerals within the crust and mantle. The amount of free water, forming the hydrosphere, is estimated at 1.4×10^9 km^3 –i.e. 17% of the total amount of water on Earth– of which 96% is stored in the oceans as saline water.

It is generally accepted that most of the water in the hydrosphere has originated from degassing of the Earth's mantle by volcanic eruptions and surfacing lava (basalt) in the course of the 5 billion years of the Earth's existence. The production by this process is estimated at about 1 km^3/year. However, it is known that Earth is also exposed to collisions with cosmic material, including ice comets. An extraterrestrial origin of at least part of the Earth's water is therefore likely. Some of the other planet's satellites and many comets consist almost completely of ice. A well-known example is Halley's Comet. A rough estimate gives a total amount of water in our solar system, that is 100 000 times the mass of water in our oceans (Kotwicki, 1991).

1.2.2 THE HYDRO-TECTONIC CYCLE

As explained before, the Earth's hydrosphere acquires water both from the mantle and possibly from space, a gain of the order of 1 km^3/year. On the other hand, a smaller quantity escapes into space and another unknown amount returns to the mantle through plate-tectonic processes. This process is driven by thermal convection currents, which move the rigid lithosphere as a coherent layer over the more plastic asthenosphere (Fig.1.1). Magma moves upward into fractures (spreading centres) in the ocean floor, where it forms new oceanic crust. This causes the lithosphere to move away from the spreading centre. At the other limb of the convection cell, the lithosphere sinks downward in a subduction zone. Where old lithosphere disappears in the mantle, ocean water is dragged with the crust to depths of hundreds of kilometres and becomes involved in the re-melting of sediments into new magma. Another part of this water is exhaled again by the associated volcanic and magmatic activity. This entire process is referred to as the *hydro-tectonic cycle*. This cycle acts on a geologic time scale of millions of years and is quantitatively negligible compared to the amount and distribution of water in the present hydrological circulation at the Earth's surface and the lower atmosphere. The difference in dynamics of this *hydrological cycle* and the hydro-tectonic cycle is also reflected in the respective energy fluxes involved.

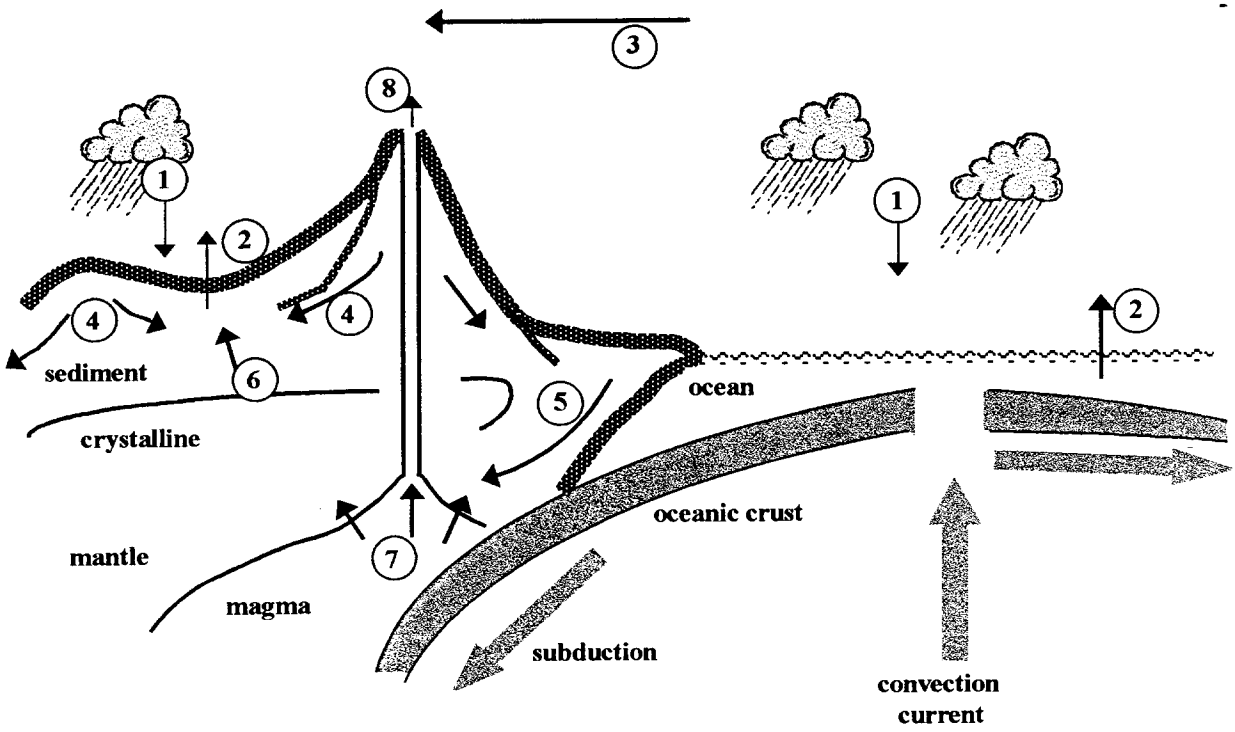

Fig.1.1 Schematic representation of the hydro-tectonic cycle, showing a cross-section through an ocean-continent boundary. The upward moving mantle material forces the oceanic crust to slide under (to subduct) the continental crust.

1. Precipitation
2. Evapo(transpi)ration
3. Vapour transport
4. Topography driven flow (meteoric water)
5. Sea(water) trapped in subducted sediments (connate water)
6. Fluid released by deformation
7. Fluid released from magma and metamorphic reactions (juvenile water)
8. Volcanic emissions

The driving force behind the hydrological cycle, solar radiation, produces a flux at the Earth's surface of 5.2×10^9 J/m^2/year, whereas the driving force behind the tectonic processes, the Earth's internal heat production, delivers about 2.0×10^6 J/m^2/year. The volcanic and magmatic exhalations, however, do have a qualitative effect on the hydrosphere by producing chemical compounds and concentrated heat. Volcanic dust and gases may influence the Earth's heat balance and thus its climate and hydrological cycle over a period of years.

Plate-tectonics and continental drift change the shape of the earth on a time scale of millions of years by a geographic re-arrangement of oceans and continents, uplift of the Earth's crust and the formation of mountain ranges. In the course of the Earth's evolution these morphological changes have caused changes in world-wide climatic conditions and in the hydrosphere. Other long-term influences on the planet's climate are caused by systematic shifts in the Earth's orbit and exposure to the sun, with associated changes in incoming solar radiation, on time scales of 10^4 to 10^5 years.

Table 1.1 Volumes and fluxes of water and their turn-over time in the different compartments of the hydrosphere. The volumes are mainly according to Baumgartner and Reichel (1975), with some additions.

	Volume in 10^3 km^3	% of total freshwater	flux 10^3 km^3/year	turn-over time year
Salt water				
Oceans	1 350 000		425	3000 [1])
Freshwater				
Ice	27 800	69.3	2.4	12 000 [2])
Groundwater	8 000*	29.9	15	500 [3])
Lakes	220**	0.55		
Soil moisture	70	0.18	90	0.8 [4])
Atmosphere	15.5	0.038	496	0.03 [5])
Reservoirs	5	0.013		
Rivers	2	0.005	40	0.05 [6])
Biomass	2	0.005		
Total	**40 114**	**100**		

* < 5000 m depth, based on a porosity of 1%, rather than porosity of 1.5%, resulting in a volume of 12×10^6 km^3 (see Volume V)

** about 50% contains salt or brackish water; cf. volume of 177×10^3 km^3 (Volume III)

[1]) Flux is oceanic evaporation

[2]) Flux estimated from discharge

[3]) Flux estimated at 37% of total continental discharge (base flow)

[4]) Flux estimated at 80% of continental rainfall

[5]) Flux is total rainfall = total evaporation

[6]) Flux is total discharge from continents

1.2.3 DISTRIBUTION OF WATER OVER THE VARIOUS RESERVOIRS

The hydrosphere can be characterised as a system of different reservoirs from which water, solutes and energy are exchanged by the hydrological cycle. On a large scale this circulation is driven by thermal energy of solar radiation and by potential- and pressure energy produced by gravity. On a small scale, capillary and osmotic forces play a role in water transport in soil and plants, whereas geothermal energy produces thermo-mineral convection currents in deep aquifers.

As mentioned before, the total amount of water in the hydrosphere is estimated at 1.4×10^9 km^3,

of which 96% resides in the oceans. The remaining 4% consists of freshwater, which exists and moves only by the virtue of the continuous distillation process that turns salt water into a freshwater by evaporation and subsequent condensation. Most of this freshwater is more or less locked up in ice caps, icebergs and glaciers, notably on Antarctica and Greenland. Were it to melt, the world's rivers could flow uninterruptedly for more than 500 years on this quantity of water.

An estimate of the distribution of freshwater over the various global reservoirs and the *turn-over time* of the different reservoirs is given in Table 1.1.

There is considerable uncertainty about some of these figures, especially for groundwater at greater depths. Also estimates of the ice volume vary considerably, from 22 000 km^3 to 43 000 km^3 . Most of the freshwater reserve actively involved in the hydrological cycle is found in the upper few kilometres of the subsurface.

The state of the still deeper water is not well known, but most of it is more or less isolated from the hydrological cycle by impervious layers and takes part in it only on a geological time scale. Moreover, most of this water is saline and probably mainly connate, i.e. water (mainly sea water) that was trapped during the deposition of sediments. Part of this water is diagenetically altered *meteoric water* (i.e. from atmospheric origin) or *juvenile magmatic water*. Hot *brines* with a temperature of 200^{0}C are still encountered in the ultra-deep Kola Peninsula (N.Russia) borehole at a depth of 12 km. Such mineralised waters normally reach the surface in thermo-mineral springs connected with (past-)volcanism or deep-seated fractures (Fig.1.1).

Another part of the groundwater reserves (Volume V, Chapter 1) at more shallow depths can also be classified as fossil, if this water was formed under different conditions than at present and if it is isolated from active circulation, either by less pervious layers or because of a lack of recharge, like in arid regions. A huge groundwater reservoir (more than 100 000 km^3) is present beneath the Sahara and the Arabian Peninsula in sandstones and limestones locally reaching a thickness of 3000 m. This water was dated at 10 000-40 000 years BP and was recharged during pluvial periods in the last ice age. It is still flowing under artesian pressure and constitutes the source behind oases. Although this water is not actively involved in the hydrological cycle, its discharge adds water to the active part, thus adding to the oceanic reservoir. Depletion of all fossil reserves on Earth, either by natural discharge or by artificial extraction, would rise the average sea level by several decimetres.

Another relatively slow part of the cycle is formed by the polar ice caps which, at least on a geological time scale, must be considered a temporary phenomenon. They have been gradually formed since the temperature at the Earth's surface started to decrease at the beginning of the Tertiary, some 50 million years ago, from about 20^{0}C to the present 15^{0}C. This eventually resulted 2 million years ago in the present Quaternary with glacial cycles of the order of 100 000 years and temperature intervals of less than 10^{0}C. During more than 90% of the Earth's history there were no polar ice caps. The origin of this cooling of the Earth is not fully understood, but a shift of the

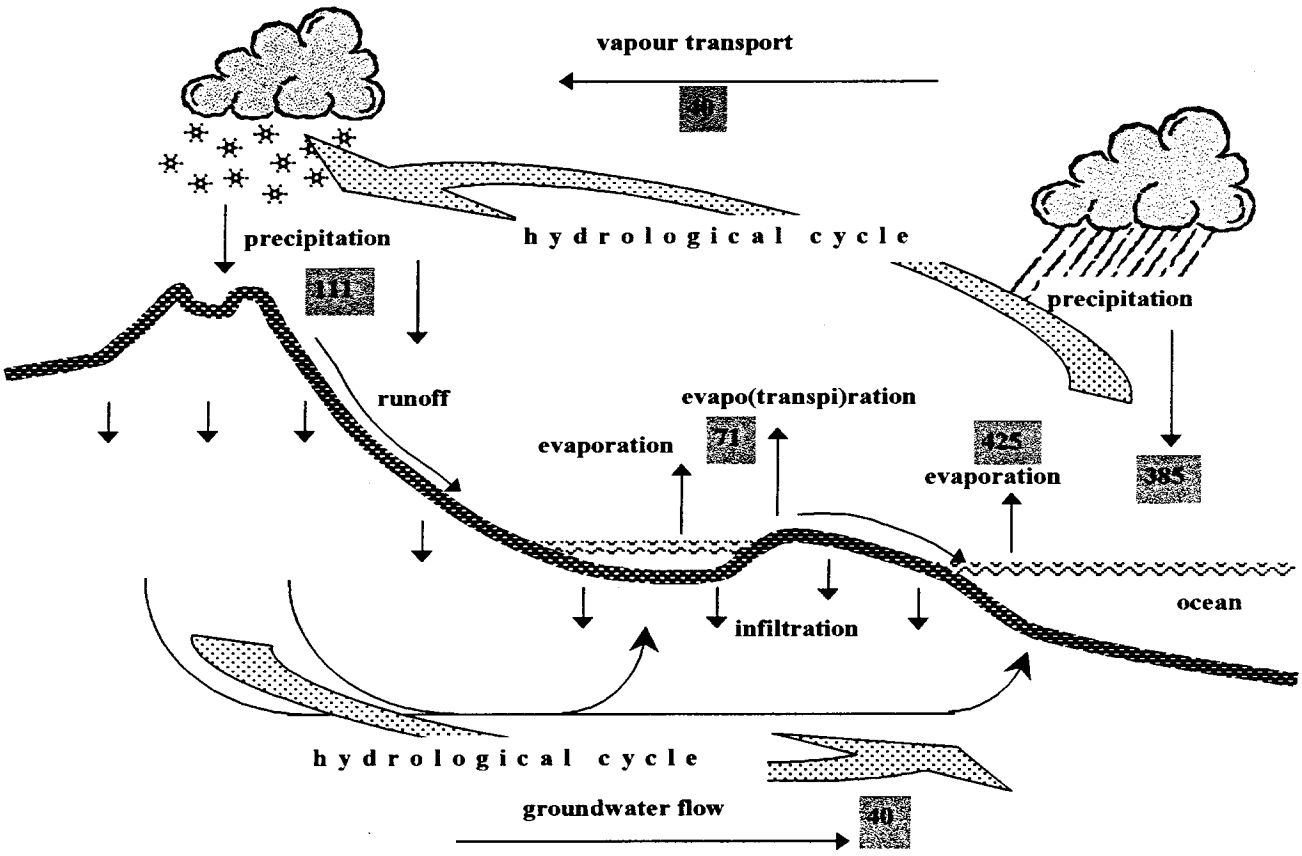

Fig.1.2 Schematic representation of the global hydrological cycle. The overall figures refer to the water fluxes in 10^3 km^3 per year (according to Table 1.2).

Antarctic landmass and the isolation of this continent by a circum-Antarctic ocean current during the Tertiary and the subsequent uplift of this continent was certainly a prerequisite for the initiation of the huge continental ice cap. The growth of the Antarctic land-ice probably began during the Middle Miocene, about 12 million years ago, but the first glaciers on the Antarctic highlands originate from the beginning of the Oligocene, about 30 million ago.

1.3 THE GLOBAL WATER BUDGET

A schematic overview of the global hydrological cycle and *water balance* is presented in Fig.1.2. The hydrological cycle starts with evaporation from the oceans, estimated at 425 000 km^3 (1176 mm) per year. Rainfall over the oceans is estimated at 385 000 km^3 (1066 mm), leaving an excess of 40 000 km^3 (equivalent to 110 mm) of water as vapour, which is transported by atmospheric circulation (advection) to the continents. The main vapour flux travels from the warm equatorial to the cool high-latitude regions.

The vapour convergence at higher latitudes becomes clear from the areal distribution of the

atmospheric vapour: the average annual vapour content decreases from 50 mm water equivalent in equatorial regions to less than 5 mm over the polar regions. Condensation of the 40 000 km^3 of vapour originating from the oceans produces rain on the continents. This precipitation is repeatedly recycled by re-evaporation. The annual cumulative evapotranspiration from the continents is estimated at 71 000 km^3 (480 mm) so that finally a total amount of 40 000 + 71 000 = 111 000 km^3 (746 mm) of precipitation is produced, leaving an excess of 40 000 km^3 (266 mm) returning to the oceans via rivers, glacial meltwater and groundwater. Table 1.2 shows the fluxes.

Table 1.2 Annual water balance at the various oceans and continents of the Earth after Baumgartner and Reichel (1975). Shiklomanov (1993) arrived at notably higher values for the oceans.

	Continents		**Oceans**		**The Earth**	
Surface area in 10^6 km^2	149		361		510	
	10^3 km^3	**mm**	**10^3 km^3**	**mm**	**10^3 km^3**	**mm**
After B.and R., 1975						
Precipitation	111	746	385	1 066	496	973
Evapo(transpi)ration	71	480	425	1 176	496	973
Discharge	40	266	40	110	—	—
After Shiklomanov, 1993						
Precipitation	119	800	458	1 270	577	1 131
Evapo(transpi)ration	72	487	505	1 400	577	1 131
Discharge	47	313	47	130	—	—

1.4 COMPONENTS OF THE HYDROLOGICAL CYCLE

1.4.1 EVAPORATION

Evaporation can only occur where a vapour pressure gradient is maintained between the evaporating surface and the overlying atmosphere. Besides this mechanism, evaporation also needs energy to convert water into vapour (2.44×10^3 J/g at 15^0C). This energy is provided by the evaporating water, and indirectly from solar radiation and heat from the atmosphere. In fact, two factors control the mechanism of evaporation. In the first place the difference between the vapour pressure of the overlying air (e_A) and the saturated vapour pressure (e_S) at the temperature of the evaporating surface. This difference (e_S-e_A) is called the saturation deficit. Secondly, the evaporation rate is determined by the vapour transport. The upward movement in a thin boundary layer is by molecular diffusion, but above this layer vapour is transferred and removed by turbulent air movement, related to the wind speed. Evaporation is strongly dependent on the temperature

determining the saturated vapour pressure, and the turbulent air exchange that is related to wind speed and surface roughness.

Methods to determine evaporation from climatic data are normally based on a combination of the energy balance for a specific surface and the aerodynamic conditions. The most well known energy balance/aerodynamic method was developed by Penman (1948). Later Monteith (1965) adapted Penman's formula so as to make it applicable to vegetated surfaces as well, by introducing biological and aerodynamic resistance factors that incorporates structure and physiology of the vegetation cover.

Although evaporation is driven by solar energy, the distribution over the oceans does not reflect the latitudinal pattern of incoming radiation, neither in time nor place. This is because the latent heat is for a large part extracted from the heat stored in the water itself, and thus influenced by warm and cold ocean currents. This occurs especially when relatively cold and dry air blows over a warm ocean current.

The high vapour pressure gradient between the warm water surface and the dry air stimulates upward vapour transport and the energy will be extracted mainly from the water. Therefore, maximum evaporation occurs in the Western Pacific and the Western Atlantic where this particular situation prevails (Fig.1.3). Relatively low values are found in the equatorial areas because of low wind velocity and high vapour pressure. Advection of warm air masses and seasonal variations in wind speed and turbulent exchange are other factors that influence the distribution of evaporation over the oceans in space and time.

Evaporation from a vegetated land surface is normally a combination of direct evaporation from a wet surface, and water consumption or transpiration by the vegetation. This combined effect is called *evapotranspiration*. The evaporation from an extensive water surface, like a lake or ocean, depends exclusively on the available energy and the atmospheric condition. Evaporation from a land surface however is often limited by the availability of water. For a well-watered vegetated surface or a wet soil, evaporation is normally close to that of an open water surface and is indicated as potential evapotranspiration.

The amount and the timing of rainfall is an important factor. Available energy, for instance, can become the limiting factor if rainfall occurs during the winter season, whereas at the other hand, more regularly distributed rainfall with frequent showers can increase evaporation from interception. Limited amounts of water at the right moment and place is one reason that the total evaporation on the continents is less than half of the amount on the oceans. The other factor is the lower net solar radiation received by the land surface. This is mainly caused by the difference in albedo (percentage incoming solar radiation that is reflected back into the atmosphere at the Earth's surface), which is 6-10% for open water and varies on the continents from 7% for tropical rain forest to 35% for dry white sand (see also Sect.1.4.3).

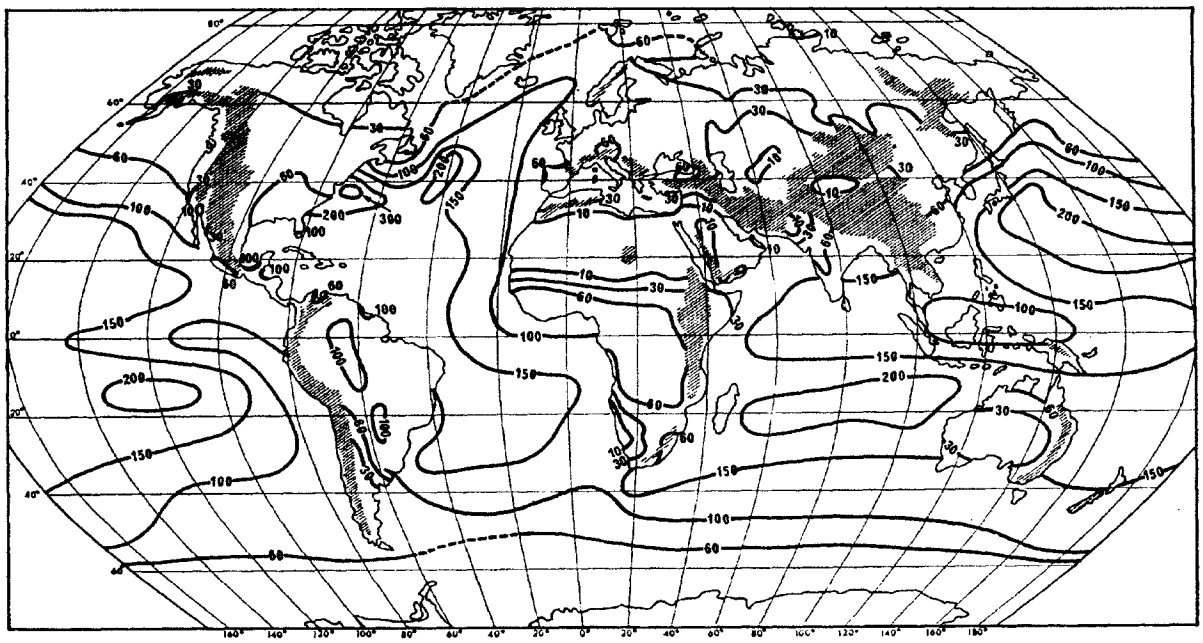

Fig.1.3 Global pattern of annual evaporation in cm (Barry, 1969; after Budyko et al., 1962).

1.4.2 PRECIPITATION AND ATMOSPHERIC CIRCULATION

In principle, rain is caused by condensation and cloud formation in the atmosphere when air is cooled to its dew-point. The cooling is normally caused by adiabatic expansion of the uplifted air, due to the decrease in atmospheric pressure with height. Heat release by condensation can subsequently provide additional energy to cause further rise of the air mass, which can result in convective thunderstorms. Most rain-producing vapour has been subjected to advective transport by atmospheric circulation.

The general atmospheric circulation is maintained by the gradient in incoming solar radiation, with an excess in the tropical belt where receipt of heat exceeds the losses back into space, and a permanent heat sink in the polar regions. Heat consumption and heat release by evaporation and condensation, respectively, are a secondary factor in the global heat distribution. The air movement itself is driven by the pressure gradient, which is caused by spatial differences in heating, but the movement deviates from the pressure gradient because of the Earth's rotation (the Coriolis effect). Other deviations superimposed on the general north-south circulation are due to the distribution of land and sea and the associated differential heating, including seasonal effects. Wind fields are further influenced by mountain ranges.

At low latitudes the air column rises and moves poleward on either side of the equator. At higher latitudes cooling air causes the column to descend. This results in the development of the large convective wind cells, the so-called Hadley Cells, with low pressure along the equator and high

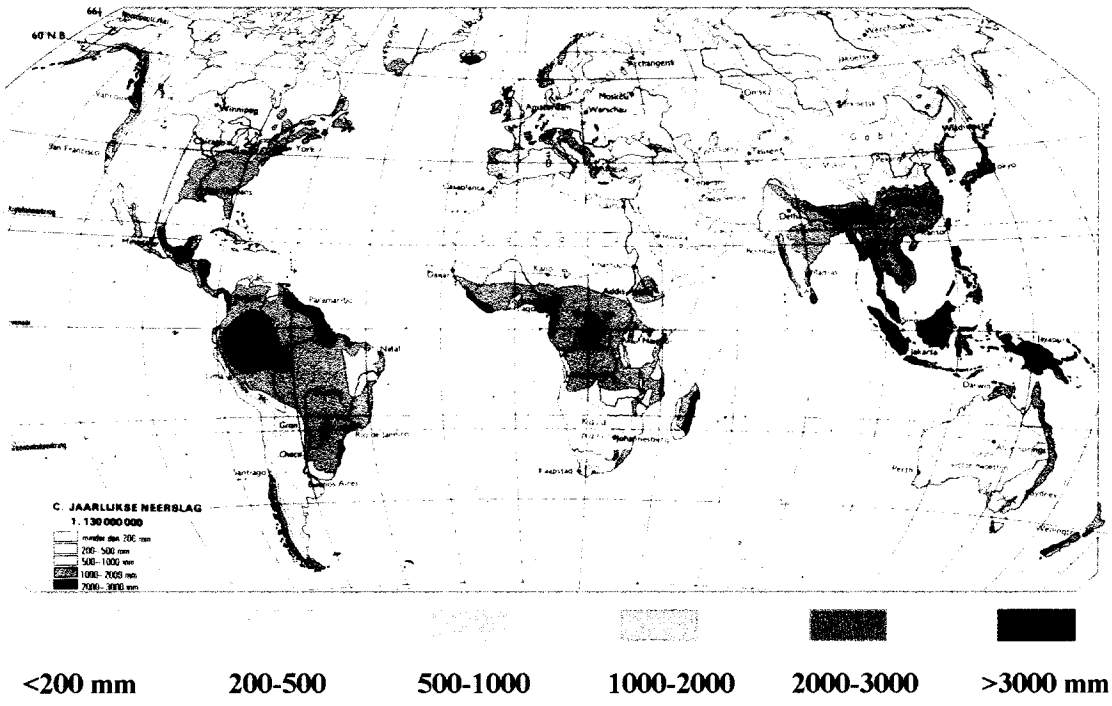

Fig.1.4 The global pattern of annual precipitation (Bos Atlas, Wolters-Noordhof, 1988).

pressure around 30^0 Latitude. The Earth's rotation causes the separation of the high pressure belt into divergent spiralling anticyclonic cells. The compensating back- flowing air produces the north-easterly and south-easterly trade winds, which converge in the equatorial area, and is therefore also known as the Inter-Tropical Convergence Zone (ITCZ). The rising air along the equatorial convergence zone produces the high rainfall of the wet-tropical rainforest areas, whereas the high pressure belt with its heating of the air by compression, results in the low rainfall zone of the dry-tropical steppe and desert areas. These arid zones extend northwards in the remote interiors of the northern hemisphere because of their distance from the moist oceanic air (Fig.1.4).

Part of the warm air from the sub-tropical high pressure belt moves to higher latitudes and forms the prevailing Westerlies on the Northern Hemisphere. Cold air sinks at the poles, spreads along an easterly course and clashes at mid-latitudes with the Westerlies. Here the warm subtropical air overrides the polar air and forms the so called polar fronts along the different air masses. The forced uplift of warm moist air, together with low pressure pulsations in the meandering Jetstreams in the upper part of the Westerlies, causes the development of low pressure cells (anticyclonic cells). Their inward and convergent, spiralling movement forces the moist air to rise and produces the frontal rains of the mid-latitudes. Convective rains are formed mainly during the summer in this area by free convection cells in overheated air.

Extreme cases of convective rains are connected with the development of devastating hurricanes or typhoons. These develop in sub-tropical areas when low pressure convection cells form over

warm sea surfaces of more than 26^0 C. Their energy is derived from the heat that is released by condensation of the rising and expanding air. This process is self- sustaining because the warm moist air is continuously sucked up from the ocean. Extreme rainfall of the order of 500 mm/day is not uncommon during the passage of hurricanes.

Other heavy rain producing winds are the seasonal Monsoons. These represent wind systems that reverse their direction because of the seasonal change from high pressure to low pressure over large continental areas. The Indian Monsoon is particularly strong. During the summer the Indian subcontinent becomes very hot and a strong thermal low-pressure cell develops. Humid air from the ocean moves in and brings high rainfall. A similar effect is caused by the southward shifting ITCZ during the southern hemisphere summer, bringing seasonal rain in the sub-tropics of southern Africa. Orographic effects are other causes of regional deviations in the global pattern. High rainfall generally occurs at the flank where air is forced upward and low rainfall is consequently observed at the lee side.

1.4.3 DISCHARGE FROM THE CONTINENTS

Part of the rainfall that reaches the earth will disappear again by evaporation, either directly from the wet soil surface or from interception on the vegetation. The remaining water may partly run off along the surface and partly infiltrate, recharging soil moisture (Volume V, Chapter 1). Soil water will percolate further downward to the saturated zone (or groundwater zone) after the soil has reached a soil-specific concentration of moisture. The remaining part is held against gravity by capillary and other forces. Part of the soil moisture and shallow groundwater is subsequently re-evaporated, mainly via transpiration by the vegetation.

Groundwater at a depth of more than 1 to 2 m below the root zone hardly participates in the evaporation process, because capillary transport from the water table upwards is then negligible. It is important to realise that two-third of continental rainfall originates from this re-evaporation and transpiration from land surfaces.

The excess of surface water as well as groundwater is eventually discharged by rivers and to a less extent by direct groundwater discharge into the sea. The character of rivers, or the river regime, follows mainly the seasonal pattern of rainfall and evapotranspiration with an attenuation and delay by the storage processes. Rivers respond fast in areas with shallow soils on steep slopes and low infiltration capacity. In contrast, level areas with high infiltration capacity, high subsurface storage and high permeability, are characterised by slowly reacting rivers and the production of extended base flow. The total global discharge is released partly by *base flow* and partly by *flood flow*. Flood flow is not exclusively generated by surface runoff. The latter type of flow, in fact, occurs only during exceptional high rainfall and in steep land with an impervious subsurface. Flood water is normally produced by a range of processes, including rapid flow through the macro-pores of the upper soil layers (throughflow) and infiltration-excess or saturation-overland flow. These (near)surface processes normally initiate rills and gullies to participate in the drainage process

during periods of high or extended rainfall, so that the drainage system expands into an ephemeral and poorly defined system of branches and associated depressions.

Soil moisture plays an important role in the exchange of water and energy with the atmosphere. Wet soils absorb and store energy and contribute to the return of moisture to the atmosphere by evapotranspiration. Part of this vapour is eventually recycled as rain in the same zone, or reappears as advective rain in adjoining areas. Water often disappears rapidly from dry and barren soil by *sheet floods*. Such surfaces receive less energy because of their higher reflection rate, increasing from 5 – 15% for dark, wet soils and vegetated surfaces, to 25 – 45% for dry, light sand. In general, removal of vegetation similarly causes unfavourable conditions; notably in semi-arid regions this can inhibit the generation of convective rain. Under specific conditions of high infiltration capacity, a reduction of vegetation with its high water consumption can result in an increase in groundwater replenishment. However, an enhancement of groundwater recharge is not always desirable, as semi-arid areas in Australia exemplify. Removal of the vegetation in parts of this country resulted in a rapid rise of the groundwater table to near or at the surface. Evaporation of this water causes severe and under the present climatic conditions irreversible salinisation (see Sect.1.4.4).

Now we can consider the rainfall-runoff balance on the continental scale (Fig.1.5). Average annual rainfall on the continents (estimated at 746 mm) represents a surplus of 50% over average annual evapotranspiration (480 mm), although on average the annual potential evaporation is higher than rainfall. This is because rainfall in many areas exceeds the maximum evaporation in one season, whereas maximum evaporation is not reached due to a lack of water in other seasons.

Changes in storage of soil water and groundwater play an important role in the smoothing of these seasonal effects, and are therefore crucial for the conversion of precipitation into runoff. The reasons are (i) because of their buffering effect on the discharge itself, and (ii) because they extend the evaporation beyond the rainy period into the subsequent drier period and thus increase total evapotranspiration.

The three components of the hydrological cycle over the continents and oceans are listed in Table 1.2. There is a global seasonal effect in the runoff that is predominantly caused by the detention storage of snow on the continents of the northern hemisphere. The North American and Eurasian landmasses receive a snow cover over 60-70% of its surface, which reaches its maximum in March-April. The maximum seasonal depletion of this cover follows at the end of the summer, causing a maximum storage in the ocean around October. Furthermore, the distribution of precipitation, evaporation and inflow from the continents eventually produces a surplus in the Indian and Atlantic Oceans, and a net loss from the Pacific and the Arctic Ocean. Consequently, there is a continuous inflow from the Indian and Atlantic oceans into the Pacific and the Arctic oceans. Table 1.3 shows the water balance between precipitation, evaporation and discharge specifically over the various continents and oceans.

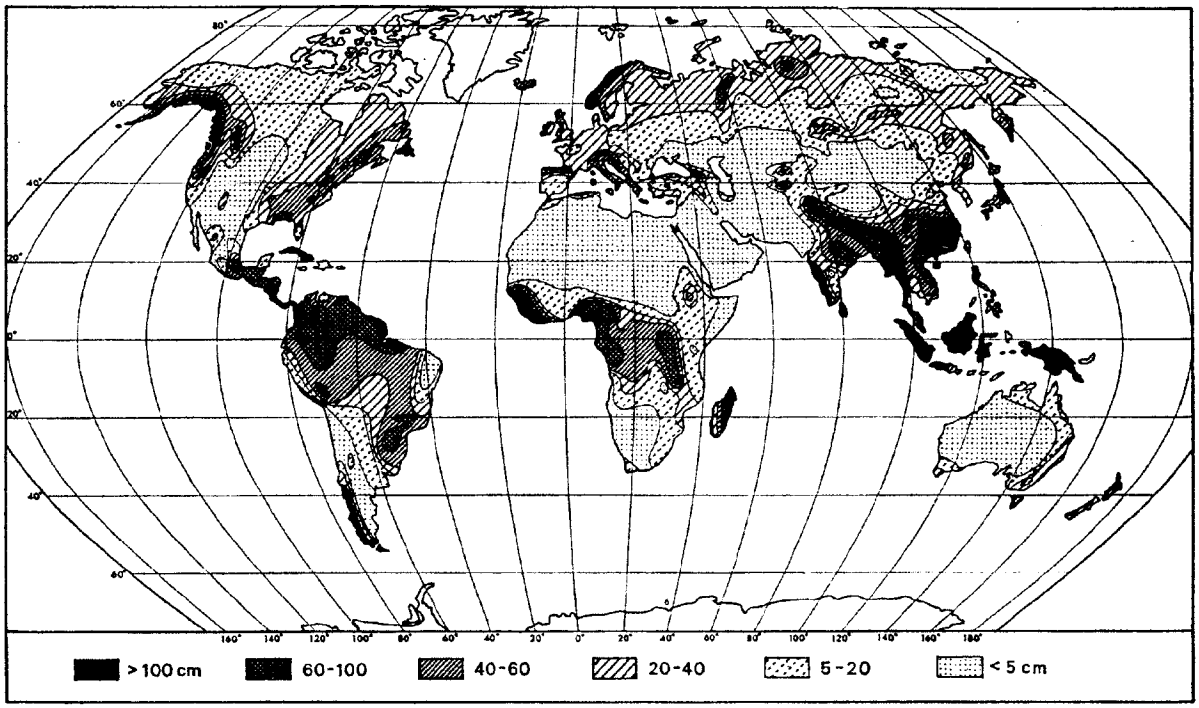

Fig.1.5 Global pattern of annual runoff in cm (Barry, 1969; after L'vovich, 1964).

1.4.4 GROUNDWATER

The subsurface consists of an upper zone with soil water and a lower saturated part with groundwater; these zones are separated by the groundwater table. The depth at which groundwater is encountered depends on topography, subsurface structure and climate. Total storage of groundwater in a layer is determined by the porosity, but the ease at which groundwater can flow depends on a combination of interconnection and size of the pores. This property is parameterised in the permeability. High porosity and high permeability are notably found in alluvial sandy deposits and to a lesser extent in sandstone. Clay on the contrary shows about the same porosity as sand (30-50 vol %), but the pores are small and consequently the flow resistance is considerable, so that saturated water flow is often negligible. Karstified limestone can produce very high permeability due to dissolution features, and can even develop subsurface streams. Relatively porous and permeable subsurface layers are indicated as water bearing layers and are called aquifers. Generally, claystones and crystalline rocks show poor aquifer characteristics, but weathering, fracturing and jointing can locally produce permeable structures.

Groundwater recharge normally takes place by diffuse infiltration according to the processes described in Sect.1.4.3. Concentrated recharge takes place via water that has accumulated in depressions or streams in cases where the stream bed is above the groundwater table. The latter situation especially occurs in arid areas where deep groundwater tables prevail. Recharge is then from episodic floods in wadi's or from river inflow from surrounding, more humid areas. Complete

Table 1.3 Annual water balance of continents and oceans after Baumgartner and Reichel (1975).

P = precipitation, E = evaporation, D = discharge

	Area in 10^3 km^2	P		E		D		D/P
		10^3 km^3	mm	10^3 km^3	mm	10^3 km^3	mm	%
Europe	10	6.6	657	3.8	375	2.8	282	43
Asia	44.1	30.7	696	18.5	420	12.2	276	40
Africa	29,8	20.7	696	17.3	582	3.4	114	16
Australia	8.9	7.1	803	4.7	534	2.4	296	33
id. w.o. islands	7.6	3.4	447	3.2	420	0.2	27	6
N. America	24.1	15.6	645	9.7	403	5.9	242	38
S. America	17.9	28.0	1564	16.9	946	11.1	618	40
Antarctica	14.1	2.4	170	0.4	28	2.0	142	83
All continents	**148.9**	**111**	**746**	**71.3**	**480**	**39.7**	**266**	**36**
Arctic Ocean	8.5	0.8	97	0.4	53	0.4	44	45
Atlantic Ocean	98.0	74.6	761	111.1	1133	–36.5	–372	–49
Indian Ocean	77.7	81	1043	11.5	1294	–19.5	–251	–24
Pacific Ocean	176.9	228.5	1292	212.6	1202	15.9	90	7
All oceans	**361.1**	**385**	**1066**	**224.7**	**1176**	**–39.7**	**–110**	**–10**

streams sometimes disappear underground in karstified limestones of high dissolution permeability.

Groundwater discharge normally takes place by subsurface drainage to streams. The average turnover time of groundwater is determined by the total flux, or recharge, and the storage of the basin. The flow density however, normally decreases downward, so that the age of the water roughly increases logarithmically with depth (see Volume 4).

Water is stored during periods of high recharge: this results in a rise of the groundwater table and an increase of the hydraulic gradient, so that the discharge increases. Moreover, a rise of the groundwater table often means that lower-order and less deeply incised stream branches are activated to take part in the drainage process, which can amplify the drainage rate by an order of magnitude. Saturation-excess overland flow through rills and gullies is the extreme condition which occurs when the groundwater table reaches the surface (Sect.1.4.3).

A dry period reverses the process: groundwater is then released from storage because discharge exceeds recharge. Consequently the groundwater table drops, discharge decreases and stops when

the water table at the divide has reached the level of the deepest incised channel and the hydraulic gradient has become zero. In arid areas where recharge is low and groundwater tables are deep, groundwater flow is more steady and fluctuations are dominated by long term cycles of drought and wet climatic spells.

Residence times of groundwater range between months for shallow drainage systems to thousands of years for deeper systems, and especially in arid areas with low recharge and large turnover time. Exceptional cases of fossil or residual groundwater flow can be found in extensive groundwater basins in desert areas. Their relaxation time is large because of a large volume of water stored and because of a high flow resistance, due to the large distances between (palaeo-)recharge and discharge areas. An example is the Sahara where huge fossil groundwater reserves from the last ice age (dated 10 000-40 000 years BP) still flow and feed springs, driven by a residual hydraulic gradient. The hydraulic gradient is slowly decreasing by depletion, but this process can proceed for thousands of years to come, unless large-scale groundwater abstraction, like in the Middle East, accelerates the depletion.

The groundwater systems discussed above are mainly driven by topography or potential energy, and their water is of meteoric origin. Groundwater occurrences at greater depths below impervious layers are more or less isolated from the active part of the hydrological cycle and their character is partly connate; i.e. they were trapped during sedimentation and are often of marine origin. These waters therefore form the connection with the geological cycle of erosion, sedimentation, diagenesis, tectonics and metamorphism, and their dynamics are interlinked with these processes. Their flow is driven by processes on a geological time and areal scale, including compaction by sediment accumulation, pressure change by tectonic deformation, thermal and geochemical convection, molecular diffusion and osmotic processes. Fluid movement under these conditions has often residual components because of the long relaxation time of the pressure gradient. The interaction of these deep seated systems with the active or meteoric part of the hydrological cycle occurs by slow upward seepage and in thermal and mineral springs in tectonically active areas.

Groundwater and surface water in humid areas finally assemble in rivers which carry the continental surplus water back to the oceans. For this purpose, stream systems consist of a highly efficient network of hierarchic and nested branches, each having their own sub-catchment. This network forms a dynamic drainage and discharge system that expands into the smallest gullies in time of high water supply, and contracts to the larger ones in dry periods.

Many arid basins do not produce a water surplus and maintain an internal ground- and surface water drainage. All rainwater eventually evaporates and the dissolved salts present in the water are left behind. The salinisation of large areas in Australia, for instance, is due to evaporation of rising groundwater, which is loaded with the accumulated salt. Most of these areas experienced wet pluvial conditions during the last ice age but started with the accumulation of salt some 10 000 years ago at the beginning of the drier Holocene.

1.4.5 CONTINENTAL WATER SURPLUS AND WATER USE

A special component of the continental water balance is the use and diversion of part of the water surplus by man. The estimated annual 40 000 km ^{3} (266 mm) of runoff from the continents (Table 1.2) represents the excess water that is left of the 111 000 km^3 (746 mm) of rainfall, after evaporation and transpiration by natural vegetation and rain-fed agriculture have taken their share. In principle, this excess water is available for domestic and industrial use and for irrigated agriculture. About 5000 km^3 of this water is nowadays withdrawn for these purposes. Irrigated agriculture takes the highest share with 65%. It is responsible for more than 50% of the world's food production on 20% of the world's arable land. The high amount of water needed for food production is exemplified by the fact that the production of 10^3 kg of corn, sufficient to feed six people for one year, requires 300×10^3 kg of water under average climatic conditions. The ratio between water use and dry mass accretion differs between crops and depends obviously on climatic conditions, particularly the potential evaporation. Observations on various types of vegetation give values between 100 and 1000 kg of water per kg dry mass production.

The uneven distribution of water resources in time and space and the irregular spread of the world's population, restrict the possibilities for increasing the application of this excess water. Most of the water is available in the equatorial tropical areas (the Amazon River, for instance, discharges 20% of the world's total runoff), whereas two-thirds of mankind live outside the tropics. Another negative factor is the variability of the supply in time. Only one-third of the runoff forms a more or less stable supply, while the remaining part occurs in floods. The irregular distribution of water in space and time has led from the earliest civilisations onwards to hydraulic engineering practices, notably the construction of water diversion, transport and storage works, including large-scale drainage and irrigation schemes. These modifications of the regional water balance have certainly resulted in a modification of the regional atmospheric and hydrological circulation and the associated climate (Sect.1.5.2).

Water resources assessment and sustainable resource development and management require a sound knowledge of the hydrological processes involved. Especially Volume V of this series is devoted to these aspects. Numerous tools and models which have been developed for analysing the hydrological situation are being treated in Volume VI.

1.5 THE HYDROSPHERE AND GLOBAL CHANGE

1.5.1 CLIMATIC CHANGE

The Earth forms a dynamic system, with internal processes driven by internal heat production and external processes driven by solar energy. Both type of processes interact in cycles of material and energy flows, each with its own temporal and spatial scales. A shift in one of the components must lead to an adjustment elsewhere in the system, which in turn can trigger changes in related systems. Regional hydrological cycles are closely linked with the prevailing climatic conditions and

associated vegetation covers, and can be expected to react accordingly to changes in the meteorological forcing or large-scale transformation in surface cover.

As explained before, the present climate deviates from the average climate during the Earth's history and is characterised by relatively low temperatures and ice caps at the poles. The present "ice age" is the sixth over the last billion years, and was preceded by the Permian glaciation some 250 million years ago. Apart from these cold eras, the Earth has experienced shifts from the domination of wet and hot swamps, as during the Carboniferous, to the hot and dry prevailing desert conditions during the Triassic. Such major shifts are basically caused by plate-tectonics induced shifts in the geographical position of the continents as well as by changes in their elevation by uplift and mountain building.

Another major player in the global climatic system is probably the carbon-dioxide content of the atmosphere. CO_2 is part of the global geochemical carbon cycle which has the following main fluxes: (i) CO_2 extracted from the atmosphere by photosynthesis, producing organic material, and by weathering of rock as well as deposition of calcium minerals; (ii) CO_2 released to the atmosphere by decay of organic matter and respiration by plants and soils; (iii) CO_2 periodically evading from and taken up by the oceans; (iv) CO_2 recycling in the Earth's interior by absorption in the mantle via the descending subduction zone and release through degassing by volcanic eruptions and by the extrusion of magma in the oceanic ridges (Fig.1.1). The oceans form a large CO_2 reservoir that act as a buffer through their physico-chemical diffusion exchange with the atmosphere. Algae play an important role in this process.

An illustration of the possible influence of the geographical position of continents and oceans, and the opening up and closing of ocean basins, as well as the influence of atmospheric levels of CO_2, is presented by the change in conditions when going from the Cretaceous to the Quaternary era. The elevation of the continents was much lower than at present, and the ocean-land ratio much larger, especially during the second half of the Cretaceous. The Antarctic Ocean was not yet isolated from warm ocean currents, whereas the landmass at the Arctic was isolated and situated far from snow producing oceans. Moreover, geochemical budget modelling suggests that the CO_2 content of the atmosphere during the last 500 million years was several times higher than at present, with a maximum of 18 times the present content in the mid-Cretaceous, some 100 million years ago. During the mid-Cretaceous the temperature of deep ocean water was 15^0 higher than at present and corals were found 1500 km nearer to the poles.

At the onset of the Tertiary, about 60 million years ago, the temperature gradually decreased, probably because of a thermal isolation of the polar regions. The separation of Antarctica from the Australian continent and the shift of this landmass to the South Pole led to the development of a circum-Antarctic ocean current that obstructs the heath exchange with warm ocean water and allowed the accumulation of snow. The Arctic opened up and came under the influence of precipitation-producing ocean water, but at the same time remained to a certain extent blocked by surrounding continents. Concurrently, the Antarctic landmass rose, which contributed further

to the cooling. Probably already during the Oligocene mountain glaciers were formed on the highest mountains. Ice caps began to develop by the mid-Miocene, about 10 million years ago. This had a positive feedback effect, firstly by an increase in the albedo, resulting in a reduction of the net radiation, and secondly by a further rise of land surface by ice accumulation by more than 1000 m. The latter effect is still clear in the Arctic where Greenland with an altitude of over 2000 m is still glaciated, whereas the Canadian Arctic at the same latitude only shows a winter snow cover. The elevation effect on temperature is a decrease of 6^0C/km under present conditions.

Another effect may have been the continental uplift of other Alpine mountains in the course of the Tertiary, notably the elevated areas of the Himalayas and the Tibetan Plateau with their associated cooling and blocking effect on atmospheric circulation. This orogenesis also caused an increase in weathering and erosion with its associated consumption of atmospheric CO_2.

The Quaternary glacial period, which began about 2.5 million years ago with a pronounced fall in temperature, is characterised by 15 to 20 glacial-interglacial cycles. During the maximum glaciations, air temperatures at the temperate climate zone dropped by 6^0 C relative to present temperature. It is generally accepted now that these cyclic fluctuations were primarily triggered by minor variations in the amounts of solar radiation reaching the top of the atmosphere. These variations originate from regular oscillations in (i) the Earth's orbit (periodicity about 100 000 years), (ii) the tilt of the Earth's axis (41 000 years), and (iii) a circular movement ("wobble") of the spin of the Earth's axis (23 000 years). These are called the Milankovitch oscillations after the Serbian engineer and astronomer Milutin Milankovitch who investigated these astronomical factors and their possible climatic impact at the beginning of the 20th century.

Superimposed on the 20 000-100 000 years astronomically driven climatic oscillations are relatively strong fluctuations in temperature on a time scale of hundreds of years during the glaciations. Fluctuations on similar time scale but lower amplitude have also been observed during the last 10 000 years, i.e. during the present (Holocene) climate. Within this climatic noise main shifts over periods of hundreds to thousands of years have been recognised in the records of the Holocene. For the mid latitudes of the northern hemisphere these climatic fluctuations seem to be connected with the persistence of (i) periods of strong zonal flow of the Westerlies with strong oceanic influence, and (ii) periods with more polar and continental influence and a more southerly track of the Westerlies. This alternating system is dominated by the pattern of high and low pressure cells, which is probably influenced by shifts in ocean currents. The impact of the shift in pressure distribution seems to reach as far south as the Sahel zone.

The most comprehensive review of climatic fluctuations in Western Europe and the Middle East was produced by Lamb (1982). His system is based on climatic proxy data (such as pollen, isotopes and tree-ring analysis), global circulation reconstructions and archaeological and historical information. A schematic review of fluctuations in Holocene climate, mainly based on Lamb (1982) and Jones (1997), is the following.

14000-8000 BC: end of glaciation; sudden and strong temperature fluctuations due to instability of glaciers and the production of huge masses of meltwater

8000-6000 BC: rapid warming and melting of mountain glaciers; humid environment in the Middle East and savannah conditions in the Sahara

5000-3500 BC: Post-Glacial "Climatic Optimum": summer temperatures in NW Europe 2-3^{0}C above that of the present day; monsoonal rains penetrate the Sahara; extensive irrigated agriculture in Mesopotamia

3500-1000 BC: drying of the Sahara (3500-1000); desertification and salinisation in Mesopotamia, Nile flow reduced; sharp decline in temperature about 1500 BC with a strong advance and initiation of new mountain glaciers (it has been suggested that the latter cooling might be connected with the huge eruption of the Santorin volcano in the Aegean Sea about 1450 BC)

900-300 BC: Iron Age Epoch: Cool and wet in northern areas; strong regrowth of bogs after a much drier period

400-800 AD: severe North Sea floods; growth of Alpine glaciers

800-1200 AD: Secondary (Early Medieval) Climatic Optimum: summer temperature at least 1^{0}C above present day; drier in NW Europe; Viking colonisation of Greenland

1430-1850 AD: Little Ice Age (polar continental climate): cool in W. Europe and the Mediterranean; temperatures 1-3^{0}C lower than at present; re-advancement of mountain glaciers; severe winters

1850 AD -present: maritime Atlantic climate; global temperature rise 0.5^{0}C; N.Atlantic sea surface warmer; increased rainfall in NW Europe.

Our knowledge of the causes of these fluctuations is still imperfect and they are probably not the same for the different periods. The exceeding of threshold values within the internal instability of the atmosphere-ocean system, which triggers a chain of feedback loops, is a distinct possibility. Other hypotheses focus on external factors, including variations in solar radiation (notably sun spot activity) and volcanic activity. The increase in temperature during the last century may be attributed to the increase in CO_2 as caused by the combustion of fossil fuel, and possibly to periodicities in the solar activity as revealed by the sunspot numbers. The latter is in accordance with the low sunspot activity during the Little Ice Age, but the mechanism behind this correlation is unclear and still a matter of debate.

1.5.2 THE HUMAN FACTOR

Our knowledge of man's influence on the global hydrological cycle is minor and mainly restricted to the direct consequences of water management for the water balance and runoff regime on the

small and medium catchment scale. The long term impact of large-scale manipulations of river basins and land use change is difficult to evaluate in the absence of long-term hydrological data. Information on the influence of land use change on evapotranspiration is rather well known, but the lack of adequate models that couple the exchange of water and energy at the surface with atmospheric circulation models make it difficult to translate this information into changes in rainfall pattern. It is even more problematic to reconstruct the effects of the large-scale reclamation and cultivation practices during the last 10 000 years, i.e. since agriculture was introduced.

The most evident influence of mankind on the hydrological cycle from the dawn of civilisations is the application of irrigation and drainage. In fact, it seems that the transition from gathering wild grains to the growth of cereal crops evolved concurrently with the beginning of diversion and control of flowing water. The oldest traces of irrigated agriculture were found with the remains of the early urban civilisation of Jericho, where already before 7000 BC water from a large spring was applied for irrigation. Different views have been developed on the impact of these early practices on the environment and on the question whether changes in climate or destructive land use and/or war caused desertification and salinisation and the fall of civilisations. Recent palaeoclimatic and archaeological research have made it plausible that wet and dry climatic episodes have often been the trigger of disasters, but that man helped to aggravate the situation.

Less direct, but probably of more regional and even global influence, must have been the effects of the large-scale removal of the temperate forests, and more recently the destruction of tropical forests. This process began more than 2000 years ago in the Mediterranean and China, 1000 years ago in Europe and 100 years ago in North America, and proceeds with the current destruction of the equatorial rain forest by logging and slash-and-burn agriculture. In addition, large-scale drainage and reclamation works have destroyed wetlands. All these changes, together with urbanisation, must be held, at least in part, responsible for lower evaporation, accelerated discharge and increased flooding.

The main question is if, and how, these changes in soil moisture, evapotranspiration and catchment runoff regimes have caused anomalies within the regional dynamic equilibrium of the general circulation, and how these in turn have affected rainfall. What we do know is that combustion of fossil fuel, irrigation and the loss of forest have caused an increase in the global atmospheric concentrations of greenhouse gasses CO_2 and CH_4. The increase rate in methane is twice that of carbon dioxide, while methane is 20 times as effective in its greenhouse effect as CO_2. During the last century, the CO_2 concentration rose from 290 ppm to 350 ppm, whereas the CH_4 concentration from 0.95 to 1.65 ppm. The global rise in temperature of 0.3 ^{0}C during the last century may well be connected with these increased emissions.

At the same time, a rise in temperature will probably also result in a higher cloud cover. This might counterbalance the greenhouse effect by an increase in the atmospheric albedo. The same could apply for the influence of dust particles from land clearance and industrial activities. However, the physics of clouds and aerosols and their interaction with radiation is not sufficiently understood

yet to assess these effects quantitatively. In the absence of concrete data, we will briefly and qualitatively summarise the possible effects of the respective man-induced environmental changes on climatic-hydrological conditions (see Volume V for a more detailed discussion).

1.5.2.1 IRRIGATION

About 3500 km^3 of the surplus water is now used for irrigation. Most of this water evaporates and the atmospheric moisture content will increase. Wet soils lower the albedo and thus enhance net radiation. These effects together might stimulate convective rain, especially in semi-arid areas. Higher atmospheric moisture levels at the other hand might hamper the moisture influx from surrounding regions.

1.5.2.2 WETLAND DRAINAGE

Large-scale drainage of wetlands diminishes evapotranspiration. The same applies to large-scale deforestation, because trees normally use more water than grassland or agricultural crops, partly because of high interception evaporation. This means that the total runoff from these areas must have increased, whereas streamflow regimes may have developed a more seasonal character due to the loss of retention storage. Losses of atmospheric moisture associated with reduced evaporation, and higher reflection may also have resulted in lower rainfall. Eagleson (1986), citing Russian sources, suggests that 10% of the precipitation in temperate humid climates probably originates from local evaporation. Much higher values were recently suggested for the Great Plains in the USA.

1.5.2.3 GROUND COVER DAMAGE

Semi-arid areas are very susceptible to damage of ground cover. The soil will dry out and erode, rainfall will generate surface runoff instead of infiltration, evaporation will be reduced, the reflection from both the surface and atmospheric dust particles may increase and convective rainfall might therefore decrease. The change in thermal and moisture regimes is then expected to result in an anomalous atmospheric situation that will be propagated by advection to surrounding areas. This may finally influence the atmospheric circulation on a larger scale. This may lead to desiccation and desertification over extensive areas. The above mentioned processes could be initiated if plans to drain the huge swamps of the White Nile in the Sudan materialise. The surface area of these Sudd swamps is about 34 000 km^2 and can produce 25 km^3 water, which would double the White Nile's discharge. The consequences for the regional rainfall are not yet known, but preliminary circulation modelling exercises suggest that 19% of the present January evaporation returns as rain on the Sudd (Eagleson, 1986).

1.5.2.4 DEFORESTATION

Deforestation of tropical forest also results in tremendous reduction of evapotranspiration and,

ultimately, of rainfall. Whereas early simulations of large-scale conversion of, for instance, the Amazonian rain forest to pasture predicted major reductions in regional rainfall (up to 30%), more recent simulations based on improved models suggest a more limited effect. Particularly disastrous conditions are known to result from the clearing of tropical steep land forest. Sheet wash and flooding during the wet season are often followed by lack of water during the dry season, because of a loss of storage capacity in the soil due to accelerated erosion (Bruijnzeel, 1996).

1.5.2.5 INTERBASIN DIVERSION

The proposed large-scale interbasinal diversion schemes of the Russian Federation and the USA would come to large-scale interferences in water circulation. Both envisage the transfer of water from the Arctic basins to the southern semi-arid areas. Both plans are shelved for the time being for various, mainly political, reasons. One of the scientific objections against the Russian plans is the fear that a substantial reduction of the inflow of freshwater in the Arctic Ocean could result in a smaller ice cover during winter, accordingly reducing the albedo. This would have a major impact on the world's heat balance. In China huge water management projects are planned and partly under construction, aiming at the transfer of water from the Yangtze River (and perhaps the Brahmaputra) to the Hwang Ho basin in the dry northern plains around Beijing.

1.5.2.6 STREAMFLOW MANAGEMENT

Most of the human endeavours to fight the irregularity in water supply are based on the management of stream flow. An alternative is the control of the atmosphere by triggering rain through cloud seeding. Many experiments have been carried out, but their effectivity is difficult to prove and the scientific results are subject to much controversy, not to speak of the social and legal aspects. Better forecast of local convective storms with radar and satellites might increase the success of this technique in the future.

1.5.2.7 LAND USE CHANGES

Evidently, the impact of large-scale water management schemes and changes in land use must create anomalies and changes in the regional moisture and heat budgets, which -by the general circulation- may be propagated to distant regions. Evidence of this type of "tele-connection" is notably available from the ocean-continent interaction. A clear example is the influence of the surface temperature anomaly in the tropical Pacific and the occurrence of the El Nino-circulation. Understanding of these processes with their regional and seasonal variability and feedback loops, and prediction of their effects, require an improvement in resolution of the General Circulation Models (GCM). Earth observation by satellite remote sensing can be a great help to monitor the input variables, whereas the application of isotopic tracers is a useful tool in analysing flow paths of vapour and identifying recycling of moisture. Notably the question of moisture recycling is challenging, because until now climate models suggest a limited contribution of local evaporation

to rainfall (see e.g. Sect.1.5.2.4), whereas two-third of the precipitation on a continental scale originates from re-evaporated rainwater (Sect.1.4.3).

1.6 ISOTOPES IN THE HYDROLOGICAL CYCLE

The original studies on isotopes in water were concerned with seawater and precipitation. The first was primarily a survey on variations in $^{18}O/^{16}O$ concentration ratios, soon to be followed by a study of the $^{2}H/^{1}H$ ratios in natural waters (Friedman, 1953). Dansgaard (1964) observed in great detail $^{18}O/^{16}O$ variations in global precipitation, including a discussion on the meteorological patterns. His work was the start of the global "isotopes-in-precipitation" network of the international organisations WMO and IAEA. In more recent years the observations became supported by theoretical and numerical modelling.

The first study on ^{14}C in groundwater, soon in combination with $^{13}C/^{12}C$, was started by the Heidelberg group in the late 1950s (Münnich, 1957; Vogel and Ehhalt, 1963). In later years this methodology became an important tool in studying groundwater movement.

The revolutionary development of the introduction of nuclear accelerators as mass spectrometers has greatly stimulated the hydrological application of isotopes with extreme low abundances in nature. Also ^{14}C research has gained tremendously by this new technological approach.

The first sections in this chapter have presented a broad picture of the global water cycle, consisting of the origins of water, the sizes of the global water reservoirs and the fluxes between them. However, in our day-to-day life, where we are dealing with stream-flow management, drinking-water supply, the propagation of the effects of surface pollution underground, et cetera, we are no less confronted with regional water bodies, streams, lakes, aquifers, their sizes and their fluxes. It will be shown that the application of isotopes as they occur in nature are an invaluable help in studying the behaviour of water and finding solutions for water problems. The remainder of this volume and the other volumes of the series are devoted to this.

The nature of the isotopic applications is of course dictated by the specific character of isotopes, radioactive and non-radioactive. We can distinguish three different types of applications.

1) Stable and radioactive isotopes can be used as *tracers*, marking a water body or a certain quantity of water; a nice example is the phenomenon that the rain water during a heavy storm is often depleted in the heavy isotope (stable ^{2}H, deuterium, or stable ^{18}O) with respect to the most abundant isotope (^{1}H and ^{16}O, respectively). This offers the possibility to follow the rain water in the surface runoff and even quantitatively analysing the runoff hydrograph.

2) During the transition of compounds such as water or carbon dioxide from one phase to another, the concentration ratio of the isotopes of an element often changes, undergoes so-called *isotope fractionation*. Conversely, observing differences in especially the stable isotopic concentration ratios informs us about certain geochemical or hydrological processes that took place. For instance, as a result of a series of processes, the isotopic composition of carbon as

well as oxygen of calcium carbonate is different for the marine and the freshwater origin. Furthermore, the isotopic composition of oxygen and hydrogen in rainwater varies with latitude, altitude, climate and time of the year.

3) *Radioactive decay* offers the possibility to determine an age, provided certain conditions are met. Noteworthy in this respect is the frequent application of dating groundwater –i.e. determining the time elapsed since the infiltration of the water- by comparing the ^{14}C or ^{3}H (tritium) activities in a groundwater sample with that of the recharge water. Moreover, also concentration differences of radioactive isotopes can also be used as a tracer.

The following chapters serve to present and explain the fundamental background of the abundance and behaviour of isotopes in nature, as well as some practical information on sample handling and analysis. The mentioning of examples will be brief; the other volumes of this series are dealing with the various compartments of the water cycle, treating the role of isotopic applications in detail.

Besides the occurrence of natural isotopes in our environment, man is able to produce radioactive isotopes. Also these can be applied as tracers, to follow water movement or reservoir leakage. The methods of applying *artificial tracers* are parallel to the use of chemical tracers, often recognisable by their fluorescent character. This methodology will not be the main subject of these volumes, despite the many successful applications. We will restrict ourselves to the isotopes found in our environment by nature. Only at few occasions we can not avoid mentioning the artificial isotopes.

2 ATOMIC SYSTEMATICS AND NUCLEAR STRUCTURE

In this chapter the principles and systematics of atomic and nuclear physics are summarised briefly, in order to introduce the existence and characteristics of isotopes.

2.1 ATOMIC STRUCTURE AND THE PERIODIC TABLE OF THE ELEMENTS

Atoms consist of a nucleus surrounded by electrons. Compared to the diameter of an atom, which is of the order of 10^{-8} cm, the size of the nucleus is extremely small ($\sim 10^{-12}$ cm). The dense concentration of matter of the nucleus mainly consists of two kinds of particles, neutrons and protons, which have about the same mass. The neutron carries no electric charge, while the proton is positively charged. The number of protons (Z), the *atomic number*, is equal to the number of electrons surrounding the nucleus. Electrons have a mass that is about 1/1800 that of the proton mass and carry an equal but negative electrical charge, so that the atom as a whole is neutral. Atoms missing one or more electrons are referred to as positive ions, atoms with a number of electrons exceeding the atomic number are called negative ions.

Protons and neutrons, the building stones of the nucleus, are called *nucleons*. The sum of the number of protons and neutrons (N) in a nucleus is the nuclear *mass number*:

$$A = Z + N \tag{2.1}$$

The notation describing a specific nucleus (= *nuclide*) of element X is:

$${}^{A}_{Z}X_{N}$$

Because the chemical properties of an element (X) are primarily determined by the number of electrons in the atom, the atomic number Z characterises the element. Therefore, writing ${}^{A}X$ alone defines the nuclide. The cloud of electrons circulating around the nucleus is well structured and consists of shells, each containing a maximum number of electrons. The chemical properties of an atom are now mainly determined by the number of electrons in the outer, incompletely filled electron shell. Because of this systematic, all atoms can be arranged in a *Periodic Table of the Elements* (part shown by Fig. 2.1).

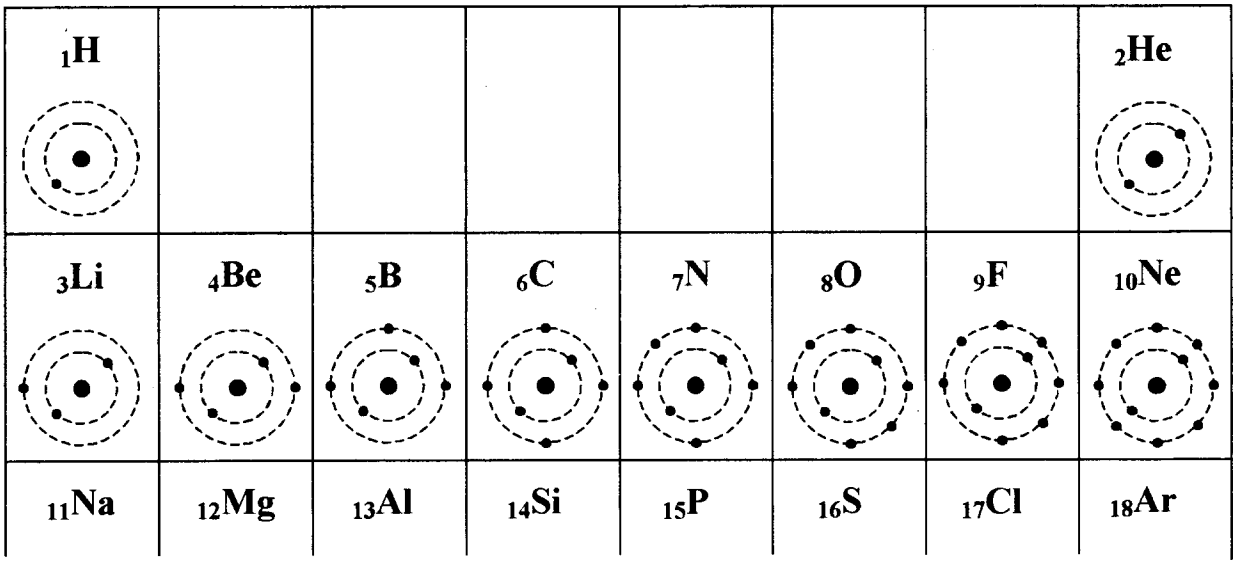

Fig. 2.1 Part of the periodic table of the elements, containing the light elements. Also shown are the electronic configurations of the respective atoms.

2.2 STRUCTURE OF THE ATOMIC NUCLEUS

The atomic nuclei are kept together by extremely strong forces between the nucleons (protons and neutrons) with a very small range. As repulsive electrical (Coulomb) forces exist between the protons, the presence of neutrons is required to stabilise the nucleus. In the most abundant nuclides of the *light elements*, the numbers of protons and neutrons are equal. Nuclei such as

$$^{2}_{1}H_{1} \qquad ^{4}_{2}He_{2} \qquad ^{12}_{6}C_{6} \qquad ^{14}_{7}N_{7} \qquad ^{16}_{8}O_{8}$$

are stable, as is the single proton (^{1}H = hydrogen). For the heavy elements the number of neutrons far exceeds the number of protons: ^{238}U contains only 92 protons, whereas the largest stable nuclide, the lead isotope ^{208}Pb has an atomic number of 82.

Instabilities are caused by an excess of protons or neutrons. Examples of such unstable or radioactive nuclei are

$$^{3}_{1}H_{2} \quad \text{and} \quad ^{14}_{6}C_{8}$$

For the light elements, a slight excess of neutrons does not necessarily result in unstable nuclei:

$$^{13}_{6}C_{7} \;,\; ^{15}_{7}N_{8} \;,\; ^{17}_{8}O_{9} \;,\; ^{18}_{8}O_{10}$$

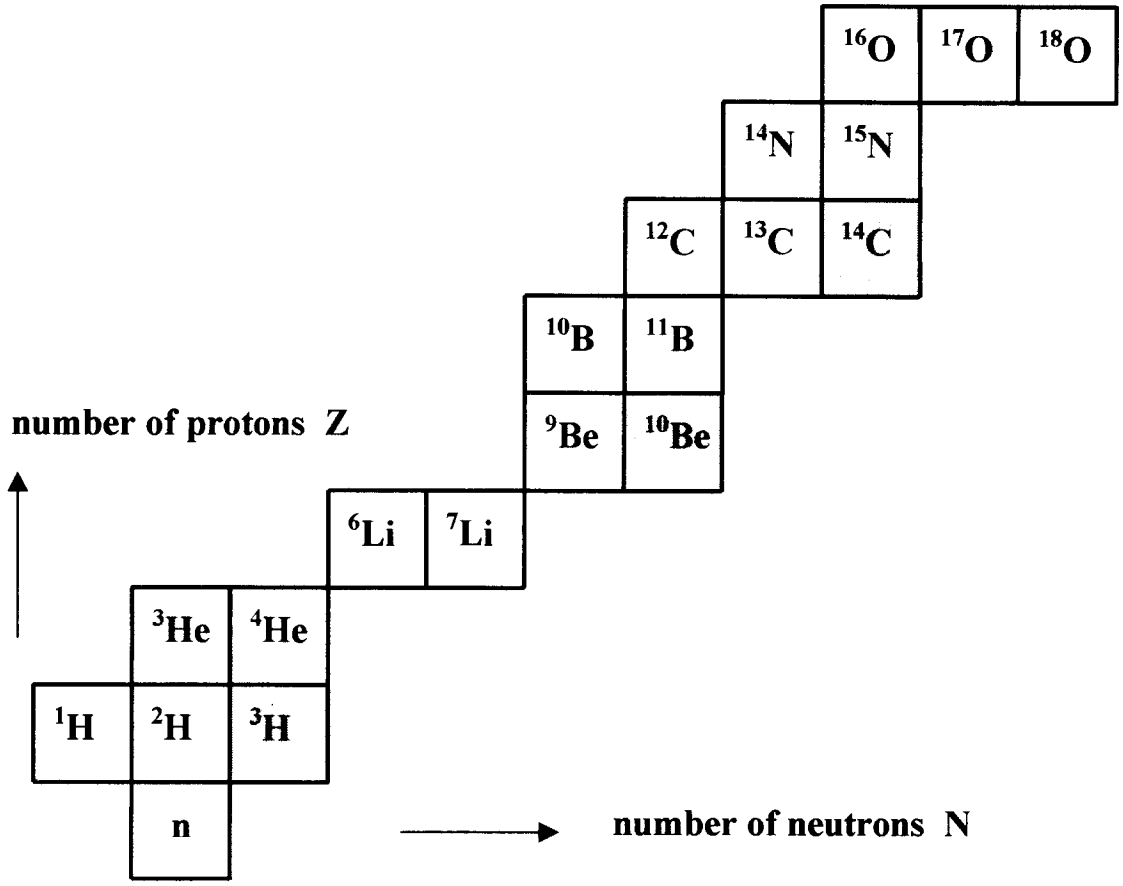

Fig. 2.2 Part of the chart of nuclides, containing the light elements. The isotopes of an element (equal Z) are found in a horizontal row, isobars (equal A) along diagonal lines, isotones (equal N) in vertical columns. The natural radioactive isotopes of H, Be, and C are marked grey.

are stable. For these "asymmetric" nuclei (Z≠N) however, the probability of formation during the "creation" of the elements, -nucleosynthesis-, was smaller, resulting in smaller natural concentrations for these nuclides.

The naturally occurring stable and radioactive isotopes of the light elements are shown in a part of the *Chart of Nuclides* (Fig. 2.2). Another part, showing some heavy nuclides is given by Fig.11.2. Note that in the higher A range N and Z are no longer about equal (^{238}U with Z=92 and N=146).

2.3 STABLE AND RADIOACTIVE ISOTOPES

The atomic nuclei of an element containing different numbers of neutrons are called *isotopes* (ισο τοπος = at the same place in the periodic table of the elements). Many elements have two or more stable, naturally occurring isotopes. In general, nuclei with even numbers of protons

or/and neutrons are more stable. Nuclei of which the number of protons or/and neutrons corresponds to some specific even number, belonging to the series of so-called *magic numbers* 2, 8, 20, 28, 50, 82, and 126, have a relatively high stability and consequently large natural occurrence.

These magic numbers can be explained by a nuclear shell model with *closed nucleon shells* within the nucleus, similar to the closed electron shells in atoms, the basis of the periodicity in the periodic table of the elements. An example of the occurrence of the magic numbers is the large number of stable isotopes of lead: the largest stable nuclide, ^{208}Pb (with Z = 82 and N = 126) is double magic. Especially the uneven-uneven nuclei are unstable and have a small chance of natural occurrence. Most uneven-Z elements have only one or at most two stable isotopes.

The earlier statement that the chemical properties of an element only depend on the atomic number, implying that the chemical properties of isotopes are equal, needs revision if we look in detail. The fact is that in nature variable relative concentrations of isotopes are observed. There are two causes for this phenomenon:

1) the chemical and some physical properties of the isotopes of one element are not exactly equal, resulting in slightly different chemical and physical properties -and consequently different concentrations- of isotopic molecules, i.e. molecules that contain different isotopes of that element

2) if the isotopes concerned are radioactive, the process of radioactive decay causes the concentration of the isotopic molecules concerned to diminish in time; this may result in concentration differences that are much larger than as caused by the isotope processes as mentioned under 1).

These phenomena will be discussed separately in the next chapters.

2.4 MASS AND ENERGY

It is inconvenient to use the real mass of atoms and molecules. Instead we define the *atomic mass* as the mass expressed in atomic mass units (amu). Originally this was equivalent to the mass of a proton; later for practical reasons, the atomic mass unit has rather become defined as 1/12 times the mass of a ^{12}C atom:

$$1 \text{ amu} = 1.6605655 \times 10^{-27} \text{ kg} \qquad \textbf{(2.2)}$$

In chemistry it is now convenient to use the *mole* quantity, defined as the number of grams of the element equal to the atomic weight. The number of atoms in one mole of the element or the number of molecules in one mole of a chemical compound is then equal for any substance and given by Avogadro's number = 6.02252×10^{23}.

If we now add up the atomic masses of the building stones of a certain nucleus X, for instance of ^{12}C consisting of 6 protons and 6 neutrons, it appears that the atomic mass of X is smaller than the sum of the 12 constituent particles:

6 protons	= 6 x 1.007825 amu	= 6.04695 amu
6 neutrons	= 6 x 1.008665 amu	= 6.05199 amu
	total mass	= 12.09894 amu
compared to	A of ^{12}C	= 12.00000 amu (by definition)
	difference	= 0.09894 amu

This so-called *mass defect* has been converted into the *binding energy*, the potential energy "stored" in the nucleus to keep the particles together. This equivalence of mass and energy is defined by Einstein's special theory of relativity as

$$E_B = Mc^2 \qquad \textbf{(2.3)}$$

where E_B is the binding energy, M is the mass, and c is the velocity of light (2.997925 x 10^8 m/s).

According to this definition the equivalence between mass and energy is expressed as

$$1 \text{ amu} \equiv 931.5 \text{ MeV (million electronvolt)} \qquad \textbf{(2.4)}$$

where 1 eV = 1.602189 x 10^{-19} J (electrical charge unit = electron charge = 1.602189×10^{-19}C).

All energies in nuclear physics, such as the particle energies after nuclear decay, are presented in MeV or keV (kilo or 10^3 electronvolt). In our case of ^{12}C the binding energy turns out to be 0.09894 amu × 931.5 MeV/amu = 92.16 MeV or 7.68 MeV per nucleon.

3 ABUNDANCE AND FRACTIONATION OF STABLE ISOTOPES

In classical chemistry isotopes of an element are regarded as having equal chemical properties. In reality variations in isotopic abundances occur far exceeding measuring precision. This phenomenon is the subject of this section.

3.1 ISOTOPE RATIOS AND CONCENTRATIONS

Before we can give a more quantitative description of *isotope effects*, we must define isotope abundances more carefully. *Isotope (abundance) ratios* are defined by the expression

$$R = \frac{\text{abundance of rare isotope}}{\text{abundance of abundant isotope}} \qquad \textbf{(3.1)}$$

The ratio carries a superscript before the ratio symbol R, which refers to the isotope under consideration. For instance:

$$^{13}R(CO_2) = \frac{[^{13}CO_2]}{[^{12}CO_2]} \qquad ^{18}R(CO_2) = \frac{[C^{18}O^{16}O]}{[C^{16}O_2]} \qquad \textbf{(3.2)}$$

$$^{2}R(H_2O) = \frac{[^{2}H^{1}HO]}{[^{1}H_2O]} \qquad ^{18}R(H_2O) = \frac{[H_2{}^{18}O]}{[H_2{}^{16}O)}$$

We should clearly distinguish between an *isotope ratio* and an *isotope concentration*. For CO_2 for instance, the latter is defined by:

$$\frac{[^{13}CO_2]}{[^{13}CO_2]+[^{12}CO_2]} = \frac{[^{13}CO_2]}{[CO_2]} = \frac{^{13}R}{1+^{13}R} \qquad \textbf{(3.3a)}$$

Especially if the rare isotope concentration is very large, as in the case of labeled compounds, the rare isotope concentration is often given in *atom %*. This is then related to the isotope ratio by:

$$R = (\text{atom \%}/100) / [1 - (\text{atom \%}/100)] \qquad \textbf{(3.3b)}$$

3.2 ISOTOPE FRACTIONATION

According to classical chemistry, the chemical characteristics of isotopes, or rather of molecules that contain different isotopes of the same element (such as $^{13}CO_2$ and $^{12}CO_2$) are

equal. To a large extent this is true. However, if a measurement is sufficiently accurate -and this is the case with the modern mass spectrometers (Chapter 11)- we observe tiny differences in chemical as well as physical behaviour of so-called *isotopic molecules* or *isotopic compounds*. The phenomenon that these isotopic differences exist is called *isotope fractionation*. (Some authors refer to this phenomenon as *isotope discrimination*; however, we see no reason to deviate from the original expression). This can occur as a change in isotopic composition by the transition of a compound from one state to another (liquid water to water vapour) or into another compound (carbon dioxide into plant organic carbon), or it can manifest itself as a difference in isotopic composition between two compounds in chemical equilibrium (dissolved bicarbonate and carbon dioxide) or in physical equilibrium (liquid water and water vapour). Throughout this volume examples of all these phenomena will be discussed.

The differences in physical and chemical properties of isotopic compounds (i.e. chemical compounds consisting of molecules containing different isotopes of the same element) are brought about by mass differences of the atomic nuclei. The consequences of these mass differences are two-fold:

1) The heavier isotopic molecules have a lower mobility. The kinetic energy of a molecule is solely determined by temperature: $kT = \frac{1}{2}mv^2$ (k = Boltzmann constant, T = absolute temperature, m= molecular mass, v = average molecular velocity). Therefore, molecules have the same $\frac{1}{2}mv^2$, regardless of their isotope content. This means that the molecules with larger m necessarily have a smaller v. Some practical consequences are:

a) heavier molecules have a lower diffusion velocity;

b) the collision frequency with other molecules - the primary condition for chemical reaction - is smaller for heavier molecules; this is one of the reasons why, as a rule, lighter molecules react faster.

2) The heavier molecules generally have higher binding energies. The chemical bond between two molecules (in a liquid or a crystal for instance, or between two atoms in a molecule) can be represented by the following simple model. Two particles exhibit competing forces on each other. The one force is repulsive and rapidly increases with decreasing distance ($\sim 1/r^{13}$). The other is attractive and increases less rapidly with decreasing distance (in ionic crystals ($\sim 1/r^2$, between uncharged particles $\sim 1/r^7$). As a result of these forces the two particles will be located at a certain distance from each other. In Fig.3.1 the potential energies corresponding to each force and to the resulting net force are drawn schematically. If one particle is located at the origin of the co-ordinate system, the other will be in the *energy well*. Escape from the well is possible only, if it obtains sufficient kinetic energy to overcome the net attractive force. This energy is called the *binding energy* of the particle. A simple example is the heat of evaporation.

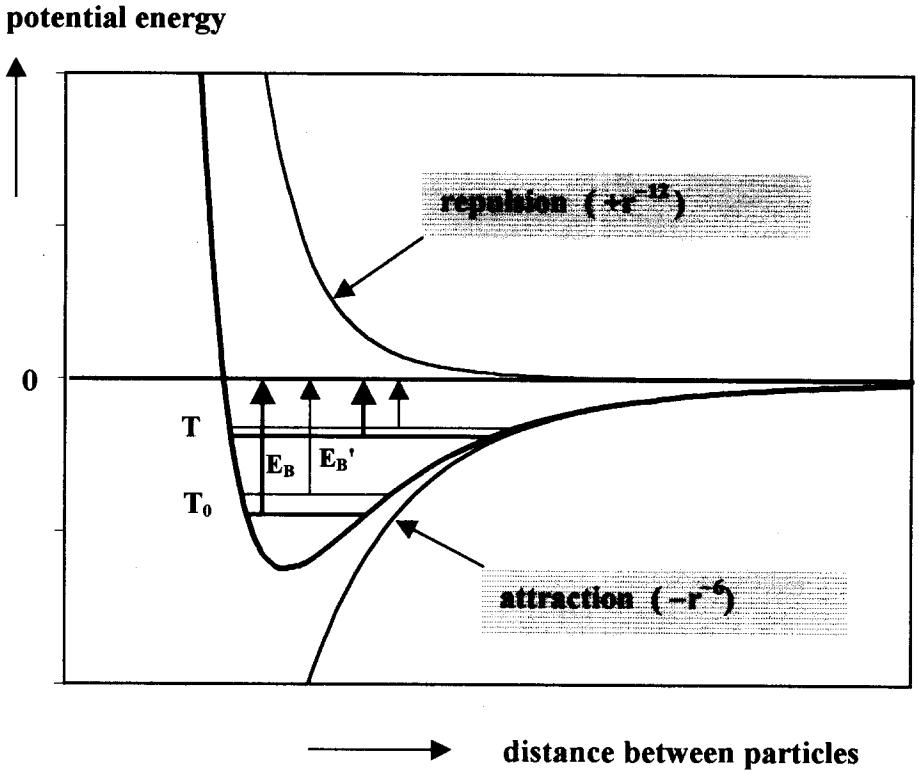

Fig.3.1 Schematic representation of the potential energy distribution caused by the repulsive and attractive forces between two particles, in this case between oppositely charged ions. The resulting potential is well-shaped (solid line). The one particle is situated at the origin (r = 0). The second particle is situated in the well. The small horizontal lines in the well are the energy levels of the system, the thin and heavy lines referring to the light and the heavy isotopic particle, respectively. The arrows indicate the respective binding energies at the zero temperature T_0 and a higher temperature T, respectively. At higher temperatures the difference between the binding energies for the isotopic particles is smaller, resulting in a smaller isotope effect.

Although the particle is in the energy well, it is not at the bottom of the well, even at the zero point of the absolute temperature scale (-273.15°C). All particles have three modes of motion: translation, i.e. displacement of the molecule as a whole, vibrations of the atoms in the molecule with respect to each other, and rotations of the molecule around certain molecular axes. In the energy well representation: the particle is not at the bottom of the well, but at a certain (energy) level above the zero energy. In Fig. 3.1 an energy level is indicated by a horizontal line. The higher the temperature of the substance, the higher energy level will be occupied by the particle.

The energy required to leave the well - i.e. to become separated from the other particle - is indicated as the binding energy E_B, whereas E_B' is the binding energy for the rare (heavy) particle. The energy of a certain particle at a certain temperature depends on its mass. The

heavier isotopic particle is situated deeper in the energy well than the lighter (heavy line in Fig.3.1) and, therefore, escapes less easily: the heavier isotopic particle (atom or molecule) generally has a higher binding energy: $E_B' > E_B$ (Fig.3.2: normal case).

Examples of this phenomenon are:

1) $^1H_2{}^{18}O$ and $^1H^2H^{16}O$ have lower vapour pressures than $^1H_2{}^{16}O$; they also evaporate less easily and

2) in most chemical reactions the light isotopic species reacts faster than the heavy. For example $Ca^{12}CO_3$ dissolves faster in an acid solution than does $Ca^{13}CO_3$.

In an isotope equilibrium between two chemical compounds the heavy isotope is generally concentrated in the compound which has the largest molecular weight.

The depth of the energy well may also depend on the particle masses in a more complicated manner. Under certain conditions with poly-atomic molecules the potential energy well is deeper for the light than for the heavy isotopic molecule. Due principally to this phenomenon the binding energy of the heavy molecule can be smaller. Because the isotope effects discussed above generally result in lower vapour pressure for the isotopically heavy species (*normal isotope effect*), this effect is referred to as the *inverse isotope effect* (Fig.3.2). Practical examples of the inverse isotope effect are the higher vapour pressure of $^{13}CO_2$ in the liquid phase as well as the lower solubility of $^{13}CO_2$ in water than of $^{12}CO_2$, both at room temperature (Vogel et al., 1970).

At high temperatures the differences between binding energies of isotopic molecules becomes smaller, resulting in smaller -an ultimately disappearing- isotope effects (Fig.3.1).

3.3 KINETIC AND EQUILIBRIUM ISOTOPE FRACTIONATION

The process of isotope fractionation is mathematically described by comparing the isotope ratios of the two compounds in chemical equilibrium (A $\Leftrightarrow$ B) or of the compounds before and after a physical or chemical transition process (A $\rightarrow$ B). The *isotope fractionation factor* is then defined as the ratio of the two isotope ratios:

$$\alpha_A(B) = \alpha_{B/A} = \frac{R(B)}{R(A)} = \frac{R_B}{R_A} \qquad \textbf{(3.4)}$$

which expresses the isotope ratio in the phase or compound B relative to that in A.

If we are dealing with changes in isotopic composition, for instance C is oxidised to CO_2, the carbon isotope fractionation refers the "new" $^{13}R(CO_2)$ value to the "old" $^{13}R(C)$, in other words $^{13}\alpha = {}^{13}R(CO_2)/{}^{13}R(C)$.

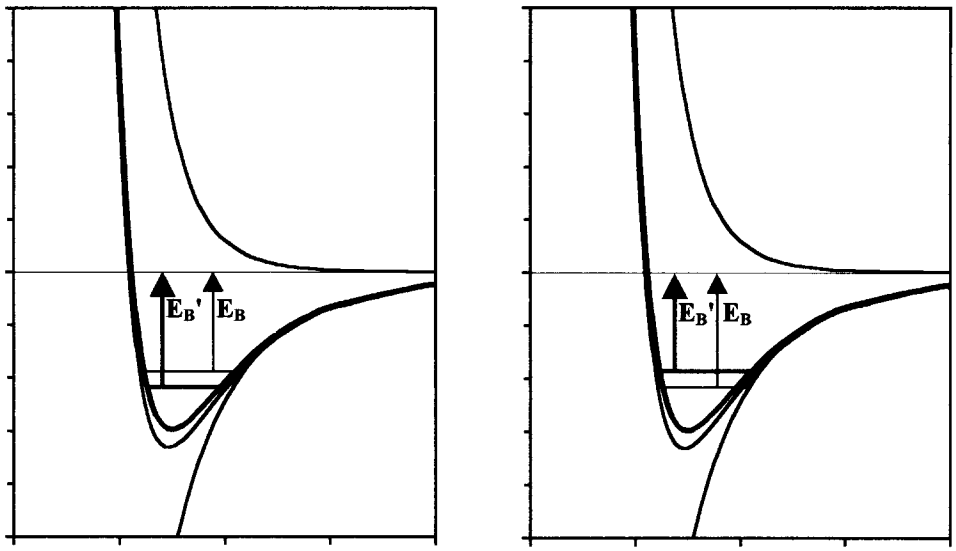

Fig.3.2 Schematic representation of the normal (left) and the inverse (right) isotope effect. For some interactions the potential energy well for the heavy particle (heavy line) is less deep than for the light particle (thin line). Depending on the specific interaction the binding energy for the isotopically heavy particle can be larger (left-hand side: normal effect) or smaller (right-hand side: inverse effect) than for the light particle.

In general isotope effects are small: $\alpha \approx 1$. Therefore, the deviation of α from 1 is widely used rather than the *fractionation factor*. This quantity, to which we refer as the *fractionation*, is defined by:

$$\varepsilon_{B/A} = \alpha_{B/A} - 1 = \frac{R_B}{R_A} - 1 \quad (\times 10^3\ ‰) \tag{3.5}$$

ε represents the *enrichment* ($\varepsilon > 0$) or the *depletion* ($\varepsilon < 0$) of the rare isotope in B with respect to A. The symbols $\alpha_{B/A}$ and $\varepsilon_{B/A}$ are equivalent to $\alpha_A(B)$ and $\varepsilon_A(B)$. In the one-way process ($A \rightarrow B$) ε is the change in isotopic composition, in other words: the new isotopic composition compared to the old.

Because ε is a small number, it is generally given in ‰ (per mill, equivalent to 10^{-3}). Note that *we do not define ε in ‰*, as many authors claim they do. (In fact they do not, as they always add the ‰ symbol). An ε value of, for instance, 5‰ is equal to 0.005. The consequence is that *in mathematical equations it is incorrect to use $\varepsilon/10^3$ instead of merely ε.* The student is to be reminded that ε is a small number; in equations one may numerically write, for instance, " −25‰ " instead of " $-25/10^3$ ".

Again, the fractionation of B with respect to A is denoted by $\varepsilon_{B/A}$ or $\varepsilon_A(B)$. From the definition of ε we simply derive:

$$\varepsilon_{B/A} = \frac{-\varepsilon_{A/B}}{1+\varepsilon_{A/B}} \approx -\varepsilon_{A/B} \qquad \textbf{(3.6)}$$

the last step because in natural processes the ε values are small.

It is important to distinguish between two kinds of isotope fractionation: kinetic fractionation and equilibrium fractionation. *Kinetic fractionation* results from *irreversible* i.e. *one-way* physical or chemical processes. Examples include the evaporation of water with immediate withdrawal of the vapour from further contact with the water; the absorption and diffusion of gases, and such irreversible chemical reactions as the bacterial decay of plants or rapid calcite precipitation. These fractionation effects are primarily determined by the binding energies of the original compounds (Sect.3.2) in that during physical processes isotopically lighter molecules have higher velocities and smaller binding energies; in chemical processes light molecules react more rapidly than the heavy. In some cases, however, the opposite is true. This *inverse kinetic isotope effect* occurs most commonly in reactions involving hydrogen atoms (Bigeleisen and Wolfsberg, 1958).

The second type of fractionation is *equilibrium* (or *thermodynamic*) *fractionation*. This is essentially the isotope effect involved in a (thermodynamic) equilibrium reaction. As a formal example we choose the isotope exchange reaction:

$$*A + B \Leftrightarrow A + *B \qquad \textbf{(3.7)}$$

where the asterisk points to the presence of the rare isotope. The fractionation factor for this equilibrium between phases or compounds A and B is the equilibrium constant for the exchange reaction of Eq.3.7:

$$K = \frac{[A]}{[*A]}\frac{[*B]}{[B]} = \frac{[*B]/[B]}{[*A]/[A]} = \frac{R_B}{R_A} = \alpha_{B/A} \qquad \textbf{(3.8)}$$

If sufficient information about the binding energies of atoms and molecules is available, the fractionation effect can be calculated, the kinetic effect (Bigeleisen, 1952) as well as the equilibrium effect (Urey, 1947). In practice, however, these data are often not known in sufficient detail. With kinetic isotope effects we are confronted with an additional difficulty which arises from the fact that natural processes are often not purely kinetic or irreversible. Moreover, kinetic fractionation is difficult to measure in the laboratory, because (i) complete irreversibility can not be guaranteed (part of the water vapour will return to the liquid), nor can the degree of irreversibility be quantified; (ii) the vanishing phase or compound will have a non-homogeneous and often immeasurable isotopic composition, because the isotope effect occurs at the surface of the compound. For example the surface layer of an evaporating water

mass may become enriched in ^{18}O and ^{2}H if the mixing within the water mass is not rapid enough to keep its content homogeneous throughout.

Isotope fractionation processes in nature which are not purely kinetic (i.e. one-way processes) will be referred to as *non-equilibrium fractionations*. An example is the evaporation of ocean or fresh surface water bodies: the evaporation is not a one-way process (certainly water vapour condenses), neither an equilibrium process as there is a net evaporation.

Equilibrium fractionation, on the other hand, can be determined by laboratory experiments and in several cases reasonable agreement has been shown between experimental data and thermodynamic calculations.

The general condition for the establishment of isotopic equilibrium between two compounds is the existence of an isotope exchange mechanism. This can be a reversible chemical equilibrium such as:

$$H_2{}^{16}O + C^{18}O^{16}O \Leftrightarrow H_2C^{18}O^{16}O \Leftrightarrow H_2{}^{18}O + C^{16}O \qquad \textbf{(3.9a)}$$

or such a reversible physical process as evaporation/condensation:

$$H_2{}^{16}O(\text{vapour}) + H_2{}^{18}O(\text{liquid}) \Leftrightarrow H_2{}^{18}O(\text{vapour}) + H_2{}^{16}O(\text{liquid}) \qquad \textbf{(3.9b)}$$

The reaction rates of exchange processes and, consequently, the periods of time required to reach isotopic equilibrium, vary greatly. For instance, the exchange of $H_2O \Leftrightarrow CO_2$ proceeds on a scale of minutes to hours at room temperature, while that of $H_2O \Leftrightarrow SO^{2-}$ requires millennia.

The fractionation resulting from kinetic isotope effects generally exceeds that from equilibrium processes. Moreover, in a kinetic process the compound formed may be depleted in the rare isotope while it is enriched in the equivalent equilibrium process. This can be understood by comparing the fractionation factor in a reversible equilibrium with the kinetic fractionation factors involved in the two opposed single reactions. As an example we take the carbonic acid equilibrium of Eq.3.9a:

$$CO_2 + H_2O \Leftrightarrow H^+ + HCO_3^-$$

For the single reactions

$$^{12}CO_2 + H_2O \rightarrow H^+ + H^{12}CO_3^-$$

and

$$^{13}CO_2 + H_2O \rightarrow H^+ + H^{13}CO_3^-$$

the reaction rates are, respectively:

$$^{12}r = {}^{12}k[{}^{12}CO_2] \qquad \text{and} \qquad {}^{13}r = {}^{13}k[{}^{13}CO_2] \tag{3.10}$$

where ^{12}k and ^{13}k are the reaction rate constants. The isotope ratio of the bicarbonate formed (ΔHCO_3^-) is:

$$^{13}R(\Delta HCO_3) = \frac{^{13}r}{^{12}r} = \frac{^{13}k[^{13}CO_2]}{^{12}k[^{12}CO_2]} = \alpha_k\, ^{13}R(CO_2) \tag{3.11}$$

where α_k is the kinetic fractionation factor for this reaction. Conversely, for:

$$H^+ + H^{12}CO_3^- \rightarrow {}^{12}CO_2 + H_2O$$

and

$$H^+ + H^{13}CO_3^- \rightarrow {}^{13}CO_2 + H_2O$$

the reaction rates are

$$^{12}r' = {}^{12}k'[H^{12}CO_3^-] \qquad \text{and} \qquad {}^{13}r' = {}^{13}k'[H^{13}CO_3^-] \tag{3.12}$$

The carbon dioxide formed (ΔCO_2) has an isotope ratio

$$^{13}R(\Delta CO_2) = \frac{^{13}r'}{^{12}r'} = \frac{^{13}k'[H^{13}CO_3^-]}{^{12}k'[H^{12}CO_3^-]} = \alpha_k'\, ^{13}R(HCO_3^-) \tag{3.13}$$

At isotopic equilibrium the isotope effects balance, in other words:

$$^{13}R(\Delta HCO_3^-) = {}^{13}R(\Delta CO_2) \tag{3.14}$$

so that combining Eqs.3.11 and 3.13 results in:

$$\frac{\alpha_k'}{\alpha_k} = \frac{^{13}R(CO_2)}{^{13}R(HCO_3^-)} = \frac{[^{13}CO_2][H^{12}CO_3^-]}{[^{12}CO_2][H^{13}CO_3^-]} = \alpha_e \tag{3.15}$$

which shows that the isotopic equilibrium fractionation α_e is equivalent to the equilibrium constant of the isotope exchange reaction:

$$H^{13}CO_3^- + {}^{12}CO_2 \Leftrightarrow H^{12}CO_3 + {}^{13}CO_2 \tag{3.16}$$

Most α_k and α_k' values are less than 1 by more than one per cent. Differences between their ratios are less - in the order of several per mill. Later we will see that rapid evaporation of water might cause the water vapour to be about twice as depleted in ^{18}O as the vapour in equilibrium with the water. The reason for this is, that $H_2{}^{16}O$ is favoured also in the condensation process.

From Eq.3.15 it is obvious that, while α_k for a certain phase transition is smaller than 1, α_e might be larger than 1. An example is to be found in the system: dissolved/gaseous CO_2: the ^{13}C content of CO_2 rapidly withdrawn from an aqueous CO_2 solution is smaller than that of the dissolved CO_2 (i.e. ^{12}C moves faster: $\alpha_k<1$), while under equilibrium conditions the gaseous CO_2 contains relatively more ^{13}C ($\alpha_e>1$; inverse isotope effect, Sect.3.2).

3.4 THEORETICAL BACKGROUND OF EQUILIBRIUM FRACTIONATION

In this section we will present a discussion of the origin of isotope effects, in particular the mass-dependent isotope fractionation, based on some principles from thermodynamics and statistical mechanics. The treatment here will not be exhaustive and so, for full details, the reader is referred to textbooks on these subjects. A basic discussion has been given by Broecker and Oversby (1971) and Richet et al. (1977).

A basic principle of quantum physics is that the energy of the particle can take only certain discrete values. This is true for any kind of motion. These discrete energy values were already mentioned in Sect.3.2, where we discussed the position of a particle at a certain time at a certain level in the energy well (Figs.3.1 and 3.2).

A basic principle of statistical mechanics states that the chance that a particle is at a certain energy level ε_r is:

$$p_r = \frac{e^{-\varepsilon_r / kT}}{q}$$

where k is the Boltzmann constant and T the absolute temperature of the compound. The value of q, the *partition function*, is determined by the requirement that the sum of all chances equals unity:

$$\sum_{r=0}^{\infty} p_r = 1$$

so that:

$$q = \sum_{r=0}^{\infty} e^{-\varepsilon_r / kT} \qquad \textbf{(3.17)}$$

The partition function is thus the summing up of the population of all energy levels of a certain system and so determines the *energy state* of the system. It is an important quantity, because thermodynamic considerations show that equilibrium conditions can be expressed as a ratio of partition functions.

Consider again the isotope exchange reaction of Eq.3.7:

$$*A + B \Leftrightarrow A + *B$$

where A and B denote two different compounds (for instance, CO_2 and HCO_3^-) or two phases of the same compound (for instance, liquid H_2O and water vapour), and the asterisk refers to the presence of a rare isotope in the molecule (^{13}C, ^{18}O, ^{2}H, etc.). In the definition of the fractionation factor -i.e. the equilibrium constant- the concentration or rather the activities are now represented by the partition functions:

$$\alpha_A(B) = K = \frac{q_A \, {}^*q_B}{{}^*q_A \, q_B} = \frac{{}^*q_B / q_B}{{}^*q_A / q_A} \qquad \textbf{(3.18)}$$

We must now evaluate the various partition functions.

In Sect.3.2 the three modes of motion were mentioned, *translation, rotation* and *vibration.* The total partition function of a system of one compound or one phase is related to the partition functions of the different motions by:

$$q = q_{trans} q_{rot} q_{vibr} \qquad \textbf{(3.19)}$$

Each partition function results from intramolecular (internal) motions, such as vibrations of atoms with respect to each other, and rotations of the molecule around molecular axes, and intermolecular (external) motions, such as vibrations and rotations of molecules with respect to each other, in a crystal lattice, for instance. Most systems are too complicated to allow an exact calculation of the partition functions. The only simple systems are ideal mono-atomic or di-atomic gases. The translations are not hindered by neighbouring atoms or molecules and intermolecular vibrations and rotations do not exist, so that only the internal components of the partition functions have to be calculated. In order to point out the mass dependence of fractionation factors and to illustrate the influence of temperature on fractionation, we will briefly mention the various partition functions.

Translation of a molecule as a whole has the partition function:

$$q_{trans} = \left[\frac{2\pi mkT}{h^2}\right]^{3/2} V \qquad \textbf{(3.20)}$$

(V = volume in which the molecules are free to move, m is the mass of the molecule, h Planck's constant). In a gas the translational contribution to the partition function ratio then is (M = molar weight):

$$\left(\frac{{}^*q}{q}\right)_{trans} = \left(\frac{{}^*m}{m}\right)^{3/2} = \left(\frac{{}^*M}{M}\right)^{3/2} \qquad \textbf{(3.21)}$$

which is temperature independent.

The partition function for internal rotational motion of a diatomic molecule is:

$$q_{rot} = \frac{8\pi^2 \mu r_0^{\,2} kT}{sh^2} \qquad \textbf{(3.22)}$$

where r_o is the equilibrium distance between the two atoms and μ is the reduced mass of the molecule = $m_1m_2/(m_1 + m_2)$; the energy of rotation is equal to that of a system where μ rotates around the centre of mass instead of m_1 and m_2 around each other. We should further remember that μr_0^2 is the moment of inertia of a rotating mass, and that s = 1, unless the molecule consists of two equal atoms in which case s = 2. In a gas the rotational contribution to the partition function ratio thus is:

$$\left(\frac{{}^*q}{q}\right)_{rot} = \frac{{}^*\mu}{\mu} = \frac{{}^*m_1}{m_1}\frac{M}{{}^*M}\frac{s}{{}^*s} \qquad \textbf{(3.23)}$$

where ${}^*m_1$ is the rare isotope of atom m_1. This ratio also is independent of temperature.

The vibrational partition function is:

$$q_{vibr} = \frac{e^{-h\nu/2kT}}{1 - e^{h\nu/kT}} \qquad \textbf{(3.24)}$$

where ν is the frequency of vibration of the two atoms with respect to each other. The frequency is generally known from experimental spectroscopic data. The temperature dependence of the fractionation effect can be shown to be caused primarily by the temperature dependence of the vibration.

The mass dependence of the vibration frequency of the harmonic oscillator is given by:

$$\nu = \frac{1}{2\pi}\left(\frac{k'}{\mu}\right)^{1/2} \qquad \textbf{(3.25)}$$

where again μ is the reduced mass of the molecule and k' is the force constant. In a first order approximation k' is not altered by an isotope substitution in the molecule, and so:

$$\frac{{}^*\nu}{\nu} = \left(\frac{\mu}{{}^*\mu}\right)^{1/2} \tag{3.26}$$

At normal temperatures (T < hν/k) the exponential function in the denominator in Eq.3.24 can be neglected. The partition function ratio then is:

$$\left(\frac{{}^*q}{q}\right)_{vibr} = e^{h(\nu-{}^*\nu)/2kT} \tag{3.27}$$

or, inserting Eq.3.26:

$$\left(\frac{{}^*q}{q}\right)_{vibr} = \exp\left[\frac{h\nu}{2kT}\left(1-\sqrt{\frac{\mu}{{}^*\mu}}\right)\right] \tag{3.28}$$

where $\mu = m_1 m_2(m_1 + m_2)$.

The partition function ratio of a di-atomic gas at normal temperatures is thus obtained by combining Eqs.3.19, 3.21, 3.23 and 3.28:

$$\frac{{}^*q}{q} = \left(\frac{{}^*M}{M}\right)^{1/2} \frac{{}^*m}{m}\frac{s}{{}^*s}\exp\left[\frac{h\nu}{2kT}\left(1-\sqrt{\frac{\mu}{{}^*\mu}}\right)\right] \tag{3.29}$$

where m and *m refer to the exchanging isotopes. The equilibrium fractionation factor between two di-atomic gases A and B is given by Eq.3.18. It should be noted that, if A or B consists of two equal atoms (such as in O_2 or CO_2), the true relation between α and K contains a factor 2 such that the factor 2 arising from s/*s is cancelled in calculating α. A simple numerical example is given in Sect.3.7.

A general approximate expression for the fractionation factor as a function of the temperature is obtained from Eqs.3.18 and 3.29:

$$\alpha = Ae^{B/T} \tag{3.30}$$

where the coefficients A and B do not depend on temperature but contain all temperature-independent quantities (mass, vibration frequency). The natural logarithm of the fractionation factor is approximated by the power series:

$$\ln\alpha = C_1 + \frac{C_2}{T} + \frac{C_3}{T^2} \tag{3.31a}$$

with the often used approximation for the fractionation:

$$\varepsilon \approx \ln(1+\varepsilon) = C_1 + C_2/T \tag{3.31b}$$

It can further be shown, that at very high temperatures the vibrational contribution to the fractionation balances the product of the translational and rotational factors, so that finally at very high temperatures $\alpha = 1$, and thus, isotope effects disappear at sufficiently high temperatures.

From the foregoing we can draw the following conclusions:

1) In a kinetic (one-way or irreversible) process the phase or compound formed is depleted in the heavy isotope with respect to the original phase or compound ($\alpha_k < 1$); theoretical predictions about the degree of fractionation can only be qualitative (fast evaporating water is depleted in ^{18}O relative to the water itself)

2) In an isotopic equilibrium (reversible) process it can not with certainty be predicted whether the one phase or compound is enriched or depleted in the heavy isotope. However, the dense phase (liquid rather than vapour) or the compound having the largest molecular mass ($CaCO_3$ versus CO_2) usually contains the highest abundance of the heavy isotope

3) Under equilibrium conditions and provided sufficient spectroscopic data on the binding energies are available, α_e may be calculated; measurements on α_e of various isotope equilibria will be reported in chapter 6

4) As a rule fractionation decreases with increasing temperature; in Chapter 6 this is shown, for instance, for the exchange equilibria of $CO_2 \Leftrightarrow H_2O$ and $H_2O_{liquid} \Leftrightarrow H_2O_{vapour}$. At very high temperatures the isotopic differences between the compounds disappear.

3.5 FRACTIONATION BY DIFFUSION

As was mentioned in Sect.3.2 isotope fractionation might occur because of the different mobilities of isotopic molecules. An example in nature is the diffusion of CO_2 or H_2O through air.

According to Fick's law the net flux of gas, F, through a unit surface area is:

$$F = -D\frac{dC}{dx} \qquad \textbf{(3.32)}$$

where dC/dx is the concentration gradient in the direction of diffusion and D is the diffusion constant. The latter is proportional to the temperature and to $1/\sqrt{m}$, where m is the molecular mass. This proportionality results from the fact that all molecules in a gas (mixture) have equal temperature and thus equal average $\frac{1}{2}mv^2$. The average velocity of the molecules and, thus, their mobilities are inversely proportional to $\sqrt{m}$.

If the diffusion process of interest involves the movement of gas A through gas B, however, m has to be replaced by the reduced mass:

$$\mu = \frac{m_A m_B}{m_A + m_B} \tag{3.33}$$

(see textbooks on the kinetic theory of gases).

The above equations hold for the abundant as well as for the rare isotope. The resulting fractionation is then given by the ratio of the diffusion coefficient for the two isotopic species. Furthermore, the molecular masses can be replaced by the molar weights M in numerator and denominator:

$$\alpha = \frac{{}^*D}{D} = \sqrt{\frac{{}^*M_A + M_B}{{}^*M_A \cdot M_B} \frac{M_A \cdot M_B}{M_A + M_B}} \tag{3.34}$$

In the example of water vapour diffusing through air, the resulting fractionation factor for oxygen is (M_B of air is taken to be 29, $M_A = 18$, ${}^*M_A = 20$):

$${}^{18}\alpha = \left[\frac{20+29}{20\times 29}\ \frac{18\times 29}{18+29}\right]^{1/2} = 0.969 \tag{3.35}$$

By diffusion through air water vapour thus will become depleted in ^{18}O (in agreement with the rules given at the end of Sect.3.4) by 31 ‰: ${}^{18}\varepsilon = -31$ ‰.

The ^{13}C fractionation factor for diffusion of CO_2 through air is:

$${}^{13}\alpha = \left[\frac{45+29}{45\times 29}\ \frac{44\times 29}{44+29}\right]^{1/2} = 0.9956 \tag{3.36}$$

in other words ${}^{13}\varepsilon = -4.4$ ‰, a depletion of 4.4 ‰.

3.6 RELATION BETWEEN ATOMIC AND MOLECULAR ISOTOPE RATIOS

We want to have a closer look at the meaning of the isotope ratio in the context of the abundance of rare isotopes of an element in poly-atomic molecules, containing at least two atoms of this element. The isotope ratio is the chance that the abundant isotope has been replaced by the rare isotope. To be more specific, we define the *atomic isotope ratio* (R_{atom}) as the abundance of all rare isotopic atoms in the compound divided by the abundance of all abundant isotopic atoms. For the sake of clarity, we select a simple example, the isotopes of hydrogen in water:

$${}^2R_{atom} = \frac{[{}^2H^{16}O^1H] + [{}^2H^{17}O^1H] + [{}^2H^{18}O^1H] + 2[{}^2H^{16}O^2H] + \ldots\ldots}{2[{}^1H^{16}O^1H] + 2[{}^1H^{17}O^1H] + 2[{}^1H^{18}O^1H] + [{}^1H^{16}O^1H] + \ldots\ldots} \tag{3.37}$$

The "second-order" abundances, such as for instance $^{2}H_2{}^{18}O$ in the nominator and $^{1}H^{2}H^{18}O$ in the denominator, have been neglected. In this context the *molecular isotope ratio* (R_{mol}) is defined as the abundance of the rare isotope of a specific element in a specific type of molecule divided by the abundance of the abundant isotope. In our example of deuterium in water:

$$ {}^{2}R_{mol} = \frac{[{}^{2}H^{16}O^{1}H]}{2[{}^{1}H^{16}O^{1}H]} \qquad \textbf{(3.38)} $$

The realistic value of this definition refers, for instance, to the measurement of isotope ratios by laser spectrometry (see Sect.10.2.1.2), where the light absorption is compared of two isotopic molecules, only differing in one isotope, contrary to **mass** spectrometry (Kerstel et al., 1999; priv.comm.).

Eq.3.37 can be rewritten as:

$$ {}^{2}R_{atom} = \frac{[{}^{2}H^{16}O^{1}H]}{2[{}^{1}H^{16}O^{1}H]} \frac{1+\frac{[{}^{2}H^{17}O^{1}H]}{[{}^{2}H^{16}O^{1}H]}+\frac{[{}^{2}H^{18}O^{1}H]}{[{}^{2}H^{16}O^{1}H]}+\frac{2[{}^{2}H^{16}O^{2}H]}{[{}^{2}H^{16}O^{1}H]}\cdots\cdots}{1+\frac{[{}^{1}H^{17}O^{1}H]}{[{}^{1}H^{16}O^{1}H]}+\frac{[{}^{1}H^{18}O^{1}H]}{[{}^{1}H^{16}O^{1}H]}+\frac{[{}^{1}H^{16}O^{2}H]}{2[{}^{1}H^{16}O^{1}H]}\cdots\cdots} \qquad \textbf{(3.39)} $$

The first factor on the right in Eq.3.39 is the molecular isotope ratio. To a very good approximation the molecular isotope ratios in the second factor may be replaced by the atomic isotope ratios:

$$ {}^{2}R_{atom} \approx {}^{2}R_{mol} \cdot \frac{1+{}^{17}R+{}^{18}R+{}^{2}R+\cdots\cdots}{1+{}^{17}R+{}^{18}R+{}^{2}R+\cdots\cdots} = {}^{2}R_{mol} \qquad \textbf{(3.40)} $$

This result means that to a first-order approximation the atomic isotope ratio is equal to a molecular isotope ratio. Although it was shown for one specific molecule, the reasoning is equally valid for the other molecules in Eq.3.39. Also for more complicated molecules the demonstration of the proof is analogous.

The approximations made are indicated as "first-order". However, if we use δ values the approximation is even better, because almost equal approximations occur in the R values of the nominator as well as the denominator of Eq.3.40 (cf. Sect.4.3.1).

3.7 RELATION BETWEEN FRACTIONATIONS FOR THREE ISOTOPIC MOLECULES

For some isotope studies, it is of interest to know the relation between the fractionations for more than two isotopic molecules. For instance, water contains three different isotopic molecules as far as oxygen is concerned: $H_2{}^{16}O$, $H_2{}^{17}O$ and $H_2{}^{18}O$; carbon dioxide consists of $^{12}CO_2$, $^{13}CO_2$ as well $^{14}CO_2$. The question now is, whether there is a theoretical relation

between the ^{17}O and ^{18}O fractionation with respect to ^{16}O (for instance, during evaporation) and between the ^{13}C and ^{14}C fractionation with respect to ^{12}C (for instance, during the uptake of CO_2 by plants).

Generally the fractionation for the heaviest isotope is taken twice as large as that for the less heavy isotope:

$$^{14}\alpha = \left(^{13}\alpha\right)^2 \qquad \text{and} \qquad ^{18}\alpha = \left(^{17}\alpha\right)^2 \tag{3.41}$$

while

$$^{14}\alpha = 1 + {}^{14}\varepsilon = \left(1 + {}^{13}\varepsilon\right)^2 = 1 + 2\,{}^{13}\varepsilon + (^{13}\varepsilon)^2 \approx 1 + 2\,{}^{13}\varepsilon$$

so that for the CO_2 uptake by plants as well as the isotope exchange between CO_2 and water, respectively:

$$^{14}\varepsilon \approx 2\,{}^{13}\varepsilon \qquad \text{and} \qquad ^{18}\varepsilon \approx 2\,{}^{17}\varepsilon \tag{3.42}$$

The approximation that these fractionations differ by a factor of 2 originates from the relation between the molecular masses as presented in Eqs. 3.21 and 3.23. For the heaviest isotope $^{m+2}\alpha$ is a function of (M+2)/M, while $^{m+1}\alpha$ is a similar function of (M + 1)/M.

Having discussed the theoretical background of isotope effects in the preceding sections, we are able to make an approximation of the exponent θ in the general relation:

$$\frac{^{m+2}R_A}{^{m+2}R_B} = \left(\frac{^{m+1}R_A}{^{m+1}R_B}\right)^{\theta} \qquad \text{or} \qquad \frac{\ln {}^{m+2}\alpha_{A/B}}{\ln {}^{m+1}\alpha_{A/B}} = \theta \tag{3.43}$$

where m = 12 for carbon or 16 for oxygen. The fractionations by diffusion are easily calculated. For the *diffusion of water vapour through air* Eqs.3.35 and 3.43 result in:

$$\ln {}^{18}\alpha \,/\, \ln {}^{17}\alpha = 1.93$$

whereas according to Eqs.3.36 and 3.43 for the *diffusion of CO_2 through air*:

$$\ln {}^{14}\alpha \,/\, \ln {}^{13}\alpha = 1.96$$

In terms of fractionation this comes to:

$$^{18}\varepsilon \approx 1.93\,{}^{17}\varepsilon \qquad \text{and} \qquad ^{14}\varepsilon \approx 1.96\,{}^{13}\varepsilon$$

Calculating the exponent θ for fractionation effects in general is quite elaborate. The relatively simple case for the CO ⇔ O_2 isotopic equilibrium may serve as an example (cf. Broecker and Oversby, 1971). The isotope exchange reactions are:

$$^{18}O^{16}O + {}^{12}C^{16}O \Leftrightarrow {}^{16}O_2 + {}^{12}C^{18}O$$

and

$$^{17}O^{16}O + {}^{12}C^{16}O \Leftrightarrow {}^{16}O_2 + {}^{12}C^{17}O$$

Inserting the proper mass numbers and the vibration frequencies: $\nu(^{12}C^{16}O) = 6.50 \times 10^{13}$/s and $\nu(^{16}O^{16}O) = 4.74 \times 10^{13}$/s in Eqs.3.18 and 3.29, the α values at 20°C are:

$$^{18}\alpha_{CO/O_2} = \frac{^{18}O/^{16}O \text{ in } CO}{^{18}O/^{16}O \text{ in } O_2} = 1.023363$$

and

$$^{17}\alpha_{CO/O_2} = \frac{^{17}O/^{16}O \text{ in } CO}{^{17}O/^{16}O \text{ in } O_2} = 1.012245$$

so that:

$$\ln {}^{18}\alpha_{CO/O_2} / \ln {}^{17}\alpha_{CO/O_2} = 1.90$$

(h = 6.626 * 10^{-34} Js; k = 1.38 * 10^{-23} J/K).

Applying the equations to poly-atomic molecules can only result in approximate θ values. However, calculations on the exchange equilibria such as CO ⇔ CO_2 and CO_2 ⇔ CH_4 result in:

$$\ln {}^{m+2}\alpha / \ln {}^{m+1}\alpha \approx 1.9 \qquad \textbf{(3.44)}$$

rather than in θ = 2 (Skaron and Wolfsberg, 1980).

In one case an experimental determination of the relation between ^{17}O and ^{18}O has been possible. A series of natural water samples was electrolytically converted into oxygen which was then analysed mass spectrometrically. The resulting relation between the $^{17}\delta$ and $^{18}\delta$ values was reported as (Meijer and Li, 1998):

$$1 + {}^{18}\delta = (1 + {}^{17}\delta)^{(1.8935 \pm 0.005)} \qquad \textbf{(3.45)}$$

Despite this, in many routine cases, where the obtainable precision is limited or irrelevant, we may still use the relation:

$$\ln^{m+2}\alpha / \ln^{m+1}\alpha = 2 \qquad \text{and} \qquad {}^{m+2}\alpha = \left({}^{m+1}\alpha\right)^2 \tag{3.46}$$

or:

$${}^{m+2}\varepsilon = 2\ {}^{m+1}\varepsilon \tag{3.47}$$

at least with a precision of 10%. In this respect, we will continue to apply the factor of 2 in the relation between the $^{13}C/^{12}C$ and $^{14}C/^{12}C$ isotope ratios for natural processes:

$${}^{14}\varepsilon = 2\ {}^{13}\varepsilon$$

as originally used by Craig (1954). The precision of a ^{14}C analysis is not sufficient to allow an experimental verification of the relation of Eq.3.42 between the fractionations for ^{13}C and ^{14}C containing molecules.

On the other hand, Eq.3.44 is to be applied if the fractionations involved are large and the measurements sufficiently accurate.

4 ABUNDANCE VARIATIONS BY NATURAL PROCESSES

In the preceding chapter we have defined isotope (abundance) ratios in various chemical compounds. Furthermore, we have presented a theoretical treatment of the physical phenomenon of isotope fractionation. In this chapter we will discuss the background of various processes occurring in nature, that may cause variations in the isotope ratios.

The equations that will be derived can be expressed practically without approximation in isotope ratios (R values) as well as in a more or less approximated format in δ values.

4.1 USE OF δ VALUES AND ISOTOPE REFERENCES

Isotope ratios such as

$$^{2}R = \frac{^{2}H}{^{1}H} \qquad ^{13}R = \frac{^{13}C}{^{12}C} \qquad ^{18}R = \frac{^{18}O}{^{16}O} \tag{4.1}$$

are generally not reported as absolute numbers. The main reasons are:

1) the type of mass spectrometers, suitable for measuring isotope abundances with high sensitivity in order to detect very small natural variations, are basically not suitable for obtaining reliable absolute ratios (see Sect.11.2)

2) the necessity of international comparison requires the use of references to which the samples have to be related

3) the use of isotope ratios would lead to reporting results as numbers consisting of a large number (5 or 6) of digits

4) absolute ratios are in principle less relevant than the changes in ratios occurring during transitions between phases or molecules.

Therefore, an isotope abundance is generally reported as a deviation of the isotope ratio of a sample A *relative* to that of a reference sample or standard, r:

$$\delta_{A/r} = \frac{R_A}{R_r} - 1 \qquad (\times 10^3\ ‰) \tag{4.2a}$$

For the specific isotopes mentioned in Eq.4.1 the respective δ values are indicated by the symbols:

$$^{2}\delta = \frac{(^{2}H/^{1}H)_A}{(^{2}H/^{1}H)_r} - 1 \qquad ^{13}\delta = \frac{(^{13}C/^{12}C)_A}{(^{13}C/^{12}C)_r} - 1 \qquad ^{18}\delta = \frac{(^{18}O/^{16}O)_A}{(^{18}O/^{16}O)_r} - 1 \quad \textbf{(4.2b)}$$

where the more often used symbols are $\delta^{2}H$ or δD, $\delta^{13}C$, and $\delta^{18}O$, respectively.

However, in this volume we will write the mass number indicating the rare isotope concerned by a superscript before the δ, as with the R symbols and the isotope symbol itself, thus making the symbols simpler and leaving space for other super- and subscripts.

As the values of δ in nature are small, they are generally given -although not defined- in ‰ (per mill ≡ parts per thousand ≡ 10^{-3}). We have to emphasise that ‰ is equivalent to the factor 10^{-3} and is not a unit as is often suggested. *A δ value is merely a small, dimensionless number.* Similarly to ε defined in Sect.3.3, it is incorrect to use $\delta/10^{3}$ instead of δ in mathematical equations. In order to avoid the negligence to realise that δ is a small number, one may choose to write in mathematical equations: δ(in ‰)10^{-3} instead of merely δ, impractical though it is.

Negative δ values indicate lower abundances of the rare isotope in these samples than in the reference material, positive δ values point to higher abundances.

Comparing the definitions of ε (Eq.3.5) and δ, the only difference is that, whereas ε was defined as the isotope ratio of a compound (then B) relative to another compound (A), δ is defined as the isotope ratio of a compound (now A) relative to the standardised reference material (r).

Although in the equations to be derived in this chapter the δ format can be applied to practically all natural processes to the precision attainable by the modern analytical instrumentation, the calculation capacity of small pocket calculators used in the field generally has come to make the approximations superfluous. The δ values delivered by isotope laboratories can easily be transformed into R values by applying (rewritten from Eq.4.2):

$$R = R_r(1 + \delta) \qquad \textbf{(4.3)}$$

where the R_r values are the isotope ratios of the international reference materials to be defined later in Chapter 7. Referring to the relation between isotope ratio and isotope concentration (Sect.3.1), the isotope concentration, C, can now be transformed into δ by inserting Eq.3.3b:

$$\delta = \frac{R}{R_r} - 1 = \frac{1}{R_r}\frac{C}{1-C} - 1 \qquad \textbf{(4.4)}$$

Examples: natural carbon contains about 1 atom % of ^{13}C; carbon with an absurdly high ^{13}C concentration of 99 atom % has a $^{13}\delta$ value (vs PDB-CO_2: R_r = 0.0112372, Sect.7.1.3) of 8809×10^{3} ‰.

If δ values are to be given relative to a secondary reference, r', rather than to the primary reference r, a conversion equation is needed.

From the isotope ratios:

$$\frac{R_A}{R_{r'}} = \frac{R_A / R_r}{R_{r'} / R_r} \tag{4.5}$$

or

$$1 + \delta_{A/r'} = \frac{1 + \delta_{A/r}}{1 + \delta_{r'/r}}$$

follows

$$\delta_{A/r'} = \frac{\delta_{A/r} - \delta_{r'/r}}{1 + \delta_{r'/r}} \tag{4.6}$$

This equation is also useful for converting between two phases or compounds A and B:

$$\delta_{A/B} = \frac{-\delta_{B/A}}{1 + \delta_{B/A}} \approx -\delta_{B/A} \tag{4.7}$$

similar to the Eq.3.6 for ε. Values of R and α are multiplicative, whereas δ and ε values are only approximately additive. In other words, the fractionation ε, as defined by Eq.3.5, is almost equal to the difference in isotopic composition between two phases:

$$\varepsilon_{B/A} = \alpha_{B/A} - 1 = \frac{R_B}{R_A} - 1 = \frac{R_B / R_r}{R_A / R_r} - 1 = \frac{1 + \delta_{B/r}}{1 + \delta_{A/r}} - 1 \approx \delta_{B/r} - \delta_{A/r} \tag{4.8}$$

For the reaction A→B, $\varepsilon_{B/A}$ is the change in isotopic composition (equal the "new" δ minus the "old" (cf. Sect.3.3).

Because strict conventions govern the use of references, we will generally drop the subscript r and designate the sample by a subscript δ_A or δ(A) instead of $\delta_{A/r}$ and δ_r(A).

The additivity of δ and ε values is commonly approximated by:

$$\delta_B \approx \delta_A + \varepsilon_{B/A} \tag{4.9}$$

This means that if air-CO_2 with a $^{13}\delta$ value of −8‰ is assimilated by plants with a carbon isotope fractionation of −17‰, the $^{13}\delta$ value of the plant carbon is −25‰.

4.2 TRACER CONCENTRATION, AMOUNT OF TRACER

Natural isotopes can be used as *tracers* to follow elements of the water cycle in their natural course. For instance, the abundance of ^{2}H and ^{18}O in precipitation can be applied to unravelling the various components of the runoff hydrograph. This application comes to calculating the amount of tracer in the different compartments of the local or regional water budget.

In Sect.3.1 we have defined the isotope concentration of, for instance, ^{18}O in water as:

$$[H_2{}^{18}O] = \frac{\text{amount of } H_2{}^{18}O}{\text{amount of water}} = \frac{H_2{}^{18}O}{H_2{}^{16}O + H_2{}^{18}O} = \frac{{}^{18}R(H_2O)}{1 + {}^{18}R(H_2O)} \approx {}^{18}R(H_2O) \qquad (4.10)$$

and in the δ notation:

$$[H_2{}^{18}O] = {}^{18}R_r \{{}^{18}R(H_2O) / {}^{18}R_r\} = {}^{18}R_r \{1 + {}^{18}\delta\} \qquad (4.11)$$

Now the rare isotope as such can not simply serve as the tracer. This becomes clear if we consider the case of the runoff hydrograph analysis. If during a storm rain would fall with a $^{18}\delta$ value equal to that of the base flow (=groundwater), there would be no isotopic change in the runoff and so we would not be able to recognise the precipitation in the runoff. The precipitation can only be "traced" if it can be distinguished isotopically from the base flow. Therefore, the *tracer concentration* has to be defined as the deviation of the rare isotope concentration from a certain base level, in our case the $^{18}\delta$ value of the base flow (= average groundwater). The concentration of the tracer is then defined as:

$$[H_2{}^{18}O] - [H_2{}^{18}O_{base}] = {}^{18}R_r \{{}^{18}\delta - {}^{18}\delta_{base}\} \qquad (4.12)$$

Here we have inserted $^{18}R_r$ as the ^{18}R value of the international reference (i.e. standard, to be introduced in Chapter 7).

If a comparison is required of, as in our present case, the amount of runoff and the amount of precipitation, we have to introduce the *amount of tracer*, defined as:

$${}^{18}R_r \{{}^{18}\delta - {}^{18}\delta_{base}\} \cdot W = {}^{18}R_r \cdot \Delta^{18}\delta \cdot W \qquad (4.13)$$

where W denotes the amount of water. Comparing specifically the amount of runoff Q and the amount of precipitation, P now comes to calculating the ratio:

$$\frac{\sum_i \left(\Delta^{18}\delta_Q \cdot Q\right)_i}{\sum_j \left(\Delta^{18}\delta_P \cdot P\right)_j} \qquad (4.14)$$

for a number of time periods i and j, respectively (i may equal j, depending on the question).

4.3 MIXING OF RESERVOIRS WITH DIFFERENT ISOTOPIC COMPOSITION

4.3.1 MIXING OF RESERVOIRS OF THE SAME COMPOUND

If two (or more) quantities of a certain compound with different δ values are being mixed (for instance, the CO_2 in the air of two different origins, such as marine and biospheric), the δ value of the mixture can be calculated from a mass balance equation (Fig.4.1A).

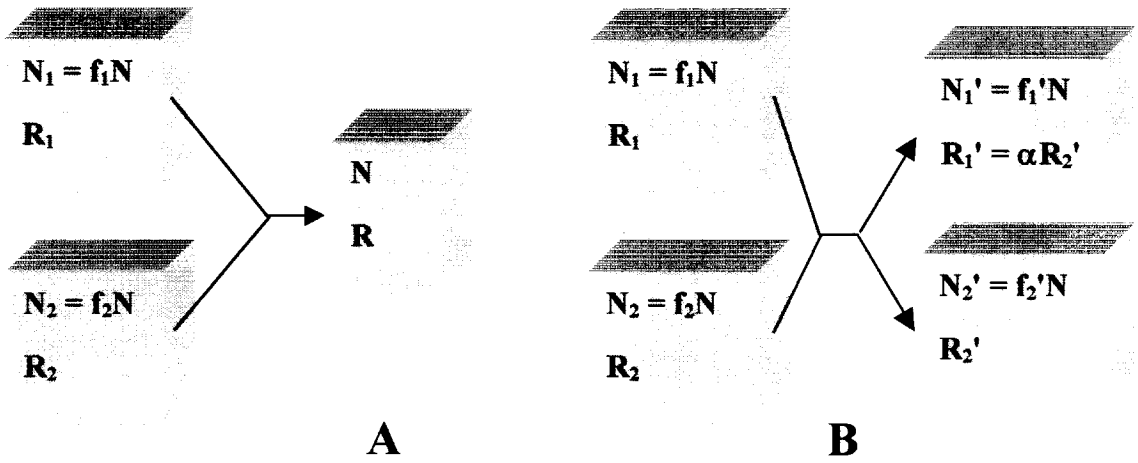

Fig.4.1 Schematic representation of (A): the mixing of two quantities of one compound with different isotopic compositions, and (B): the mixing and reaction of two different compounds or two phases of the same compound with different isotopic composition that will be subjected to isotope exchange and will ultimately become a fractionation factor (α) apart.

N_1 molecules of a certain compound with an isotope ratio R_1 contain $N_1/(1 + R_1)$ molecules of the abundant, $R_1N_1/(1 + R_1)$ molecules of the rare isotopic species (cf. Eq.3.3).If this quantity is mixed with another quantity N_2 (with isotopic composition R_2), a simple mass balance gives the isotope ratio of the mixture:

$$\frac{RN}{1+R} = \frac{R_1N_1}{1+R_1} + \frac{R_2N_2}{1+R_2} \quad \text{or} \quad RN \approx R_1N_1 + R_2N_2 \qquad (4.15)$$

where $N = N_1 + N_2$. The approximation is valid for $R \approx R_1 \approx R_2$ (note that the R values have not been neglected in comparison to 1).

Replacing the R values by $R_r(1 + \delta)$ and denoting the fractional contributions to the mixture by f_1 (= N_1/N) and f_2 (= N_2/N), where $f_1 + f_2 = 1$, the δ value of the mixture is:

$$\delta = \frac{f_1\delta_1[1+R_r(1+\delta_2)]+f_2\delta_2[1+R_r(1+\delta_1)]}{1+R_r[f_1(1+\delta_2)+f_2(1+\delta_1)]} \qquad \textbf{(4.16)}$$

For natural abundances of isotopes within a δ range of 100‰ this equation can be approximated (to within ± 0.03 ‰) by:

$$\delta = f_1\delta_1 + f_2\delta_2 \qquad \textbf{(4.17)}$$

which means that to a very good approximation additivity applies to δ values. Fig.4.2 shows the example of mixing seawater and river water in an estuary. Additivity is valid for the Chloride content of the water (*conservative tracer*) as well as for $^{18}\delta$. The relation between the two is consequently a straight line.

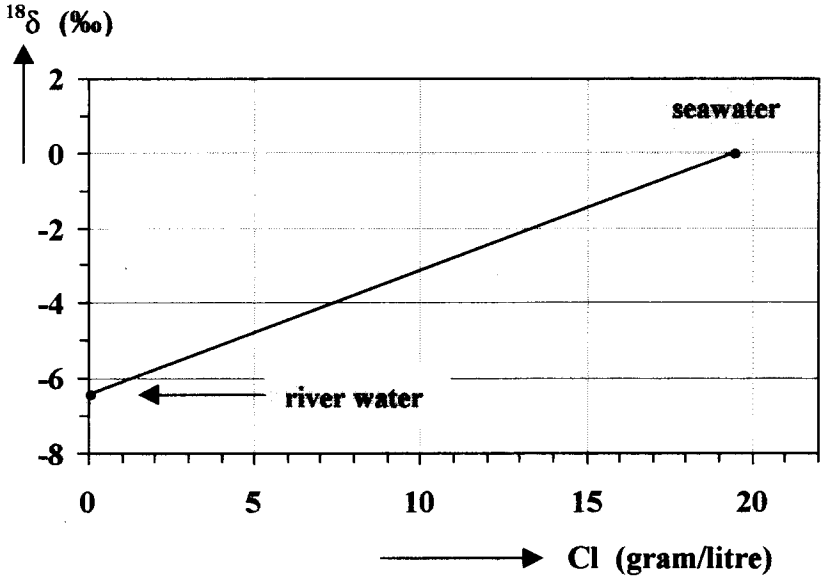

Fig.4.2 Linear relation between the Chlorinity (Cl concentration) and $^{18}\delta$ of water in the estuary of the Western Scheldt, where water from the Belgian river Scheldt (Cl = 0‰ (=g/kg); $^{18}\delta$ = −6.5‰) mixes with water from the North Sea (Cl = 19.36‰; $^{18}\delta$ = 0‰).

4.3.1.1 ISOTOPIC DILUTION ANALYSIS

A practical application of the previous section is the so-called *Isotopic Dilution Analysis*, a method used in radiochemistry. By this method an amount of radioactive material can be determined without the chemical separation procedures being complete. For instance, if small traces of radioactivity are to be quantified, a known amount of the same, but inactive compound is added and the chemical separation procedure is carried out (not necessarily quantitative). From the final specific activity of the compound the quantity of the original radioactive compound can then be calculated.

In general, the conservation of mass during the addition of material requires (cf. Eq.4.15):

$$A_{or} + A_{ad} = A_{mix} \quad \text{or} \quad N_{or}a_{or} + N_{ad}a_{ad} = (N_{or} + N_{ad})a_{mix} \tag{4.18a}$$

and

$$N_{or}C_{or} + N_{ad}C_{ad} = (N_{or} + N_{ad})C_{mix} \tag{4.18b}$$

where the subscripts or, ad and mix refer to the original material, the added material and the mixture, respectively. N is the respective quantity, C the concentration, A the amount of radioactivity and a the specific activity. Here we briefly mention a few examples.

Example 1. Determination of an unknown quantity/concentration of inactive compound by adding a known amount of the same compound with a known specific activity

$a_{or} = 0$

N_{ad} and a_{ad} are known

Specific activity a_{mix} is to be measured

N_{or} is unknown and wanted (Eq.4.16a):

$$N_{or} = \left(\frac{a_{ad}}{a_{mix}} - 1 \right) \times N_{ad} \tag{4.19}$$

If the added radioactive solution is carrier free, i.e. $N_{ad} = 0$ and thus the specific activity a_{ad} is ∞, we have to write:

$$A_{ad} = A_{mix} = N_{mix} \times a_{mix} = N_{or} \times a_{mix}$$

and thus: $N_{or} = A_{ad} / a_{mix}$

Example 2. Determination of an unknown amount of (human or animal) body fluid by adding deuterium enriched water

C_{or} is known; has to be calculated from the ^2R or $^2\delta$ water of the original body fluid (blood), because using $^2\delta$ as a concentration (cf. Eq.4.17) is not accurate enough

N_{ad} is known but may be negligibly small

C_{ad} is known

C_{mix} is to be measured

N_{or} is unknown and wanted (from Eq.4.18b):

$$N_{or} = \left(\frac{C_{ad}}{C_{mix}} - 1 \right) \times N_{ad} \qquad \textbf{(4.20)}$$

Example 3. Determination of an unknown carrier-free radioactivity (A_{or}) by adding a known quantity of the inactive compound (N_{ad})

Here the total amount of activity before and after the addition is the same ($A_{mix} = A_{or}$), while the final quantity of mixture (N_{mix}) is equal to the quantity added (N_{ad}):

$$A_{or} = N_{ad} \times a_{mix} \qquad \textbf{(4.21)}$$

This method is known as the *Reverse Isotope Dilution Analysis*.

4.3.2 MIXING OF RESERVOIRS OF DIFFERENT COMPOUNDS

If the mixing process includes chemically different but reactive compounds of quantities N_1 and N_2 with different isotopic compositions R_1 and R_2, the final stage is characterised by a fractionation between the compounds. During there action a chemical shift between the two compounds will often occur. The quantities change into N_1' and N_2' with isotopic compositions of R_1' and R_2' where the latter values are a fractionation factor α apart. An example is the exchange between gaseous CO_2 and a bicarbonate solution as, for instance, between lake water and atmospheric CO_2, or the mixing of fresh and seawater with different pH.

A similar mass balance for the rare isotope can be written (Fig.4.1B):

$$\frac{R_1'N_1'}{1+R_1'} + \frac{R_2'N_2'}{1+R_2'} = \frac{R_1N_1}{1+R_1} + \frac{R_2N_2}{1+R_2}$$

or $$R_1'N_1' + R_2'N_2' \approx R_1N_1 + R_2N_2 \qquad \textbf{(4.22)}$$

where $N_1' + N_2' = N_1 + N_2$, and the same approximation applies as in Eq.4.15 for the range of δ values of all natural samples.

This results in:

$$R_2' = \frac{R_1N_1 + R_2N_2}{\alpha N_1' + N_2'} \qquad \text{and} \qquad R_1' = \alpha R_2' \qquad \textbf{(4.23)}$$

or

$$\delta_2' \approx \frac{f_1\delta_1 + f_2\delta_2 - f_1'\varepsilon}{1 + f_1'\varepsilon} \qquad \text{and} \qquad \delta_1' \approx \delta_2' + \varepsilon \text{ or} \qquad \textbf{(4.24)}$$

with $f_1 = N_1/(N_1+N_2)$, et cetera.

These equations are applied to the indirect determination of $^{18}\delta$ of a water sample, viz. by measuring $^{18}\delta$ of CO_2 equilibrated with the water rather than the water itself (Sect.10.2.1.1 and 11.2.3.4).

4.4 ISOTOPIC CHANGES IN RAYLEIGH PROCESSES

It is common in isotope studies to be concerned with the change in isotopic composition of a reservoir because of the removal of an increasing fraction of its contents accompanied by isotope fractionation. We will discuss the process under two conditions, (i) removal of a compound (=*sink*) from a reservoir without an additional input (evaporation from a confined water basin for example); (ii) removal accompanied by a constant input (=*source*) (such as evaporation from a lake with a river input).

4.4.1 RESERVOIR WITH ONE SINK

A simple box model describing a reservoir with only one sink. is presented by Fig.4.3. Here N is the total number of molecules, and R is the ratio of the rare to abundant molecular concentrations, so that

N/(1+R) is the number of abundant isotopic molecules and

RN/(1+R) is the number of rare isotopic molecules

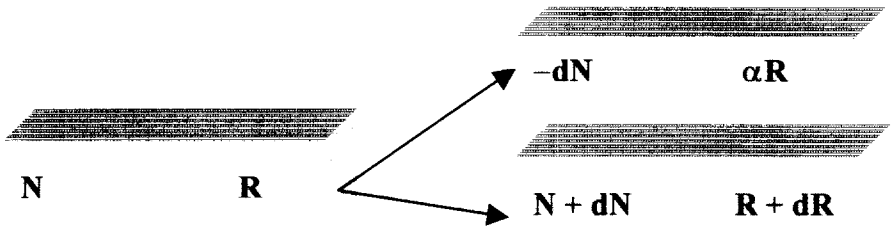

Fig.4.3 Schematic representation of the Rayleigh process. N is the number of abundant isotopic molecules (≈ total number of molecules), R is the isotope ratio, α is the (equilibrium or kinetic) fractionation factor involved.

For the removal of dN molecules with an accompanying fractionation factor α, the mass balance for the rare isotope gives:

$$\frac{R}{1+R}N = \frac{R+dR}{1+R+dR}(N+dN) - \frac{\alpha R}{1+\alpha R}dN$$

To a good approximation we will furthermore take the total number of molecules equal to the number of abundant isotopic molecules: in fact, for this approximation all denominators are taken equal 1+R (which is not the same as neglecting R completely!). The mass balance for the rare isotope now becomes:

$$RN = (R + dR)(N + dN) - \alpha R dN$$

and neglecting the products of differentials:

$$dR/R = (\alpha - 1)dN/N$$

Integration and applying the boundary condition: $R = R_o$ at $N = N_o$ (nothing has been neglected yet) gives:

$$\frac{R}{R_0} = \left(\frac{N}{N_0}\right)^{\alpha-1} \qquad \textbf{(4.25a)}$$

or in δ values with respect to the standardised reference:

$$\delta = (1 + \delta_0)(N/N_0)^{\varepsilon} - 1 \qquad \textbf{(4.25b)}$$

where N/N_o represents the remaining fraction of the original reservoir; R_o and δ_0 refer to the original isotopic composition. Once more we have to remind the reader that ε (= α-1) is a small number, for instance –0.004 if the fractionation is –4‰.

The increase in $^{18}O/^{16}O$ of a confined water body by evaporation with $\alpha<1$ (Fig.4.4: upper curve) serves as an example of this simple Rayleigh process. Another case is presented by the $^{13}C/^{12}C$ increase in lake-water bicarbonate due to the growth of plankton.

We have now focussed our attention on the isotopic change of the reservoir. It is also relevant to calculate the isotopic composition of the compound which is gradually built up by the infinitesimal increments dN. This is not a simple additive procedure, because the isotopic composition of the reservoir changes during the process and thus also that of the increments dN. An example is found in the formation of a carbonate deposit from a groundwater mass which looses CO_2 when exposed to the atmosphere.

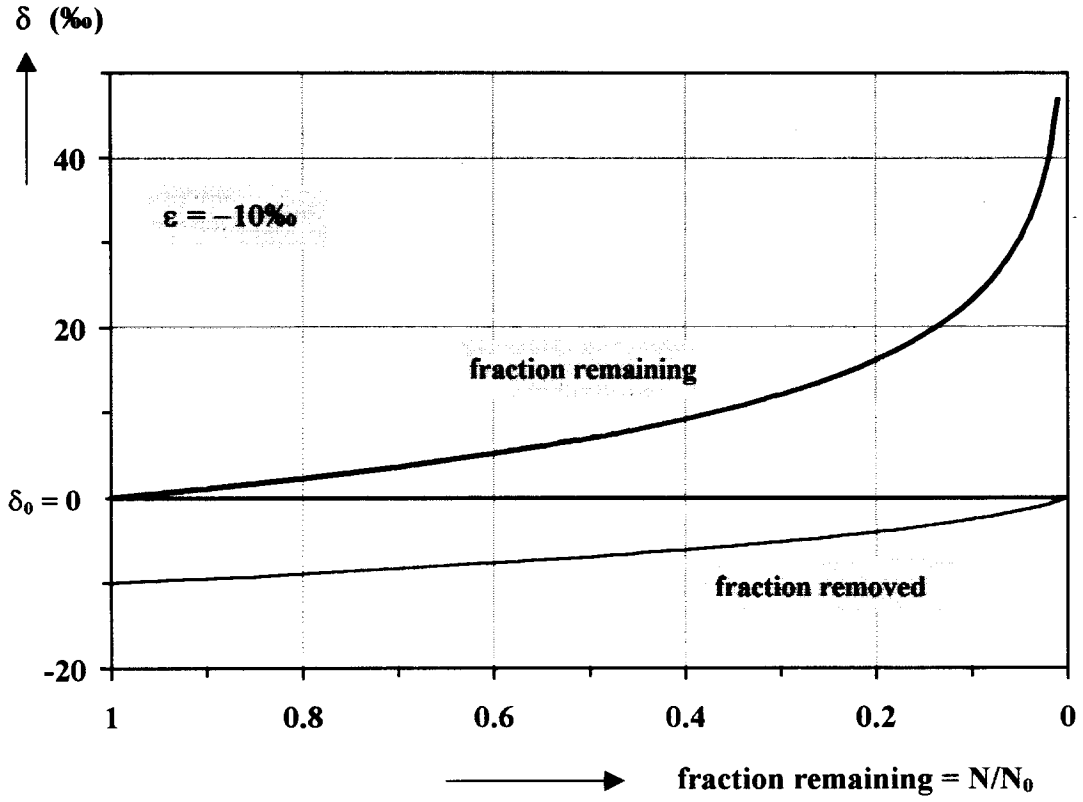

Fig.4.4 The enrichment of a rare heavy isotope in a reservoir by the Rayleigh process as a function of the fraction removed. The preferential removal of the light isotopic species is accompanied by a fractionation of $\alpha < 1$. The lower line present the average cumulative isotopic composition of the compound formed by the process, δ_Σ (Eq.4.26).

The average isotopic composition of the formed compound (= of the sum (Σ) of the increments) at a certain time is:

$$R_\Sigma = \frac{1}{N_0 - N}\int_N^{N_0} \alpha R \cdot dN = \frac{1}{N_0 - N}\frac{\alpha R_0}{N^{\alpha-1}}\int_N^{N_0} N^{\alpha-1}\, dN$$

where R is given by Eq.3.25a. Integration of this equation gives:

$$R_\Sigma = \frac{N_0}{N_0 - N} R_0 \left(\frac{N}{N_0}\right)^{\alpha} \Bigg|_N^{N_0} = R_0 \frac{1-(N/N_0)^{\alpha}}{1-N/N_0} \qquad \textbf{(4.26)}$$

or

$$\delta_{\Sigma} = (1+\delta_0)\frac{1-(N/N_0)^{\alpha}}{1-N/N_0} - 1 \qquad (4.27)$$

The resulting change in δ_e (for $\delta_0 = 0$) is shown in Fig.4.4 by the lower line.

4.4.2 RESERVOIR WITH TWO SINKS

A slightly more complicated, but nevertheless realistic phenomenon occurs if two processes simultaneously withdraw two different compounds from the reservoir (Fig.4.5). This process occurs when, through growth of algae in surface water, the pH of the water increases causing the formation of calcium carbonate. Both processes have characteristic carbon isotope fractionation involved.

The rare isotope mass balance now gives:

$$RN = (R + dR)(N + dN) - \alpha_1 R \cdot f_1 dN - \alpha_2 R \cdot f_2 dN$$

Here $f_1 + f_2 = 1$: a total amount dN of the element under consideration is removed from the reservoir. As with the previous case, we have:

$$\frac{dR}{R} = (\alpha_1 f_1 + \alpha_2 f_2 - 1)\frac{dN}{N}$$

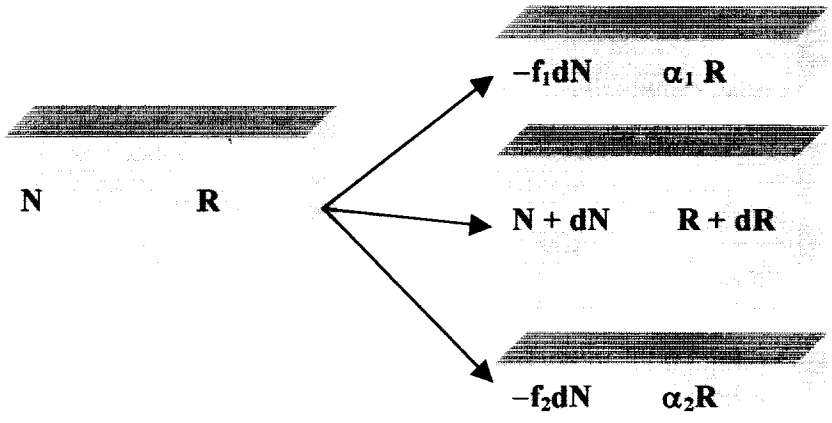

Fig.4.5 Schematic representation of the Rayleigh process where two compounds are being removed from the reservoir with different fractionation (α_1 and α_2); f_1 and f_2 refer to the fractional contributions to the total sink ($f_1 + f_2 = 1$).

which after integration gives:

$$R = R_0\left(\frac{N}{N_0}\right)^{\alpha_1 f_1+\alpha_2 f_2-1} \qquad \textbf{(4.28a)}$$

or

$$\delta = (1+\delta_0)(N/N_0)^{\varepsilon_1 f_1+\varepsilon_2 f_2} \qquad \textbf{(4.28b)}$$

This reduces to the simple case of one sink (Eqs.4.25a and 4.25b) if $f_2 = 0$, while the exponent reduces to $\varepsilon_1 f_1$ if the removal of the second compound occurs without fractionation.

4.4.3 RESERVOIR WITH ONE SOURCE AND ONE SINK, AS A FUNCTION OF TIME

Although the previous are practical examples of Rayleigh processes, the general case includes the existence of a source as well as a sink. These are represented by a supply rate i (in quantity per unit time) and a loss rate u (Fig.4.6A), while the fractionation with input, α_i, is not necessarily equal to unity.

The rare isotope mass balance is:

$$RN + \alpha_i R_i \cdot i dt = (R + dR)[N + (i - u)dt] + \alpha R \cdot u dt$$

from which we have by separation of variables (with $\alpha - 1 = \varepsilon$):

$$\frac{dR}{(i+\varepsilon u)R - \alpha_i R_i i} = \frac{dt}{N_0 + (i-u)(t-t_0)}$$

where N at a time t has been replaced by the denominator on the right ($N = N_0$ at $t = t_0$).

Integration and applying the boundary condition that $R = R_0$ at $t = t_0$ results in:

$$R = \frac{\alpha_i R_i}{1+(u/i)\varepsilon} + \left[R_0 - \frac{\alpha_i R_i}{1+(u/i)\varepsilon}\right]\left[1+\frac{i-u}{N_0}(t-t_0)\right]^{-\frac{i+u\varepsilon}{i-u}} \qquad \textbf{(4.29)}$$

for the case where $i \neq u$.

If $i = u$, the mass balance is:

$$RN_0 + \alpha_i R_i \cdot i dt = (R + dR)N_0 + \alpha R \cdot u dt$$

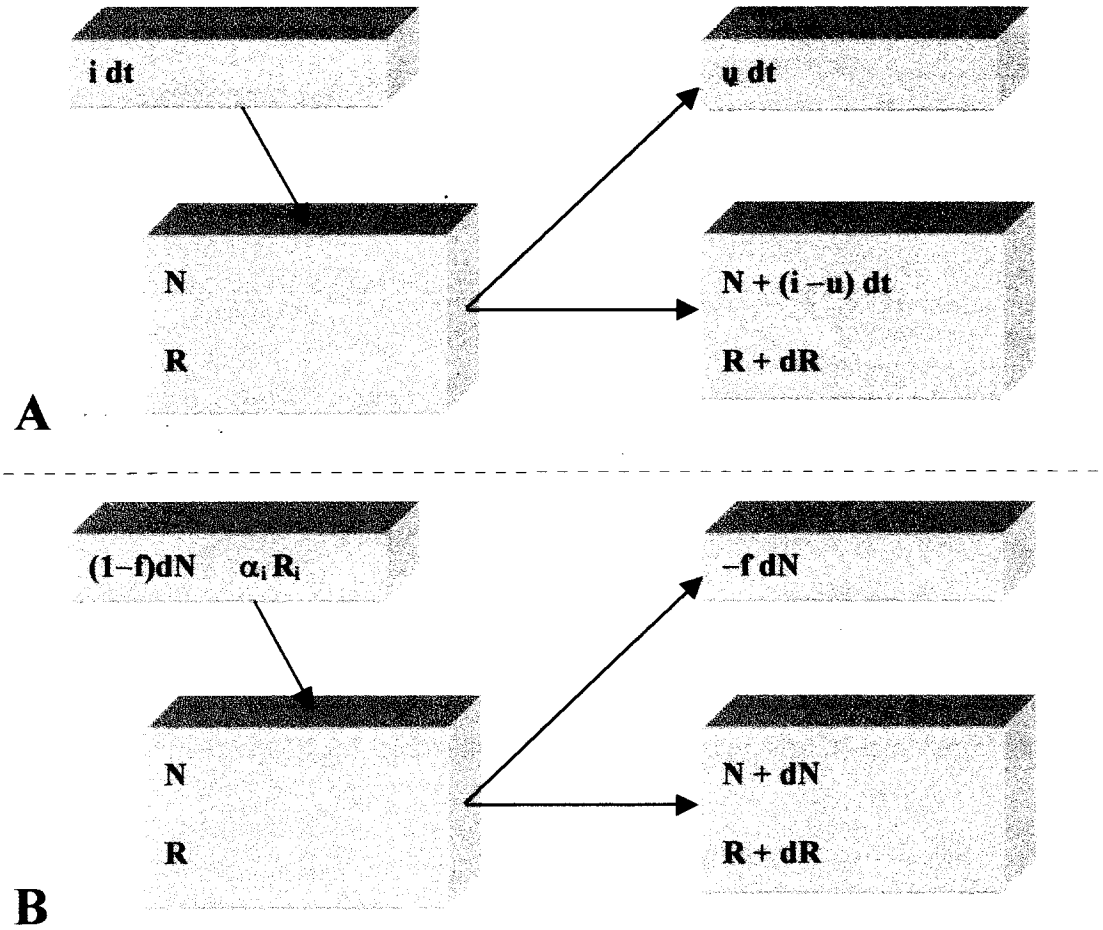

Fig.4.6 Schematic representation of the Rayleigh process with one source and one sink (A) as a function of time with n and m denoting the input and output rates respectively, and (B) as a function of the quantities of in- and outflow with determining the relation between input and output rates.

from which we can similarly derive:

$$R = \frac{\alpha_i R_i}{\alpha} + \left[R_0 - \frac{\alpha_i R_i}{\alpha} \right] e^{-\alpha(i/N_0)(t-t_0)} \qquad \textbf{(4.30)}$$

As $t \rightarrow \infty$, a steady-state situation is reached with:

$$R = \frac{\alpha_i R_i}{\alpha} \qquad \text{or} \qquad \delta = \frac{(1+\varepsilon_i)(1+\delta_i)}{1+\varepsilon} \qquad \textbf{(4.31)}$$

which is approximated by

$$\delta = \delta_i + (\varepsilon_i - \varepsilon) \qquad \textbf{(4.32)}$$

Such a situation occurs where the evaporation of a lake is balanced by the inflow of water from a river (Dead Sea, Lake Titicaca, Lake Chad). In this case $\alpha_i = 1$ because the inflow occurs without fractionation. The meaning and value of α has to be considered separately. It also describes the incongruent dissolution process which occurs in some groundwater systems. The result is simply understood by noting that steady state requires the input to be isotopically equal to the output ($R_i = \alpha R$).

Another important example is the fact that *evapotranspiration* (the phenomenon that water from the soil is taken up by a plant through capillary action of the plant vessels, and subsequently evaporates from the leaf surface) causes water to be transported by a plant from the soil to the air with no net isotope fractionation. The process is demonstrated by Fig.4.7.

The small diameter of the capillary results in a relatively high flow rate. This is essential, because it prevents the isotopically heavy leaf water to diffuse downward.

If there is no source, i = 0 and Eq.4.29 reduces to Eq.4.25a, the simple case with only one sink.

If the sink is absent, the isotopic composition approaches for $t \rightarrow \infty$ to $R = \alpha_i R_i$.

In the general cases where $i \neq u$, (for instance, slowly increasing or decreasing surface water bodies in which cases $\alpha_i = 1$), the resulting isotopic composition of the reservoir depends on the competition between sink and source. If $u < i$ and for $t \rightarrow \infty$, R approaches $\alpha_i R_i[1 + (u/i)\varepsilon]$, while in the opposite case ($u > i$): $R \rightarrow \infty$, as with the simple Rayleigh process discussed in Sect.4.4.1.

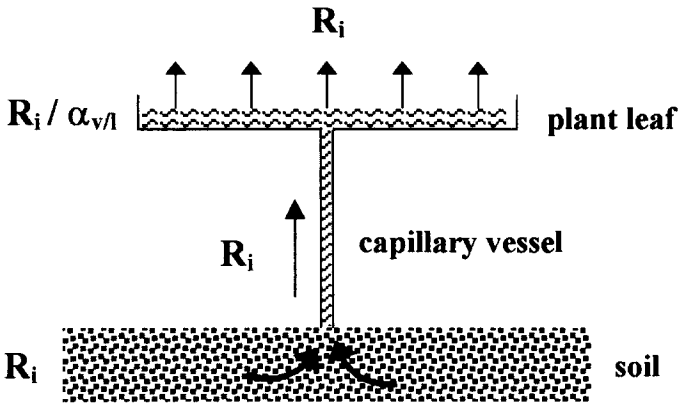

Fig.4.7 Schematic representation of the evapotranspiration process. The capillary flow of the soil water with isotope ratio R_i (for ^{18}O or ^{2}H) occurs without fractionation. At the surface of the plant leaf evaporation is accompanied by fractionation $A_{v/l}$ (Table 7.3 or 7.4). In a stationary state the escaping vapour should have the same R value as the transpired water. The result is that the (supposedly well-mixed) leaf water is enriched in ^{18}O and ^{2}H by $\alpha_{v/l}$.

4.4.4 RESERVOIR WITH ONE SOURCE AND ONE SINK, AS A FUNCTION OF MASS

If the Rayleigh process involves one source and one sink there is an alternative mathematical approach in which the isotopic composition is considered to be a function of changes in quantity N, rather than of time (Fig.4.6B). The isotope mass balance now gives:

$$RN + \alpha_i R_i(1 - f)dN = (R + dR)(N + dN) - \alpha R \cdot f dN$$

This results in the differential equation:

$$\frac{dR}{(\alpha f - 1)R + (1 - f)\alpha_i R_i} = \frac{dN}{N}$$

Integration and application of the boundary condition that $R = R_o$ at $N = N_o$ results in:

$$R = \frac{(1-f)\alpha_i}{1-\alpha f} R_i + \left[R_0 - \frac{(1-f)\alpha_i}{1-f} R_i \right] \left(\frac{N}{N_0} \right)^{\alpha f - 1} \qquad \textbf{(4.33)}$$

where N/N_0 denotes the remaining fraction of the original reservoir. A common example of this process in nature is represented by the evaporation of an isolated water body. With decreasing size of the reservoir N, R approaches:

$$R_\infty = \frac{(1-f)\alpha_i}{1-\alpha f} \qquad \textbf{(4.34)}$$

4.4.5 RESERVOIR WITH TWO SOURCES AND TWO SINKS, WITH AND WITHOUT FRACTIONATION

Finally we will treat the conditions at a stationary state, i.e. a situation in which in- and outflow of a well-mixed reservoir are balanced such that the isotopic composition of the reservoir compound has become constant in time (Fig.4.8). A practical example of this model is presented by a river in a tropical region where evaporation is significant, resulting in gradually increasing $^{2}\delta$ and $^{18}\delta$ values along the course of the river; α represents the evaporation and exchange with atmospheric vapour; I_0 is the original water flow rate at the river source.

The stationary state requires that the sinks and sources are balanced for the abundant as well as for the rare isotope. This condition is mathematically presented by:

$$I + dI + \frac{f}{1-f} dI = \frac{1}{1-f} dI + I$$

and

$$(R + dR)(I + dI) + \alpha_i R_i \frac{f}{1-f} dI = \alpha_u R \frac{1}{1-f} dI + RI$$

or

$$\left(\frac{\varepsilon_u + f}{1-f} R - \frac{\alpha_i f}{1-f} R_i \right) dI = I dR$$

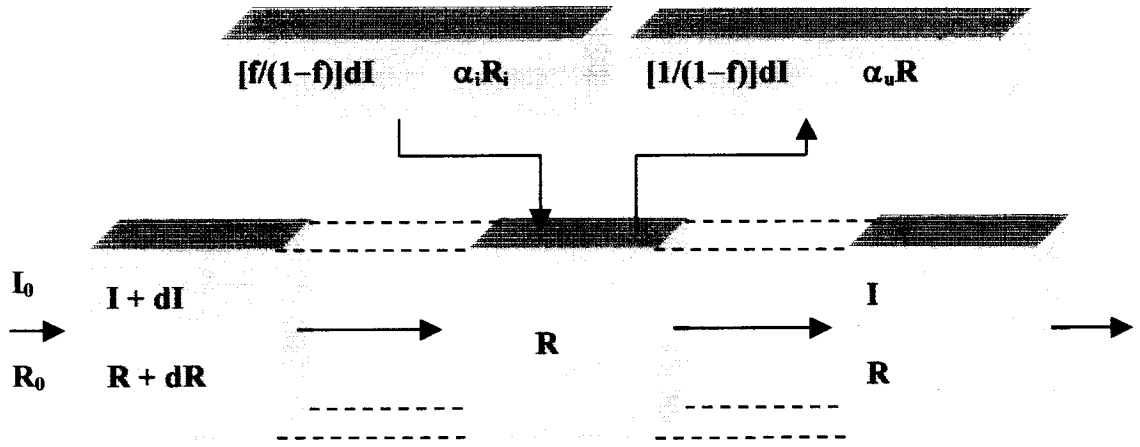

Fig.4.8 Model representing a well-mixed reservoir with simple in- and outflow as well as with a source and sink affecting the isotopic composition of the reservoir. For instance, during an infinitesimal time period dI has escaped from the (river) water into the air through evaporation and exchange with the ambient vapour.

Integration and applying the boundary condition $R = R_0$ at $I = I_0$ results in:

$$\ln \frac{\left[\frac{\varepsilon_u + f}{1-f} R - \frac{\alpha_i f}{1-f} R_i \right]}{\left[\frac{\varepsilon_u + f}{1-f} R_0 - \frac{\alpha_i f}{1-f} R_i \right]} = \frac{\varepsilon_u + f}{1-f} \ln \frac{I}{I_0}$$

Finally, after some rearrangement:

$$R = \frac{\alpha_i f}{\varepsilon_u + f} R_i + \left[R_0 - \frac{\alpha_i f}{\varepsilon_u + f} R_i \right] \left(\frac{I}{I_0} \right)^{\frac{\varepsilon_u + f}{1-f}} \qquad \textbf{(4.35)}$$

or

$$\delta = \frac{\alpha_i f}{\varepsilon_u + f}(1+\delta_i) + \left[1 + \delta_0 - \frac{\alpha_i f}{\varepsilon_u + f}(1+\delta_i)\right]\left(\frac{I}{I_0}\right)^{\frac{\varepsilon_u + f}{1-f}} - 1 \qquad \textbf{(4.36)}$$

The result of the last model calculation is shown in Fig.4.9 for δ and ε values as indicated in the graph. In the case of flowing river water that is subjected to evaporation, the value of f depends on the relative humidity. For the calculation of Fig.4.9, f has arbitrarily been chosen 0.5.

The difference between the simple, one-directional evaporation of Fig.4.4 is obvious: while in the former case the remaining δ of the remaining water approaches infinity, here the δ increase is very regular. The important result of comparing the trends for $^{18}\delta$ and $^{2}\delta$ with increasing I/I_0 will be discussed in Sect.7.5.

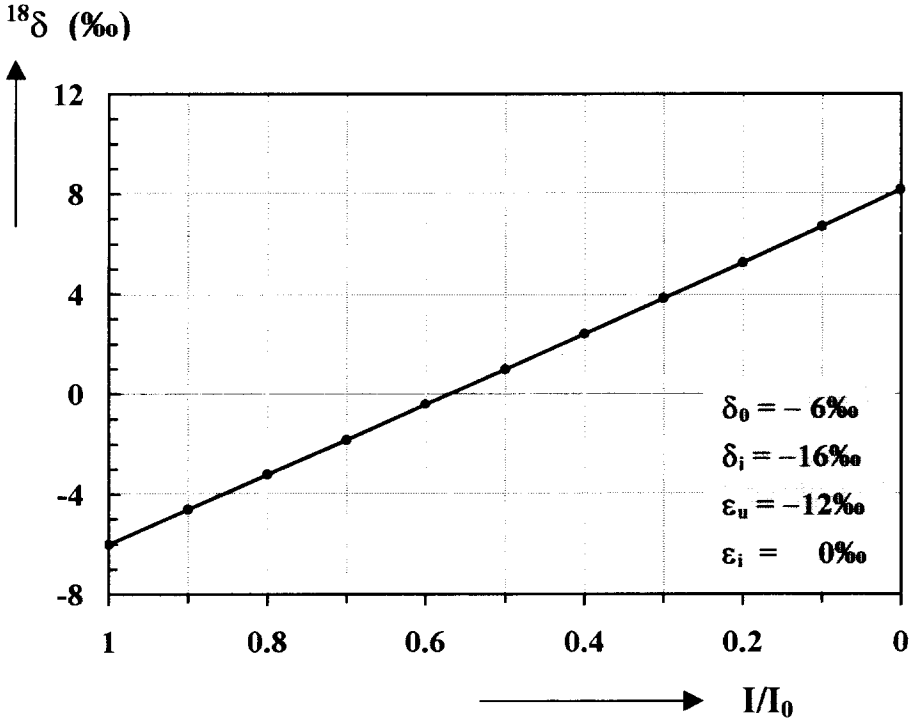

Fig.4.9 Result of the model of Fig.4.8, representing, for instance, a river which evaporates continuously during its course (Eq.4.36). The value of f has been chosen 0.5. The δ and ε values can be realistic. The shape of the curve is almost a straight line, contrary to the simple evaporation presented in Fig.4.4. A similar curve can be calculated for $^{2}\delta$. The ratio between these two curves will be discussed in Sect.7.5.

5 RADIONUCLIDE DECAY AND PRODUCTION

This section contains a brief review of relevant facts about radioactivity, i.e. the phenomenon of nuclear decay, and about nuclear reactions, the production of nuclides. For full details the reader is referred to textbooks on nuclear physics and radiochemistry, and on the application of radioactivity in the earth sciences (cited in the list of references).

5.1 NUCLEAR INSTABILITY

If a nucleus contains too great an excess of neutrons or protons, it will sooner or later disintegrate to form a stable nucleus. The different modes of radioactive decay will be discussed briefly. The various changes that can take place in the nucleus are shown in Fig.5.1 In transforming into a more stable nucleus, the unstable nucleus looses potential energy, part of its binding energy. This energy Q is emitted as kinetic energy and is shared by the particles formed according to the laws of conservation of energy and momentum (see Sect.5.3).

The energy released during nuclear decay can be calculated from the mass budget of the decay reaction, using the equivalence of mass and energy, discussed in Sect.2.4. The atomic mass determinations have been made very accurately and precisely by mass spectrometric measurement:

$$E = [M_{parent} - M_{daughter}] \times mc^2 \qquad \textbf{(5.1)}$$

with

$$1 \text{ amu} \equiv 931.5 \text{ MeV} \qquad \textbf{(5.2)}$$

Disintegration of a parent nucleus produces a daughter nucleus which generally is in an excited state. After an extremely short time the daughter nucleus looses the excitation energy through the emittance of one or more *γ (gamma) rays*, electromagnetic radiation with a very short wavelength, similar to the emission of light (also electromagnetic radiation , but with a longer wavelength) by atoms which have been brought into an excited state. In some cases, however, ß decay is directly to the ground state of the daughter nucleus, without the emission of γ radiation. Fig.5.2 shows the various decay schemes of some familiar nuclides.

5.2 NUCLEAR DECAY AND RADIATION

In the now following sections the various types of spontaneous nuclear disintegration will be discussed.

5.2.1 NEGATRON (β^-) DECAY

The most abundant decay mode is ß$^-$ decay, involving the emission of a negative electron, a *negatron or β^- (beta) particle* because of a transformation inside the nucleus of a neutron into a proton:

$$n \rightarrow p^+ + \beta^- + \bar{\nu} + Q \qquad \textbf{(5.3)}$$

This results in a daughter nucleus with equal A and a change in atomic number Z to Z+1, and the emission of an electron and an anti-neutrino. A (anti)neutrino is a particle with mainly a relativistic mass, i.e. *mass because of its motion*. (Neutrino's and negatrons have their spin anti-parallel to their direction of motion and anti-neutrino's and positrons parallel).

The total reaction energy Q is shared between the β particle and the (anti)neutrino. The consequence is that, although Q is a specific amount of energy, the energy spectrum of the ß$^-$ particles is continuous from zero to a certain maximum energy at $E_{\beta max} = Q$. The energy distribution is such that the maximum in this distribution is at an energy about one third of the maximum energy.

As mentioned above, in some cases the resulting daughter nucleus is not in an excited state, so that no γ radiation is emitted. This happens to be the case with the two isotopes that are relevant in isotope hydrology, viz. ^{3}H and ^{14}C.

5.2.2 POSITRON (β^+) DECAY

This type of nuclear transformation involves the emission of a *positron or β^+ (beta plus) particle* as the result of a transformation inside the nucleus of a proton into a neutron:

$$p^+ \rightarrow n + e^+ + \nu + Q \qquad \textbf{(5.4)}$$

and, because after slowing down the positron reacts fast with an electron anywhere present:

$$e^+ + e^- \rightarrow 2\gamma \qquad \textbf{(5.5)}$$

Here two electron masses are transformed into energy. The process is called *annihilation*, the energy released *annihilation energy*. With the mass of the electron

$$m_e = 5.4858026 \times 10^{-4} \qquad \textbf{(5.6)}$$

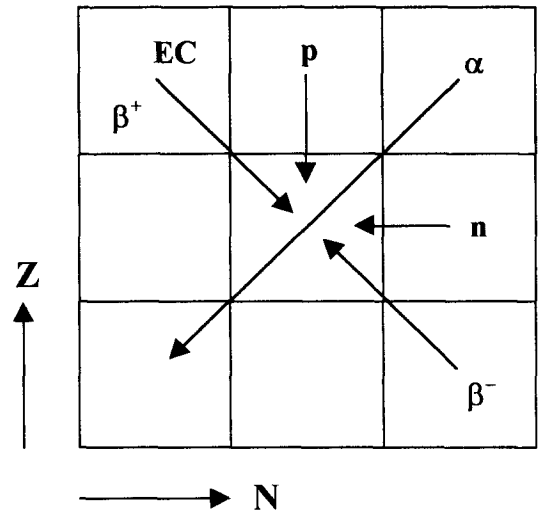

Fig.5.1 Different modes of radioactive decay visualised on one spot of the chart of nuclides (cf. Fig. 1.2). N is the number of neutrons, Z the number of protons.

the resulting energy is 1.022 MeV, which is represented by two oppositely directed γ particles of 511 keV each. This type of decay is, for instance, known from naturally occurring ^{40}K (Fig.5.2).

5.2.3 ELECTRON CAPTURE (EC)

The nucleus may pick up one electron from the atomic electrons circling the nucleus in consecutive shells. In that case the following reaction takes place:

$$p^+ + e^- \rightarrow n + \nu + Q \qquad \textbf{(5.7)}$$

Depending on from which atomic shell the electron is caught by the nucleus, electron capture is called K capture, L capture, and so on. β^+ decay and EC leave the mass number A of the nucleus unchanged, while Z becomes Z-1 (Fig.5.1). The atom is left in an excited state and returns to the ground state by emitting short-wave electromagnetic radiation, viz. low-energy γ rays or X rays. As in the previous decay modes, the excited state of the nucleus causes the emission of one or more γ rays.

5.2.4 ALPHA (α) DECAY

α (alpha) decay involves the emission of an *α particle* (a ^4He nucleus):

$$^{A}_{Z}X \rightarrow {}^{A-4}_{Z-2}Y + {}^{4}_{2}He \qquad \textbf{(5.8)}$$

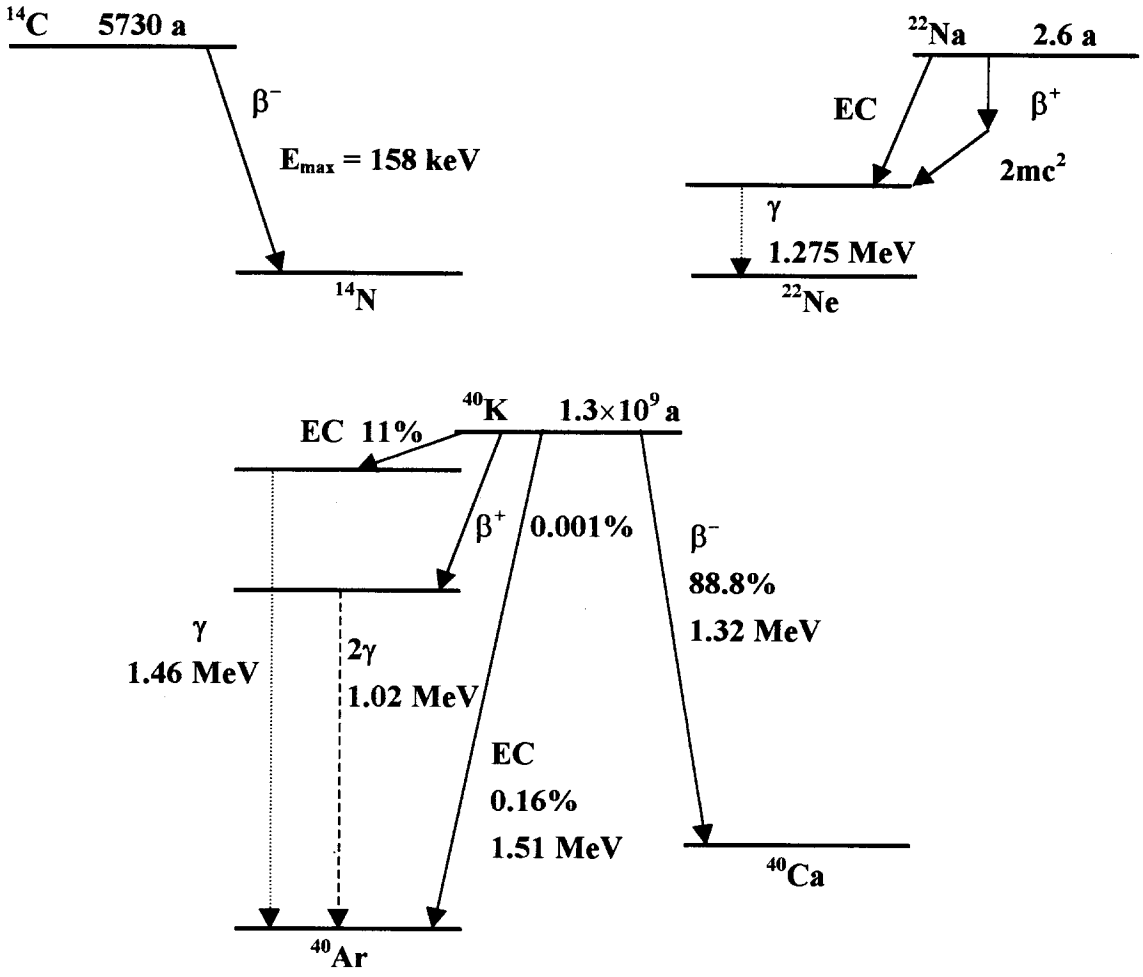

Fig.5.2 Decay schemes for some nuclides obeying β^-, β^+ or EC decay, the latter example of ^{40}K in branching decay, and the consecutive γ radiation by the excited daughter nucleus as well as the formation of 2 γ by annihilation of an emitted β^+ particle.

This type of decay occurs primarily within the heavy elements such as in the uranium and thorium series. The emission of the heavy α particle practically coincides with the emission of relatively large-energy γ rays.

Because as in all cases the reaction energy Q is shared by the atoms Y and He according to the two conservation laws, the case of α emission is special. As with a gun shot, where the rifleman feels a large momentum against his shoulder, the daughter nucleus receives a relatively large so-called *recoil*. This is particularly important where the *recoil energy* is large enough to loose the daughter nucleus from its chemical bond. This phenomenon is the basis for studying the natural abundance of the decay nuclides of uranium and thorium. In Sect.5.3 we will deal with recoil energy quantitatively.

5.2.5 SPONTANEOUS AND INDUCED FISSION, NEUTRON EMISSION

Nuclides of the heavy elements have the possibility of breaking up into two relatively large daughter nuclei together with the emission of a number of neutrons. This decay may occur spontaneously as well as induced by the bombardment of the parent nucleus by a neutron from elsewhere, for instance from a neighbouring nucleus. This is the dominant process in nuclear reactors (Sect.5.4.2; Chapter 12).

5.3 RECOIL BY RADIOACTIVE DECAY

In the preceding chapter we mentioned the phenomenon of the recoil momentum and energy which any decaying nucleus experiences. However, in the case of a heavy particle such as the α particle leaving the nucleus, the effect is not negligibly small. We will now calculate the recoil energy by considering the classical mechanics of this process (Fig.5.3).

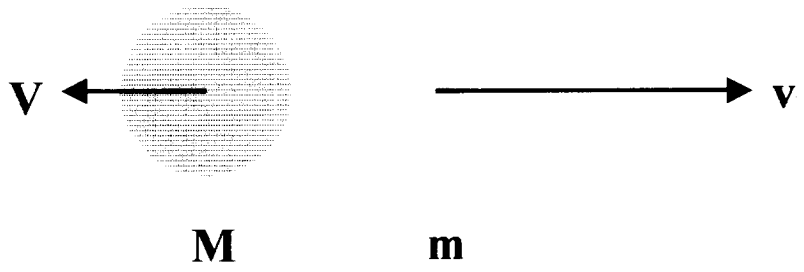

Fig.5.3 After radioactive decay the daughter nucleus M and the smaller emitted particle m (for instance, an α particle) move in opposite direction, together carrying the decay energy as the respective kinetic energies.

The *principle of conservation of momentum* requires:

$$MV + mv = 0 \qquad \text{or} \qquad M^2V^2 = m^2v^2 \tag{5.9}$$

while the *principle of conservation of energy* requires the decay energy to be equal to the sum of the two kinetic energies:

$$E_{decay} = \tfrac{1}{2} MV^2 + \tfrac{1}{2} mv^2 = E_M + E_m \tag{5.10}$$

From Eq.5.9 we have:

$$E_M = \frac{1}{2}MV^2 = \frac{1}{2M}M^2V^2 = \frac{1}{2M}m^2v^2 = \frac{m}{M}E_m \tag{5.11}$$

With Eq.5.10:

$$E_{decay} = \left(1 + \frac{m}{M}\right) E_m$$

so that the two particle energies are, respectively:

$$E_m = \frac{M}{M+m} E_{decay} \qquad \text{and} \qquad E_M = \frac{m}{M+m} E_{decay} \tag{5.12}$$

In the case of the α decay of ^{238}U with a decay energy of about 4.2 MeV, the daughter nucleus, ^{234}Th, receives a recoil energy of [4/(234+4)] × 4.2 MeV = 71 keV, more than enough to break the chemical bond between the Th atom and the surrounding atoms in the mineral (see Sect.12.14 and Volume 4 on Groundwater) for a discussion of the consequences.

5.4 NUCLEAR REACTIONS

The overall principle of a *nuclear reaction* is that a nucleus is bombarded by a particle that is in the first instance taken up by the nucleus to form a *compound nucleus*. This does not result in a stable particle. Within an extremely short time the compound nucleus will loose the excess energy by the release of one or more particles, ultimately forming a new nuclide. The bombarding particles may be "man-made" and originate from a nuclear particle accelerator (electrically charged particles) or a nuclear reactor (high- or low-energy neutrons), or may be from natural origin.

A few examples may serve to show the convention of writing nuclear reactions:

$$^{36}Ar + n \rightarrow p + {}^{36}Cl \qquad \text{or} \qquad {}^{36}Ar(n,p)^{36}Cl$$

$$^{40}Ca + n \rightarrow \alpha + {}^{37}Ar \qquad \text{or} \qquad {}^{40}Ca(n.\alpha)^{37}Ar \tag{5.13}$$

$$^{40}Ar + n \rightarrow 2n + {}^{39}Ar \qquad \text{or} \qquad {}^{40}Ar(n,2n)^{39}Ar$$

5.4.1 NATURAL PRODUCTION

Nature is constantly and intensively performing nuclear reactions. The bombarding particles originate from two sources:

1) from **cosmic radiation**, an avalanche of fragments of atmospheric nuclei, a wide range of particles from photons and electrons to neutrons and mesons. These are primarily produced as secondary and tertiary particles in the upper atmosphere in a process called

spallation, by very-high-energy cosmic protons and a smaller percentage of helium nuclei from the sun, from further away in our Galaxy and probably from extragalactic space. Mesons reaching the earth surface have a very high penetrating power and can be observed at great depth below the ground or water surface.

Variations in cosmic radiation occur because the origin is to be found in events such as solar flares and supernova explosions. Also indirectly does the sun influence the cosmic ray flux in the atmosphere. The fact is that part of the incoming primary particles are deflected away from the earth by the earth' magnetic field, which has not been entirely constant through geologic times. The variable magnetic field of the sun now adds to the variations in the earth' magnetic field and thus in the shielding capacity of the earth against cosmic particles.

Cosmic radiation produces radioactive nuclei in the atmosphere primarily through two different types of reactions:

(i) high-energy reactions by the secondary particles such as protons, neutrons and He nuclei bombarding atmospheric nuclei (N, O, Ar); these reactions are the origin of the atmospheric abundance of nuclides such as ^{3}H, ^{7}Be, ^{26}Al, ^{32}Si, ^{39}Ar and ^{85}Kr;

(ii) low-energy reactions by thermal neutrons, of which the production of ^{14}C in the air is the best known example.

These reactions will be discussed later together with the specific treatment of the various isotopes (Chapters 8 and 12).

2) from **nuclear decay particles**, primarily neutrons from spontaneous decay of nuclides of the uranium, actinium and thorium decay series. These processes occur underground depending on the U or Th content of the soil minerals (Chapter 12).

5.4.2 ANTHROPOGENIC RELEASES OF RADIONUCLIDES

Also man has become able to produce nuclei and even elements, presently unknown in nature, on a small scale in the laboratory, but also on a large scale in the natural environment by the test explosion of nuclear weapons.

The anthropogenic releases of radioactivity are related to these nuclear weapons testings as well as to the regular or incidental releases by nuclear (power) industries.

The release of radioactivity related to the testing of nuclear weapons has two main causes, viz.:

1) **Fission bombs**, based on the neutron-induced fission reaction of uranium or plutonium:

$$^{235}U + n \rightarrow \text{nucleus with } A \approx 85 - 100 + \text{nucleus with } A \approx 130 - 145 + \text{neutrons}$$

and likewise

$$^{239}Pu + n \rightarrow \text{nucleus with } A \approx 95 - 105 + \text{nucleus with } A \approx 132 - 142 + \text{neutrons}$$

Well-known examples of radioactive nuclides as products of the asymmetrical mass distribution of the long-living fission products are ^{93}Zr and ^{99}Tc on the one hand, and ^{129}I and ^{137}Cs on the other. Industrial activities concerning nuclear power production and fuel reprocessing may bring on a small scale nuclear waste materials in the environment, similar to those that are being produced by the bomb explosions.

A special case of nuclear waste release is the occurrence of nuclear reactor incidents. In some cases (Chernobyl in 1986) sufficient radioactivity was injected into the environment to detect certain isotopes in nature, for instance in sediments and ice cores.

2) During the nuclear explosions especially the neutron density in the surrounding air is sufficiently high to **produce radioactive nuclides** that are also being made by nature itself:

$$^{14}N + n \rightarrow {}^{12}C + {}^{3}H \qquad \text{or} \qquad {}^{14}N(n,{}^{3}H){}^{12}C$$

and

$$^{14}N + n \rightarrow {}^{14}C + {}^{1}H \qquad \text{or} \qquad {}^{14}N(n,p){}^{14}C$$

^{3}H (tritium) and ^{14}C (radiocarbon), and other cosmogenically as well as anthropogenically produced isotopes will be discussed in detail in Chapter 8 and 12.

6 EQUATIONS OF RADIOACTIVE DECAY AND GROWTH

The mathematical expressions presented in this chapter are generally applicable to all those processes in which the transition of the *parent nucleus* to a *daughter nucleus* , i.e. the process of radioactive decay, is governed by statistical chance. This chance of decay is equivalent to the degree of instability of the parent nucleus. Each radioactive nuclide has its specific degree of instability which, as we will see, is going to be expressed by the half-life assigned to this nuclide.

The radioactivity of a sample is more complicated if it consists of two or more components, such as: (i) in the case of a mixture of independent activities, (ii) if one specific type of nuclide shows two modes of decay, so-called branching decay, and (iii) if we are dealing with a nuclear decay series in which also the daughter nuclides are radioactive. All these phenomena will be discussed separately.

6.1 LAW OF RADIOACTIVE DECAY

The fundamental law of radioactive decay is based on the fact that the decay, i.e. the transition of a parent nucleus to a daughter nucleus is a purely statistical process. The disintegration (decay) probability is a fundamental property of an atomic nucleus and remains equal in time. Mathematically this law is expressed as:

$$dN = \lambda N \cdot dt \tag{6.1}$$

and

$$\lambda = \frac{(-dN/dt)}{N} \tag{6.2}$$

where N is the number of radioactive nuclei, -dN/dt the decrease (negative) of this number per unit of time and λ is thus the probability of decay per nucleus per unit of time. This *decay constant* λ is specific for each decay mode of each nuclide.

The *radioactivity* or *decay rate* is defined as the number of disintegrations per unit of time:

$$A = -dN / dt = \lambda N \tag{6.3}$$

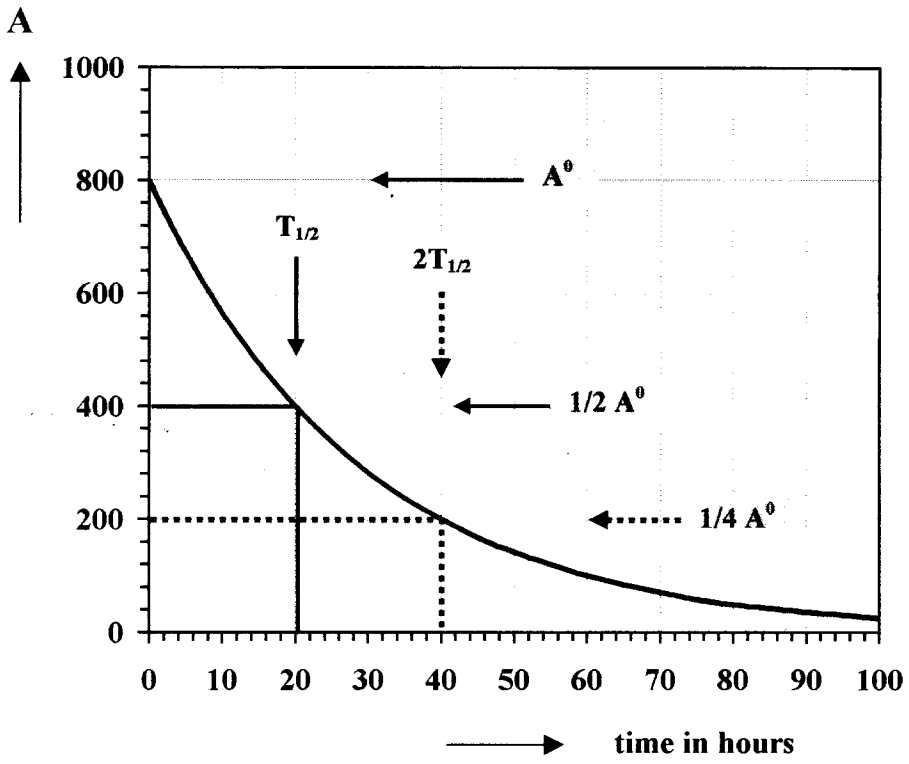

Fig.6.1 The rate of radioactive decay. After each subsequent half-life of 20 hours the number of radioactive nuclei and the original radioactivity of 800 units are divided into half.

By integration of this relation and applying the boundary conditions that at in the beginning t = 0 and $N = N^0$ we obtain:

$$\ln(N/N_0) = -\lambda t \qquad \textbf{(6.4)}$$

and subsequently the equation of *exponential decay*:

$$N = N^0 e^{-\lambda t} \qquad \textbf{(6.5)}$$

or using Eq.6.3:

$$A = A^0 e^{-\lambda t} \qquad \textbf{(6.6)}$$

The time during which A^0 decreased to A (= the age of the material) is:

$$T = (1/\lambda)\ln(A/A_0) \qquad \textbf{(6.7)}$$

The relations of Eqs.6.5 and 6.6 indicate the rate at which the original number of radioactive nuclei (N^0) and the original radioactivity (A^0) decrease in time (Fig.6.1).

6.2 HALF-LIFE AND MEAN LIFE

It is a common practice to use the *half-life* ($T_{1/2}$) instead of the decay constant (λ) for indicating the degree of instability or the decay rate of a radioactive nuclide. This is defined as the period of time in which half of the radioactivity has disappeared (half of the nuclei have disintegrated, Fig.6.1):

$$T_{1/2} = (-1/\lambda)\ln(1/2) \tag{6.8}$$

from which:

$$\lambda = \frac{\ln 2}{T_{1/2}} = \frac{0.693}{T_{1/2}} \tag{6.9}$$

The *mean life* of a nuclide is the sum of the life times of a certain number of nuclei (before they have all disintegrated) divided by the number of nuclei. During the time interval dt a number of dN nuclei disintegrate. These "lived" during a period t, which amounts to a total life time for dN nuclei of (cf. Eq.6.3):

$$t \cdot dN = t \cdot \lambda N \cdot dt$$

Integrating over all nuclei (N) gives the mean life (time):

$$\begin{aligned} \tau &= \frac{1}{N^0}\int_0^\infty t \cdot \lambda N \cdot dt = \lambda \int_0^\infty t \cdot e^{-\lambda t} dt = \lambda\left\{-\frac{t}{\lambda}e^{-\lambda t}\Big|_0^\infty + \frac{1}{\lambda}\int_0^\infty e^{-\lambda t} dt\right\} \\ &= \lambda\left\{0 + \frac{1}{\lambda}\left(-\frac{1}{\lambda}e^{-\lambda t}\Big|_0^\infty\right)\right\} = \frac{1}{\lambda} \end{aligned} \tag{6.10}$$

As an example, the mean life of a ^{14}C nucleus with $T_{1/2}$ = 5730 a is 8267 years. Then λ = 1/8267, which means that a sample activity decreases by 1‰ in about 8 years; a ^{3}H sample activity ($T_{1/2}$ = 12.43 a) decreases by 5.6% per year.

6.3 ACTIVITY, SPECIFIC ACTIVITY AND RADIONUCLIDE CONCENTRATION

The *activity* of a certain sample is the number of a radioactive disintegrations per sec for the sample as a whole. The *specific activity*, on the other hand, is defined as the number of disintegrations *per unit weight or volume* of sample (see spec.act. of ^{14}C and ^{3}H, Chapter 8). The unit of radioactivity is the *Becquerel* (Bq), which is defined as a decay rate of one disintegration per second (dps) or the now obsolete Curie (Ci) which was defined as a decay rate of 3.7×10^{10} dps.

As an example of the relation between the specific activity of a sample and the actual *concentration* of the radioactive nuclide, we will calculate the specific tritium (^3H) activity of water containing one ^3H atom per 10^{18} hydrogen atoms (equivalent to 1 TU = Tritium Unit (Chapter 8):

$$A_{spec} = \lambda N \text{ (per litre)}$$

where:

$\lambda = (\ln 2)/T_{1/2} = (\ln 2)/12.43$ a (1 year = 3.16×10^7 s)
$N = 2 \times 10^{-18} \times (G/M) \times A$ (G/M = number of moles)
A = Avogadro's number = 6.02×10^{23}/mol
M = molecular weight = 18.0
pCi = pico-Curie = 10^{-12} Curie = 3.7×10^{-2} dps = 0.037 Bq

The numerical result for water with 1 TU of tritium is:

$$A_{spec} = 0.118 \text{ Bq/L} = 3.19 \text{ pCi/L} \qquad \textbf{(6.11)}$$

As another example we can calculate the ^{14}C concentration in carbon, which has a specific ^{14}C activity of 13.56 dpm per gram of carbon (in the year AD 1950) (see ^{14}C standard activity, Chapter 8):

$$\frac{^{14}C}{C} = \frac{13.56 \times 5730 \times (3.16 \times 10^7) \times 12}{60 \times \ln 2 \times (6.02 \times 10^{23})} = 1.2 \times 10^{-12} \qquad \textbf{(6.12)}$$

6.4 MIXTURE OF INDEPENDENT RADIOACTIVITIES

Fig.6.2 shows a semi-logarithmic decay curve of a mixture of two activities that are completely independent, a *composite decay curve*. If the half-life values are sufficiently apart, it is seen to be possible to unravel the two separate decay curves, starting at the right-hand side of the curve, where the one activity has already disappeared. Subtracting the straight semi-logarithmic curve from the composite curve gives the straight line for the shorter-lived nuclide.

6.5 BRANCHING DECAY

Also in nature radioactive nuclides exist that show two different modes of decay. One example is presented by ^{40}K that can decay with the emission of a β^- or a β^+ particle (Fig.5.1).

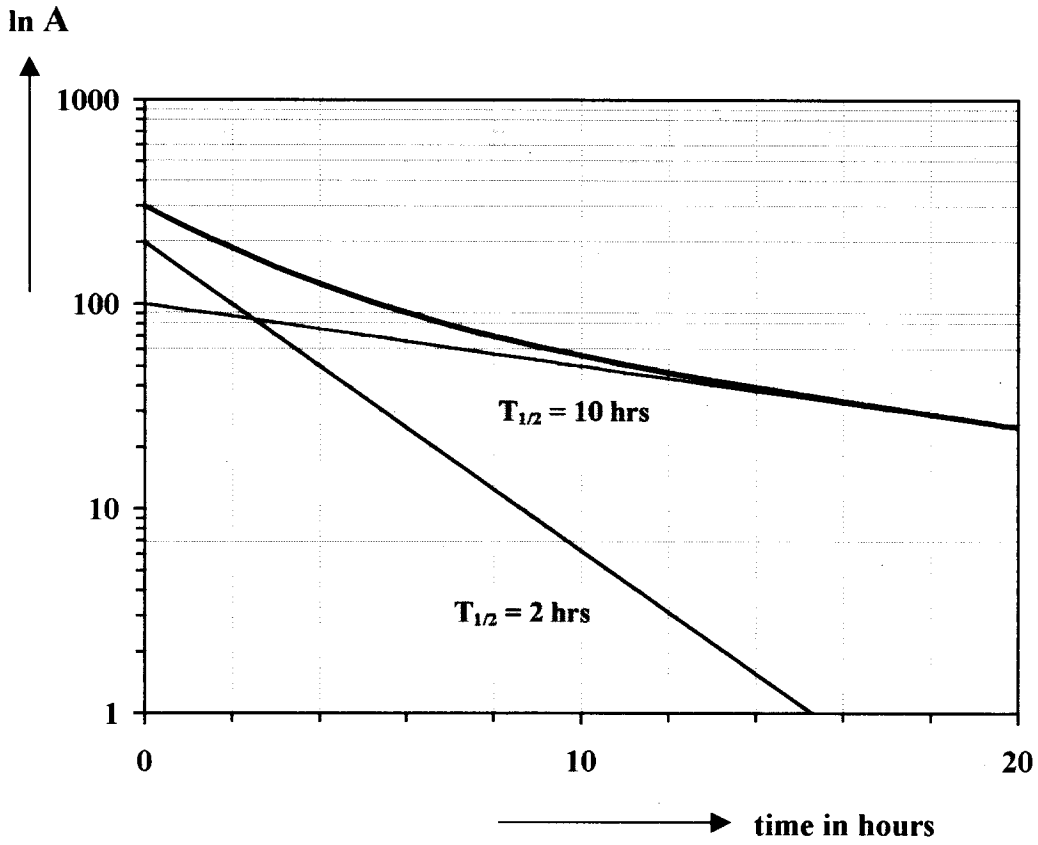

Fig.6.2 Semi-logarithmic plot of a composite decay curve for a mixture of two independent radioactive compounds with half-lives of 2 and 10 hours. The longer-lived activity can be subtracted from the sum curve (heavy line) to produce the semi-logarithmic straight decay curve for the shorter-lived nuclide.

Each decay mode has its specific decay constant or half-life. The total decay is simply the sum of both single chances and is thus given by:

$$\lambda_{total} = \lambda_1 + \lambda_2 \qquad \textbf{(6.13)}$$

and the total half-life consequently by:

$$(1/T_{1/2})_{total} = (1/T_{1/2})_1 + (1/T_{1/2})_2 \qquad \textbf{(6.14)}$$

6.6 RADIOACTIVE DECAY SERIES

If a radioactive nuclide is situated in the Chart of Nuclides far from the stability line (for the light elements at Z=N), the daughter nucleus after radioactive decay may be radioactive as well. In nature this occurs with the heavy nuclides in the uranium and thorium decay series (Chapter 12). Here the original decay of ^{238}U or ^{232}Th is followed by a series of radioactive decay products. Fig.6.3 shows schematically how the elements of such decay series are related.

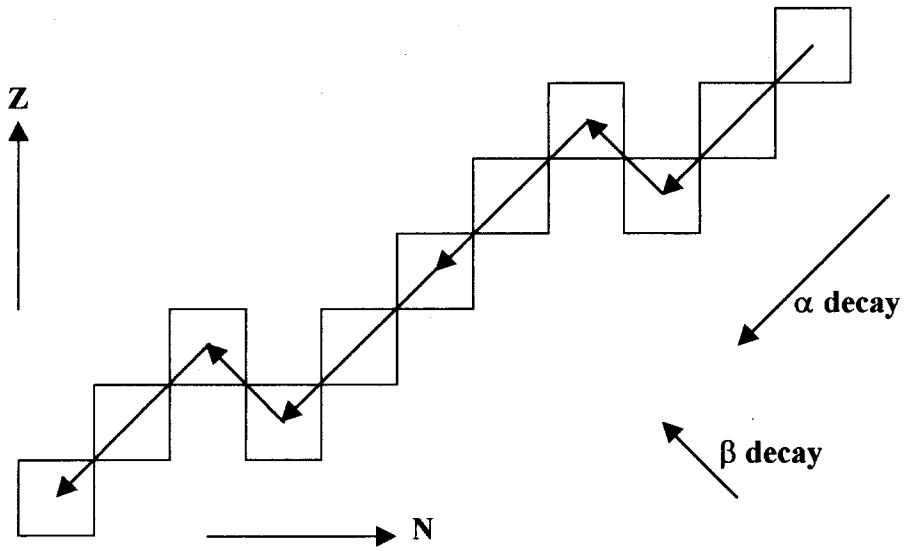

Fig.6.3 Schematic representation of a hypothetical multiple decay curve, analogous to the decay curves of the U and Th decay series (Sect.12.14-12.16).

In this context we can restrict ourselves to one element from the multiple decay chain: the relation between a parent and a daughter activity. The relations in a second and higher degree have been treated elsewhere (see textbooks by Friedlander et al. and by Faure).

The parent nucleus decays according to the equations of radioactive decay which we have treated in this section:

$$A_1 = -\frac{dN_1}{dt} = \lambda_1 N_1 \qquad \textbf{(6.15)}$$

and

$$N_1 = N_1^0 e^{-\lambda_1 t} \qquad \text{and} \qquad A_1 = A_1^0 e^{-\lambda_1 t} \qquad \textbf{(6.16)}$$

The amount of daughter nuclei is determined by two processes: (i) radioactive decay and (ii) radioactive growth by decay of the parent nuclei, respectively:

$$\frac{dN_2}{dt} = -\lambda_2 N_2 + \lambda_1 N_1 \qquad \textbf{(6.17)}$$

The solution of this differential equation is:

$$N_2 = \frac{\lambda_1}{\lambda_2 - \lambda_1} N_1{}^0 \left(e^{-\lambda_1 t} - e^{-\lambda_2 t}\right) + N_2{}^0 e^{-\lambda_2 t} \qquad \textbf{(6.18)}$$

while at zero activity at zero time ($N_2^0 = 0$):

$$A_2 = \lambda_2 N_2 = \frac{\lambda_2}{\lambda_2 - \lambda_1} A_1^0 \left(e^{-\lambda_1 t} - e^{-\lambda_2 t}\right) \qquad \textbf{(6.19)}$$

The last term represents the decay of the amount of daughter nuclide that was present at the time t = 0. It is obvious that the ratio between λ_1 and λ_2 is the dominating factor that determines the course of the daughter activity in time. We shall now briefly mention the 3 different cases for this ratio.

6.6.1 SECULAR EQUILIBRIUM

This type of relation between parent and daughter activity occurs when the half-life of the parent nuclide is infinitely larger than that of the daughter nuclide. Examples are the relations between the long-living isotopes of uranium and thorium, ^{238}U, ^{235}U and ^{232}Th, and their decay products (see Chapter 12):

$$\lambda_1 << \lambda_2$$

Eq.6.16 properly describes the parent activity in time, whereas Eq.6.19 turns into:

$$A_2 = A_1^0 \left(e^{-\lambda_1 t} - e^{-\lambda_2 t}\right) \qquad \textbf{(6.20)}$$

or for $\lambda_1 = 0$,

$$A_2 = A_1^0 \left(1 - e^{-\lambda_2 t}\right) \qquad \textbf{(6.21)}$$

describing the growth of the daughter activity in time if we take $A_2 = 0$ in the beginning. Fig.6.4 shows the courses of both activities. Finally (at $t \rightarrow \infty$ with $\lambda_2 t \rightarrow \infty$ in Eq.6.20) the daughter activity reaches a value of:

$$A_2 = A_1^0 e^{-\lambda_1 t} = A_1 \qquad \textbf{(6.22)}$$

in other words, parent and daughter activity become equal.

The phenomenon that in a sample containing a long-living nuclide a short-living daughter activity may grow is applied, for instance in cases where the radioactivity measurement of the daughter nuclide is easier than that of the parent activity. Such case is the activity determination of ^{32}Si with a half-life of about 140 years, which decays through a low-energetic β^- decay to ^{32}P with a half-life of 14.3 days and a high-energetic β^- decay. Eq.6.21 shows that after separating chemically a pure ^{32}Si activity ^{32}P is growing into this sample at a

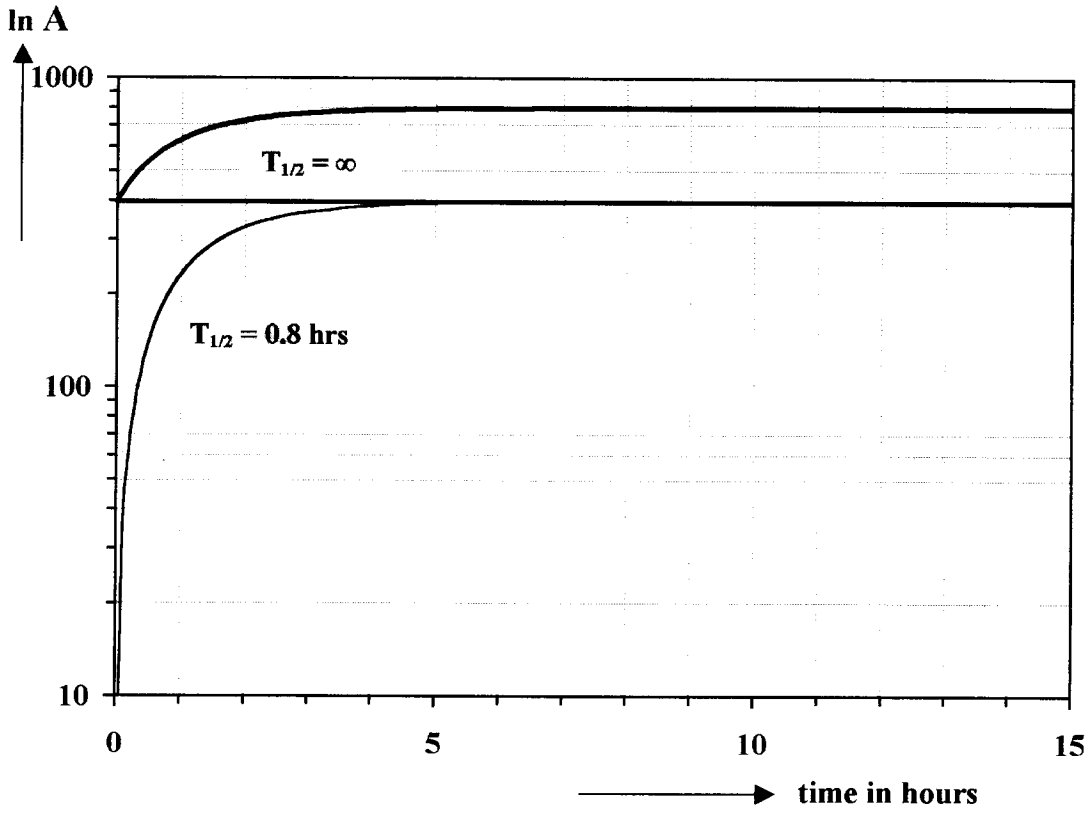

Fig.6.4 Relation between the radioactivities of a parent (straight line) and a daughter nuclide when the parent nuclide decays infinitely slow as compared to the daughter nuclide (half-lives of ∞ and 0.8 hours, respectively), i.e. the case of secular equilibrium. The upper line represents the sum of parent and daughter activity.

rate such that after one daughter half-life the daughter activity has increased to 50 % of its maximum value of A_1:

$A_2 = 1/2\ A_1$ after one $T_{1/2}$

$A_2 = 3/4\ A_1$ after two $T_{1/2}$

$A_3 = 7/8\ A_1$ after three $T_{1/2}$, and so on.

This consideration gives the time required to gain sufficient daughter activity for a proper measurement after chemical separation of the parent and daughter nuclides.

6.6.2 TRANSIENT EQUILIBRIUM

In this case, the half-life of the parent nuclide is still larger than that of the daughter nuclide but not infinitely:

$\lambda_1 < \lambda_2$

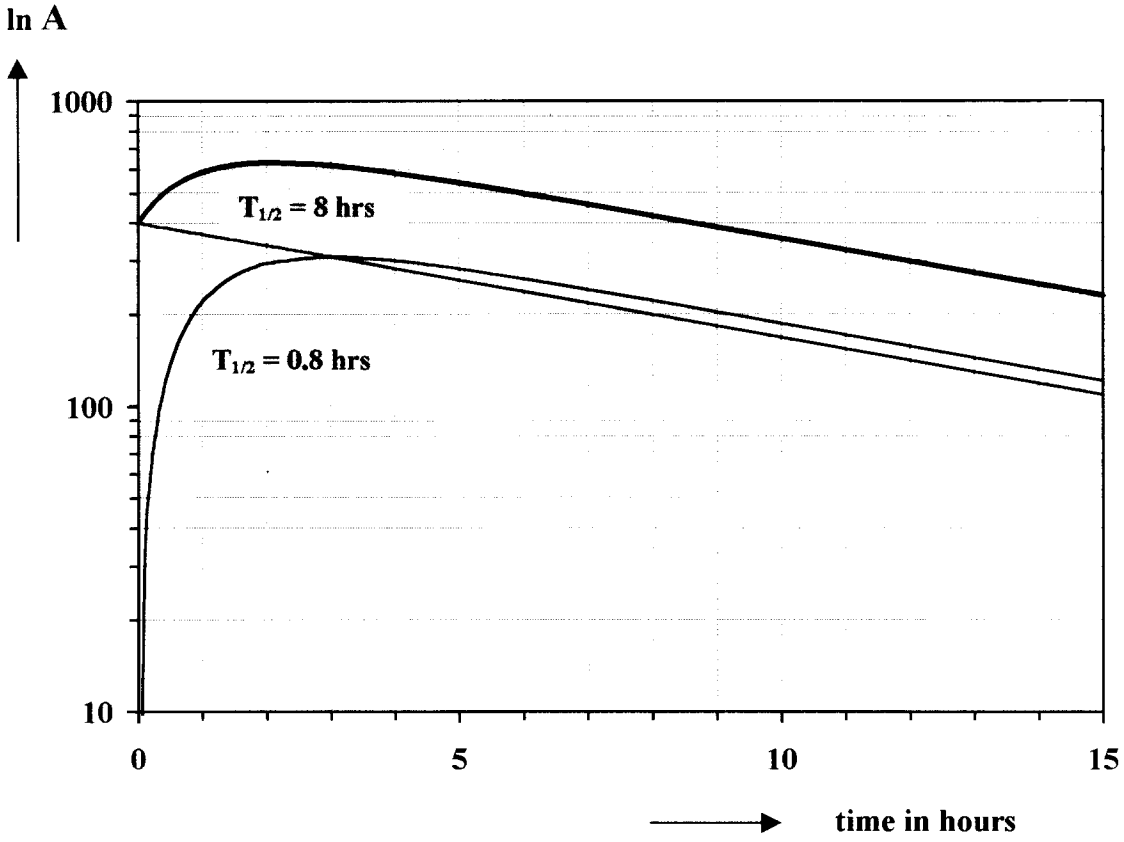

Fig.6.5 Relation between the radioactivities of a parent and a daughter nuclide, when the half-life of the parent is larger (but not infinitely) than that of the daughter (half-lives of 8 and 0.8 hours, respectively): the case of transient equilibrium. The heavy line shows the sum activity of parent and daughter.

Growth of the daughter after zero activity at zero time now occurs according to Eq.6.19. A stationary state is reached after sufficient time in which the daughter activity is larger than the parent activity, as is to be expected. Fig.6.5 shows the course of both activities:

$$A_2 = \frac{\lambda_2}{\lambda_2 - \lambda_1} A_1^0 e^{-\lambda_1 t} = \frac{\lambda_2}{\lambda_2 - \lambda_1} A_1 \qquad \textbf{(6.23)}$$

6.6.3 NO-EQUILIBRIUM

Here the half-life of the daughter nuclide is larger than that of the parent:

$$\lambda_1 > \lambda_2$$

The daughter activity is growing in the sample according to Eq.6.19 (Fig.6.6).

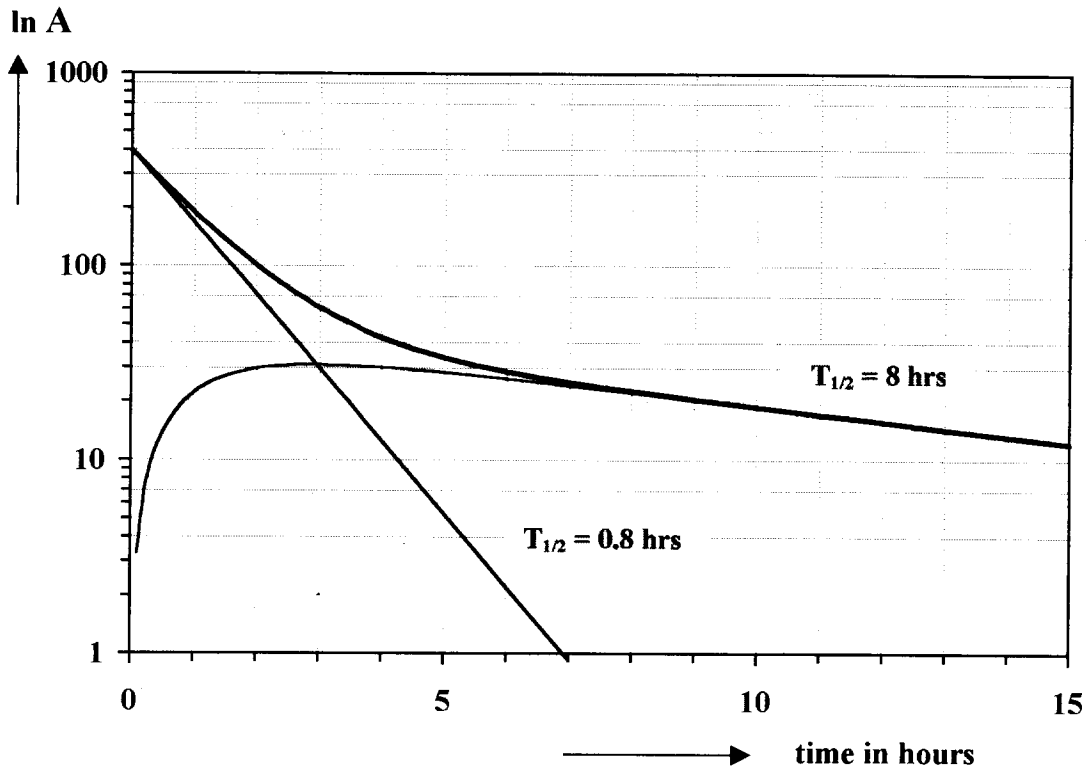

Fig.6.6 Relation between the radioactivities of a parent and a daughter nuclide, when the half-life of the daughter exceeds that of the parent (half-lives of 8 and 0.8 hours, respectively): the case of no-equilibrium. The straight line is the semi-logarithmic plot of the parent activity. The upper curve is the total activity of the mixture.

Finally, after sufficiently long time, only daughter activity will be left, since the parent activity is disappearing at a higher rate:

$$A_2 = \frac{\lambda_2}{\lambda_1 - \lambda_2} A_1^0 e^{-\lambda_2 t} \qquad \textbf{(6.24)}$$

After a period of t_{max} the daughter activity reaches a maximum value for:

$$\frac{dA_2}{dt} = 0 = \frac{-\lambda_1\lambda_2}{\lambda_2 - \lambda_1} A_1^0 e^{-\lambda_1 t_{max}} + \frac{\lambda_2^{\,2}}{\lambda_2 - \lambda_1} A_1^0 e^{-\lambda_2 t_{max}}$$

or

$$\lambda_1 e^{-\lambda_1 t_{max}} = \lambda_2 e^{-\lambda_2 t_{max}} \qquad \textbf{(6.25)}$$

The maximum value of the daughter activity is thus reached at:

$$t_{max} = \frac{1}{\lambda_2 - \lambda_1} \ln \frac{\lambda_2}{\lambda_1} \qquad \textbf{(6.26)}$$

Inserting Eq.6.25 in Eq.6.19 shows that at the time this maximum is reached, the parent and daughter activity are equal (Fig.6.6).

6.7 ACCUMULATION OF STABLE DAUGHTER PRODUCT

A special case of "no-equilibrium" as discussed in the preceding paragraph occurs if the daughter product is not radioactive, in other words:

$$\lambda_2 = 0$$

This can be illustrated by two examples, (i) the accumulation of ^{40}Ar during the decay of ^{40}K in rock (Fig.6.2) and the accumulation of ^{3}He in water during the decay of ^{3}H. We will take the latter process as an example to calculate the age of a sample from the remaining parent activity and the accumulated amount of daughter product.

Starting from the general relation of Eq.6.18 or 6.19 we can simply correct for $\lambda_2 = 0$ and the absence of an original quantity of daughter (a hard condition for a successful application of the dating methods mentioned):

$$N_2 = N_1^0 \, (1 - e^{-\lambda_1 t}) \qquad \textbf{(6.27)}$$

where the amount of gas accumulated (V in litres STP) is related to the number of atoms N_2 by:

$$V = \frac{N_2}{6 \times 10^{23}} 22.4 \ \text{L}$$

Since, instead of the original ^{3}H activity, the activity after the unknown period of time is known (to be measured), N_1^0 in Eq.6.27 has to be replaced by N_1, and subsequently N_1 by the activity ($A_1=\lambda N_1$), so that:

$$\frac{6 \times 10^{23}}{22.4} V = N_1 e^{\lambda T} (1 - e^{-\lambda T}) = \frac{A_1}{\lambda} e^{+\lambda T} (1 - e^{-\lambda T}) = \frac{A_1}{\lambda} (e^{\lambda T} - 1)$$

The period of time elapsed since time zero (the "age" T) is:

$$T = \frac{1}{\lambda} \ln \left(2.7 \times 10^{22} \frac{\lambda}{A_1} V + 1 \right) \qquad \textbf{(6.28)}$$

This dating method –especially applied in oceanography, but recently also in hydrology (Schlosser et al., 1998)– makes a very strong appeal to the experimental (mass spectrometric) technique, as the amount of ^{3}He produced is extremely small. This is shown here by an example of one litres of water with a present-day ^{3}H activity of 100 TU which over a period of 20 years has accumulated of 5.1×10^{-10} mL STP (0°C and 1033 hPa) of ^{3}He.

6.8 RADIOACTIVE GROWTH

For the sake of completeness we will mention here the production of radionuclides by nuclear reactions, because this phenomenon is, from a mathematical point of view, very similar to the case of secular equilibrium as discussed in Sect.6.6.1, if the production rate (P) is constant. The reactions may take place in a nuclear particle accelerator or in a nuclear reactor. The production rate of the radionuclide is:

$$\frac{dN}{dt} = P - \lambda N \qquad \textbf{(6.29)}$$

where N is the number of radioactive nuclei and λ is the decay constant. Similar to Eq.6.21, the solution for the activity produced is:

$$\lambda N = A = P(1 - e^{-\lambda t}) \qquad \textbf{(6.30)}$$

At time approaches infinity, a stationary is being reached in which the radionuclide production and decay are equal. Thus, at $t = \infty$:

$$A_{max} = P \qquad \textbf{(6.31)}$$

This is shown in Fig.6.7, representing the course of the radioactivity in time, comparably to Fig.6.4.

The time required to produce certain fractions of the maximum attainable activity is now:

$A = 1/2\ P = 1/2\ A_{max}$ after one half-life

$A = 3/4\ P$ after a period of time $= 2T_{1/2}$

$A = 7/8\ P$ after $3T_{1/2}$, and so on.

This means that after 3 half-lives the maximum attainable activity has practically been reached.

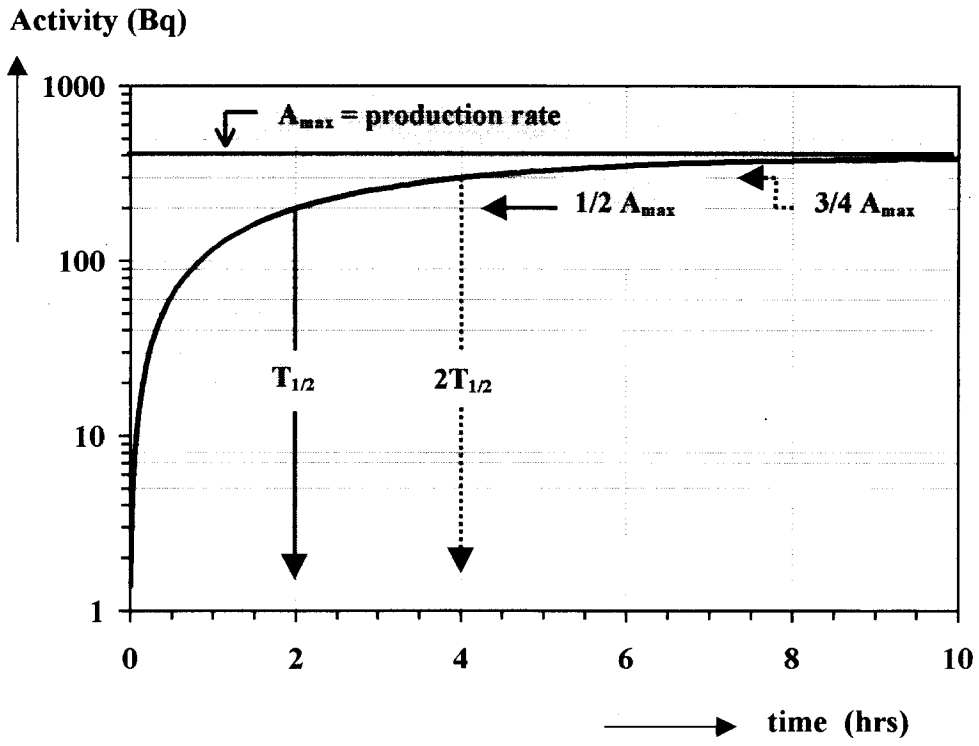

Fig.6.7 Growth of radioactivity by a constant production rate P of 400 nuclides/sec, resulting in a maximum activity of 400 Bq. The half-life of the produced nuclide is 2 hours.

7 NATURAL ABUNDANCE OF THE STABLE ISOTOPES OF C, O AND H

This chapter is concerned with the natural concentrations of the stable isotopes of hydrogen, carbon and oxygen, with particular attention paid to those compounds relevant in the hydrological cycle. For each isotope separately, we discuss the natural fractionation effects, internationally agreed definitions, standards, and reference materials, and variations in the natural abundances.

In order to help the reader to appreciate isotopic abundance values as they occur in nature, Fig.7.1 shows some actual isotope ratios and fractionations in a choice of equilibrium systems. Surveys of some practical data of all isotopes concerned are given in the respective Sections.

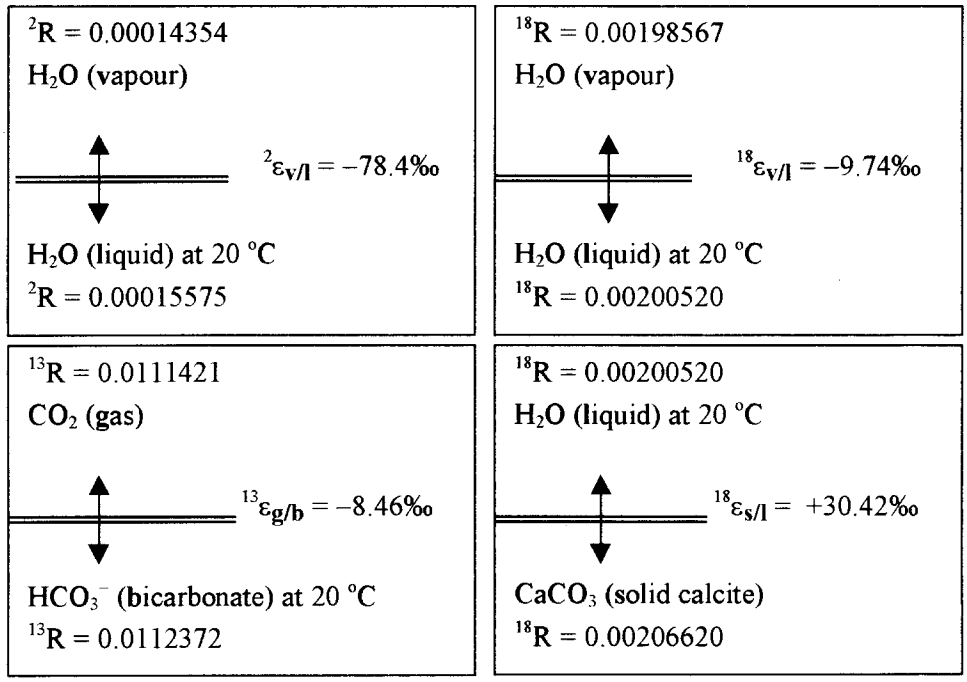

Fig.7.1 Examples of isotope ratios of compounds in isotopic equilibrium and the respective isotope fractionations, as defined in Sect.3.3. As an example may serve the calculation of $^{13}\varepsilon_{g/b}$ as $^{13}\alpha_{g/b} - 1$ with $^{13}\alpha_{g/b} = 0.0111421/0.0112372 = 0.99154$.

7.1 STABLE CARBON ISOTOPES

Table 7.1 The stable and radioactive isotopes of **carbon**: practical data for the natural abundance, properties, analytical techniques and standards. Further details are given in Sect.7.1 and 8.1, and in Chapters 10 and 11.

MS = mass spectrometry, PGC = proportional gas counting, LSS = liquid scintillation spectrometry, AMS = accelerator mass spectrometry

	^{12}C	^{13}C	^{14}C
stability	stable	stable	radioactive
natural abundance	0.989	0.011	$< 10^{-12}$
natural specific activity			< 0.25 Bq/gC
decay mode / daughter			β^- / ^{14}N
half-life ($T_{1/2}$)			5730 a
decay constant (λ)			1.21×10^{-4}/a = 1/8267 a^{-1}
max. β energy			156 keV
abundance range in hydrological cycle		30‰	0 to 10^{-12}
reported as		$^{13}\delta$ or $\delta^{13}C$	^{14}A, ^{14}a, $^{14}\delta$, or $^{14}\Delta$
in		‰	dpm/gC, Bq/gC, %, or ‰
instrument		MS	PGC, LSS, AMS
analytical medium		CO_2	CO_2, C_2H_2, CH_4, C_6H_6, graphite
usual standard deviation		0.03‰	1‰ to 1% at natural level
international standard		VPDB	Oxalic acid: Ox1, Ox2
with absolute value		0.0112372	13.56 dpm/gC

7.1.1 THE NATURAL ABUNDANCE

The chemical element carbon has two stable isotopes, ^{12}C and ^{13}C. Their abundance is about 98.9% and 1.1%, so that the $^{13}C/^{12}C$ ratio is about 0.011 (Nier, 1950). As a result of several fractionation processes, kinetic as well as equilibrium, the isotope ratio shows a natural variation of almost 100‰.

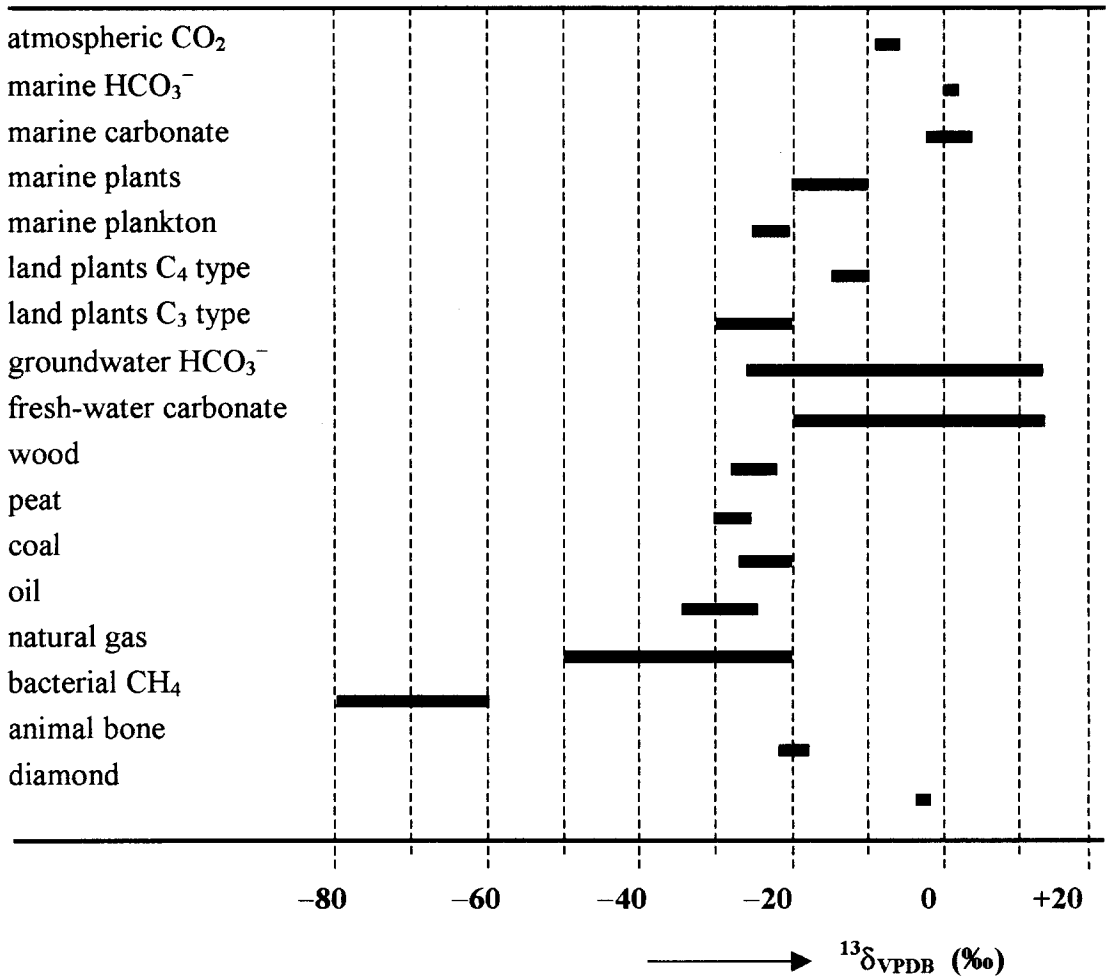

Fig.7.2 General view of $^{13}C/^{12}C$ variations in natural compounds. The ranges are indicative for the materials shown.

Fig.7.2 presents a broad survey of natural abundances of various compounds, at the low-^{13}C end bacterial methane (marsh-gas), at the high end the bicarbonate fraction of groundwater under special conditions. In the carbonic acid system variations up to 30‰ are normally observed. Wider variations occur in systems in which carbon oxidation or reduction reactions take place, such as the CO_2 (carbonate) – CH_4 (methane) or the CO_2 – $(CH_2O)_x$ (carbohydrate) systems.

7.1.2 CARBON ISOTOPE FRACTIONATIONS

It will later be shown that the presence of *dissolved inorganic carbon* (DIC) in sea-, ground-, and surface water presents the possibility of studying gas-water exchange processes and of measuring water transport rates in oceans and in the ground. In connection with studying these phenomena, the stable and radioactive isotopes of carbon and their interactions pay an important contribution, often together with the water chemistry.

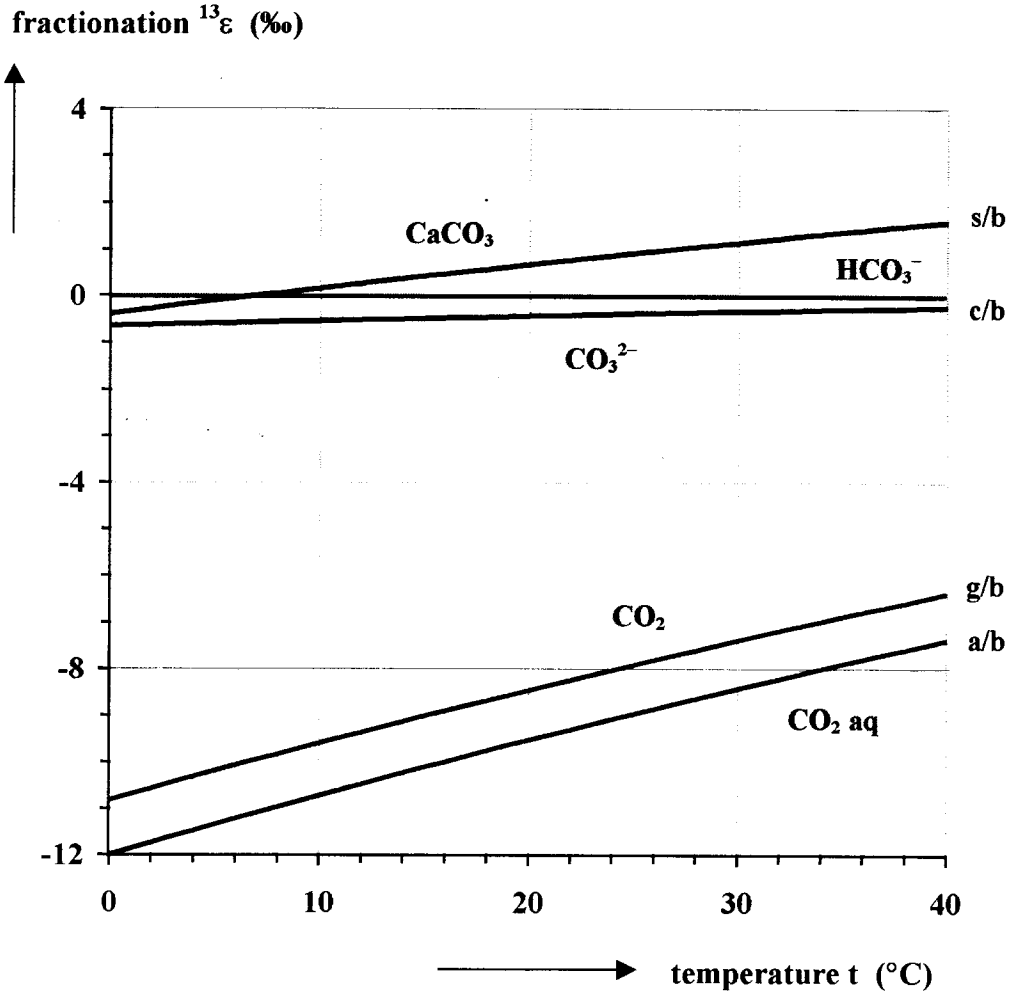

Fig.7.3 Temperature-dependent equilibrium isotope fractionation for carbon isotopes of gaseous CO_2 (g), dissolved CO_2 (a), dissolved carbonate ions (c), and solid carbonate (s) with respect to dissolved HCO_3^- (b). The actual data and equations are given in Table 7.2.

In nature equilibrium carbon isotope effects occur specifically between the phases CO_2 – H_2O – H_2CO_3 – $CaCO_3$. Values for the fractionations involved only depend on temperature and are obtained from laboratory experiments. A survey is presented in Fig.7.3 and Table 7.2.

The kinetic fractionation of specific interest is that during carbon dioxide assimilation, i.e. the CO_2 uptake by plants. The relatively large fractionation (up to about −18‰) is comparable to the effect observed during absorption of CO_2 by an alkaline solution. A quantitative estimate shows that the isotope effect as a result of diffusion of CO_2 through air can not explain the fractionation (Sect.3.5). The resulting value of $^{13}\alpha$ is 0.9956, so that only −4.4‰ of the total assimilation fractionation in favour of ^{12}C can be explained by the diffusion. The remaining −13.6‰, therefore, has to be found in the surface of the liquid phase and in the subsequent biochemical process.

Table 7.2 Carbon isotope fractionation in the equilibrium system CO_2–HCO_3–CO_3–$CaCO_3$; $^{13}\varepsilon_{y/x}$ represents the fractionation of compound y relative to compound x. Values for intermediate temperatures may be calculated by linear interpolation (see also Fig.7.3). T = t (°C) + 273.15 K

g = gaseous CO_2 , a = dissolved CO_2 , b = dissolved HCO_3^- , c = dissolved CO_3^{2-} ions, s = solid calcite.

t (°C)	$^{13}\varepsilon_{g/b}$ [1] (‰)	$^{13}\varepsilon_{a/g}$ [2] (‰)	$^{13}\varepsilon_{a/b}$ [3] (‰)	$^{13}\varepsilon_{c/b}$ [4] (‰)	$^{13}\varepsilon_{s/b}$ [5] (‰)	$^{13}\varepsilon_{s/g}$ [6] (‰)
0	−10.83	− 1.18	−12.00	− 0.65	− 0.39	+10.55
5	−10.20	− 1.16	−11.35	− 0.60	− 0.11	+10.19
10	− 9.60	− 1.13	−10 72	− 0.54	+ 0.15	+ 9.85
15	− 9.02	− 1.11	−10.12	− 0.49	+ 0.41	+ 9.52
20	− 8.46	− 1.09	− 9.54	− 0.44	+ 0.66	+ 9.20
25	− 7.92	− 1.06	− 8.97	− 0.39	+ 0.91	+ 8.86
30	− 7.39	− 1.04	− 8.42	− 0.34	+ 1.14	+ 8.60
35	− 6.88	− 1.02	− 7.90	− 0.29	+ 1.37	+ 8.31
40	− 6.39	− 1.00	− 7.39	− 0.25	+ 1.59	+ 8.03

[1]) Mook et al., 1974 : $^{13}\varepsilon_{g/b} = -9483/T + 23.89‰$ **(7.1)**

[2]) Vogel et al., 1970 : $^{13}\varepsilon_{a/g} = -373/T + 0.19‰$ **(7.2)**

[3]) From [1]) and [2]) : $^{13}\varepsilon_{a/b} = -9866/T + 24.12‰$ **(7.3)**

[4]) Thode et al., 1965 and [1]) : $^{13}\varepsilon_{c/b} = -867/T + 2.52‰$ **(7.4)**

[5]) Our evaluation of the original data from Rubinson & Clayton, 1969 and Emrich et al., 1970 : $^{13}\varepsilon_{s/b} = -4232/T + 15.10‰$ **(7.5)**

[6]) From [1]) and [5]) : $^{13}\varepsilon_{s/g} = +5380/T - 9.15‰$ **(7.6)**

Another kinetic process occurring in the soil is the bacterial decomposition of organic matter to form methane (CH_4). Here the largest fractionation amounts to about −55‰. In this process CO_2 is simultaneously produced with a fractionation of +25‰, resulting in a $^{13}\delta$ value of about 0‰.

A special problem is the kinetic fractionation during uptake and release of CO_2 by seawater. This fractionation is included in calculations on global ^{13}C modelling.

First we have to emphasise that the difference in isotopic composition between, for instance, gaseous CO_2 and the dissolved inorganic carbon content of water can not be addressed by *isotope fractionation between CO_2 and DIC*.

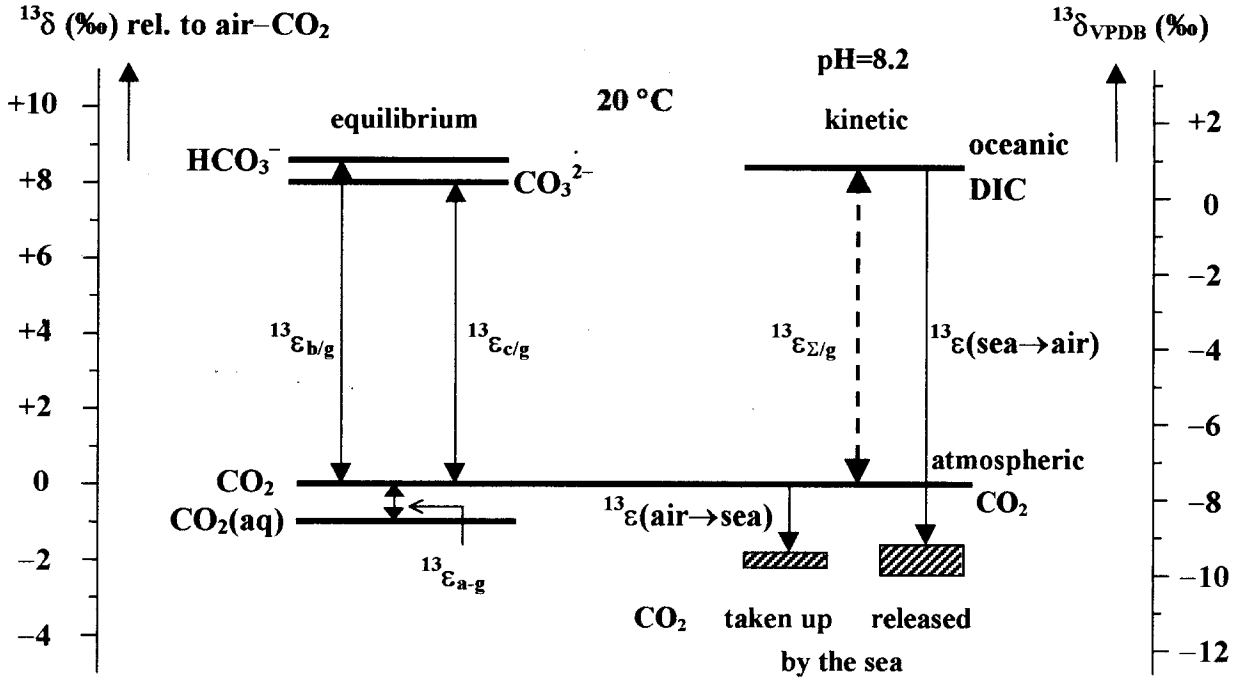

Fig.7.4 Fractionation for the isotopic equilibrium between CO_2(gas)–dissolved CO_2(aq)–dissolved bicarbonate (HCO_3^-)–dissolved carbonate (CO_3^{2-}) (Mook, 1986). The right-hand scale indicates approximate natural $^{13}\delta$ values with respect to VPDB. The right-hand part shows kinetic fractionations during uptake and release of atmospheric oceanic CO_2, respectively. DIC is the total dissolved inorganic carbon content (C_T).

Isotope fractionation is the phenomenon that, due to an isotope exchange process, a difference between the isotopic composition *of two compounds* occurs, while seawater carbon consists of 3 fractions, i.e. dissolved CO_2 (H_2CO_3 is hardly present), dissolved HCO_3^-, and dissolved CO_3^{2-}. All these fractions are fractionated isotopically with respect to each other. The ^{13}R value of DIC is:

$$^{13}R_{DIC} = \frac{[CO_2aq]^{13}R_{CO_2aq} + [HCO_3]^{13}R_{HCO_3} + [CO_3^{2}]^{13}R_{CO_3}}{[CO_2aq] + [HCO_3] + [CO_3^{2}]}$$

or in terms of the respective fractionations:

$$^{13}R_{DIC} = \frac{a \cdot {}^{13}\alpha_{a/b} + b + c \cdot {}^{13}\alpha_{c/b}}{C_T} \; {}^{13}R_b \qquad (7.7)$$

or in terms of δ values:

$$^{13}\delta_{DIC} = \frac{a \cdot {}^{13}\alpha_{a/b} + b + c \cdot {}^{13}\alpha_{c/b}}{C_T} \, {}^{13}\delta_b + \frac{a \cdot {}^{13}\varepsilon_{a/b} + c \cdot {}^{13}\varepsilon_{c/b}}{C_T} \qquad \textbf{(7.8)}$$

where the brackets indicate the respective concentrations, which are also denoted by a (acid), b (bicarbonate), and c (carbonate ions), so that $a + b + c = C_T$. The α values are given in Table 7.2. The chemical fractions are quantitatively treated in Chapter 9.

Originally $^{13}\varepsilon_k$ values for the uptake of CO_2 by seawater of about −15‰ were assumed, based on experimental results of CO_2 absorption by an alkaline solution (Baertschi, 1952). However, Siegenthaler & Münnich (1981) have reasoned that this effect does not apply to the dissolving action of seawater. Calculations by these authors as well as by Inoue & Sugimura (1985) and Wanninkhof (1985) have shown the kinetic fractionation during CO_2 uptake to be

$$^{13}\varepsilon_k \text{ (air} \Rightarrow \text{sea)} = {}^{13}\varepsilon_k \text{ (atm.}CO_2 \text{ to } CO_2 \text{ taken up)} = -2.0 \pm 0.2‰$$

This value was confirmed by experiments of the last author (−2.4 ± 0.8‰).(We have to remind the reader that these $^{13}\varepsilon_k$ values as well as those below are for kinetic fractionations and *do not* refer to Table 7.2).

The kinetic fractionation during CO_2 release by the ocean reported by Siegenthaler & Münnich (1981) needs a correction (Mook, 1986). By application of the most recent equilibrium fractionations of Table 7.2 the equilibrium fractionation ($^{13}\alpha_{a/DIC}$) for dissolved CO_2 with respect to total dissolved carbon at 20 °C is 0.99055. This fractionation factor is also determined by the chemical composition of seawater, which adds to the overall temperature dependence.

At 20 °C the respective relative concentrations in seawater at pH = 8.20 are: $CO_2(aq)/C_T$ = 0.006, HCO_3^-/C_T = 0.893 and CO_3^{2-}/C_T = 0.102 where C_T is the total inorganic carbon concentration. By incorporation of the $CO_2 + OH^-$ reaction (0.9995), the resulting $^{13}\delta$ value is −10.1 to −10.6‰, depending on whether the hydration of CO_2 to H_2O is to be included.

According to Inoue & Sugimura (1985) the value is about -10‰, so that we can conclude to a fractionation of released CO_2 with respect to DIC of:

$$^{13}\varepsilon_k \text{ (sea} \Rightarrow \text{air)} = {}^{13}\varepsilon_k \text{ (DIC rel. to } CO_2 \text{ released)} = -10.3 \pm 0.3‰$$

Figure 7.4 represents a review of equilibrium and kinetic fractionations relative to gaseous CO_2 (left-hand scale) and the actual $^{13}\delta$ values based on $^{13}\delta$ (atm.CO_2) = −7.0‰ (right-hand scale). It is obvious that the isotopic compositions of CO_2 released and taken up by the ocean are equal, as is required by the condition of stationary state of isotopic equilibrium between ocean and atmosphere.

7.1.3 REPORTING ^{13}C VARIATIONS AND THE ^{13}C STANDARD

As described in Sect.4.1, isotopic compositions expressed as $^{13}\delta$ values are related to those of specific reference materials. By international agreement PDB was used as the *primary carbon reference* (*standard*) material. PDB (Pee Dee Belemnite) was the carbonate from a certain (marine) belemnite found in the Cretaceous Pee Dee formation of North America. This material was the original standard sample used in the early days in Chicago and at CalTech, but has long been exhausted. The US National Bureau of Standards therefore distributed another (marine) limestone of which $^{13}\delta$ had been accurately established in relation to PDB. This first standard available to the community, Solenhofen limestone NBS20, was analysed by Craig (1957) and consecutively defined as:

$$^{13}\delta_{NBS20\,/\,PDB} = -1.06‰$$

In this way the PDB scale was indirectly established. Meanwhile NBS20 is considered to be no longer reliable, probably because of improper storage, and has been replaced by another limestone, NBS19, of which the $^{13}\delta$ value has been compared by a number of laboratories with the previous standard.

Based on this comparison an IAEA panel in 1983 (Gonfiantini, 1984) adopted this new standard to define the new *VPDB (Vienna PDB) scale* as:

$$^{13}\delta_{NBS19\,/\,VPDB} = +1.95‰ \qquad \textbf{(7.9)}$$

The absolute $^{13}C/^{12}C$ ratio of PDB was originally reported as 0.0112372 (Craig, 1957), whereas a slightly different value of 0.011183 (± 0.1‰) was reported by Zhang and Li (1987). The distinction between PDB and VPDB has been made for formal reasons, but the difference is negligibly small (< 0.01‰).

Henceforth all $^{13}\delta$ values are reported relative to VPDB, unless stated otherwise.

More details on measurement and calculation procedures are given in Chapter 11. A survey of other reference samples is given in Table 11.2.

7.1.4 SURVEY OF NATURAL ^{13}C VARIATIONS

In the other volumes certain aspects of natural $^{13}\delta$ variations will be discussed in more detail. Here we will restrict ourselves to a general survey, particularly with regard to the hydrological cycle (Fig. 7.5).

7.1.4.1 ATMOSPHERIC CO_2

The least depleted atmospheric CO_2 had originally $^{13}\delta$ values near −7‰. Since the 19th century this value has undergone relatively large changes. In general, high values are observed in

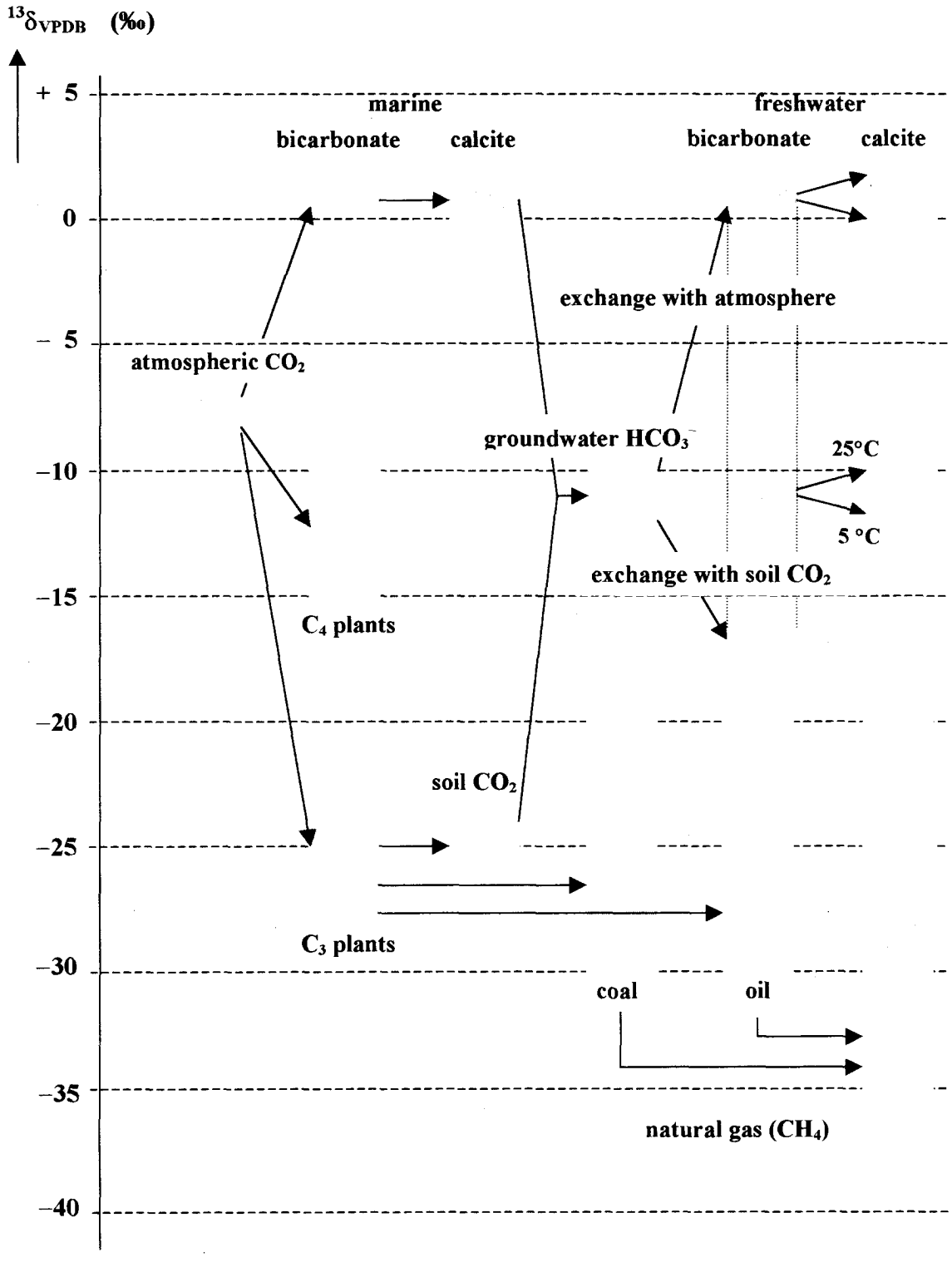

Fig.7.5 Schematic survey of $^{13}\delta$ variations in nature, especially of compounds relevant in the hydrological cycle.

oceanic air far removed from continental influences and occurs in combination with minimal CO_2 concentrations. More negative $^{13}\delta$ values are found in continental air and are due to an admixture of CO_2 of biospheric and anthropogenic origin ($^{13}\delta \approx -25‰$), in part from the decay of plant material, in part from the combustion of fossil fuels (Keeling, 1958; Mook et al., 1983).

7.1.4.2 SEAWATER AND MARINE CARBONATE

Atmospheric CO_2 appears to be nearly in isotopic equilibrium with the oceanic dissolved bicarbonate. The $^{13}\delta(HCO_3^-)$ values in the ocean are about +1 to +1.5‰, in agreement with the equilibrium fractionation $\varepsilon_{g/b}$ at temperatures between 15 and 20 °C (Table 7.2). According to the fractionation $\varepsilon_{s/b}$ we should expect calcite slowly precipitating in equilibrium with oceanic bicarbonate to have $^{13}\delta$ values of +2.0 to +2.5‰. This is indeed the normal range found for recent marine carbonates. Mook and Vogel (1968) observed this isotopic equilibrium between marine to brackish-water shells and dissolved bicarbonate in the water.

7.1.4.3 VEGETATION AND SOIL CO_2

Plant carbon has a lower ^{13}C content than the atmospheric CO_2 from which it was formed. The fractionation which occurs during CO_2 uptake and photosynthesis depends on the type of plant and the climatic and ecological conditions. The dominant modes of photosynthesis give rise to strongly differing degrees of fractionation (Lerman, 1972; Throughton, 1972). The Hatch-Slack photosynthetic pathway (C_4) results in $^{13}\delta$ figures of −10 to −15‰ and is primarily represented by certain grains and desert grasses (sugar reed, corn). In temperate climates most plants employ the Calvin mechanism (C_3), producing $^{13}\delta$ values in the range of $-26 \pm 3‰$. A third type of metabolism, the Crassulacean Acid Metabolism (CAM) produces a large spread of $^{13}\delta$ values around −17‰ (Deines, 1980).

The CO_2 content of the soil atmosphere can be orders of magnitude larger than that of the free atmosphere. The additional CO_2 is formed in the soil by decay of plant remains and by root respiration and consequently has $^{13}\delta$ values centring around −25‰ in temperate climates where Calvin plants dominate.

7.1.4.4 FOSSIL FUEL

As complicated biogeochemical processes are involved in the degradation of terrestrial and marine plant material ultimately into coal, oil, and natural gas, the range of $^{13}\delta$ values of these fossil fuels is larger, extending to more negative values, especially of biogenic methane (Fig.7.5). The global average of CO_2 from the combustion of these fuels is estimated to be about −27‰.

7.1.4.5 GLOBAL CARBON CYCLE

Biospheric carbon has a direct influence on $^{13}\delta$ of atmospheric CO_2. The large uptake of CO_2 by the global biosphere during summer and the equal release of CO_2 during winter causes a seasonal variation in the atmospheric CO_2 concentration as well as in $^{13}\delta$. The simple mixing of CO_2 from these two components, atmospheric CO_2 (atm) and biospheric CO_2 (bio) is represented by the equation (cf. Eqs.4.13 and 4.15):

$$(^{13}\delta_{atm} + \Delta^{13}\delta)(C_{atm} + \Delta C_{bio}) = {}^{13}\delta_{atm}C_{atm} + {}^{13}\delta_{bio}\Delta C_{bio} \qquad (7.10)$$

where C stands for the CO_2 concentration, ΔC for the biospheric addition, and $\Delta^{13}\delta$ for the variation in the δ value.

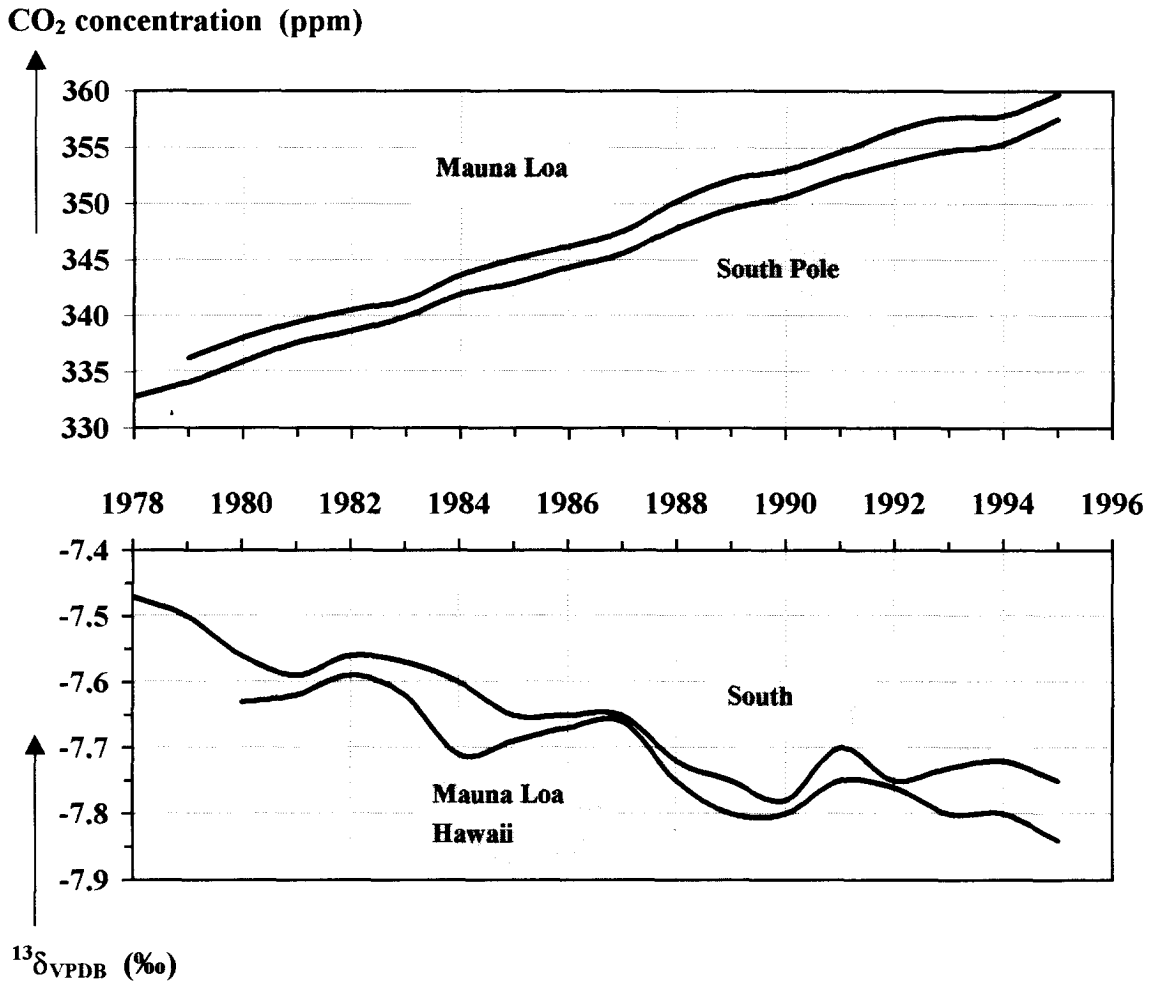

Fig.7.6 Trends of the concentration and $^{13}\delta$ of atmospheric CO_2 of air samples collected by C.D.Keeling on top of the Mauna Loa volcano at the Island of Hawaii and at the South Pole. The seasonal variations have been removed from the original data (Roeloffzen et al., 1991). The dates refer to 1 January of each year.

Numerically this comes to a periodic (seasonal) variation of

$$\frac{\Delta^{13}\delta}{\Delta C_{bio}} = \frac{^{13}\delta_{bio} - ^{13}\delta_{atm}}{C_{atm} + \Delta C_{bio}} = \frac{-25+7.85}{353} \approx -0.05‰ \text{ per ppm of } CO_2 \qquad \textbf{(7.11)}$$

Superimposed on this phenomenon is the gradual increase in the concentration and the accompanying decrease in $^{13}\delta$ by the emission of fossil-fuel CO_2. The trends are shown in Fig.7.6 and can be approximated by:

$$\Delta^{13}\delta / \Delta CO_2 = -0.015 \text{ ‰ / ppm} \quad \text{or} \quad \Delta^{13}\delta = -0.025‰ \text{ / year} \qquad \textbf{(7.12)}$$

at a CO_2 concentration of 353 ppm and $^{13}\delta$ = −7.85‰ over the Northern Hemisphere, valid for 01/01/1990.

The smaller ‰/ppm value of Eq.7.12 compared to Eq.7.11 shows that the long-term trend is not due to simple addition and mixing of additional CO_2 in the atmosphere. The large oceanic DIC reservoir is levelling out the purely atmospheric mixing effect through isotope exchange.

7.1.4.6 GROUNDWATER AND RIVERWATER

Soil CO_2 is important in establishing the dissolved inorganic carbon content of groundwater. After dissolution of this CO_2 the infiltrating rain water is able to dissolve the soil limestone:

$$CO_2 + H_2O + CaCO_3 \rightarrow Ca^{2+} + 2HCO_3^- \qquad \textbf{(7.13)}$$

(Fig.7.7). Because limestone generally is of marine origin ($^{13}\delta \approx +1‰$), this process results in $^{13}\delta$ of the dissolved bicarbonate of about −11 to −12‰ (in temperate climates).

In the soil the HCO_3^- first formed exchanges with the often present excess of gaseous CO_2, **ultimately** resulting in $^{13}\delta(HCO_3^-) = {}^{13}\delta(\text{soil } CO_2) + {}^{13}\varepsilon_{b/g} \approx -25‰ + 9‰ = -16‰$ (Fig.7.5). Consequently, $^{13}\delta(HCO_3^-)$ values significantly outside the range of −11 to −12‰ are observed in soil water as well as in fresh surface water such as rivers and lakes. In surface waters such as lakes ^{13}C enrichment of dissolved inorganic carbon can be caused by isotope exchange with atmospheric CO_2 ($^{13}\delta \approx -7.5‰$), **ultimately** resulting in values of $^{13}\delta + {}^{13}\varepsilon_{b/g} = -7.5‰ + 9‰ = +1.5‰$, identical to oceanic values. Consequently, freshwater carbonate minerals may have "marine" $^{13}\delta$ values. In these cases the marine character of the carbonate is to be determined by $^{18}\delta$ (Sect.7.3).

In addition to HCO_3^-, natural waters contain variable concentrations of CO_2 with the effect that the $^{13}\delta$ value of DIC is lower than that of the bicarbonate fraction alone: in groundwater (Vogel and Ehhalt, 1963), and in stream and river waters derived from groundwater (Fig.7.8) the $^{13}\delta$(DIC) values are generally in the range of −12 to −15‰.

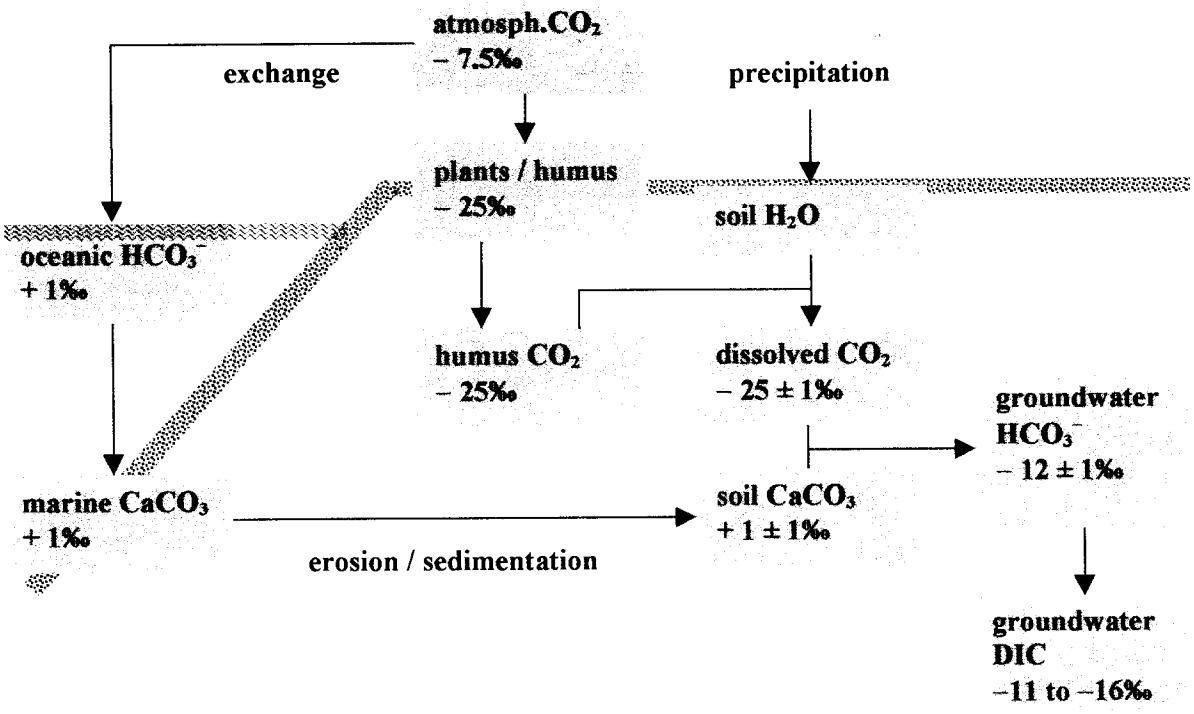

Fig. 7.7 Schematic representation of the formation of dissolved inorganic carbon in groundwater from soil carbonate and soil CO_2. This is the main process responsible for the carbonate content of groundwater and the consecutive components of the water cycle. Generally, dissolved bicarbonate is by far the largest component. The ‰ values referring to the respective $^{13}\delta$ have been kept simple for the sake of clarity. DIC is the dissolved inorganic carbon content of the water, i.e. HCO_3^-, CO_2(aq) and CO_3^{2-}.

7.2 STABLE OXYGEN ISOTOPES

7.2.1 THE NATURAL ABUNDANCE

The chemical element oxygen has three stable isotopes, ^{16}O, ^{17}O and ^{18}O, with abundances of 99.76, 0.035 and 0.2%, respectively (Nier, 1950). Observation of ^{17}O concentrations provides little information on the hydrological cycle in the strict sense above that which can be gained from the more abundant and, consequently, more accurately measurable ^{18}O variations (Sect.3.7). We shall, therefore, focus our attention here on the $^{18}O/^{16}O$ ratio (≈ 0.0020).

Values of $^{18}\delta$ show natural variations within a range of almost 100‰ (Fig.7.9). ^{18}O is often enriched in (saline) lakes subjected to a high degree of evaporation, while high-altitude and cold-climate precipitation, especially in the Antarctic, is low in ^{18}O. Generally in the hydrological cycle in temperate climates we are confronted with a range of $^{18}\delta$ not exceeding 30‰.

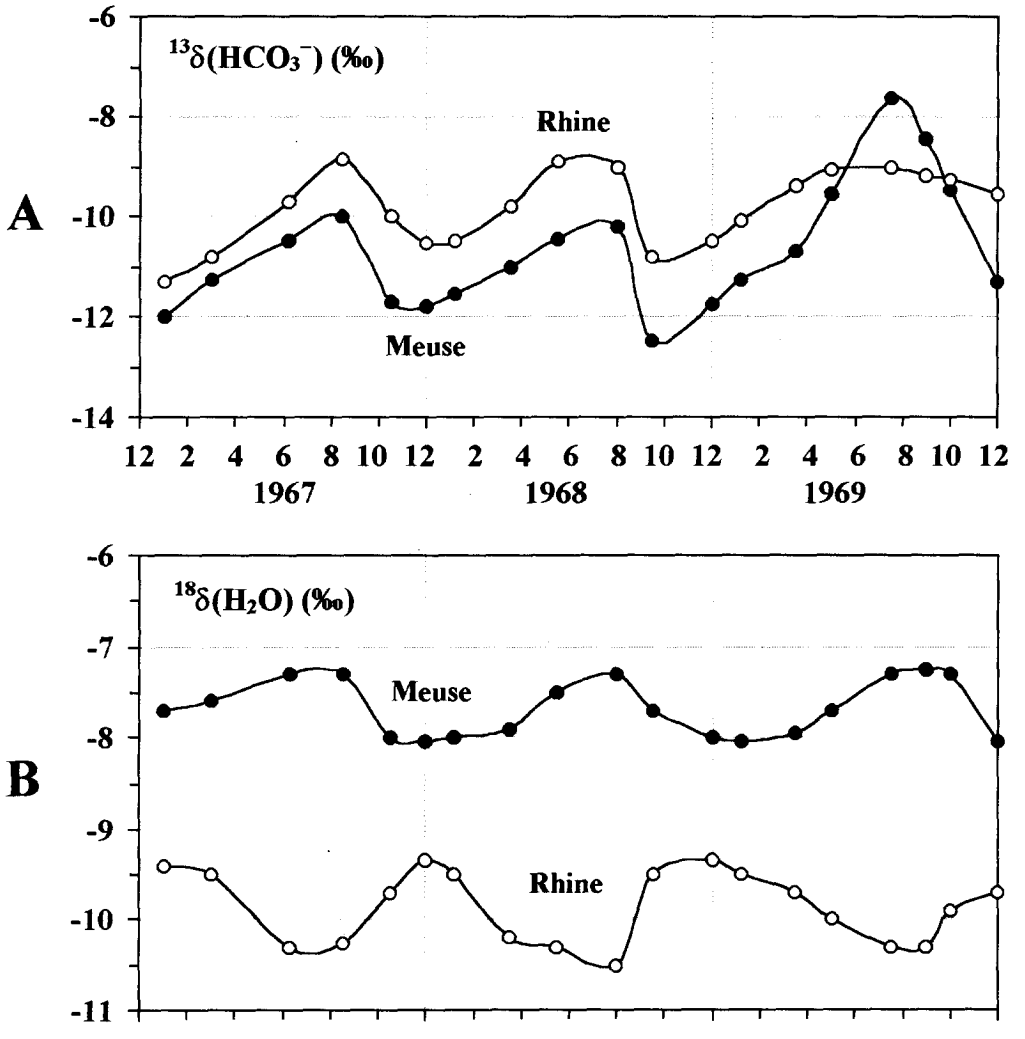

Fig.7.8 A three-year observation of the isotopic composition of water from the N.W.European rivers Rhine and Meuse (Mook, 1970):

A. $^{13}\delta$ values of the dissolved bicarbonate fraction, showing normal values during winter and relatively high values in summer, probably because of isotopic exchange of the surface water bicarbonate with atmospheric CO_2.

B. $^{18}\delta$ values, where the river Meuse is showing the average value and the seasonal variations of $^{18}\delta$ in the precipitation: high values in summer, low during winter; during early spring and summer the Rhine receives meltwater from the Swiss Alps with relatively low $^{18}\delta$ because of the high-altitude precipitation.

Table 7.3 The stable isotopes of **oxygen**: practical data for the natural abundance, properties, analytical techniques and standards. Further details are given in Sect.7.2, and in Chapters 10 and 11.

MS=mass spectrometry

	^{16}O	^{17}O	^{18}O
stability	stable	stable	stable
natural abundance	0.9976	0.00038	0.00205
abundance range in hydrological cycle		15‰	30‰
reported as		$^{17}\delta$ or $\delta^{17}O$	$^{18}\delta$ or $\delta^{18}O$
in		‰	‰
instrument		MS	MS
analytical medium		O_2	CO_2 or O_2
usual standard deviation			0.05‰
international standard			VSMOW for water VPDB for carbonate etc
with absolute value			VSMOW: 0.0020052 VPDB: 0.0020672

7.2.2 OXYGEN ISOTOPE FRACTIONATIONS

The isotope effects to be discussed are within the system H_2O (vapour) – H_2O (liquid) – $CaCO_3$. The equilibrium fractionation values have been determined by laboratory experiments. Fig.7.1 shows some actual isotope ratios. Fig.7.10 and Table 7.4 present a survey of the temperature dependent equilibrium isotope effects.

Equilibrium fractionations determined in the laboratory are also found in nature. The most striking observation is that the carbonate shells of many molluscs appear to have been formed in isotopic equilibrium with seawater. The *palaeotemperature scale* as presented by Eq.7.18 was presented by Epstein et al. (1953) (cf. Friedman & O'Neil, 1977). This relation is deduced from ^{18}O measurements on carbonate laid down by marine shell animals at known temperatures and water isotopic compositions. These data lost the original interpretation of the temperature dependence of the $\alpha_{s/l}$ by the later realisation that the major oceanic palaeotemperature effect is the change in $^{18}\delta$ of seawater –and, consequently of carbonate formed in this water- by the formation viz. melting of enormous ice caps on the poles during or after ice ages.

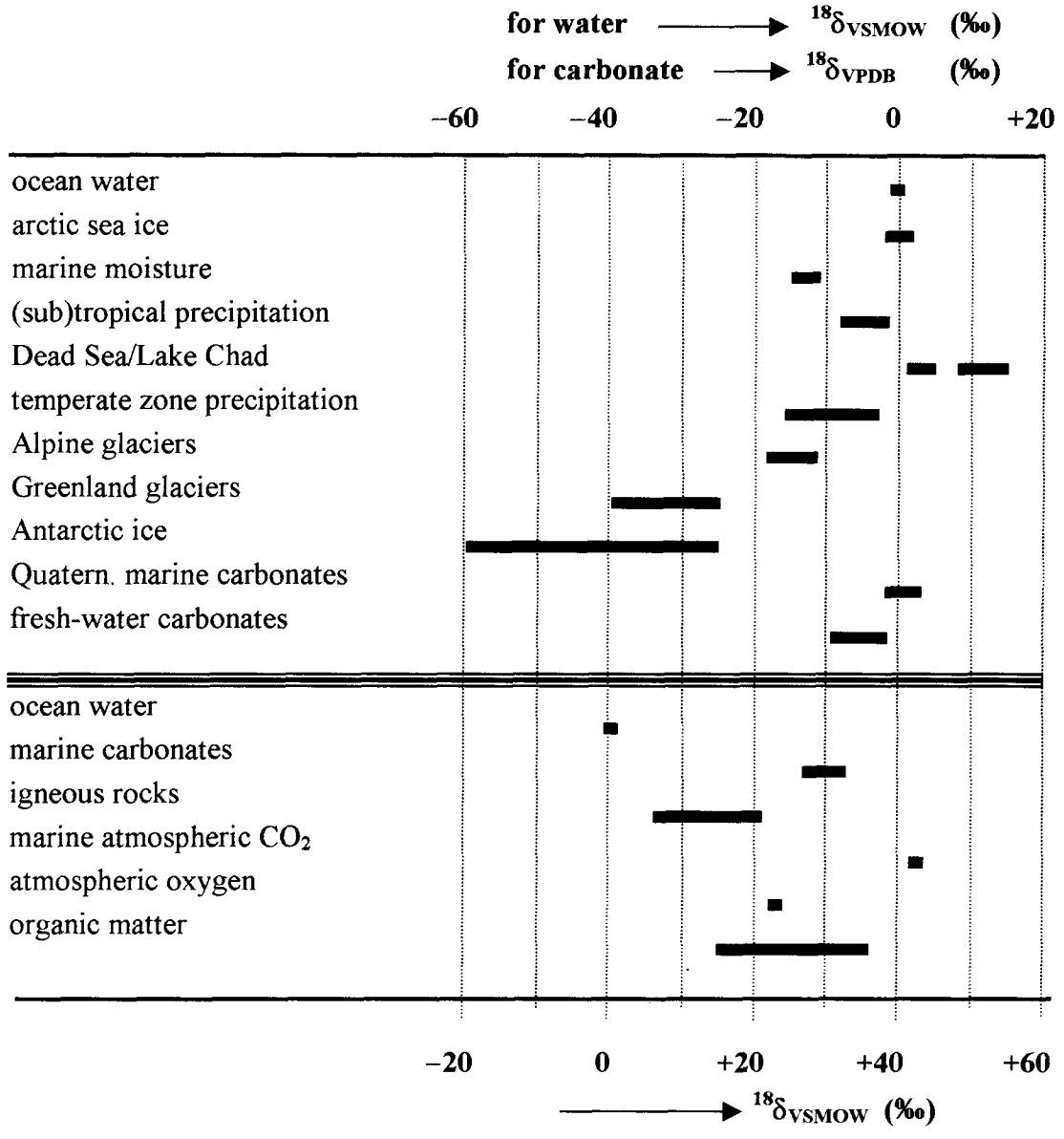

Fig.7.9 General view of $^{18}O/^{16}O$ variations in natural compounds. The ranges are indicative for the majority of materials shown. The relation between the VPDB and VSMOW scales is given in Sect.7.2.3 and Fig.7.11.

Kinetic effects are observed during the evaporation of ocean water, as oceanic vapour is isotopically lighter than would result from equilibrium fractionation alone. The natural isotope effect for oxygen (≈ -12‰) is smaller than could be brought about by fractionation by diffusion. Laboratory measurements resulted in $^{18}\varepsilon_d$ = -27.3 ± 0.7‰ (Merlivat, 1978) and $^{18}\varepsilon_d$ = -27.2 ± 0.5‰ (unpubl.). These experimental values are again smaller than results from Eq.(3.35) (-31.3‰), which may be explained by the water molecules forming clusters of

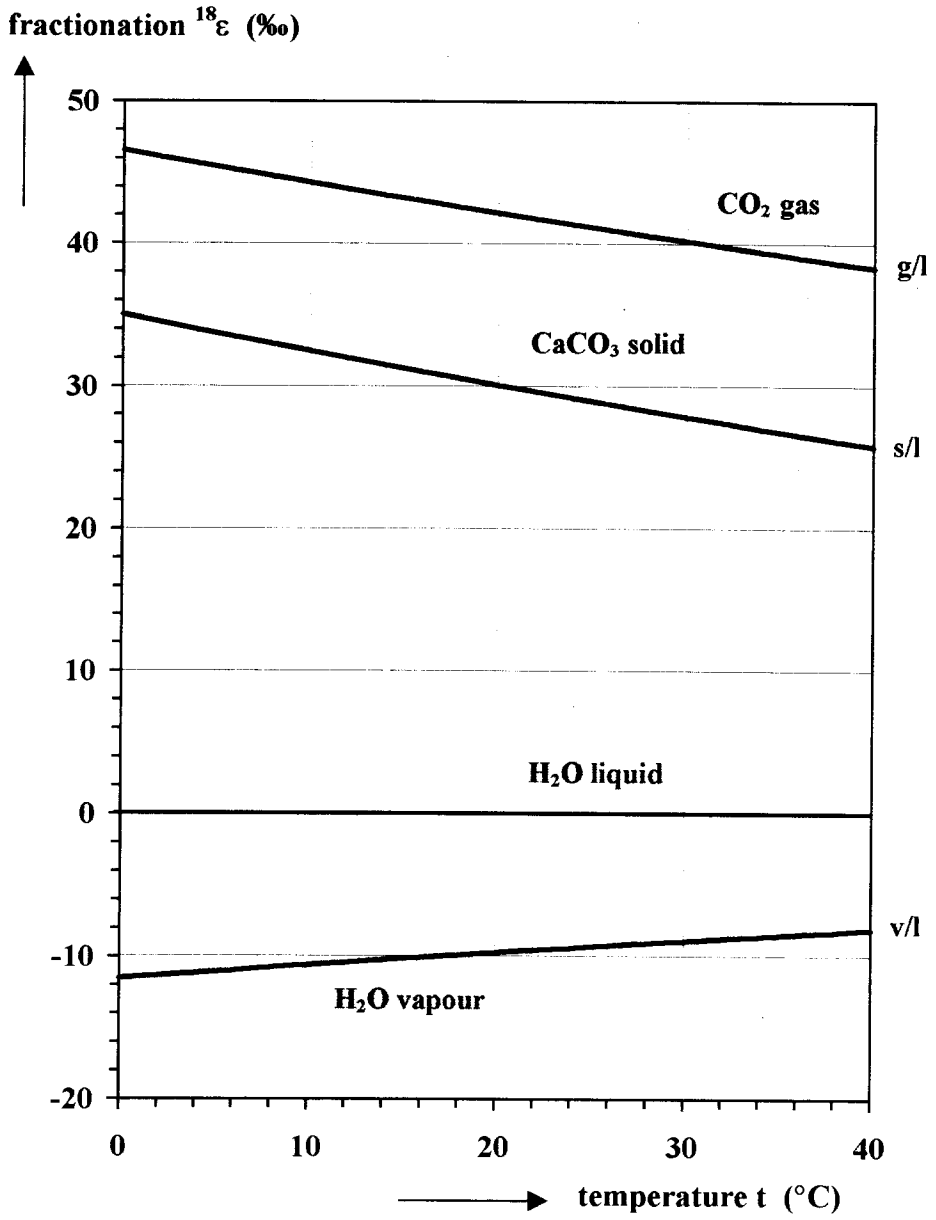

Fig.7.10 Temperature dependent equilibrium fractionations for oxygen isotopes of water vapour (v), gaseous CO_2 (g), and solid calcite (s) with respect to liquid water (l).

larger mass in the vapour phase. Furthermore, evaporation of ocean water includes sea spray by which water droplets evaporate completely without fractionation, thus reducing the natural isotope effect.

Table 7.4 Oxygen isotope fractionation in the equilibrium system CO_2–H_2O–$CaCO_3$; $^{18}\varepsilon_{y/x}$ represents the fractionation of compound y relative to compound x, and is approximately equal to $\delta_y - \delta_x$. Values for intermediate temperatures may be calculated by linear interpolation (Fig.7.9). T = t (°C) + 273.15 K

l = liquid H_2O , v = H_2O vapour , i = ice , g = gaseous CO_2 , s = solid $CaCO_3$, lg = CO_2 (g) isotopic equilibrium with H_2O (l) at 25°C , sg = CO_2 (g) from $CaCO_3$ (s) by 95% H_3PO_4 at 25°C.

t °C	$^{18}\varepsilon_{v/l}$ [1] (‰)	$^{18}\varepsilon_{s/l}$ [2] (‰)	$^{18}\varepsilon_{g/l}$ [3] (‰)	$^{18}\varepsilon_{g/lg}$ [4] (‰)	$^{18}\varepsilon_{sg/lg}$ [5] (‰)
0	−11.55	+ 34.68	+ 46.56	+ 5.19	+ 3.98
5	−11.07	+ 33.39	+ 45.40	+ 4.08	+ 2.72
10	−10.60	+ 32.14	+ 44.28	+ 3.01	+ 1.51
15	−10.15	+ 30.94	+ 43.20	+ 1.97	+ 0.34
20	− 9.71	+ 29.77	+ 42.16	+ 0.97	− 0.79
25	− 9.29	+ 28.65	+ 41.15	0	− 1.88
30	− 8.89	+ 27.56	+ 40.18	− 0.93	− 2.93
35	− 8.49	+ 26.51	+ 39.24	− 1.84	− 3.96
40	− 8.11	+ 25.49	+ 38.33	− 2.71	− 4.94

[1]) Majoube, 1971 : $\ln{}^{18}\alpha_{v/l} = -1137/T^2 + 0.4156/T + 0.0020667$ **(7.14a)**

1/T adjustment : $^{18}\varepsilon_{v/l} = -7\,356/T + 15.38‰$ **(7.14b)**

Values at higher temperatures can be obtained from Horita and Wesolowski, 1994

The fractionation between vapour and liquid water is independent of the NaCl concentration of the solution, contrary to some other salts (Friedman and O'Neil, 1977)

[2]) From [3]) and [5]) and Friedman and O'Neil, 1971

: $^{18}\varepsilon_{s/l} = 19\,668/T - 37.32‰$ **(7.15)**

[3]) Brenninkmeijer et al., 1983 : $^{18}\varepsilon_{g/l} = 17\,604/T - 17.89‰$ **(7.16)**

[4]) From [3]), where lg is obtained from l by applying the $^{18}\varepsilon_{g/l}$ value at 25°C (concluded by an IAEA panel to be +41.2‰ : $^{18}\varepsilon_{g/lg} = 16\,909/T - 56.71‰$ **(7.17)**

This fractionation is independent of the salt content of the solution

[5]) Epstein et al., 1953, 1976: $t(°C) = 16.5 - 4.3(^{18}\delta_s - {}^{18}\delta_w) + 0.14(^{18}\delta_s - {}^{18}\delta_w)^2$ **(7.18)**

where $^{18}\delta$ refers CO_2 prepared from solid carbonate with 95% H_3PO_4 at 25°C and $^{18}\delta_w$ to CO_2 in isotopic equilibrium with water at 25°C, both relative to VPDB-CO_2

sg is obtained from s by applying the fractionation for the CO_2 production at 25°C

: $^{18}\varepsilon_{sg/s} = + 10.25‰$

: $^{18}\varepsilon_{sg/lg} = 19\,082/T - 65.88‰$ **(7.19)**

Majoube, 1971: $^{18}\varepsilon_{i/l} = + 3.5‰$ (0°C); $^{18}\varepsilon_{i/v} = + 15.2‰$ (0°C); $^{18}\varepsilon_{i/v} = + 16.6‰$ (−10°C)

7.2.3 REPORTING ^{18}O VARIATIONS AND THE ^{18}O STANDARDS

Originally *$^{18}O/^{16}O$ of an arbitrary water sample* was (indirectly, via a local laboratory reference sample) compared to that of average seawater. This *Standard Mean Ocean Water* in reality never existed. Measurements on water samples from all oceans by Epstein and Mayeda (1953) were averaged and referred to a truly existing reference sample, NBS1, that time available at the US National Bureau of Standards (NBS). In this way the isotope water standard, SMOW, became indirectly defined by Craig (1961a) as:

$$^{18}\delta_{NBS1\,/\,SMOW} = -7.94‰$$

The International Atomic Energy Agency (IAEA), Section of Isotope Hydrology, in Vienna, Austria and the US National Institute of Standards and Technology (NIST, the former NBS) have now available for distribution batches of well preserved standard mean ocean water for use as a standard for ^{18}O as well as for ^{2}H. This standard material, VSMOW, prepared by H.Craig to equal the former SMOW as closely as possible both for $^{18}\delta$ and $^{2}\delta$, has been decided by an IAEA panel in 1976 to replace the original SMOW in fixing the zero point of the $^{18}\delta$ scale. All water samples are to be referred to this standard.

From an extensive laboratory intercomparison it became clear that the difference between the early SMOW and the present VSMOW is very small (IAEA, 1978), probably:

$$^{18}\delta_{SMOW\,/\,VSMOW} = +0.05‰ \qquad \textbf{(7.20)}$$

At present two standard materials are available for reporting $^{18}\delta$ values, one for water samples, one for carbonates. This situation arises from the practical fact that neither the isotope measurements on water nor those on carbonates are performed on the original material itself, but are made on gaseous CO_2 reacted with or derived from the sample.

The laboratory analysis of $^{18}O/^{16}O$ in water is performed by equilibrating a water sample with CO_2 of known isotopic composition at 25°C (Sect.10.2.1), followed by mass spectrometric analysis of this equilibrated CO_2 (Sect.11.1). This equilibration is generally carried out on batches of water samples, consisting of the unknown samples (x) and the standard or one or more reference samples. After the correction discussed in Sect.11.2.3.4 is made, it is irrelevant whether the water samples themselves are being related or the CO_2 samples obtained after equilibration, provided sample and standard are treated under equal condition:

$$^{18}\delta_{x\,/\,VSMOW} = {}^{18}\delta_{xg\,/\,VSMOWg} \qquad \textbf{(7.21)}$$

where g refers to the equilibrated and analysed CO_2.

The absolute $^{18}O/^{16}O$ ratio of VSMOW is reported as $(2005.2 \pm 0.45) \times 10^{-6}$ (Baertschi, 1976). Reference and intercomparison samples are available from the IAEA and the NIST. A survey of the data is given in Table 11.2. In order to overcome small analytical errors, some laboratories prefer to fix their VSMOW scale by two extreme points (Sect.11.2.3.5). Using

this procedure, the sample $^{18}\delta$ is located on a linear δ scale between VSMOW (0‰) and SLAP (Standard Light Antarctic Precipitation) with a defined value of

$$^{18}\delta_{SLAP\,/\,VSMOW} = -55.5‰ \qquad \textbf{(7.22)}$$

$^{18}\delta$ values of carbonates are given with reference to the same PDB calcite used for ^{13}C (Sect.7.1.3). The zero point of this PDB scale was fixed by means of the NBS20 reference sample (Solenhofen limestone) which originally was defined as (Craig, 1957):

$$^{18}\delta_{NBS20\,/\,PDB} = -4.14‰$$

The absolute $^{18}O/^{16}O$ ratio of PDB-CO_2 was originally reported as 0.0020790 (Craig, 1957). This value, however, does not agree with Baertschi's ratio for VSMOW and the accurately measured difference between the two standards (Fig.7.10). At present a value of 0.0020672 is considered to be more realistic (Table 11.1).

Recently, samples from NBS20 do not always show the above value. Probably because of exchange with atmospheric vapour due to improper storage, the $^{18}\delta$ value may have shifted to close to –4.4‰. Therefore, a new set of carbonate reference materials has been introduced by the IAEA where NBS19 replaces NBS20. The VPDB (Vienna PDB) scale has now been defined by using NBS19:

$$^{18}\delta_{NBS19\,/\,VPDB} = -2.20‰ \qquad \textbf{(7.23)}$$

The carbonate itself is not analysed for $^{18}\delta$ but rather the CO_2 prepared according to a standard procedure which involves treatment in vacuum with 95% (or 100%) orthophosphoric acid at 25°C. If samples and reference are treated and corrected similarly,

$$^{18}\delta_{x\,/\,VPDB} = {}^{18}\delta_{xg\,/\,VPDBg} \qquad \textbf{(7.24)}$$

where g refers to the prepared and analysed CO_2, so that neither the fractionation between the carbonate and the CO_2 prepared from it (Table 7.4) nor the reaction temperature need to be known.

The relations between the VPDB, VPDB-CO_2 (VPBDg), VSMOW and VSMOW-CO_2 (VSMOWg) scales are derived from the equations given in Table 7.4, according to Eq.7.24:

$$^{18}\delta_{x\,/\,VSMOW} = 1.03086\ {}^{18}\delta_{x\,/\,VPDB} + 30.86‰ \qquad \textbf{(7.25)}$$

$$^{18}\delta_{x\,/\,VSMOW} = 1.04143\ {}^{18}\delta_{x\,/\,VPDBg} + 41.43‰ \qquad \textbf{(7.26)}$$

$$^{18}\delta_{x\,/\,VSMOWg} = 1.00027\ {}^{18}\delta_{x\,/\,VPDBg} + 0.27‰ \qquad \textbf{(7.27)}$$

The relations are visualised in Fig.7.11.These are of interest in isotope studies on silicates, oxides, carbonates, organic matter, and their correlation with water.

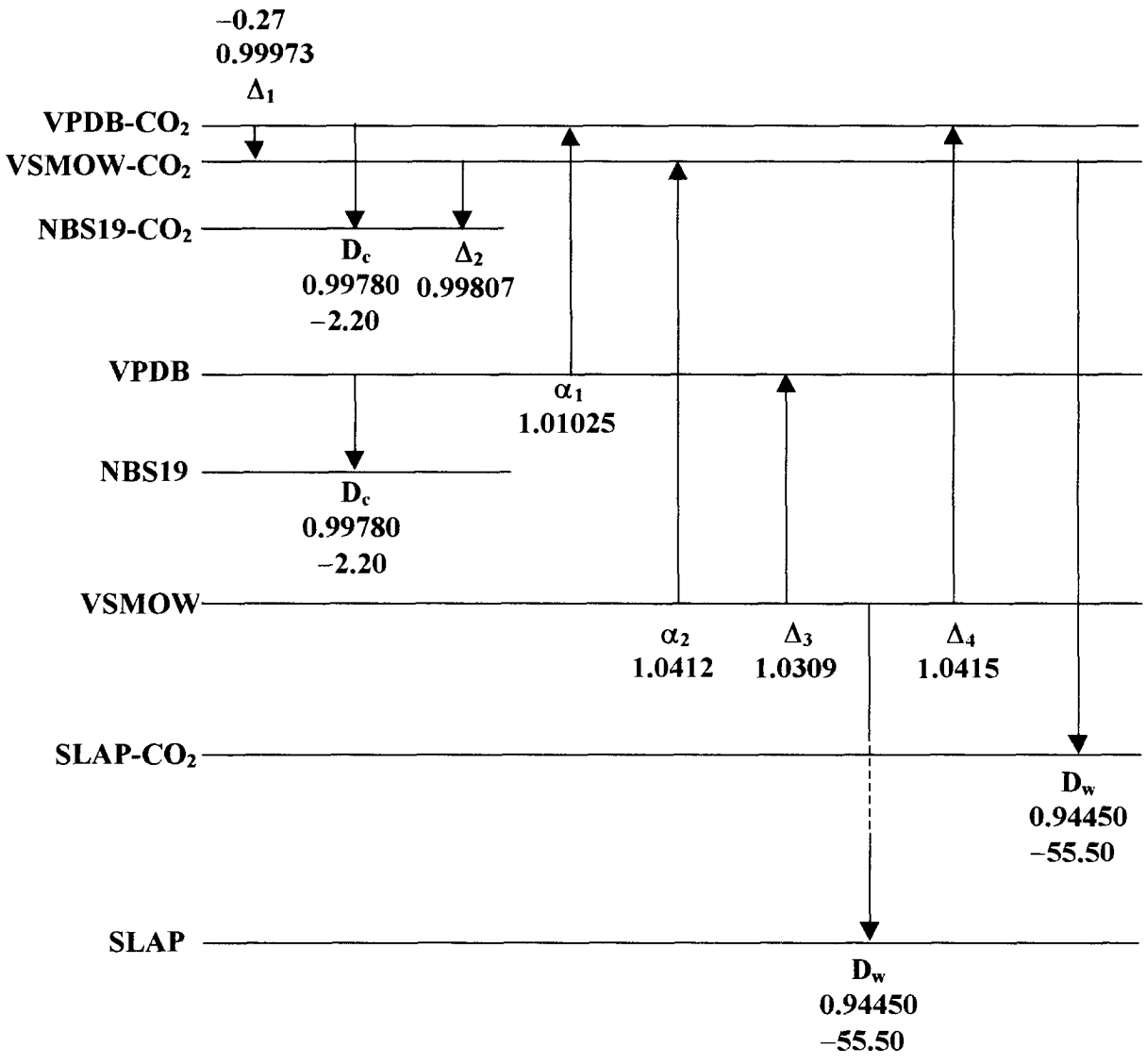

Fig.7.11 Relations between ^{18}O reference and intercomparison samples with respect to VPDB and VSMOW (IAEA, 1986). VPDB–CO_2 refers to CO_2 prepared from hypothetical VPDB by treatment with H_3PO_4 (95%) at 25°C, VSMOW–CO_2 to CO_2 equilibrated with VSMOW at 25°C. The vertical scale is indicative and not entirely proportional to real numbers.

Δ_1 : Difference between VPDB–CO_2 and SMOW–CO_2 (−0.22‰) (Craig and Gordon, 1965; Mook, 1968) plus the difference between SMOW(CO_2) and VSMOW(CO_2) (−0.05‰) (Eq.7.20)

D_c : defined value of NBS19 relative to VPDB (Eq.7.24)

Δ_2 : = $D_c - \Delta_1$

α_1 : according to Friedman and O'Neil (1977)

α_2 : average of 3 independent methods applied by 4 different laboratories

Δ_3 : from α_2 , α_1 , and Δ_1 ; 1.03086 is the exact figure quoted by Friedman and O'Neil (1977), in agreement with $\alpha_2 = 1.04115$ (Brenninkmeijer et al., 1983)

Δ_4 : from Δ_3 and α_1

The conversion equations are in general:

$$^{18}\delta_{lower} = \alpha_i \, ^{18}\delta_{upper} + \varepsilon_i \qquad \textbf{(7.28)}$$

where $\alpha_i = \Delta$, D , or α , and "lower" and "upper" refer to the levels in the scheme.

Henceforth, all $^{18}\delta$ values of carbonates are reported relative to VPDB, $^{18}\delta$ of gaseous (atmospheric) CO_2 relative to VPDB–CO_2, and all $^{18}\delta$ values of water relative to VSMOW, unless stated otherwise.

More details on the measurement and calculation procedures are given in Chapter 11.

7.2.4 SURVEY OF NATURAL ^{18}O VARIATIONS

$^{18}\delta$ variations throughout the hydrologic cycle will be discussed in detail in the other volumes. Here we present only a broad survey (Fig.7.12).

7.2.4.1 SEAWATER

The oceans form the largest global water reservoir. The ^{18}O content in the surface layer is rather uniform, varying between +0.5 and –0.5‰ (Epstein & Mayeda, 1953). Only in tropical and polar regions larger deviations are observed. In tropical regions more positive values are caused by strong evaporation: $^{18}\delta$ of water in the Mediterranean amounts to +2‰ ($^{2}\delta$ = +10‰). In polar regions more negative values originate from water melting from isotopically light snow and ice.

If ocean water were evaporating under equilibrium conditions, the vapour resulting would be 8 to 10‰ depleted in ^{18}O, depending on temperature. However, oceanic vapour appears to have an average $^{18}\delta$ value of -12 to -13‰, which must partly be due to kinetic fractionation. The relative humidity of the air and the evaporation temperature influence the amount of non-equilibrium fractionation occurring (see Volume 2 on Precipitation).

7.2.4.2 PRECIPITATION

The transformation of atmospheric water vapour to precipitation depends on so many climatological and local factors, that the $^{18}\delta$ variations in precipitation over the globe are very large. As a general rule $^{18}\delta$ becomes more negative the further the rain is removed from the

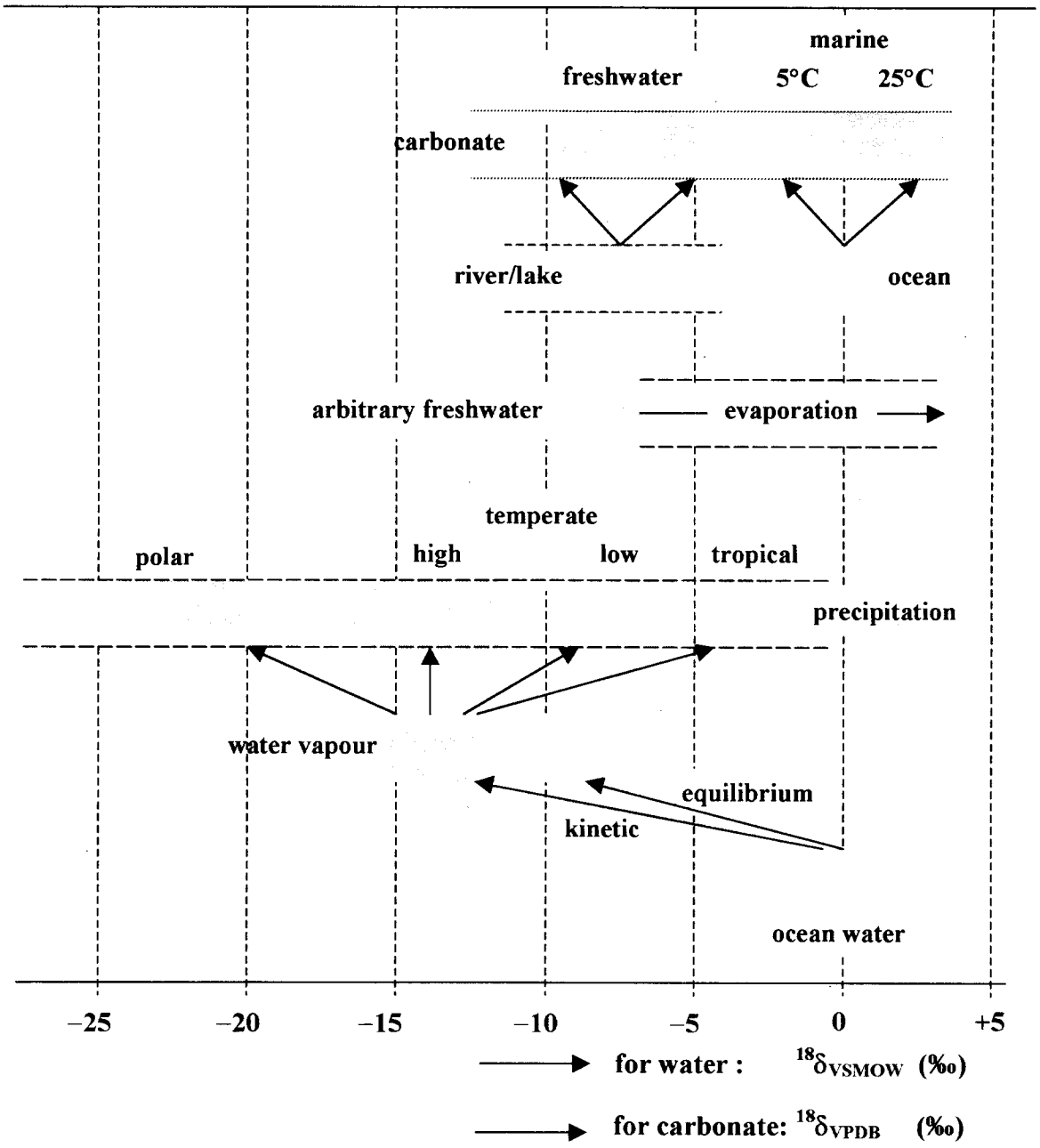

Fig.7.12 Schematic survey of natural $^{18}\delta$ variations in nature, especially relevant in the hydrological cycle. The marine vapour gradually becomes depleted in ^{18}O during the transport to higher latitudes (Fig.7.13). Evaporation of surface water may cause the water to become enriched in ^{18}O. Finally the formation of solid carbonate results in a shift in $^{18}\delta$ depending on temperature (cf. Fig.7.5).

main source of the vapour in the equatorial regions. In the Arctic and Antarctic, $^{18}\delta$ of the ice can be as low as -50‰. This gradual ^{18}O depletion model is schematically shown in Fig.7.13.

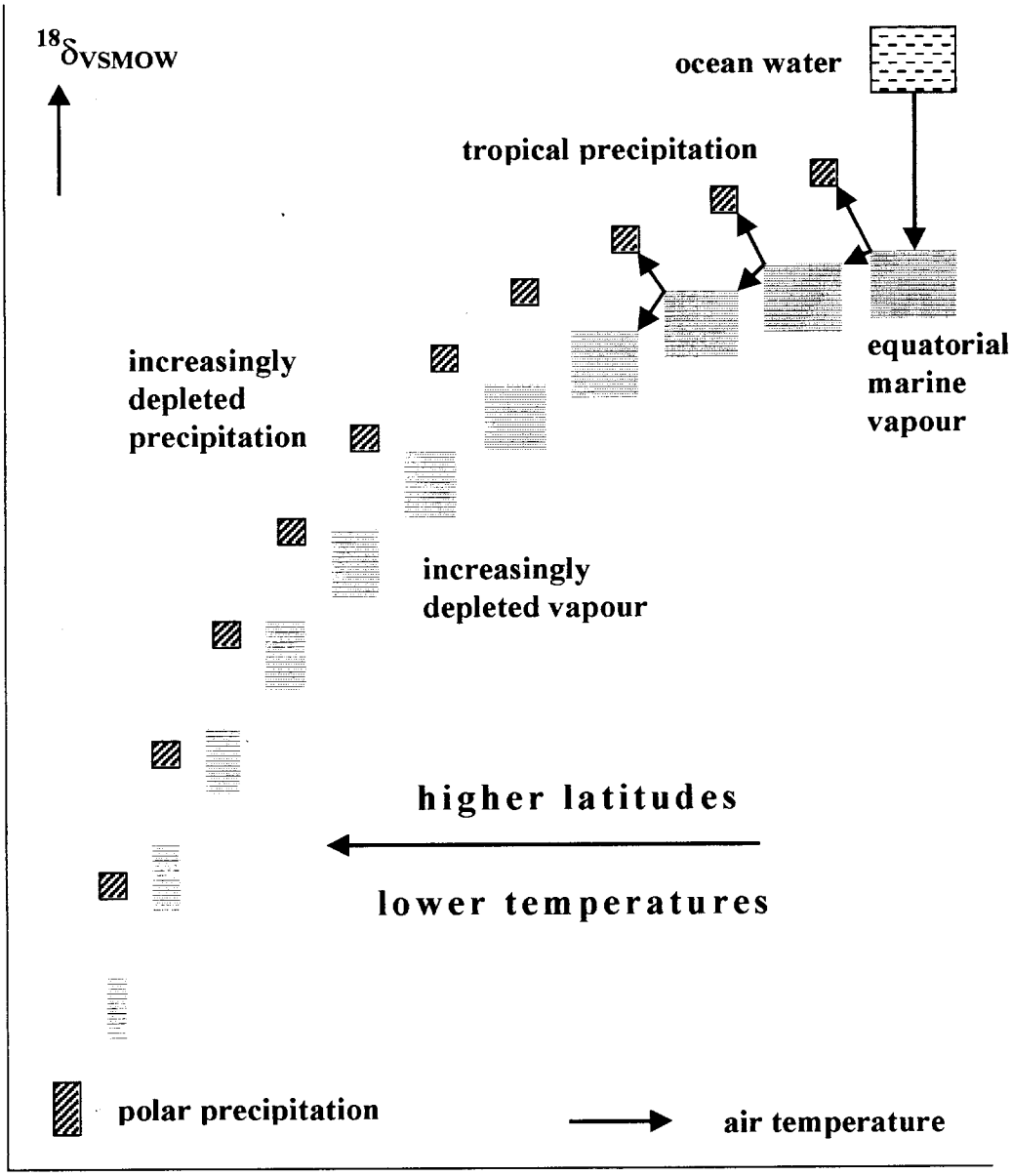

Fig.7.13 Schematic representation of the gradual depletion in ^{18}O of atmospheric water vapour and the condensing precipitation, the further the vapour and precipitation process are removed from the main source of the vapour: the tropical marine belt. At lower temperatures the isotope fractionation between water vapour and liquid water is larger, counteracting but loosing from the Rayleigh depletion process (cf. Fig.7.7 and 7.12).

In Volume 2 the various effects will be discussed in detail, causing regional and temporal variations on $^{18}\delta$ of precipitation.

We can distinguish between:

1) **latitudinal effect** with lower $^{18}\delta$ values at increasing latitude
2) **continental effect** with more negative $^{18}\delta$ values for precipitation the more inland
3) **altitude effect** with decreasing $^{18}\delta$ in precipitation at higher altitude
4) **seasonal effect** (in regions with temperate climate) with more negative $^{18}\delta$ values during winter
5) **amount effect** with more negative $^{18}\delta$ values in rain during heavy storms.

7.2.4.3 SURFACE WATER

In Fig.7.8 some data are shown on $^{18}\delta$ variations in riverwater. The seasonal variation with relatively high values in summer is characteristic for precipitation in temperate regions. The basis of both curves represents the average $^{18}\delta$ values of precipitation and groundwater in the recharge areas, i.e. N.W.Europe (Meuse) and Switzerland/S.Germany (Rhine), the latter with a large transport of relatively isotopically light meltwater in spring.

Evaporation, especially in tropical and semi-arid regions, causes ^{18}O enrichment in surface waters. This results, for instance, in $^{18}\delta$ of the river Nile to be +3 to +4‰, and of certain lakes as high as +20‰ (Sect.4.4.5 and 7.5).

7.2.5 CLIMATIC VARIATIONS

The slow precipitation of calcium carbonate is a process during which carbonate and water are in isotopic equilibrium, as was pointed out earlier. The ^{18}O content of the carbonate is, therefore, primarily determined by that of the water. The second determining factor is the temperature, as is indicated in Fig.7.10. Consequently we can in principle deduce the water temperature from $^{18}\delta$ of carbonate samples in marine sediment cores, provided $^{18}\delta$ of the water is known ($\approx$ 0‰). This was originally believed to be the basis of the ^{18}O palaeothermometry of fossil marine shells (Epstein et al., 1953).

The present-day opinions assume a varying $^{18}\delta$ of the surface ocean water during glacial/interglacial transitions (Emiliani, 1971; Olausson, 1981), due to varying amounts of accumulated ice with low $^{18}\delta$ as polar ice caps. As a realistic order of magnitude, an estimated amount of 5.10^5 km^3 of ice (= V_{ice}) laid down especially on the northern polar ice cap during the last ice age with an average $^{18}\delta$ value of –20 ‰ changes the $^{18}\delta$ value (at present = 0 ‰) of the 10^7 km^3 of ocean water (=V_{ocean}) by +1 ‰, as is simply deduced from the mass balance:

$$V_{\text{present ocean}} \times {}^{18}\delta_{\text{present seawater}} = V_{\text{ice-age ocean}} \times {}^{18}\delta_{\text{ice-age seawater}} + V_{\text{ice caps}} \times {}^{18}\delta_{\text{ice}} \quad \textbf{(7.29)}$$

Another spectacular application of isotope variations in nature is the deduction of climatic changes in the past from $^{18}O/^{16}O$ or $^{2}H/^{1}H$ ratios in polar ice cores. If the process of gradual

isotope depletion of precipitation is studied in detail as a function of latitude and thus of air temperature, a relation can be derived (Volume 2) which comes to the temperature dependence:

$$d^{18}\delta / dt \approx +0.7‰ / °C \qquad \textbf{(7.30)}$$

(Dansgaard, 1964; Van der Straaten and Mook, 1983). By this relation it is possible to translate isotope variations into climatic variations during geologic times. Records have been obtained on ice cores from Greenland and the Antarctic, showing the alternation of low-$^{18}\delta$ (or low-$^{2}\delta$) and high-$^{18}\delta$ (or high-$^{2}\delta$) periods, respectively cold and warm periods (Eq.7.30).

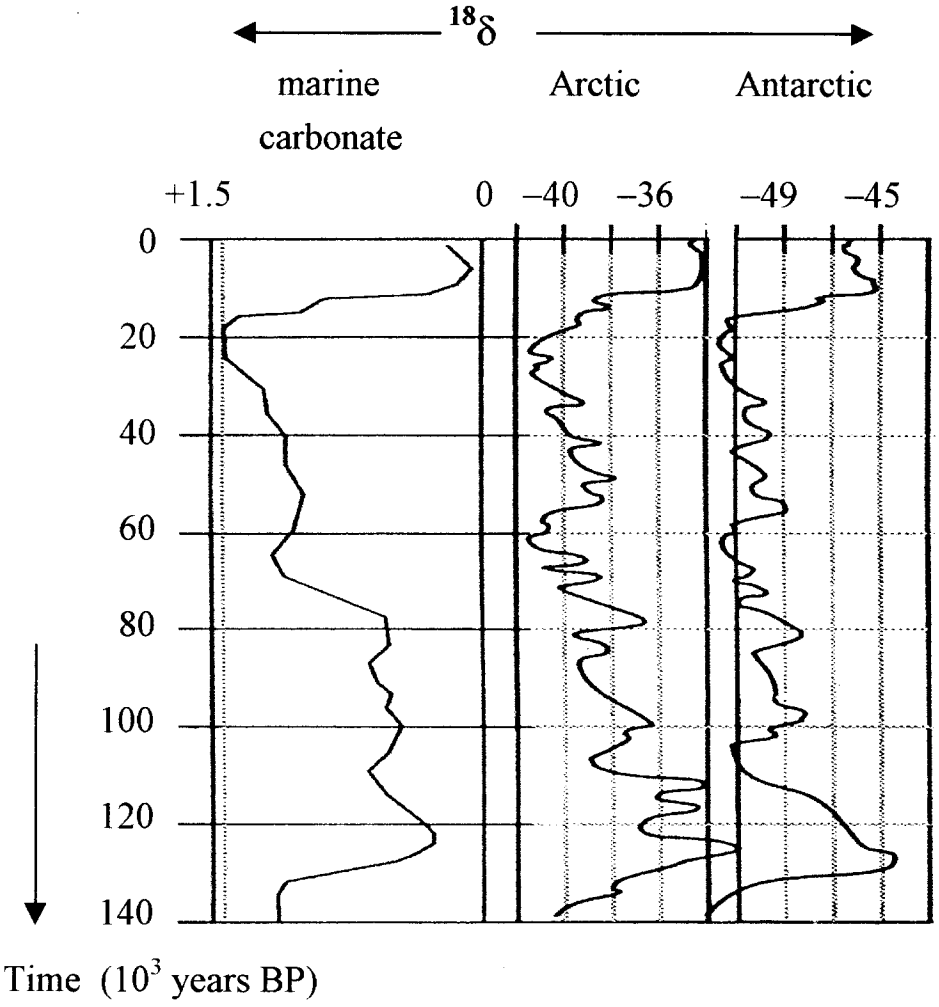

Fig.7.14 Palaeotemperature records represented by $^{18}\delta$ variations in time in the $CaCO_3$ fraction from foraminifera shells in deep-sea core sediments (left), in glacier ice of a Northern Greenland glacier (at Summit), and in glacier ice of an Antarctic ice core (at Vostok), respectively from left to right (figure modified from Lorius and Oeschger, 1994). In each record the left side indicates the lower temperatures, for instance, at 20 000 years BP each curve shows the most recent glacial maximum. The upper 10 000 years contain the present warm interglacial, the Holocene.

7.3 RELATION BETWEEN ^{13}C AND ^{18}O VARIATIONS IN H_2O, HCO_3^-, AND CO_3^{2-}

Differences and the relations between the various natural water-carbonate systems can nicely be displayed by considering both $^{18}\delta$ of the water and $^{13}\delta$ of the dissolved bicarbonate. Fig.7.15 is a schematic representation of three waters of realistic isotopic composition, each provided with the temperature dependent range of calcite precipitated under equilibrium conditions. This figure essentially is a combined graph of Figs.7.5 and 7.12.

From an isotopic point of view, the 4 common types of water are:

1) *Seawater*, with $^{18}\delta$ values around 0‰ (by definition) at present; the carbonate range is that of recent marine carbonates. Because of changing glacial and interglacial periods the $^{18}\delta$ of ocean water varied in the past. Also the $^{18}\delta$ values of marine limestone have increased during the course of geological time, while the $^{13}\delta$ values have essentially remained the same (Veizer & Hoefs, 1976).

2) *Ground- and river water*, with an arbitrarily chosen value of $^{18}\delta$. In freshwater bicarbonate $^{13}\delta$ generally is around -11 to -12‰. The isotopic compositions of fresh-water carbonates derived from this water may result from the known equilibrium fractionations (Tables 6.2 and 6.4), in a similar way as is indicated for marine carbonate.

3) *Stagnant surface or lake water* can be subjected to processes altering the isotopic composition. Provided the water has a sufficient residence time in the basin, isotope exchange will cause the ^{13}C content to reach isotopic equilibrium with atmospheric CO_2. Then $^{13}\delta$ equals that in the ocean. Carbonate $^{13}\delta$ and $^{18}\delta$ are related to, respectively, HCO_3^- and H_2O as indicated for the marine values. The ^{18}O content of the water, especially in warmer climates, will change towards less negative or even positive values due to evaporation.

4) *Estuarine water* has intermediate values of $^{13}\delta(HCO_3^-)$ or $^{13}\delta$(DIC) and $^{18}\delta(H_2O)$, depending on the degree of mixing of the river- and seawater. The latter behaves conservatively, i.e. is only determined by the mixing ratio; $^{13}\delta$(DIC) also depends on the DIC values of the mixing components. Therefore, the mixing line is generally not straight. The relation with $^{13}\delta$ of the bicarbonate fraction is even more complicated, as the dissociation equilibria change with pH (even the pH does not at all behave conservatively) (Sect.9.5.4).

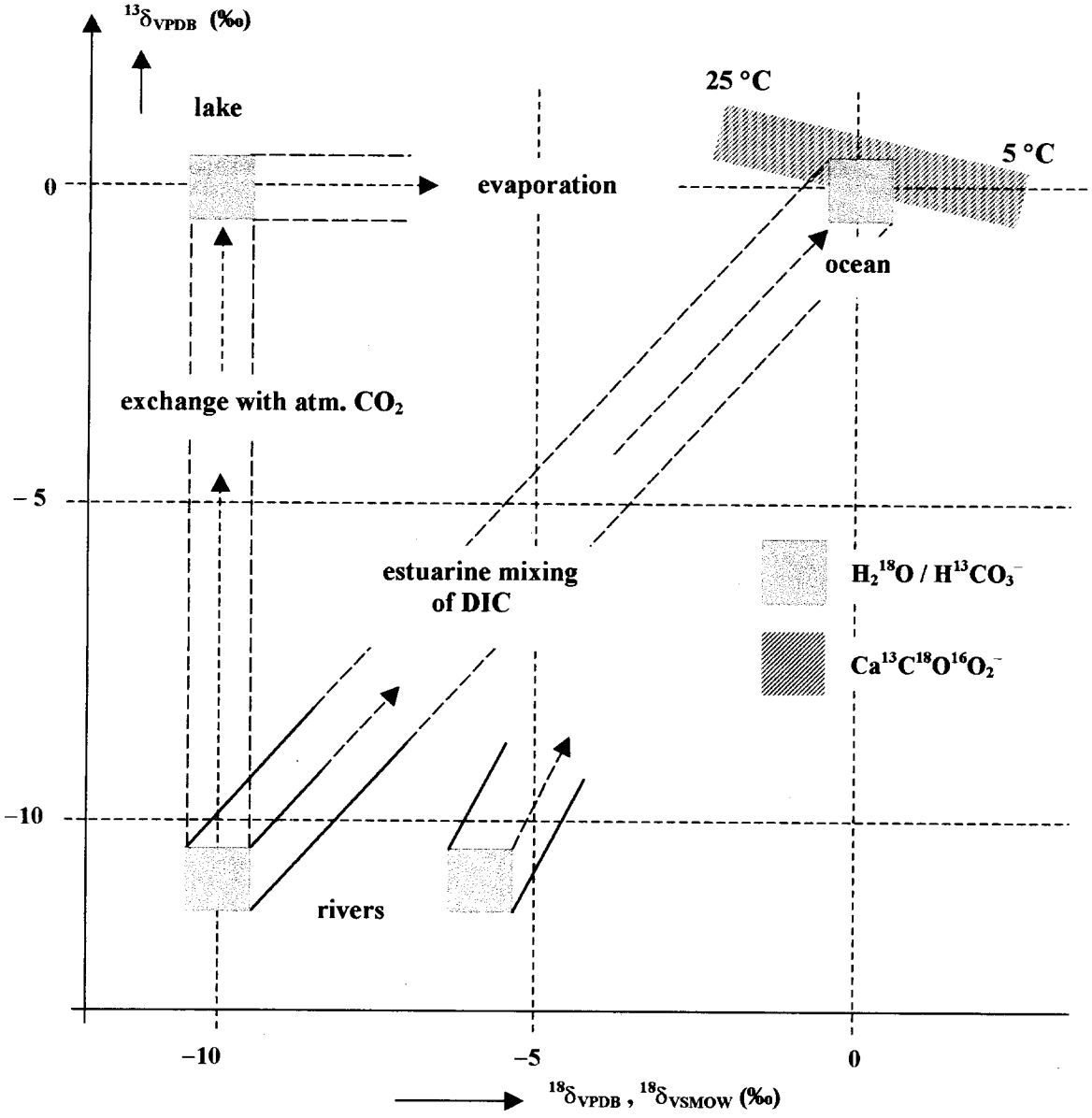

Fig.7.15 Relation between the natural variations of $^{13}\delta(HCO_3^-$ and $CaCO_3)$ and $^{18}\delta(H_2O$ and $CaCO_3)$. The graph is essentially a combination of Figs.7.5 and 7.12. Estuarine mixing only results in a straight line between the river and sea values of $^{13}\delta_{DIC}$, if C_T of the components is equal. Because this is rarely the case, the relation between the two members mostly is observed as a slightly curved line. Additionally, $^{13}\delta(HCO_3^-)$ in estuaries is not subject to conservative mixing, because the mixing process rearranges the carbonate fractions (Sect.9.5.4). Depending on the residence times of the water at the surface, evaporation and isotope exchange changes the isotopic composition to higher δ values.

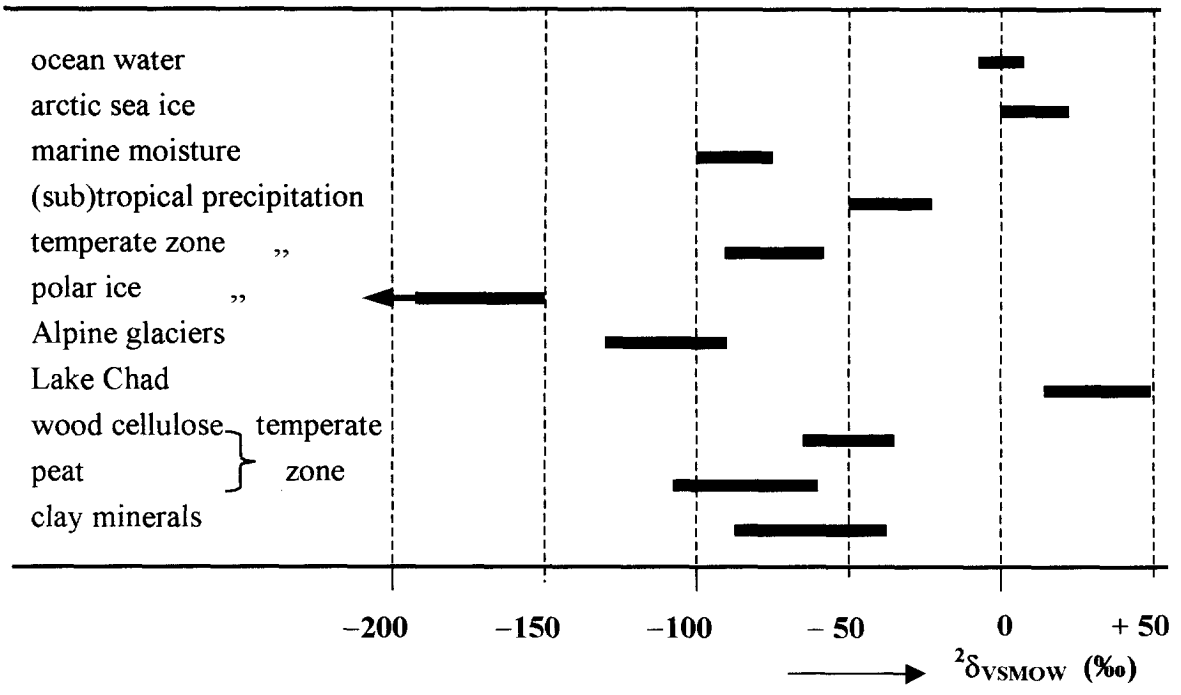

Fig.7.16 General view of $^2H/^1H$ variations in natural compounds. The ranges are indicative for the majority of materials shown.

7.4 STABLE HYDROGEN ISOTOPES

7.4.1 THE NATURAL ABUNDANCE

The chemical element hydrogen consists of two stable isotopes, ^1H and ^2H (D or Deuterium), with an abundance of about 99.985 and 0.015% and an isotope ratio $^2H/^1H \approx 0.00015$ (Urey et al., 1932). This isotope ratio has a natural variation of about 250‰, higher than the $^{13}\delta$ and $^{18}\delta$ variations, because of the relatively larger mass differences between the isotopes (Fig.7.16).

As with ^{18}O, high ^2H concentrations are observed in strongly evaporated surface waters, while low ^2H contents are found in polar ice. Variations of about 250‰ are present in the part of the hydrological cycle to be discussed here.

7.4.2 HYDROGEN ISOTOPE FRACTIONATIONS

The most important hydrogen isotope fractionation is that between the liquid and the vapour phases of water. Under equilibrium conditions water vapour is isotopically lighter (contains less ^2H) than liquid water by amounts given in Table 7.6. Fig.7.3 shows some actual isotope ratios of equilibrium systems and the matching $^2\delta$ values. The fractionation by diffusion of H_2O through air ($^2\delta_d$) varies between −22.9 ± 1.7‰ (Merlivat, 1978) and −20.4 ± 1.4‰. (unpubl.), slightly more than the value calculated from Eq.3.34 (−16.3‰) (cf. Sect. 7.3.2).

7.4.3 REPORTING ^2H VARIATIONS AND THE ^2H STANDARD

VSMOW is the *standard* for $^2H/^1H$ as it is for $^{18}O/^{16}O$ ratios. Values for the absolute $^2H/^1H$ ratio of VSMOW and SLAP are reported to be $(155.76 \pm 0.07)\times10^{-6}$ and $(89.02 \pm 0.05)\times10^{-6}$, respectively, by Hagemann et al. (1970), $(155.75 \pm 0.08)\times10^{-6}$ and $(89.12 \pm 0.07)\times10^{-6}$ by De Wit et al. (1980), and $(155.60 \pm 0.12)\times10^{-6}$ and $(88.88 \pm 0.18)\times10^{-6}$ by Tse et al. (1980).

Table 7.5 The stable and radioactive isotopes of **hydrogen**: practical data for the natural abundance, properties, analytical techniques and standards. Further details are given in Sect.7.4 and 8.3, and in Chapters 10 and 11.

MS=mass spectrometry, PGC=proportional gas counting, LSS=liquid scintillation spectrometry, AMS=accelerator mass spectrometry

	^1H	^2H	^3H
natural abundance	0.99985	0.00015	$< 10^{-17}$
stability	stable	stable	radioactive
natural specific activity			< 1.2 Bq/L water
decay mode / daughter			β^- / ^3He
half-life ($T_{1/2}$)			12.320 ± 0.022 a
decay constant (λ)			5.576×10^{-2}/a = 1/18.33 a^{-1}
max. β energy			18 keV
abundance range in hydrological cycle		250‰	0 to 10^{-16}
reported as		$^2\delta$ or δ^2H or δD	^3A
in		‰	TU, Bq/L H_2O
instrument		MS	PGC, LSS
analytical medium		H_2	H_2O, C_2H_6, C_6H_6
usual standard deviation		0.5‰	≥ 1% at high level
international standard		VSMOW	NBS-SRM 4361
with absolute value		$^2H/^1H$ = 0.00015575	$^3H/^1H$ = 6600 TU or = 0.780 Bq/g H_2O as of Jan.1, 1988

The average $^2\delta$ value of the secondary standard SLAP on the VSMOW scale (Sect.7.2.3) consequently is −428.2 ± 0.1‰. Based on these data the $^2\delta$ value has been defined as:

$$^2\delta_{SLAP\,/\,VSMOW} = -428.0‰ \qquad \textbf{(7.33)}$$

No significant difference in $^2\delta$ has been detected between the original SMOW standard and VSMOW (IAEA, 1978).

Table 7.6 Hydrogen isotope fractionation in the equilibrium system liquid water (l), water vapour (v), and ice (i); $\varepsilon_{y\,/\,x}$ represents the fractionation of compound y relative to compound x and is approximately equal to $^2\delta(y) - {}^2\delta(x)$. Values for intermediate temperatures may be obtained by linear interpolation; $T = t\,(°C) + 273.15$ K.

t °C	$^2\varepsilon_{v/l}$ [1]) (‰)	$^{18}\varepsilon_{v/l}$ (‰)	$^2\varepsilon_{v/l} / {}^{18}\varepsilon_{v/l}$ [2])
0	−101.0	−11.55	8.7
5	− 94.8	−11.07	8.5[5]
10	− 89.0	−10.60	8.4
15	− 83.5	−10.15	8.2[5]
20	− 78.4	− 9.71	8.1
25	− 73.5	− 9.29	7.9
30	− 68.9	− 8.89	7.7[5]
35	− 64.6	− 8.49	7.6
40	− 60.6	− 8.11	7.4

[1]) Majoube, 1971 $: \ln {}^2\alpha = -24\,844/T^2 + 76.248/T - 0.052612$ **(7.31a)**

1/T adjustment $: {}^2\varepsilon_{v/l} = -85\,626/T + 213.4‰$ **(7.31b)**

Values at higher temperatures can be obtained from Horita and Wesolowski(1994)

[2]) The ratios between the fractionations for ^{18}O and ^2H at the liquid–vapour equilibrium are obtained from Majoube (1971).

Majoube, 1971 $: {}^2\varepsilon_{i/l} = +\,19.3‰$ (at 0°C) **(7.32)**

Reference and intercomparison water samples are available from the IAEA (Table 11.3). The ^2H contents of hydrogen-containing samples are determined by completely converting them to hydrogen gas. Therefore, fundamental problems of isotope fractionation during sample preparation, as with ^{18}O, do not occur; however, the analyses are more troublesome (Sect.10).

Henceforth all $^2\delta$ values will be reported relative to VSMOW.

More details on the measurement and calculation procedures, and on isotope reference samples are given in Chapter 10.

7.4.4 SURVEY OF NATURAL ^{2}H VARIATIONS

From the foregoing it is evident that some correlation should exist between ^{2}H and ^{18}O fractionation effects. Therefore, in natural waters a relation between $^2\delta$ and $^{18}\delta$ values is to be expected. Indeed, the $^2\delta$ and $^{18}\delta$ variations in precipitation, ice, most groundwaters and non-evaporated surface waters have appeared to be closely related. Therefore, the qualitative discussion given in Sect.7.2.4 for $^{18}\delta$ applies to $^2\delta$ equally well. The next section is devoted to this relation.

7.5 RELATION BETWEEN ^{2}H AND ^{18}O VARIATIONS IN WATER

If we simply assume that evaporation and condensation in nature occur in isotopic equilibrium, the relation between the $^2\delta$ and $^{18}\delta$ values of natural waters is determined by both equilibrium fractionations $^2\varepsilon_{v/l}$ and $^{18}\varepsilon_{v/l}$. In Table 7.6 the ratio of these factors is presented for the temperature range of 0 – 40°C.

Craig (1961b) and Dansgaard (1964) found a relation between the $^2\delta$ and $^{18}\delta$ values of precipitation from various parts of the world:

$$^2\delta = 8\ ^{18}\delta + 10\ ‰ \qquad \textbf{(7.34)}$$

This relation, shown in Fig.7.17 has become known as the *Global Meteoric Water Line* (GMWL) and is characterised by a *slope* of 8 and a certain *intercept* with the ^{2}H axis (= the $^2\delta$ value at $^{18}\delta$ = 0‰). The general relation is of the MWL is:

$$^2\delta = s\cdot{}^{18}\delta + d \qquad \textbf{(7.35)}$$

where the slope s = 8, as is explained by the ratio between the equilibrium isotope fractionations of hydrogen and oxygen for the rain condensation process (Table 7.6); d is referred to as the *deuterium excess* (*d-excess*), the intercept with the $^2\delta$ axis. In several regions of the world as well as during certain periods of the year and even certain storms the $^2\delta$ value is different from 10 ‰, depending on the humudity and temperature conditions in the evaporation region.

The isotopic composition of water vapour over seawater with $^2\delta = {}^{18}\delta = 0$ ‰ vs VSMOW is somewhat lighter than would follow from isotopic equilibrium with the water: the evaporation

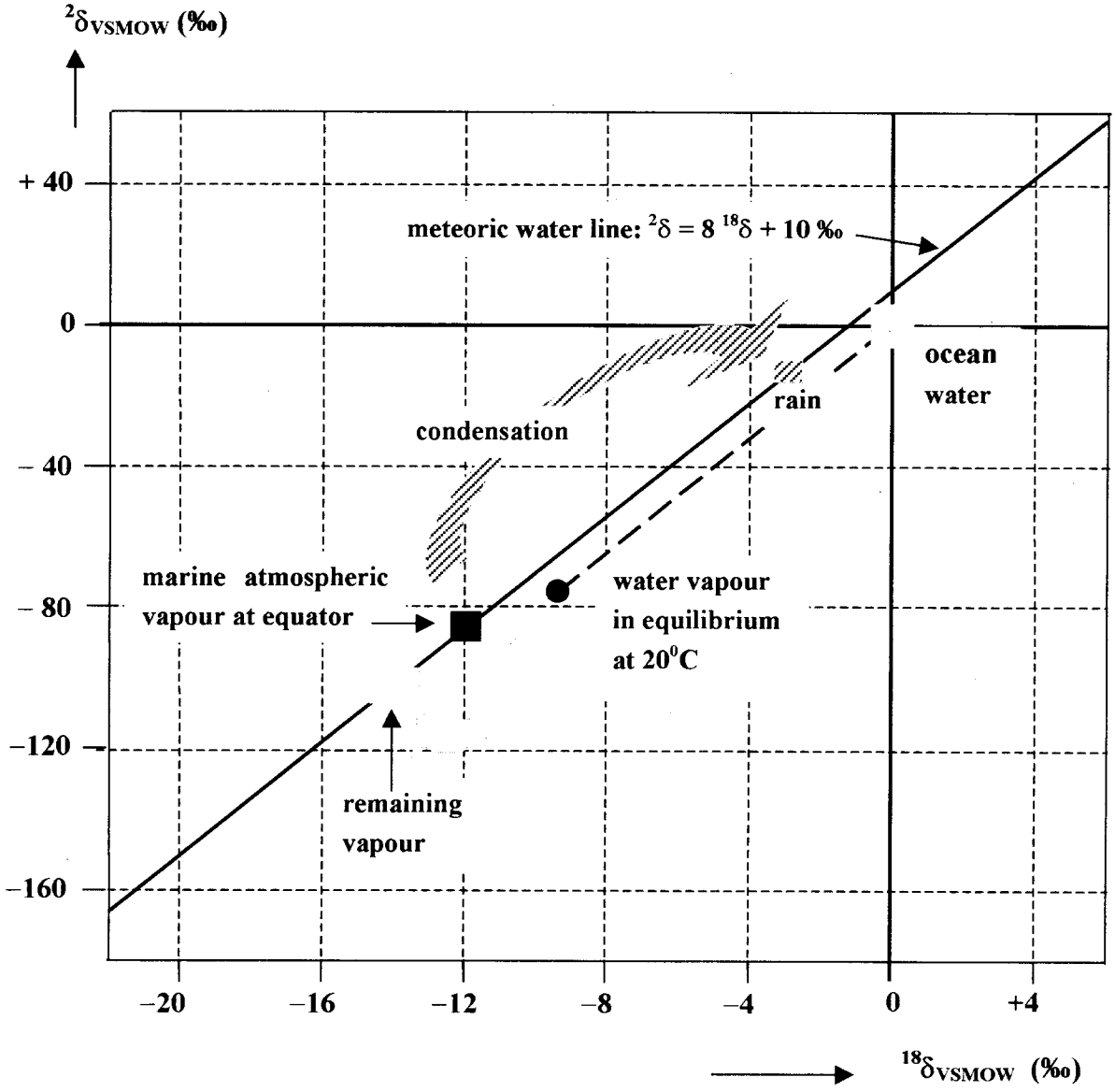

Fig.7.17 Relation between natural variations of $^{18}\delta$ and $^{2}\delta$ ocean water, atmospheric vapour and precipitation. The black round represents the hypothetical value of water vapour in isotopic equilibrium with ocean water, black square the observed isotopic composition of equatorial marine vapour, originated from the more realistic non-equilibrium fractionation. Marine vapour gradually condenses into precipitation (hatched arrow) with a positive fractionation, leaving the vapour progressively depleted in ^{18}O and ^{2}H (grey arrow) (cf. Fig.7.13).

is a non-equilibrium (partly kinetic) process. However, from the observed vapour composition onward the vapour and precipitation remain in isotopic equilibrium, because the formation of precipitation is likely to occur from saturated vapour (i.e. vapour in physical equilibrium with water). Consequently the $^{18}\delta$ and $^{2}\delta$ values both move along the meteoric water line (Eq.7.33).

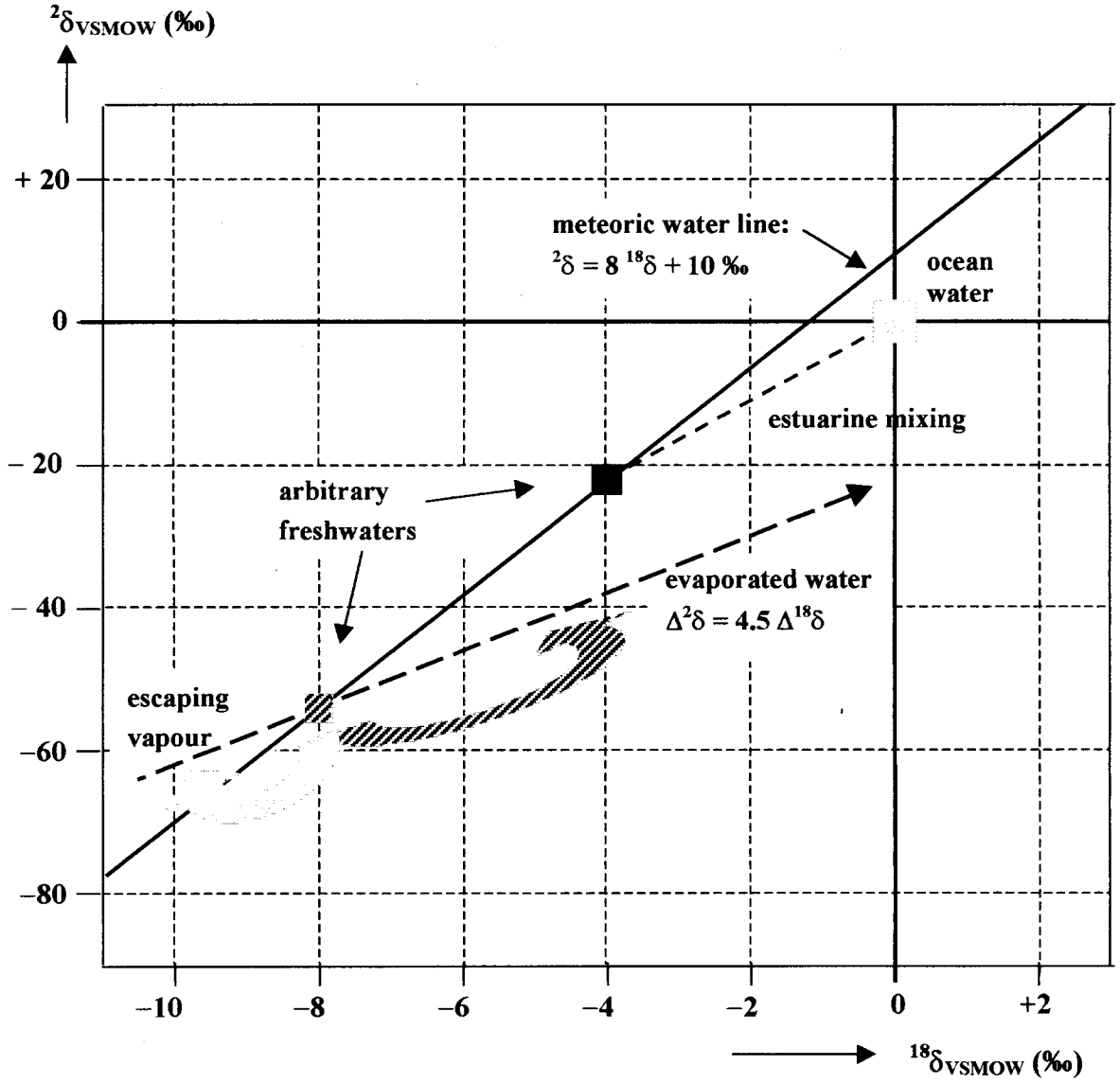

Fig.7.18 Relation between $^{18}\delta$ and $^{2}\delta$ for estuarine mixing and for evaporating surface water. Because the evaporation is a non-equilibrium process, isotope fractionations involved are not necessarily related by a factor of 8, as is the equilibrium condensation process, the basis for the meteoric water line (Fig.7.17). As in the preceding figure, the arrows indicate the direction of change of the isotopic composition of the escaping vapour and of the remaining evaporated water.

In Volume 3 (Surface Water) certain circumstances will be discussed leading to deviations from the common MWL. For instance, larger values of d are occasionally observed.

Apart from this, deviations occur in evaporating surface waters, showing slopes of 4 to 5 rather than 8. If $^{2}\delta_o$ and $^{18}\delta_o$ denote the original isotopic composition of an arbitrary surface water, the δ values after evaporation are related by:

$$^{2}\delta - {}^{2}\delta_o \approx 4.5\,(^{18}\delta - {}^{18}\delta_o) \quad \text{or} \quad \Delta^{2}\delta \approx 4.5\,\Delta^{18}\delta \qquad \textbf{(7.35)}$$

(Fig.7.18). The release of relatively low-δ water vapour to the air results in a increase in δ of the remaining water, as illustrated by the model of Sect.4.4.5, here for $^{2}\delta$ as well as $^{18}\delta$.

8 NATURAL ABUNDANCE OF RADIOACTIVE ISOTOPES OF C AND H

In this chapter the two nuclides, ^{14}C and ^{3}H, will be treated that are the most relevant in the hydrological cycle. Chapter 12 contains a survey of the isotopes with less extensive applications.

8.1 THE RADIOACTIVE CARBON ISOTOPE

8.1.1 ORIGIN OF ^{14}C, DECAY AND HALF-LIFE

The natural occurrence of the radioactive carbon isotope, ^{14}C or radiocarbon, was first recognised by W.F. Libby (1946). It is naturally formed in the transitional region between the stratosphere and troposphere about 12 km above the earth's surface through the nuclear reaction:

$$^{14}N + n \rightarrow {}^{14}C + p \qquad \textbf{(8.1)}$$

The thermal neutrons required are produced by reactions between very high-energy primary cosmic ray protons and molecules of the atmosphere. ^{14}C thus formed very soon oxidises to ^{14}CO, and ultimately to $^{14}CO_2$ which mixes with the inactive atmospheric CO_2 (Fig.8.1). Through exchange with oceanic dissolved carbon (primarily bicarbonate), most $^{14}CO_2$ molecules enter the oceans and living marine organisms. Some are also assimilated by land plants, so that all living organisms, vegetable as well as animal, contain ^{14}C in concentrations about equal (Sect.8.1.3) to that of atmospheric CO_2.

^{14}C decays according to:

$$^{14}C \rightarrow {}^{14}N + \beta^- \qquad \textbf{(8.2)}$$

with a maximum β^- energy of 156 keV and a half-life of 5730 ± 40 years (Godwin, 1962) (Fig.8.2). Originally the half-life was thought to be 5568 years, so that during the first decade or two ^{14}C age determinations were based on the "wrong" half-life. Later, when the "better" half-life became known, so many ^{14}C ages were already published that, in order to avoid confusion, it was decided that the original half-life should continued to be used for reporting ^{14}C ages. Moreover, it was meanwhile known that ages would still be in error, even using the right half-life, because of the natural variations in the ^{14}C content of atmospheric CO_2 during geologic times and deviating from the present. These errors were even larger. Nowadays the

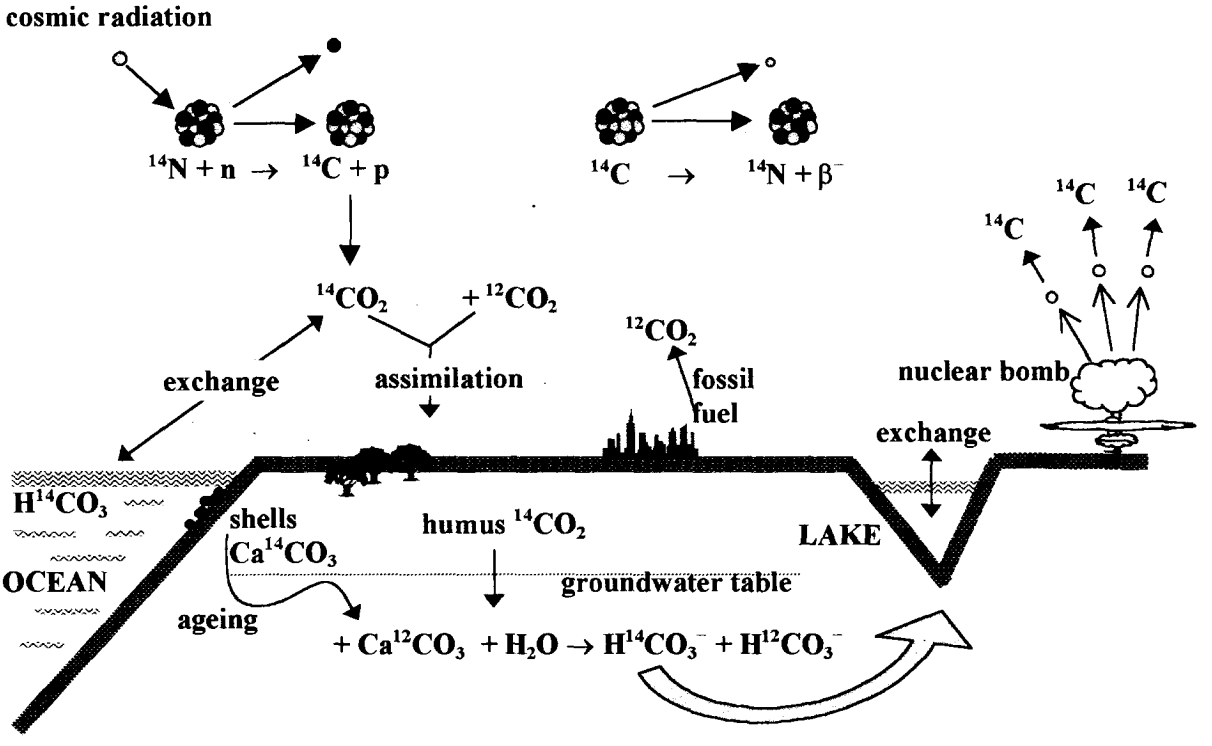

Fig.8.1 Origin and distribution of ^{14}C in nature. The natural ^{14}C concentration by the production by neutrons from cosmic radiation has been influenced by -chronologically- the addition to the air of CO_2 without ^{14}C by the combustion of fossil fuels and the production of ^{14}C by neutrons released by the fission and fusion reactions during nuclear explosions.

^{14}C calibration, based on the known ^{14}C content of tree rings with exactly known age, removes both errors at once (Sect.8.1.4).

The production and distribution of ^{14}C in nature occurs through series of chemical and biological processes which has become stationnary throughout much of geologic time. As a consequence, the concentration of ^{14}C in the atmosphere, oceans and biosphere reached a steady-state value which has been almost constant during a geologic period which is long compared to the life span of a ^{14}C nucleus. This natural concentration, $^{14}C/C$, is of the order of 10^{-12}, which is equivalent to a specific activity of about 0.25 Bq/gC (disintegrations per second per gram of carbon) (Sect.5.3).

8.1.2 REPORTING ^{14}C VARIATIONS AND THE ^{14}C STANDARD

Three modes of reporting ^{14}C activities are in use, in part analogous to the conventions internationally agreed (IAEA) for stable isotopes (Stuiver and Polach, 1977; Mook and Van der Plicht, 1999).

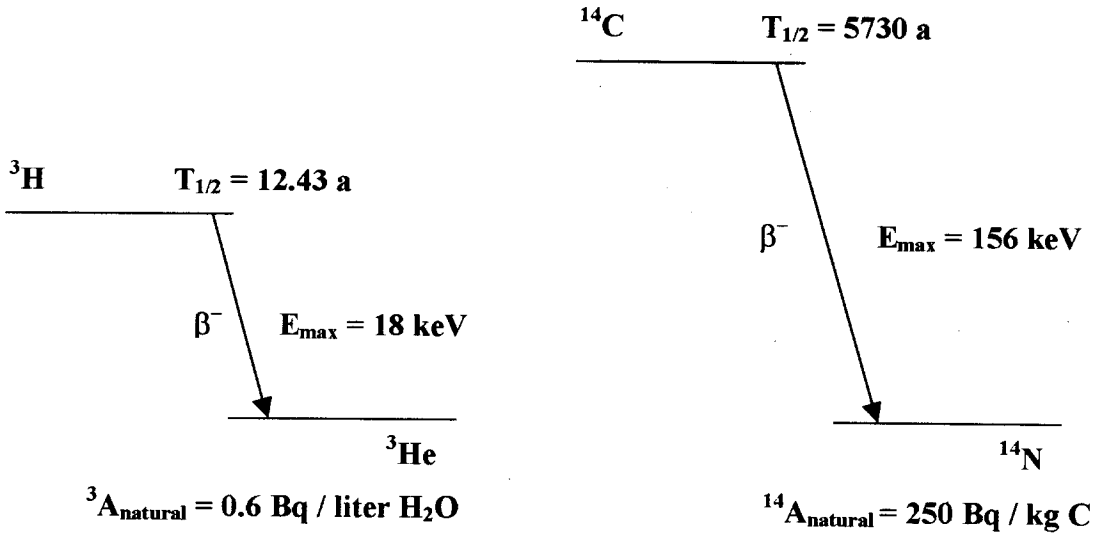

Fig.8.2 Decay schemes of tritium and radiocarbon. Both nuclides are pure β^- emitters. The present-day specific activities are given as ^{3}A and ^{14}A.

The *absolute (specific) ^{14}C activity*, that is the ^{14}C radioactivity (in Bq or, conventionally, in disintegrations per minute (dpm) per gram of carbon) is given the symbol

$$^{14}A = \text{number of disintegrations per minute (dpm/gC)} \qquad \textbf{(8.3)}$$

It is extremely difficult to make an absolute measurement of a ^{14}C activity. Moreover, the absolute ^{14}C content of a sample is generally not relevant. Therefore, the sample activities are compared with the activity of a standard. In reality, the number of ^{14}C registrations (β registrations from ^{14}C decay in radiometric detectors such as proportional counters and liquid scintillation counters, registrations of ^{14}C concentration in AMS systems) are related to the number of registrations from the standard under equal conditions.

This results in a *^{14}C activity ratio* or *^{14}C concentration ratio*:

$$^{14}a = \frac{^{14}A_{sample}}{^{14}A_{reference}} = \frac{^{14}A}{^{14}A_R} =$$

$$= \frac{^{14}C \text{ decay rate in the sample}}{^{14}C \text{ decay rate in the reference}} = \frac{^{14}C \text{ concentration in the sample}}{^{14}C \text{ concentration in the reference}} \qquad \textbf{(8.4)}$$

Because in the nominator and denominator of the last two fractions the detection efficiencies are cancelled being equal for sample and reference material, the use of the ratio ^{14}a is adequate for any type of measuring technique.

Henceforth, the symbol ^{14}A may be used for the *^{14}C content* (radioactivity or concentration) of a sample, whether the analytical technique applied is radiometric or mass spectrometric (AMS).

Under natural circumstances the values of ^{14}a are between 0 and 1. In order to avoid the use of decimals, it is general practice to report these values in %, which is equivalent to the factor 10^{-2} (see also Sect.11.5.1). It is incorrect to write $^{14}a/10^2$ instead of merely ^{14}a.

In several cases the differences in ^{14}C content between the project samples are small. Therefore, the use has been taken over from the stable-isotope field to define relative abundances, in casu the *relative ^{14}C content (activity or concentration)*, $^{14}\delta$, defined as the difference between sample and reference ^{14}C content as a fraction of the reference value:

$$^{14}\delta = \frac{^{14}A - {}^{14}A_R}{^{14}A_R} = \frac{^{14}A}{^{14}A_R} - 1 = {}^{14}a - 1 \quad (\times 10^2\ \%) \qquad \textbf{(8.5)}$$

The values of δ are small numbers and therefore generally given in ‰, which is equivalent to the factor 10^{-3} (cf. Sect.4.1).

In Chapter 7 we have seen that during any process in nature isotope fractionation occurs, not only for the stable isotopes but similarly for the radioactive isotope such as ^{14}C. Neglecting this effect would introduce an error in an age determination, because the original ^{14}C content of the material would be different from what we assume. The degree of fractionation is nicely indicated by the $^{13}\delta$ value of the material. An example is the apparent difference in age between C_3 plants such as trees ($^{13}\delta \approx -25$‰) and a C_4 plant such as sugar cane ($^{13}\delta \approx -10$‰), each assimilating the same atmospheric CO_2. Therefore, in defining the standard activity, but also in our treatment of all ^{14}C data, we have to *normalise* the ^{14}C results to the same $^{13}\delta$ value. In Chapter 11 we will go into more detail. Here we suffice by stating that by international agreement all ^{14}C results have to be corrected for a deviation of the $^{13}\delta$ value from −25‰, with the exception of Ox1 which has to be corrected to −19‰.

The ^{14}C *standard activity* or *concentration* was chosen to represent as closely as possible the ^{14}C content of carbon in naturally growing plants. The ^{14}C standard activity does not need to be, in fact it is not, equal to the ^{14}C activity of the standard. The definition of the standard ^{14}C activity is based on 95% of the specific activity of the original NBS oxalic acid (Ox1) in the year AD1950 (Karlén et al., 1966), as will be discussed in more detail later.

The ^{14}C *standard activity* is defined by:

$$^{14}A^0_{standard} = 0.95\ {}^{14}A^0_{Ox1} = 13.56 \pm 0.07\ \text{dpm/gC} = 0.226 \pm 0.001\ \text{Bq/gC} \qquad \textbf{(8.6)}$$

dpm/gC means disintegrations per minute per gram of carbon, while the superscript ^{0} refers to the fact that the definition is valid for the year 1950 only.

Because the original supply of oxalic acid has been exhausted, a new batch of oxalic acid (Ox2) is available for distribution by the NIST (formerly US-Nat. Bureau of Standards).

Through careful measurement by a number of laboratories (Mann, 1983), the ^{14}C activity has become related to that of the original Ox1 by:

$$^{14}A^0_{Ox2} = (1.2736 \pm 0.0004)\ ^{14}A^0_{Ox1} \qquad \textbf{(8.7)}$$

Both activities refer to AD1950. Consequently the standard activity is:

$$^{14}A^0_{standard} = 0.7459\ ^{14}A^0_{Ox2} \qquad \textbf{(8.8)}$$

where the $^{14}A^0$ values for Ox1 and Ox2 refer to the activity of the material in 1950, irrespective of the time of measurement.

Details on the measurement and calculation procedures are given in Chapter 11.

A survey of available ^{14}C reference samples of different compounds and ages is given in Table 11.5.

8.1.3 SURVEY OF NATURAL ^{14}C VARIATIONS

8.1.3.1 ATMOSPHERIC CO_2

Certain fluctuations occur in the stationary state mentioned in Sect.8.1.1. Because of variations in cosmic ray intensity, and in climate affecting the size of the carbon reservoirs, the ^{14}C content of atmospheric carbon has not always been precisely the same as at present. This phenomenon has been observed by measuring the ^{14}C content of tree rings (see Fig.8.5).

These fluctuations do not exceed a few per cent over relatively short periods, and are, therefore, of very little relevance to the hydrologist who is generally confronted with dissolved carbon from a variable vegetation covering a long and uncertain period of time.

The strong increase in the atmospheric ^{14}C level due to the nuclear test explosions is of more relevance to the hydrologist. During the bomb explosions ^{14}C (and ^3H) is being produced by the same nuclear reactions that are responsible for the natural production. In the northern hemisphere the peak concentration occurred during the spring of 1963, when it was about double the natural concentration (Fig.8.3). In the southern hemisphere a more gradual increase has taken place. This is due to the fact that the seasonal injections of ^{14}C from the stratosphere into the troposphere primarily occurred over the northern hemisphere, while air is not easily and simply transported across the equator. The ^{14}C increase only gradually leaked through the equatorial regions to the southern troposphere.

8.1.3.2 VEGETATION AND SOILS

The higher ^{14}C levels have entered the soil vegetation, and have become detectable in the CO_2 gas, present in the soil and playing a major role in the formation of dissolved inorganic carbon in groundwater. In this way the "bomb effect" possibly increases the ^{14}C content of young groundwater.

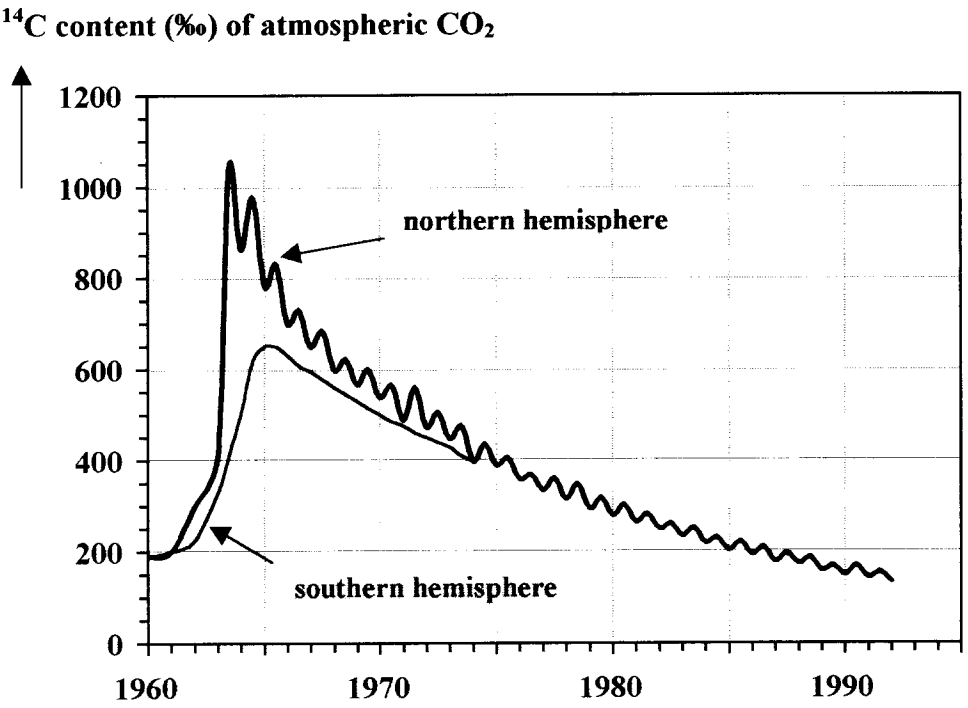

Fig.8.3 Curve representing the natural ^{14}C content of atmospheric CO_2 (data for Nordkapp, Norway, representative for the northern hemisphere) (Nydal, pers.comm.). Test explosions of nuclear weapons since the fifties and especially the early sixties have temporarily increased the concentration by a factor of two. Due to isotopic exchange with the oceans, ^{14}C is slowly returning to "normal". The influence on the southern hemisphere was obviously smaller. The seasonal variation of some per cent during the late 1960s has been smoothed out, since they are not relevant in hydrology, contrary to the ^{3}H variations to be discussed later in this chapter.

The CO_2 generated in the soil by decaying plant remains and by root respiration is relatively young and therefore contains about the atmospheric ^{14}C concentration (^{14}a = 100%) (Fig.8.3).

8.1.3.3 SEAWATER AND MARINE CARBONATE

Because seawater is in constant exchange with atmospheric CO_2, one would expect that, like the stable carbon isotopes, that an isotopic equilibrium exists between the two reservoirs. This is not the case, due to the phenomenon of *upwelling* of water from greater depth and a

considerable age. This may extent to ages of 1500 years, equivalent to an ^{14}a value of the order of 85%. In general, in surface seawater ^{14}C contents are observed in the range of 95%.

8.1.3.4 GROUNDWATER

By processes of erosion and re-sedimentation fossil carbonate is generally part of terrestrial soils. Here it may be dissolved by the action of soil-CO_2, which is contained by the infiltrating rain water. In this way the dissolved inorganic carbon in groundwater also contains ^{14}C (Münnich, 1957). As the carbonate is very old and thus without ^{14}C ($^{14}a = 0\%$) - generally, but not always (see Volume 4 on Groundwater) - the bicarbonate resulting from the reaction:

$$CO_2 + H_2O + CaCO_3 \rightarrow Ca^{2+} + 2HCO_3^- \qquad (8.9)$$

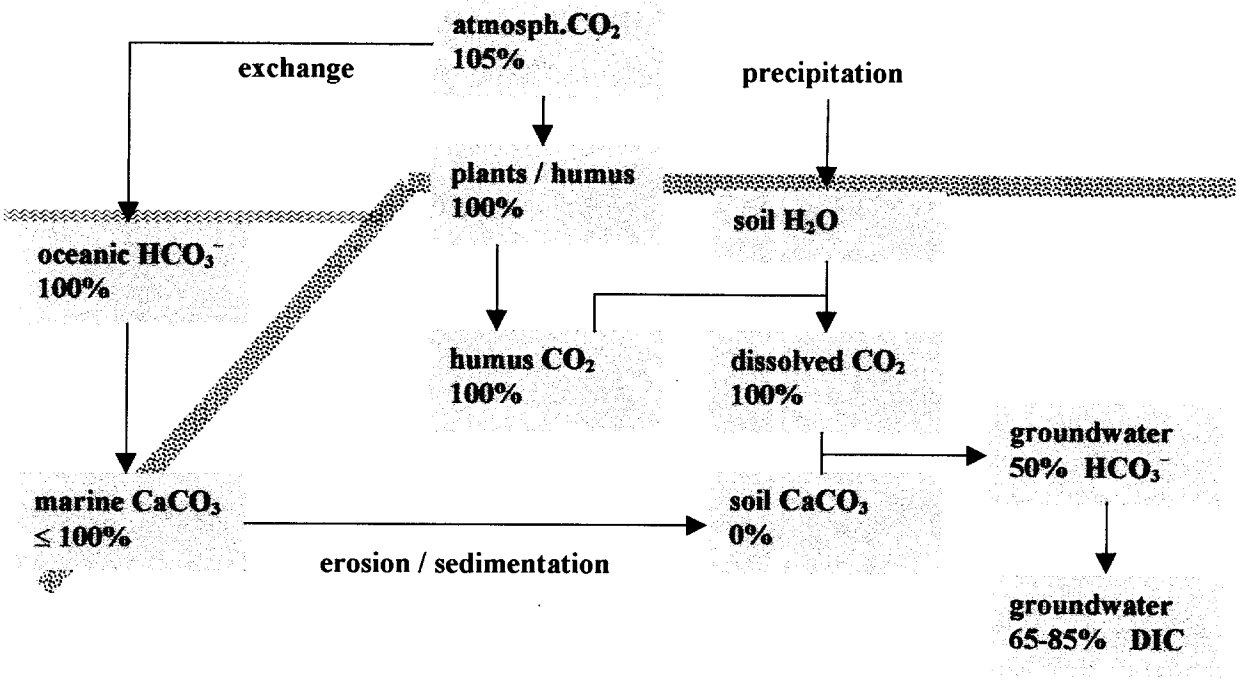

Fig.8.4 Schematic representation of the formation of dissolved inorganic carbon in groundwater. The percentages are the ^{14}a values indicative for the carbonate dissolution, which is the most relevant process in most types of groundwater. The ^{14}a value of groundwater HCO_3^- of 50% results in higher values of ^{14}a in the total dissolved carbon because of the additional CO_2 and of isotopic exchange with the soil-CO_2.

will have a ^{14}C content one half that of the CO_2 ($^{14}a = 50\%$) (cf. ^{13}C, Fig. 7.7). Isotopic exchange with soil CO_2 or atmospheric CO_2 lead to higher ^{14}C concentrations of the inorganic carbon fraction of recent groundwater, in combination with respectively decreased or increased $^{13}\delta$ (see Sect.7.2). The increased level of ^{14}C in atmospheric CO_2 since 1963 can

lead to ^{14}C contents in soil organic matter and soil CO_2, which even exceed the natural atmospheric value.

8.1.4 ^{14}C AGE DETERMINATION

Knowing the rate of radioactive decay (λ or $T_{1/2}$), the age (T = time elapsed since death) of a carbonaceous sample, organic or inorganic, can be calculated from the measured activity, ^{14}A, if the ^{14}C activity at the time of death, $^{14}A^{initial}$, is known (Eq.6.7):

$$T = -(T_{1/2}/\ln 2)(^{14}A/^{14}A^{initial})$$

Considering this equation, 3 quantities have to be well established: $T_{1/2}$, $^{14}A^{i}$ and the proper value ^{14}A of the ^{14}C activity of the sample. As was explained before, the condition that sample and reference activity are determined at the same time and under similar conditions results in the ^{14}a value valid for the year 1950, i.e. the age obtained counts back from 1950.

By international convention:

1) the initial activity equals the standard activity in AD1950
2) the ^{14}C activities have to be normalised for fractionation (samples to $^{13}\delta = -25‰$, Ox1 to $-19‰$, Ox2 to $-25‰$) (see Chapter 10)
3) the original (Libby) half-life of 5568 has to be used.

This results in the relation:

$$T = -\frac{T_{1/2}}{\ln 2}\ln\frac{^{14}A_{sample}}{^{14}A_{standard}} = -\frac{5568}{0.693}\ln\frac{^{14}A^{0}_{sample}}{^{14}A^{0}_{standard}} = -8033\ln {}^{14}a_{sample} \qquad \textbf{(8.10)}$$

The result is called the *conventional ^{14}C age BP* of the sample, that is the age Before Present (by definition: before AD1950).

In order to avoid confusion, the original (conventional) half-life of $T_{1/2}$ = 5568 years is still being used by international agreement for geological and archaeological dating. In hydrology, however, we will apply the true half-life of 5730 years.

The practice using these conventional ages is neat but of course a simplification. Apart from using the "wrong" half-life, the assumption of a constant ^{14}C content of living organic matter is proven untrue. However, by applying the *^{14}C calibration curve*, i.e. the empirical relation between the conventional age of treerings (to 10 000 years BC) and their real age, both problems are solved and ^{14}C ages are translated into real ages (Fig.8.5). The "wiggles" of the calibration curve are due to the natural variations in the atmospheric ^{14}C content, mentioned in Sect.8.1.3. Further details about radiocarbon dating are, for instance, given by Mook and Streurman, 1983 and by Mook and Waterbolk, 1985).

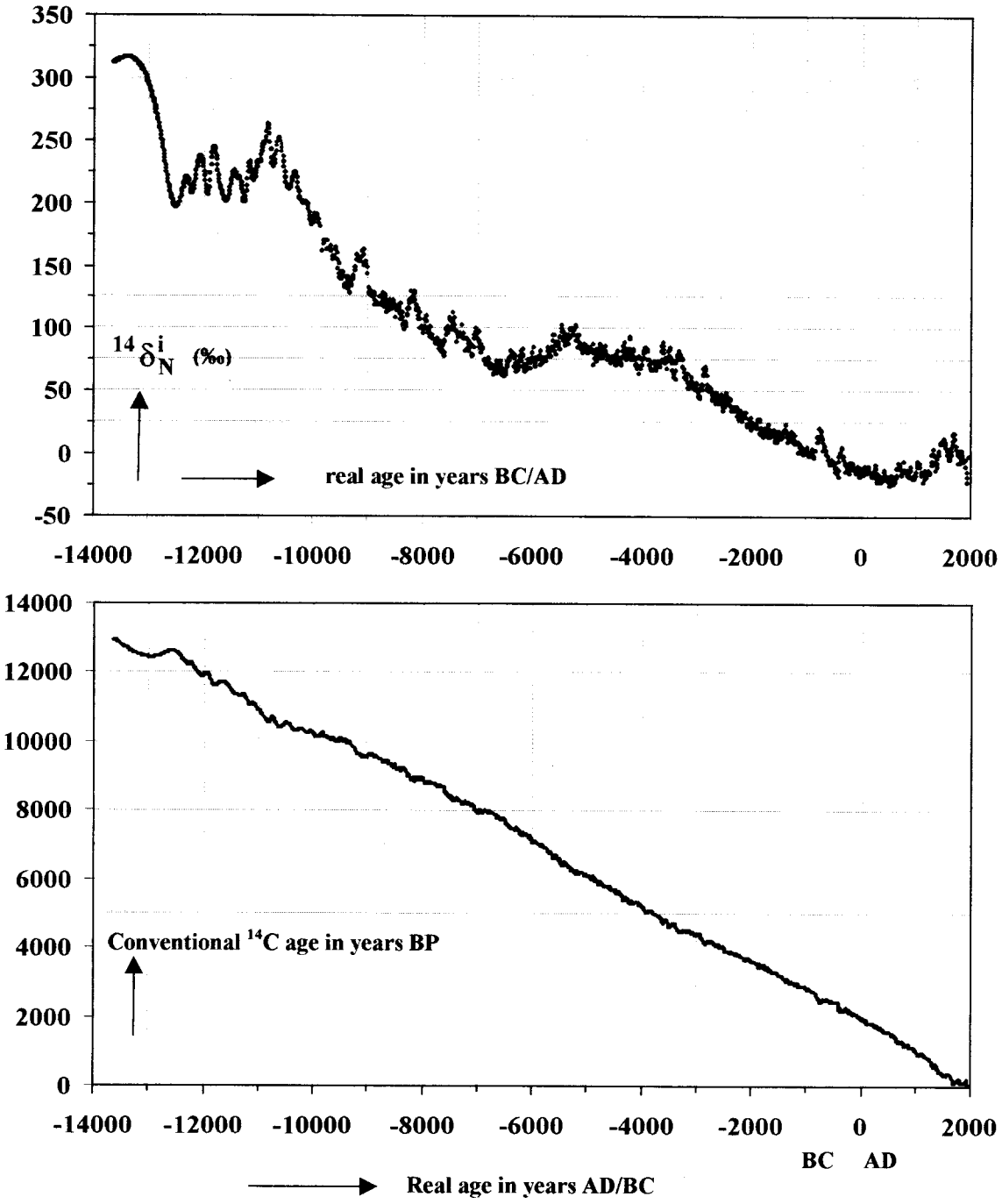

Fig.8.5 Variations in the ^{14}C content of atmospheric CO_2 in the past (upper curve), resulting from ^{14}C measurements of treerings of accurately known age by a number of laboratories, and of annual growthrings in corals (Bard et al., 1998). The parameter showing the deviations from the standard is defined by Eq.11.47. The data result in the calibration curve (lower curve), used for translating conventional ^{14}C ages into real ages (Stuiver and Van der Plicht, 1999)(Sect.11.5.4.3). The straight line in the calibration curve represents y = x.

8.1.5 DATING GROUNDWATER

Dating water as such has no meaning. Dating groundwater is determining the age of groundwater, i.e. the time elapsed since the water became groundwater, in other words, since it infiltrated into the soil as precipitation or any other type of surface water (rivers, lakes).

In principle there are some methods of calculating or estimating groundwater ages, for instance, based on hydrodynamical modelling. Here we discuss the application of radioactive decay.

Essential to know is the input function, i.e. the (time dependent) amount of radioactive tracer that infiltrated. The water molecule itself has one radioactive isotope, tritium or ^{3}H. The disadvantages are that both the activity and the half-life are very small. Possible applications will be discussed in Sect.8.3. Therefore, we are driven back on radioactive compounds dissolved in the water, rather than the water itself. In Chapter 12 we will discuss several radioactive isotopes that can be applied. Here we are concerned with ^{14}C, which has a very attractive half-life for solving hydrological problems. It is contained by dissolved inorganic carbon (DIC) as well as dissolved organic molecules (DOC).

8.1.5.1 DATING GROUNDWATER WITH DIC

If $^{14}a^{i}$ were known and if no carbon entered or escaped the groundwater in the course of time, the water age (since infiltration) would be given by:

$$T = -8267 \ln [(^{14}A / {}^{14}A^{0}_{standard}) / (^{14}A^{i} / {}^{14}A^{0}_{standard})] = -8267 \ln(^{14}a / {}^{14}a^{i}) \quad \textbf{(8.11)}$$

It is tempting to apply this ^{14}C method to DIC: the sampling and measuring techniques are relatively simple and available. However,

> we have to warn the reader that, for geochemical reasons, to obtain trustworthy groundwater ages by applying the radiocarbon dating technique to DIC is by no means simple and straightforward.

Volume 4 of this series will discuss the various problems. Here we limit ourselves with a brief review.

The initial ^{14}C activity $^{14}A^{initial}$ (= $^{14}A^{i}$) in the total dissolved inorganic carbon content (DIC) of infiltrating groundwater can not simply be taken as being equal to $^{14}A_{standard}$, as in the procedure of calculating conventional ages (Eq.8.9). Estimating the original, real value $^{14}A^{i}$ or $^{14}a^{i}$ of recent groundwater is more complicated.

8.1.5.1.1 The origin of ^{14}C in DIC

In general, the formation of DIC in groundwater essentially consists of two processes: (i) the dissolution of carbonate by H^{+} in H_2CO_3 from atmospheric CO_2 (in arid regions) or soil CO_2,

or in organic acids, and (ii) isotopic exchange with CO_2 as mentioned in Sect.8.1.3. Various models are dealing with the development of DIC and the concurrent $^{13}\delta$ and ^{14}a values.

8.1.5.1.2 The chemical/isotopic mass balance

The CO_2–$CaCO_3$ concept first proposed by Münnich (1975) is based on the mass balance of inorganic carbon (Fig.8.4) in the *closed system* of soil CO_2, soil $CaCO_3$ and water. $CaCO_3$ is dissolved by an equal molar amount of biogenic CO_2 (0.5b), whereas an additional amount of CO_2 (a) is required to stabilise the solution chemically. For the ^{14}C analysis of ground water all CO_2 is extracted from the solution after acidification. Rewriting Eq.8.9 in a more complete form gives:

$$(a + 0.5\,b)CO_2 + 0.5b\,CaCO_3 + H_2O \rightarrow 0.5b\,Ca^{2+} + b\,HCO_3^- + a\,CO_2 \qquad \textbf{(8.12)}$$

where a and b are the respective concentrations of dissolved carbon dioxide and bicarbonate. In this simple concept the chemical composition of the water, in casu the carbonic acid fractions, determine the original ^{14}a value of the mixture of CO_2 and HCO_3^- :

$$(a + b)^{14}a = 0.5b\ ^{14}a_l + (a + 0.5b)^{14}a_g \qquad \textbf{(8.13)}$$

where the subscripts l and g refer to the solid carbonate and the gaseous CO_2, respectively. As in most groundwaters, pH is low so that the only carbonic acid fractions are the dissolved CO_2 (a) and HCO_3^- (b). With the ^{14}a values given in Fig.8.4 the dissolved bicarbonate is expected to have a ^{14}C content of 50%, while an additional amount of CO_2 (with $^{14}a = 100\%$) shifts the ^{14}C content of DIC (= a + b) to a somewhat higher value. This method of estimating the original ^{14}C content of groundwater, and thus correcting the apparent age for the fact that $^{14}a^i \neq 100\%$ is referrred to as the *chemical dilution correction* (Ingerson and Pearson, 1964; Geyh and Wendt, 1965). With $^{14}a_l = 0$ % the original ^{14}C content of the DIC is:

$$^{14}a^i = \frac{a + 0.5b}{a + b}\ ^{14}a_g = \frac{a + 0.5b}{a + b} \times 100\% \qquad \textbf{(8.14)}$$

The factor $^{14}a^i/^{14}a_g = {}^{14}a^i/^{14}a_0$ is called the *dilution factor* with a value between 0.5 and 1.

An alternative approach is to consider the stable carbon isotopic composition of DIC in the groundwater, instead of the chemical composition. For ^{13}C a similar mass balance can be written as for ^{14}C in Eq.8.13:

$$(a + b)^{13}\delta_{DIC} = 0.5b\ ^{13}\delta_l + (a + 0.5b)^{13}\delta_g \qquad \textbf{(8.15)}$$

where the subscripts are the same as in Eq.8.13. The *isotopic* and the *chemical dilution correction* are now related by (Pearson, 1965):

$$\frac{^{13}\delta_{DIC} - {}^{13}\delta_l}{^{13}\delta_g - {}^{13}\delta_l} = \frac{a + 0.5b}{a + b} \qquad (8.16)$$

with the respective expression for $^{14}a^i$ and $^{13}\delta$ values instead of a and b (Eq.8.14). Numerically, using the $^{13}\delta$ and ^{14}a values of Figs.7.7.and 8.4 a 20% fraction of dissolved CO_2 in groundwater results in $^{13}\delta$ and $^{14}a^i$ values of −14.6‰ and 60%, respectively.

8.1.5.1.3 Isotopic exchange in an open system

In an *open system* the $^{13}\delta$ and ^{14}a values may further change by isotopic exchange of DIC thus formed with surrounding CO_2, which may be soil- as well as atmospheric CO_2 in the unsaturated zone. In principle both values change in parallel to an isotopic equilibrium situation between DIC and the CO_2, so that the ^{14}a and $^{13}\delta$ values are coupled by:

$$\frac{^{14}a_{ex} - {}^{14}a_0}{^{14}a_{eq} - {}^{14}a_0} = \frac{^{13}\delta_{ex} - {}^{13}\delta_0}{^{13}\delta_{eq} - {}^{13}\delta_0} \qquad (8.17)$$

where the subscripts ex, eq and 0 respectively refer to the actual values after isotopic exchange, the ultimate values when isotopic equilibrium with the surrounding CO_2 has been reached and the original values after closed-system dissoloution, respectively. The combination of the isotopic dilution correction and the exchange correction have been used by several authors (Gonfiantini, 1971; Mook, 1976; 1980; Fontes and Garnier, 1979). However, the chemical and geochemical conditions underground are so complicated that the above models may be reasonable approaches but are not to be considered clean correction methods.

In temperate climates where the land has a vegetation cover, the observed values of $^{13}\delta_{DIC}$ and $^{14}a_{DIC}$ are generally in the range of −11 to −14‰ and 65 to 85%, respectively.

8.1.5.2 DATING GROUNDWATER WITH DOC

Attempts were made to determine the age of groundwater, i.e. the time elapsed since infiltration, by means of dating the *dissolved organic carbon (DOC)* content of the water sample. Based on their solubilities in specific acid solutions, the soluble and thus mobile organic compounds are subdivided in *fulvic acids* (soluble at low pH) and *humic acids*. These organic molecules, originating from the decomposition of organic matter, are relatively resistent against further degradation.

Also here we are confronted with the problem to assign $^{14}a^i$ values to the recently infiltrated water. Geyer et al. (1993) concluded that only the fulvic fraction originates with certainty in the soil zone and thus is able to produce reliable ^{14}C ages, based on an $^{14}a^i$ value in the range of 85 ± 10%. This range of values depends on the average age of the soil organic matter in the recharge zone, which can be hundreds of years.

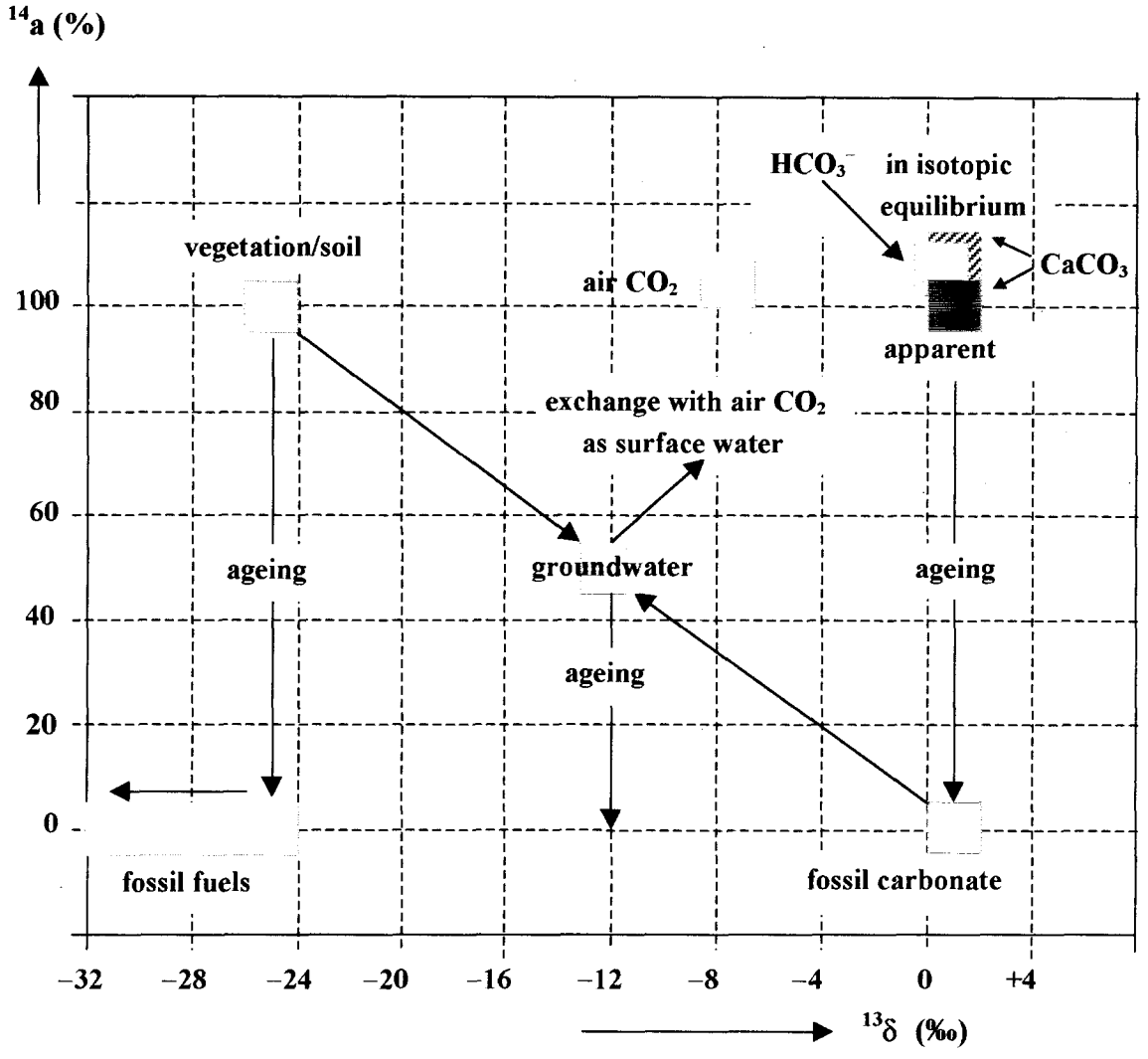

Fig.8.6 Schematic representation of the relation between variations in ^{13}C and ^{14}C in nature. The groundwater values have been explained in the Figs.7.7 and 8.5. The marine bicarbonate and solid carbonate (vertically dashed) values for the case of an isotopic equilibrium with atmospheric CO_2 are not observed in the ocean. The upwelling of deep, relatively old (1500 a) water causes the surface water to be lightly depleted in ^{14}C. The apparent age of this water -and consequently of the marine carbonate formed in this water (horizontally dashed)- is about 400 years (equivalent to 5%^{14}C).

8.2 RELATION BETWEEN ^{13}C AND ^{14}C VARIATIONS

A survey of the relevant values of the ^{14}C (^{14}a in %) and ^{13}C content ($^{13}\delta$ in ‰) in the reservoirs relevant for the hydrological cycle is given in Fig.8.6.

The values are merely indicative and do not exclude deviations. The figure is a combination of the above discussions represented schematically in the Figs.7.5, 7.7 and 8.4.

Special attention in this figure needs the value for marine carbonate. Accidentally the observed ^{14}a values for vegetation and marine carbonate are almost equal. The fact is that two processes cancel each other: (i) starting with organic matter on land with $^{13}\delta$ about –25‰ and ^{14}a = 100% (by definition, cf. Sect.7.1.2), the difference in $^{13}\delta$ between land vegetation and marine carbonate (via atmospheric CO_2) of about 25‰ requires ^{14}a of the latter to be 5%(=2×25‰) larger; (ii) the upwelling of deep sea water with ages of up to 1500 years generally causes the surface ocean water to be depleted by (accidentally) also 5%.

8.3 THE RADIOACTIVE HYDROGEN ISOTOPE

8.3.1 ORIGIN OF ^3H, DECAY AND HALF-LIFE

The radioactive isotope of hydrogen, ^3H (tritium or T), originates (as does ^{14}C) from a nuclear reaction between atmospheric nitrogen and thermal neutrons (Libby, 1946):

$$^{14}N + n \rightarrow {}^{12}C + {}^3H \qquad \textbf{(8.18)}$$

The ^3H thus formed enters the hydrologic cycle after oxidation to $^1H^3HO$ (Fig.8.7). It finally decays according to:

$$^3H \rightarrow {}^3He + \beta^- \qquad \textbf{(8.19)}$$

with $E_{\beta max}$ = 18 keV and a half-life of 12.430 years (Unterweger et al., 1980) (Fig.8.2).

According to a recent re-evaluation (Lucas and Unterweger, 2000), a more preferable value is 4500 ± 8 days (equivalent to 12.32 year; the former value has been used in this text).

8.3.2 REPORTING ^3H ACTIVITIES AND THE ^3H STANDARD

Because the nuclear reaction (Eq.8.18) has a lower probability than reaction (Eq.8.1) and because the residence time of ^3H in the atmosphere is much smaller than that of ^{14}C, the natural ^3H concentration in the air is much smaller than that of ^{14}C. Natural ^3H abundances are either presented as specific activities in Bq per litre of water) or in Tritium Units (TU), the latter by definition equivalent to a concentration of $^3H/^1H = 10^{-18}$ (1 TU = 3.19 pCi/L = 0.118 Bq/L) (Sect. 4.3).

For ^3H, as for ^{14}C, it is extremely difficult to determine the absolute specific activities. Tritium activities, are therefore related to a reference water sample which is measured under equal conditions. For this purpose the IAEA and NIST (the former NBS) has available a tritium standard NBS-SRM 4361 of 11 100 TU as of September 3, 1978 (Unterweger et al., 1978). After being related to this standard, ^3H concentrations are reported in absolute values (^3A in TU), corrected for decay to the date of sample collection.

8.3.3 SURVEY OF NATURAL ^3H VARIATIONS

Under undisturbed natural conditions the ^3H concentration in precipitation was probably about 5 TU, which is equivalent to a specific activity of about 0.6 Bq/L (Roether, 1967).

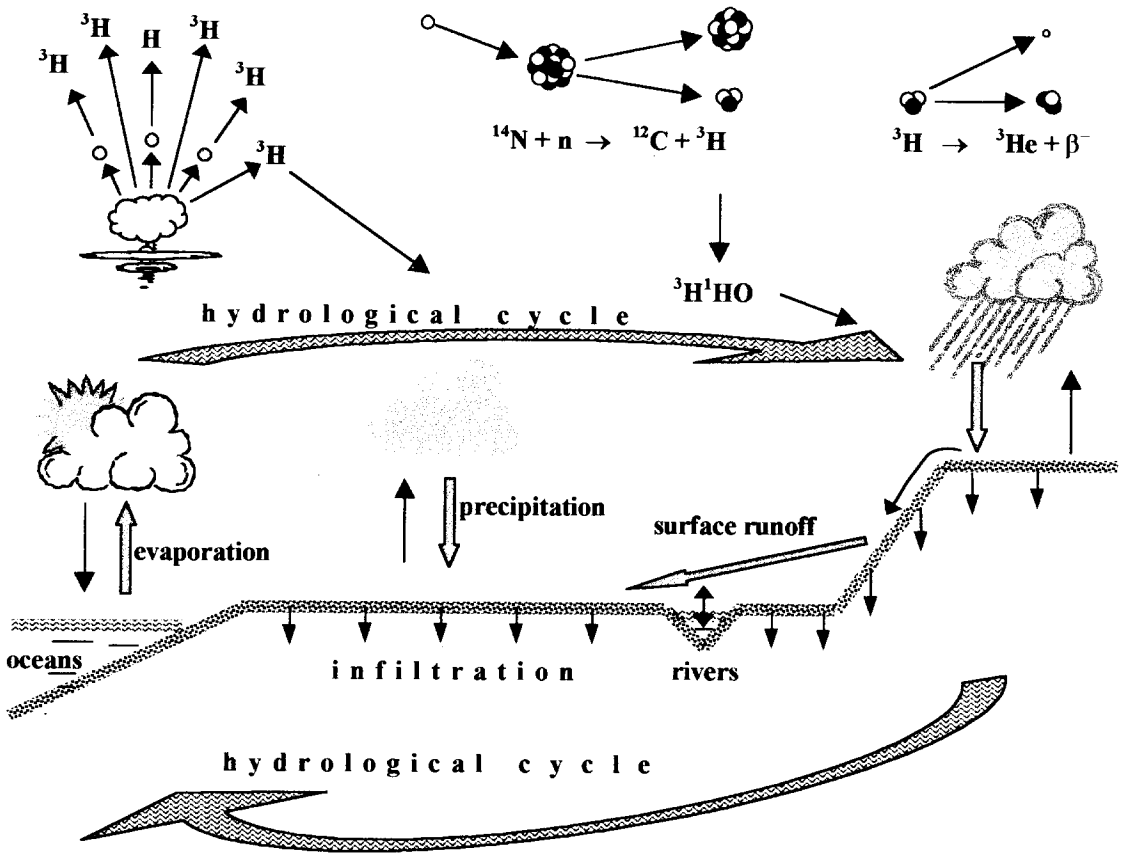

Fig.8.7 Origin and distribution of ^3H in nature. Contrary to ^{14}C, the turnover of ^3H is very fast, except where it is fixed in glacier ice or groundwater.

Following the nuclear weapon tests of the early sixties, the ^3H content of precipitation temporarily increased by a 1000-fold in the northern hemisphere (Fig.8.8). Since 1963 this extreme ^3H content has decreased to essentially natural values in winter and about twice natural in summer.

A large part of the ^3H (as well as ^{14}C) produced by the nuclear explosions has been injected into the stratosphere and returns to the troposphere each year during spring and early summer. This causes the seasonal variation in both ^3H and ^{14}C, more pronounced in the former, because the residence time of H_2O to which ^3H is coupled in the atmosphere is very small (in the order of weeks).

The probability of contamination of young groundwater by bomb ^3H prevents the water to be simply dated by measuring the degree of ^3H decay. Nevertheless, ^3H data can often be used to determine dates ante quem or post quem. For instance, water with $^3A < 5$ TU must have a mean residence time of more than 40 years; water having $^3A > 20$ TU must date from after 1961. The tracer use of ^3H will further be discussed in the Volume 4 of this series.

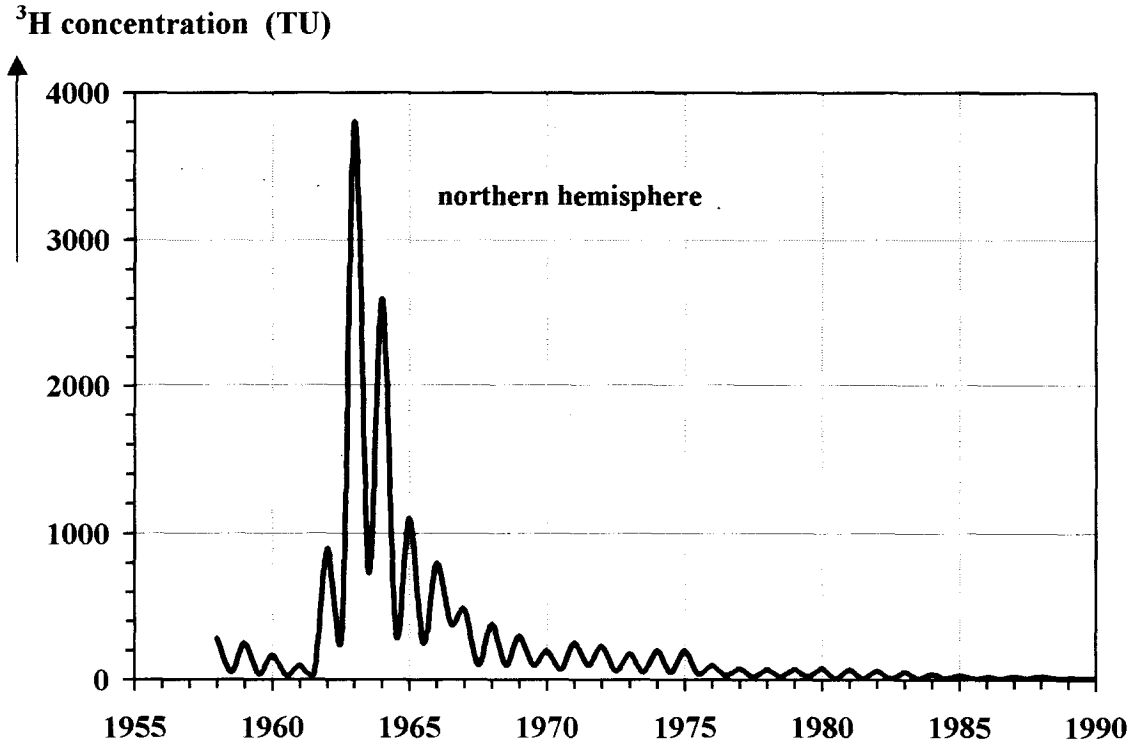

Fig.8.8 Smoothed curve representing the average ^3H content of precipitation over the continental surface of the Northern hemisphere.

8.4 COMPARISON OF ^3H AND ^{14}C VARIATIONS

8.4.1 RELATION BETWEEN ^3H AND ^{14}C IN THE ATMOSPHERE

At first we will compare the curves showing the ^{14}C and ^3H variations in atmospheric CO_2 and H_2O, respectively (Figs.8.3 and 8.8), because they give important information on the global carbon and water cycle, respectively. The main differences are the following.

1) The effect of the nuclear bomb ^{14}C and ^3H had a much more pronounced effect on the atmospheric content of the latter, because the natural ^3H concentration is so much lower.

2) The restoration to natural conditions goes faster for ^3H than for ^{14}C, because the turnover time of water in the atmosphere from evaporation of ocean water to precipitation very

short (in the order of weeks), while the exchange of CO_2 between the atmosphere and ocean water is very slow (in the order of years).

3) For the same reason does ^{14}C show much smaller seasonal amplitudes than ^{3}H; the consequence for the latter is that in temperate climates, where the main infiltration of rain occurs during the winter half-year, groundwater rarely shows the high ^{3}H values observed in precipitation during the early 1960s.

4) The ^{14}C increase after 1960 in the air over the southern hemisphere is less pronounced than over the northern hemisphere, as the majority of the nuclear tests took place in the north and, moreover, since the air is not easily transported across the equator; for ^{3}H the consequences are that the equivalent curve for the Southern hemisphere is much different: it is less regular, shows a maximum at 30 TU around 1963-65 with occasional peaks up to 80 TU, and a slow decrease to the natural level (5 TU) at present.

5) ^{14}C is being used to calibrate global carbon cycle models, indicating the exchange (and transition) time of (additional) CO_2 between air and sea; ^{3}H is being applied in oceanography, indicating the rate of vertical water movement and lateral water flow.

8.4.2 RELATION BETWEEN ^{3}H AND ^{14}C IN GROUNDWATER

We have already emphasised that our discussion of the occurrence of ^{14}C and ^{3}H in groundwater may not lead to the idea that, using these isotopes, we are able to simply measure the *age of groundwater*, i.e. the period of time elapsed since the infiltration of the water.

The main obstacle is the unknown isotopic values at time zero, the moment of infiltration, for ^{3}H as well as for ^{14}C. However, ^{14}C and ^{3}H together certainly offer the possibility to set limits to *absolute ages*, especially in combination with hydrogeological and hydrochemical evidence.

Determining *relative ages* (i.e. the age differences between neighbouring samples, which is often equally relevant) is less complicated, at least if the chemistry does not point to the action of processes underground -such as carbonate dissolution, decomposition of additional (old) organic matter, and certainly if we are dealing with a mixture of different water- that could influence the carbon isotopic composition. In that case the age difference between water samples collected at two geographical locations k and k+1 is expressed as:

$$\Delta T = 8270 \ln \frac{^{14}a_{k+1}}{^{14}a_k} \qquad \textbf{(8.20)}$$

where $8270 = (\ln 2)/T_{1/2}$ years. From a qualitative point of view, a few approximate conclusions can be drawn from isotopic data. For instance, if the water sample shows a measurable ^{3}H activity (larger than 1 TU), the water is *subrecent*, i.e. less than 50 years old, or is a mixture of young and old water, or at least contains an admixture of a certain percentage of recent water. With no measurable ^{14}C and ^{3}H the water is certainly a few tens of

thousands of years old. If the water is very recent, the ^{14}C content is expected to be close to or above 100%, because the soil-CO_2 then is likely to contain bomb ^{14}C.

Volume 4 of this series is especially devoted to these problems and (im)possibilities.

A general and simplified survey is shown in Fig.8.9. With *recent groundwater* we refer to water that infiltrated not more than some tens of years ago. *Young groundwater* may have any age of hundreds of years, old groundwater thousends. Finally *very old*, also referred to as *fossil groundwater* does not contain ^{3}H and ^{14}C and is several tens of thousands of years old. Waters which are relatively high in ^{3}H and lower in ^{14}C than recent water are likely to be mixtures of young and old water.

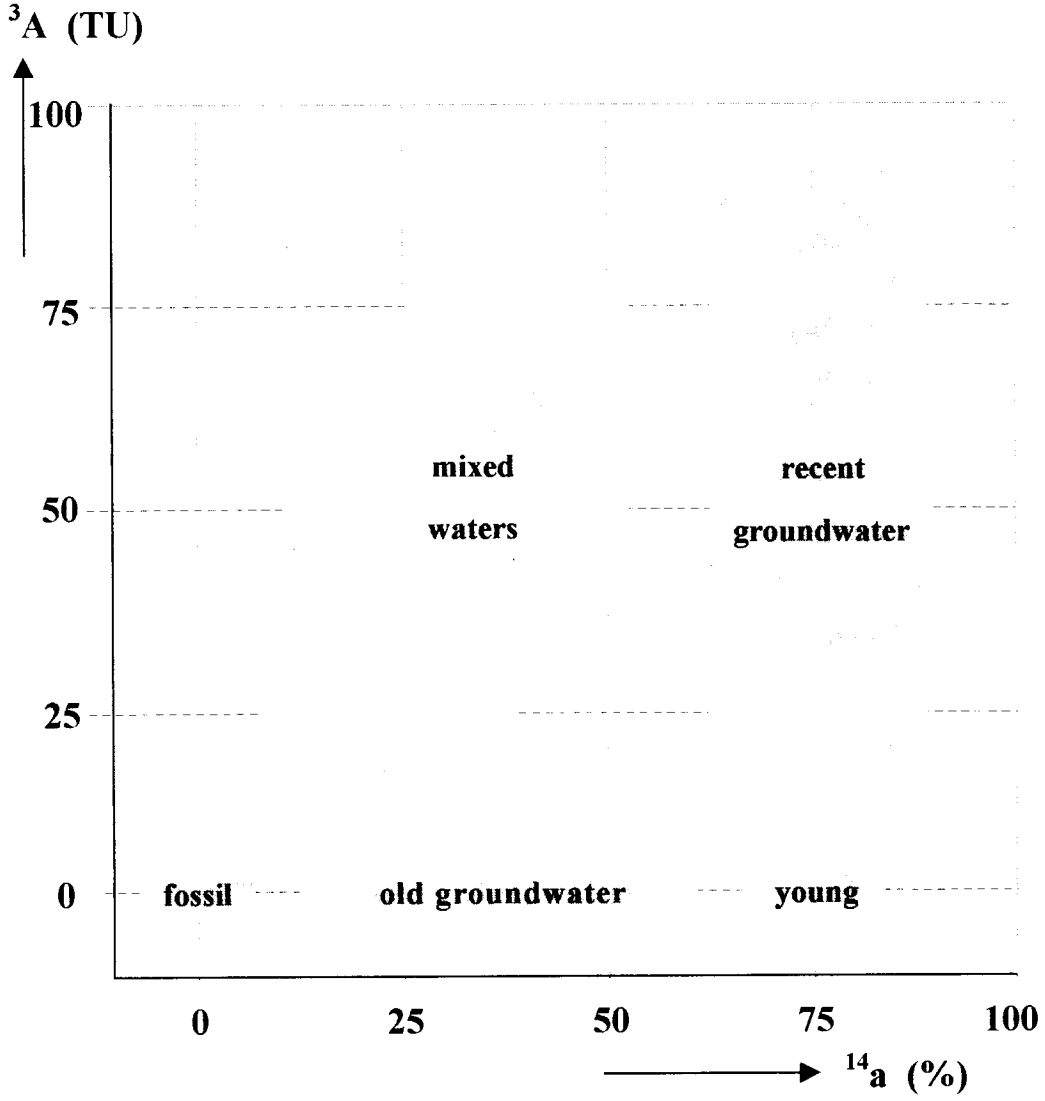

Fig.8.9 Schematic representation of relations between the ^{14}C and ^{3}H content in groundwater. The scheme is merely indicative and serves to give a general impression. The terminology is discussed in the text.

9 CHEMISTRY OF CARBONIC ACID IN WATER

9.1 INTRODUCTION

Studying the carbon isotopic composition of water, whether it concerns freshwater or seawater, a complication arises from the fact that the dissolved inorganic carbon always consists of more than one compound, while also the presence of gaseous CO_2 and solid calcium carbonate may be relevant. In fact we are dealing with the following compounds and concentrations:

gaseous CO_2 (occasionally denoted by CO_2g) with a partial pressure P_{CO2}
dissolved CO_2 (denoted by CO_2aq)
dissolved carbonic acid, H_2CO_3 with $a = [H_2CO_3] + [CO_2aq]$
dissolved bicarbonate, HCO_3^- with $b = [HCO_3^-]$
dissolved carbonate, CO_3^{2-} with $c = [CO_3^{2-}]$
total dissolved inorganic carbon, DIC, with $C_T = a + b + c$
solid carbonate, $CaCO_3$ (occasionally denoted by s)

The ambiguity in using carbon isotopes now consists of two observations:

1) On the one hand, only the isotopic composition of a single compound in relation to that of another compound is geochemically or hydrologically meaningful. We have seen an example of this statement while discussing the carbon isotopic composition of groundwater, for ^{13}C as well as ^{14}C (Figs.7.7 and 8.4). In other words: an isotopic fractionation factor is a fundamental, physico/chemical quantity only if it is the ratio between two isotopic ratios of single compounds. For instance:

$$^{13}\alpha_{a/b} = {}^{13}R_a/{}^{13}R_b \qquad \text{and} \qquad {}^{13}\alpha_{c/b} = {}^{13}R_c/{}^{13}R_b$$

2) **a)** On the other hand, in mass balance considerations the carbon isotopic composition of a mixture of compounds is relevant. For instance, if CO_2 or $CaCO_3$ are being removed from a dissolved carbon solution, of for estuarine mixing of fresh- and seawater, the total ^{13}C mass balance has to be taken into account. In this chapter some examples are given.

b) Measuring the carbon isotopic composition of a solution comes to extracting the total CO_2 from the sample after acidification, instead of single compounds.

For the essential translation of $^{13}\delta$ of total dissolved carbon to $^{13}\delta$ of single compounds, and conversely, the inorganic carbon chemistry, i.e. of the dissolved inorganic carbon is required.

Once the various concentrations of the dissolved species -to be deduced in the next sections are known, the ^{13}C mass balance:

$$\begin{aligned}&\left([CO_2aq]+[H_2CO_3]+[HCO_3^-]+[CO_3^{2-}]\right)^{13}R_{DIC} = \\ &=[CO_2aq]^{13}R_{CO_2aq}+[H_2CO_3]^{13}R_{H_2CO_3}+[HCO_3^-]^{13}R_{HCO_3}+[CO_3^{2-}]^{13}R_{CO_3}\end{aligned} \quad (9.1)$$

or, inserting the previously mentioned symbols for the various concentrations and combining the concentration of CO_2aq and the carbonic acid, H_2CO_3, the latter being a negligibly small fraction, the isotopic composition of the total dissolved carbon (C_T = a + b + c) is:

$$^{13}R_{C_T} = \frac{a \cdot R_a + b \cdot R_b + c \cdot R_c}{C_T} \quad (9.2)$$

and conversely, inserting the proper fractionation factors as mentioned before:

$$^{13}R_b = \frac{C_T \cdot {}^{13}R_{C_T}}{a \cdot \alpha_{a/b} + b + c \cdot \alpha_{c/b}} b \quad (9.3)$$

The next sections will be devoted to analysing the chemical composition of carbonate waters.

9.2 CARBONIC ACID EQUILIBRIA

In the presence of gaseous CO_2, dissolved CO_2 exchanges with CO_2 gas:

$$CO_2(g) + H_2O \Leftrightarrow CO_2(aq) + H_2O \quad (9.4)$$

$$CO_2(aq) + H_2O \Leftrightarrow H_2CO_3 \quad (9.5)$$

where g and aq refer to the gaseous and dissolved phase, respectively. Although the concentration of $CO_2(aq)$ far exceeds that of dissolved H_2CO_3 (in the order of 10^3) we denote the concentration of all dissolved CO_2 by $[H_2CO_3]$. The equilibrium condition between the phases is quantified by the *molar solubility* K_o (Henry's law):

$$K_0 = \frac{[H_2CO_3]}{P_{CO_2}} \quad (9.6)$$

where the atmospheric CO_2 partial pressure, P_{CO2}, is in atm, K_o is the solubility in mol L^{-1} atm^{-1} and $[H_2CO_3]$ is the dissolved CO_2 concentration in mol/kg of water.

H_2CO_3 dissociates in water according to

$$H_2CO_3 + \Leftrightarrow H^+ + HCO_3^- \quad (9.7)$$

and

$$HCO_3^- \Leftrightarrow H^+ + CO_3^{2-} \quad \textbf{(9.8)}$$

where the equilibrium conditions are quantified by the *dissociation* or *acidity constants*:

$$K_1 = \frac{[H^+][HCO_3^-]}{[H_2CO_3]} \quad \textbf{(9.9)}$$

and

$$K_2 = \frac{[H^+][CO_3^{2-}]}{[HCO_3^-]} \quad \textbf{(9.10)}$$

Finally the dissociation of water obeys the equilibrium condition

$$K_w = [H^+][OH^-] \quad \textbf{(9.11)}$$

Here we have to emphasise that, although the hydrogen ion, H^+, is commonly hydrated to form H_3O^+ or even to multiple hydrated ions, we will write the hydrated hydrogen ion as H^+ as the hydrated structure does not enter the chemical models.

The $[H^+]$ concentration is generally given as a pH value, defined as the negative logarithm:

$$pH = -^{10}\log[H^+] \quad \textbf{(9.12)}$$

The total concentration of dissolved inorganic carbon (= total carbon, also denoted by ΣCO_2 or ΣC or DIC) is defined by:

$$C_T = [CO_2aq] + [H_2CO_3] + [HCO_3^-] + [CO_3^{2-}] = a + b + c \quad \textbf{(9.13)}$$

The *alkalinity* is a practical quantity, following from the conservation of electroneutrality in solutions where the metal-ion concentrations (Na, Ca, Mg) and pH are constant:

$$A_T = [HCO_3^-] + 2[CO_3^{2-}] + [OH^-] - [H^+] + [\text{other weak acid anions}] \quad \textbf{(9.14)}$$

in which concentrations of other weak acids may be included in the interest of high precision, such as humic acids in freshwater or borate, $[B(OH)_4^-]$, in seawater.

Under natural conditions $[H^+]$ and $[OH^-]$ are negligibly small compared to the carbonate species concentrations. The sum of the weak acid and alkali-ion concentrations, determined by an acid titration, referred to as the total alkalinity, thus about equals the *carbonate alkalinity* defined as:

$$A_C = [HCO_3^-] + 2[CO_3^{2-}] = b + 2c \quad \textbf{(9.15)}$$

If the water contains Ca^{2+} (or Mg^{2+}) and carbonate or is in contact with calcite also the dissociation equilibrium of calcite affects the carbon chemistry:

$$CaCO_3 \Leftrightarrow Ca^{2+} + CO_3^{2-} \tag{9.16}$$

where the concentrations are limited by the solubility product:

$$K_{CaCO3} = [Ca^{2+}][CO_3^{2-}] \tag{9.17}$$

9.3 THE EQUILIBRIUM CONSTANTS

Basically all values of the solubilities and dissociation constants are temperature dependent. However, the K values also depend on the solute concentrations, because the formation of ion complexes between the carbonic ions and molecules and ions in the solution hinder the dissolved carbonic molecules and ions to take part in the thermodynamic equilibrium reactions. Therefore, in the thermodynamic equation, the concentrations have to be replaced by their *activities*, that are smaller than the concentrations. The *thermodynamic solubility constant* is:

$$K_0 = \frac{a_{H_2CO_3}}{P_{CO_2}} = \frac{\gamma_a[H_2CO_3]}{P_{CO_2}} \tag{9.18a}$$

where in general the *activity coefficients* $\gamma < 1$ ($\gamma = 1$ for an *ideal solution*, i.e. with zero solute concentrations or zero *ionic strength*).

In the non-ideal solutions of seawater and brackish water it is more practical to describe the relation between the real, *measurable* concentrations by the *apparent solubility constant*:

$$K_0' = \frac{[H_2CO_3]}{P_{CO_2}} = \frac{K_0}{\gamma_a} \tag{9.18b}$$

The *thermodynamic* and the *apparent acidity (dissociation) constants* of the first and second dissociation of carbonic acid (Eqs.9.6, 9.9 and 9.10) are now related by:

$$K_1 = \frac{a_H \cdot a_{HCO_3}}{a_{H_2CO_3}} = \frac{\gamma_H[H^+] \cdot \gamma_b[HCO_3^-]}{\gamma_a[H_2CO_3]} \tag{9.19a}$$

and

$$K_1' = \frac{[H^+][HCO_3^-]}{[H_2CO_3]} = \frac{\gamma_a}{\gamma_H \cdot \gamma_b} K_1 \tag{9.19b}$$

and with respect to the second dissociation constant:

$$K_2 = \frac{a_H \cdot a_{CO_3}}{a_{HCO_3}} = \frac{\gamma_H[H^+] \cdot \gamma_c[CO_3^{2-}]}{\gamma_b[HCO_3^-]} \qquad \textbf{(9.20a)}$$

and

$$K_2' = \frac{[H^+][CO_3^{2-}]}{[HCO_3^-]} = \frac{\gamma_b}{\gamma_H \cdot \gamma_c} K_2 \qquad \textbf{(9.20b)}$$

The definition also takes into account that in reality instead of $[H^+]$ the pH is being measured based on a series of buffer solutions. Therefore, in these equations $[H^+]$ is to be replaced by 10^{-pH}.

Comparing fresh and seawater, the differences in the first and second dissociation constants of carbonic acid -K_1 and K_2 for freshwater, and K_1' and K_2' for seawater- and the consequences thereoff will appear spectacular.

For practical reasons the values of the dissociation constants are generally given as:

$$pK = -\,^{10}\log K \qquad \text{or} \qquad K = 10^{-pK} \qquad \textbf{(9.21)}$$

The K_0, K_1 and K_2 values for freshwater (ideal solution) and seawater as a function of the water temperature and the water salinity are discussed in the next section and shown in Figs.9.1 - 9.4.

9.3.1 IDEAL SOLUTIONS

Most freshwaters can be considered as ideal solutions (extrapolated to zero ionic strength). Values for the temperature range of 0 to 40 °C and the salinity range of 0 to 40 ‰ are shown in Figs.9.1 to 9.4 and in Table 9.1 (left-hand shaded column). The classic data of Harned and co-authors are practically equal to those reported by Millero and Roy (1997) for freshwater (at S = 0‰):

$$pK_0 = -2622.38/T - 0.0178471T + 15.5873 \text{ (Harned and Davis, 1943)} \qquad \textbf{(9.22)}$$

$$pK_1 = 3404.71/T + 0.032786T - 14.8435 \text{ (Harned and Davis, 1943)} \qquad \textbf{(9.23)}$$

$$pK_2 = 2902.39/T + 0.02379T - 6.4980 \text{ (Harned and Scholes, 1941)} \qquad \textbf{(9.24)}$$

$$\ln K_w = 148.9802 - 13847.26/T - 23.6521 \ln T \text{ (Dickson and Riley, 1979)} \qquad \textbf{(9.25)}$$

where the *absolute temperature* T = t(°C) + 273.15 K.

9.3.2 SEAWATER

The salt concentration of seawater is defined by the *salinity*, given in g/kg of seawater, or in ‰. Probably the best data have been reported by Millero and Roy (1997); these values for the temperature range of 0 to 40°C and the salinity range of 0 to 40‰ are shown in Figs.9.1 to 9.4 and in Table 9.1 (right-hand shaded column). The seawater values (at S = 35‰) are practically equal to the values published by Weiss (1974) and by Mehrbach et al. (1973), as reported by Dickson and Millero (1987):

$$\ln K_o' = -60.2409 + 9345.17 / T + 23.3585 \ln(0.01T) + \\ + S\,[0.023517 - 0.023656\,(0.01T) + 0.0047036\,(0.01T)^2 \qquad \textbf{(9.26)}$$

$$pK_1' = 3670.7 / T - 62.008 + 9.7944 \ln T - 0.0118\,S + 0.000116\,S^2 \qquad \textbf{(9.27)}$$

$$pK_2' = 1394.7 / T + 4.777 - 0.0184\,S + 0.000118\,S^2 \qquad \textbf{(9.28)}$$

(K_0': Weiss, 1974), (K_1', K_2': Mehrbach et al. (1973), reported by Dickson and Millero (1987).

The *salinity* values S are related to the originally used *chlorinity*, i.e. the concentration of chloride (+bromide and iodide, also given in g/kg or ‰), by:

$$S = 1.80655\,Cl \qquad \textbf{(9.29)}$$

The solubility product of calcium carbonate differs for the two different crystalline types, calcite and aragonite. Figs.9.5 and 9.6 show values at specific temperatures and salinities.

9.3.3 BRACKISH WATER

The large differences between K and K', i.e. the large effect of salt concentrations on the acidity constants (Fig.9.4), result in an entirely different chemical character of freshwater and seawater, as will be illustrated in the next sections. The acidity constants for freshwater with zero salinity and for seawater have extensively been studied experimentally. The problem remains the proper treatment of waters with varying low salt concentrations. In order to obtain the proper K' values, the K values must be corrected with the help of the Debye-Hückel theory applicable at low concentrations. The treatment of non-ideal solutions is illustrated here by considering freshwaters with less dissolved salts than about 400mg/L (Stumm and Morgan, 1970).

A measure for the salt concentration is the *ionic strength* (I) of the water. This can be approximated by:

$$I \cong 2.5\times10^{-5}\,S \qquad \textbf{(9.30)}$$

where S is the salt concentration in mg/l. The approximate values for the two acidity constants then are:

$$pK_1' = pK_1 - \frac{0.5\sqrt{I}}{1+1.4\sqrt{I}} \qquad \text{and} \qquad pK_2' = pK_2 - \frac{2\sqrt{I}}{1+1.4\sqrt{I}} \qquad \textbf{(9.31)}$$

Table 9.1 Apparent solubility and acidity (dissociation) constants of carbonic acid for various temperatures and salinities. The values are according to Millero and Roy (1997).

$K_0.10^2$	S (‰)								
t (°C)	0	5	10	15	20	25	30	35	40
0	**7.691**	7.499	7.295	7.112	6.934	6.761	6.592	**6.412**	6.252
5	**6.383**	6.223	6.067	5.916	5.754	5.610	5.470	**5.321**	5.188
10	**5.370**	5.236	5.105	4.977	4.842	4.721	4.603	**4.477**	4.365
15	**4.571**	4.457	4.345	4.236	4.121	4.018	3.917	**3.811**	3.715
20	**3.936**	3.837	3.741	3.648	3.556	3.459	3.373	**3.289**	3.199
25	**3.428**	3.342	3.258	3.177	3.090	3.013	2.938	**2.858**	2.786
30	**3.013**	2.938	2.864	2.793	2.723	2.655	2.582	**2.518**	2.449
35	**2.679**	2.612	2.547	2.483	2.415	2.355	2.296	**2.234**	2.178
40	**2.404**	2.344	2.286	2.223	2.168	2.113	2.061	**2.004**	1.954

$K_1.10^7$									
t (°C)	0	5	10	15	20	25	30	35	40
0	**2.667**	4.667	5.433	5.984	6.412	6.761	7.047	**7.278**	7.464
5	**3.069**	5.420	6.353	7.015	7.534	7.962	8.299	**8.610**	8.851
10	**3.467**	6.194	7.295	8.072	8.690	9.204	9.638	**10.00**	10.30
15	**3.846**	6.966	8.241	9.162	9.908	10.52	11.04	**11.48**	11.86
20	**4.188**	7.727	9.183	10.26	11.12	11.83	12.45	**13.00**	13.46
25	**4.498**	8.433	10.09	11.32	12.33	13.18	13.90	**14.52**	15.07
30	**4.753**	9.099	10.96	12.36	13.52	14.49	15.35	**16.11**	16.75
35	**4.966**	9.705	11.80	13.37	14.69	15.81	16.79	**17.66**	18.41
40	**5.105**	10.26	12.56	14.32	15.81	17.06	18.20	**19.19**	20.09

$K_2.10^{10}$									
t (°C)	0	5	10	15	20	25	30	35	40
0	**0.240**	1.291	1.879	2.355	2.773	3.155	3.508	**3.837**	4.150
5	**0.284**	1.600	2.339	2.951	3.491	3.981	4.436	**4.864**	5.272
10	**0.331**	1.950	2.877	3.639	4.325	4.943	5.534	**6.095**	6.607
15	**0.380**	2.350	3.491	4.436	5.284	6.081	6.823	**7.516**	8.185
20	**0.430**	2.793	4.188	5.346	6.397	7.379	8.299	**9.183**	10.05
25	**0.479**	3.289	4.966	6.383	7.656	8.872	10.02	**11.12**	12.19
30	**0.527**	3.828	5.834	7.534	9.099	10.57	11.99	**13.34**	14.66
35	**0.573**	4.426	6.792	8.831	10.72	12.50	14.22	**15.89**	17.50
40	**0.617**	5.070	7.870	10.28	12.53	14.69	16.79	**18.79**	20.75

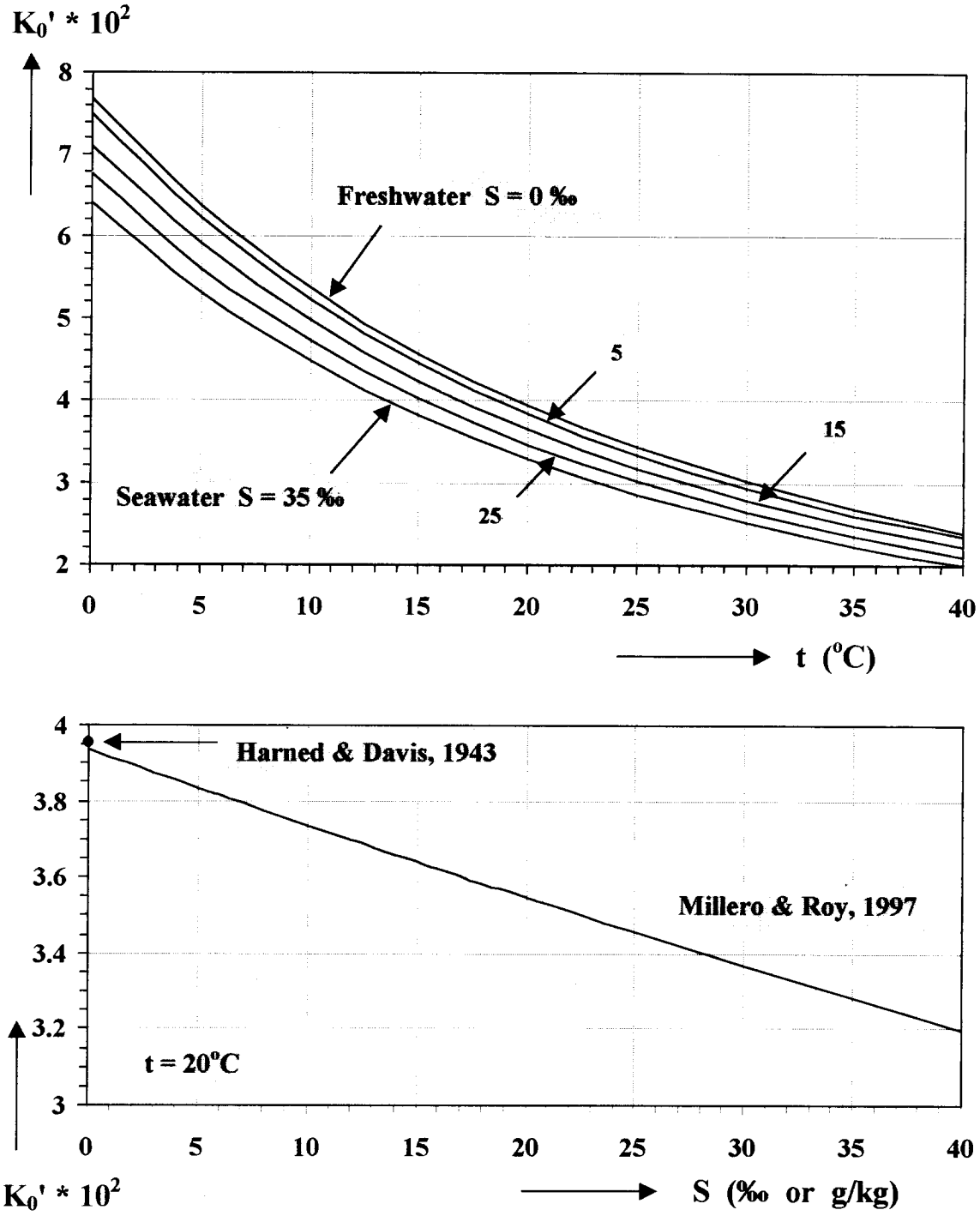

Fig.9.1 The solubility constants (= solubilities in M/L.atm) for CO_2 in freshwater, seawater and brackish water as a function of temperature at salinities of 0, 5, 15, 25, and 35‰ (= g of salt per kg of water) (upper graph) and as a function of salinity at 20 °C (lower graph). All values are according to Millero and Roy (1997), at higher salinities similar to Weiss (1974) (Eq.9.26); the values for freshwater are similar to those of Harned and Davis (1943) (Eq.9.22).

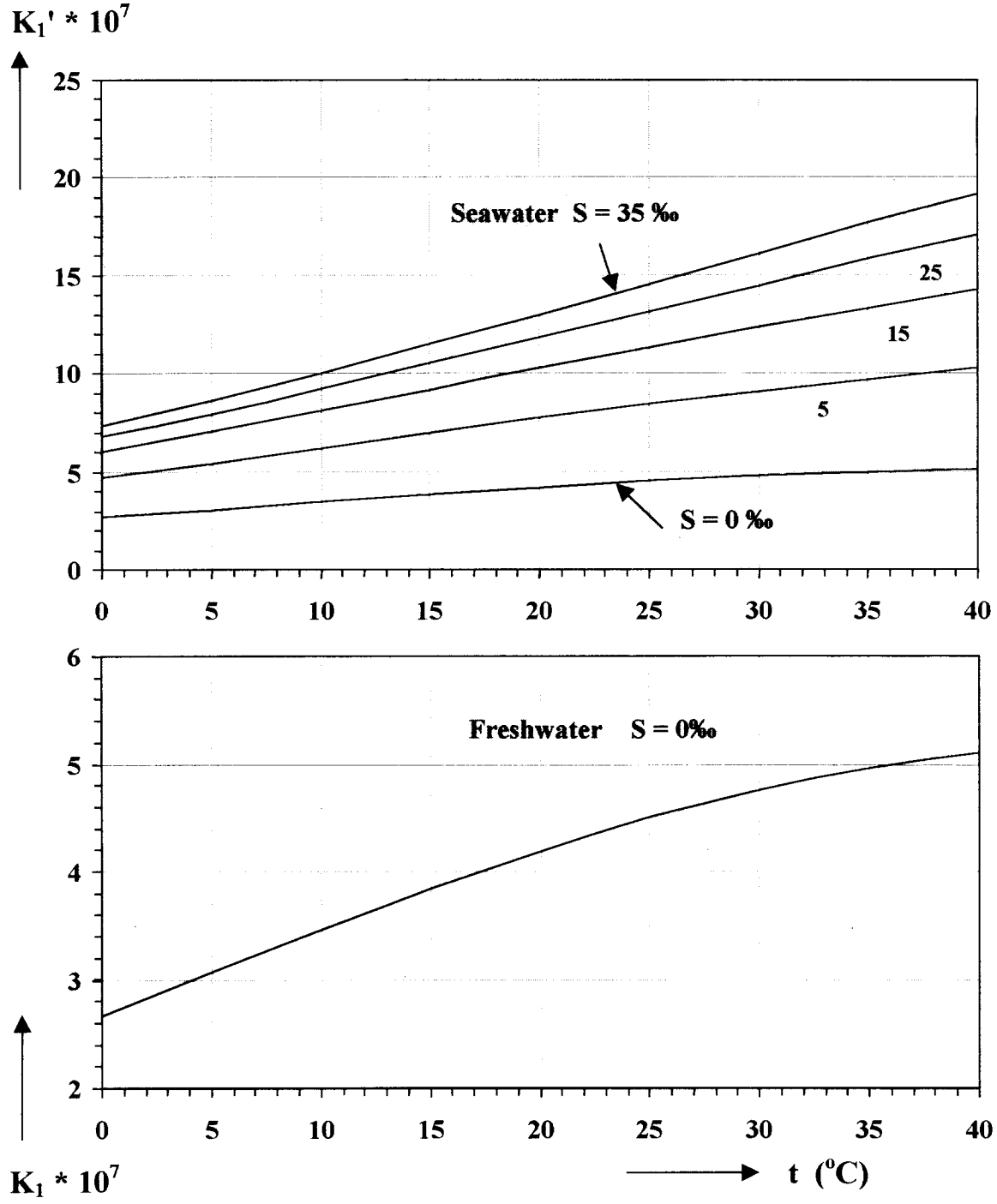

Fig.9.2 The acidity constants for the first dissociation of carbonic acid in freshwater and seawater as a function of the water temperature at salinities of 0, 5, 15, 25, and 35‰. The values are according to Millero and Roy (1997). The freshwater values are equal to those of Harned and Davis (1943) (Eq.9.23), the marine values are in good agreement with those reported by Mehrbach et al. (1973) as discussed by Dickson and Millero (1987) (Eq.9.27).

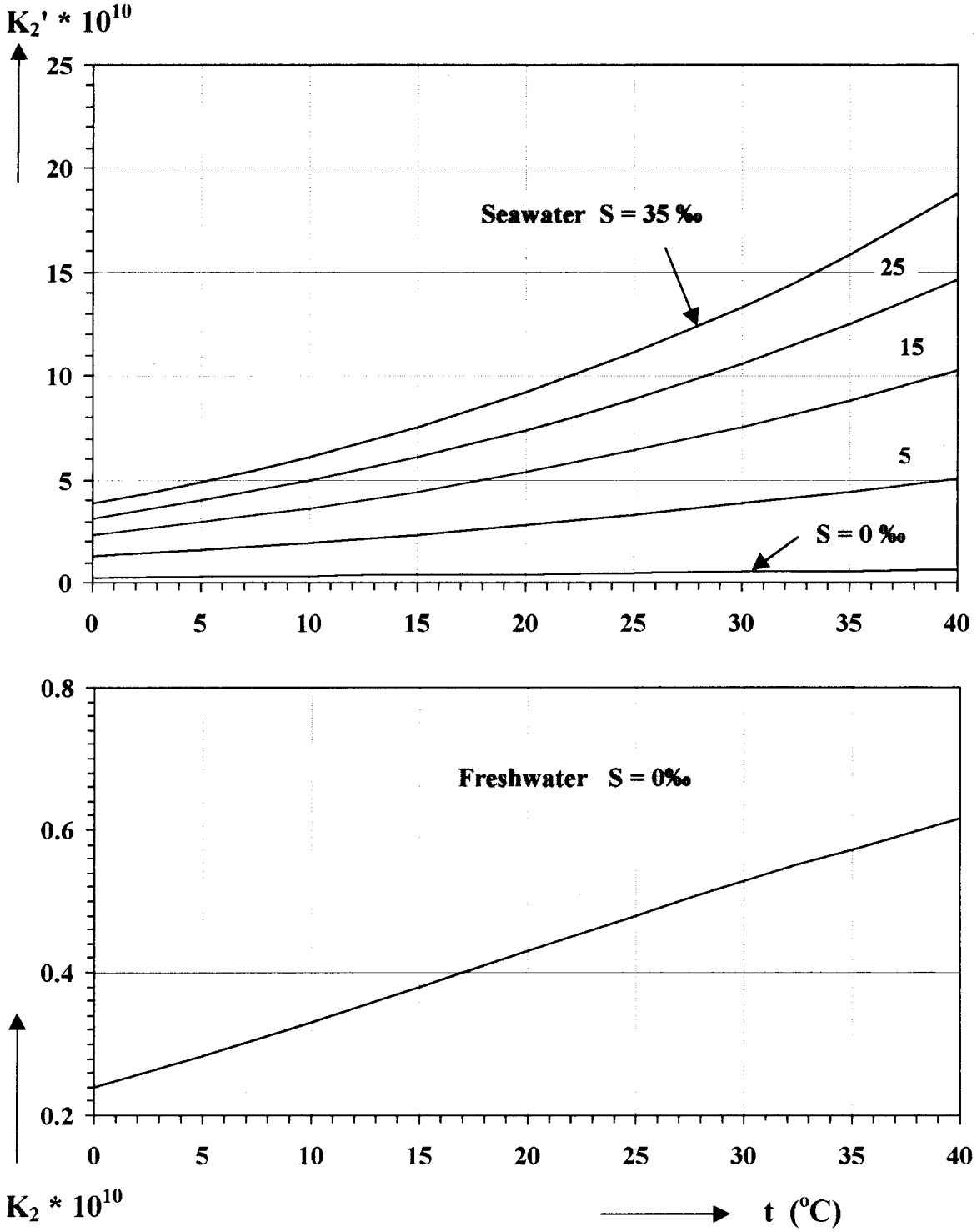

Fig.9.3 The acidity constants for the second dissociation of carbonic acid in freshwater and seawater as a function of the water temperature at salinities of 0, 5, 15, 25, and 35‰. The values are according to Millero and Roy (1997). The freshwater values are equal to those of Harned and Scholes (1941) (Eq.9.24), the marine values are in good agreement with those reported by Mehrbach et al. (1973) as reported by Dickson and Millero (1987) (Eq.9.28).

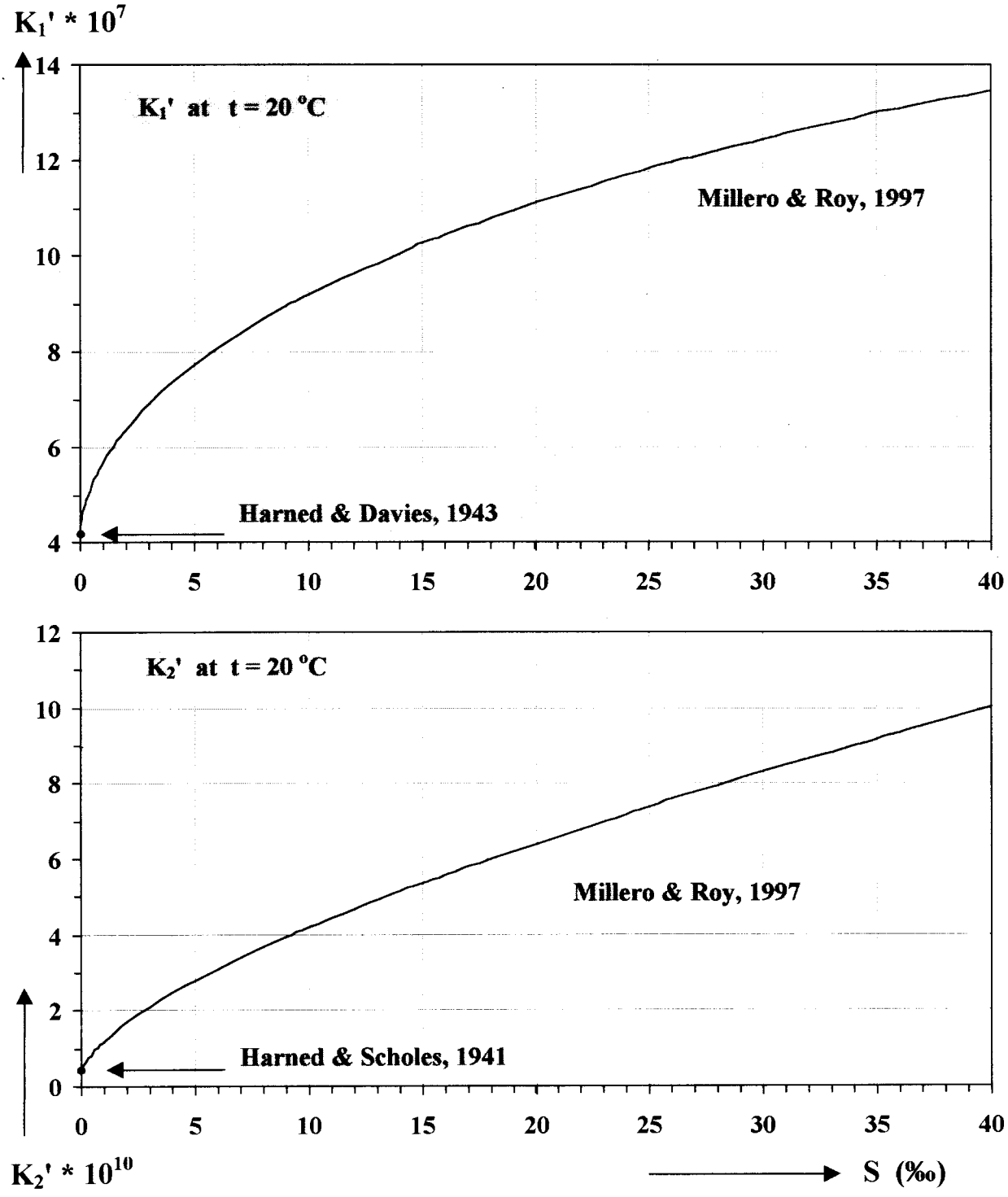

Fig.9.4 Values for the first and second dissociation constants of dissolved carbonic acid as a function of the salinity (Millero and Roy, 1997). The values are valid for a water temperature of 20 °C.

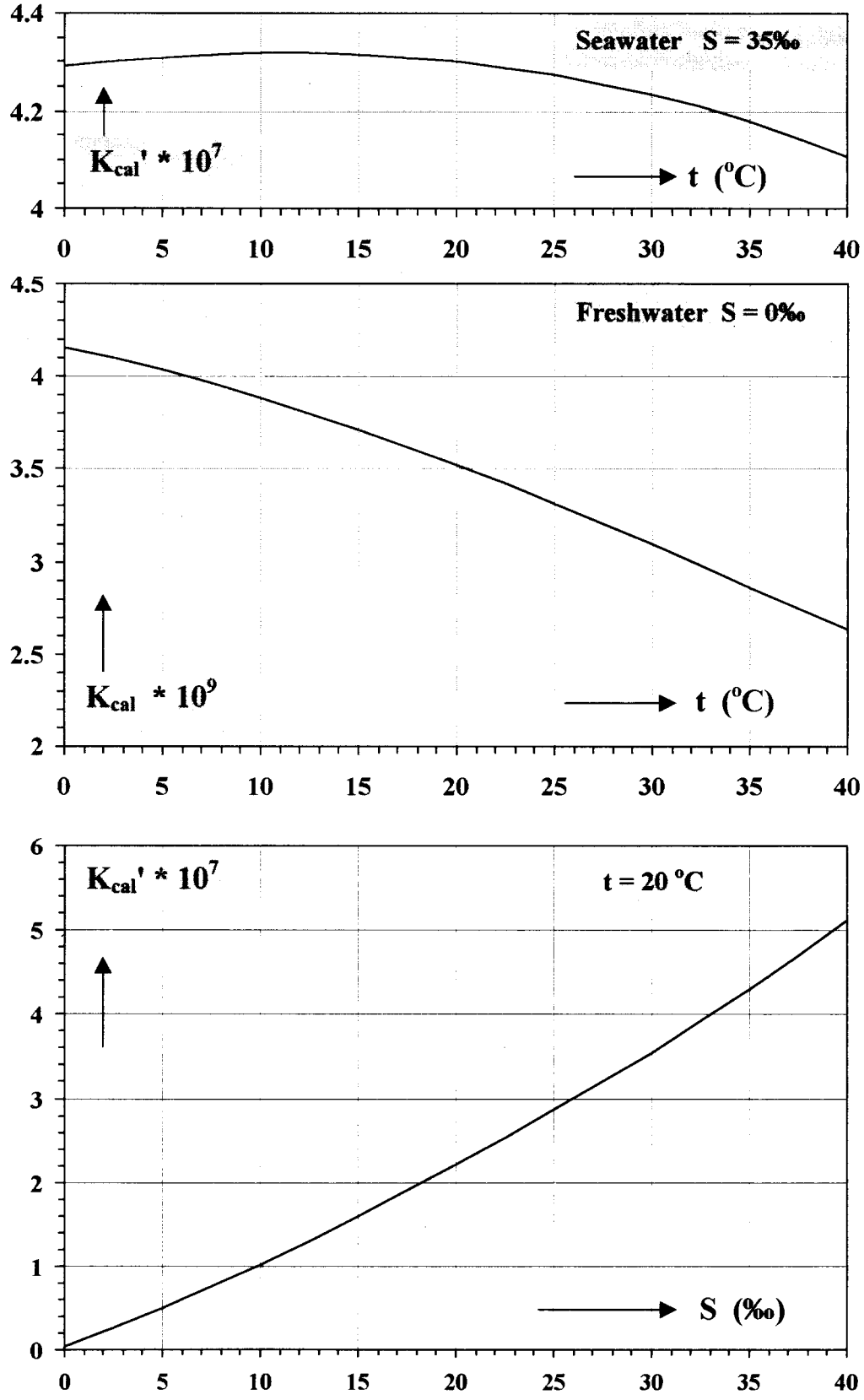

Fig.9.5 The solubility product (Eq.9.17) of calcite ($CaCO_3$) depending on the water temperature and salinity during precipitation (values according to Eq.9.43 (Mucci, 1983)).

The acidity constant values published by Millero and Roy (1997) are derived from the above considerations on non-ideal solutions taking into account a series of different compounds. Sets of data for various temperatures and salinities are further presented in Table 9.1.

Values of the solubility product of calcite ($CaCO_3$) (Eq.9.17) used in this volume are taken from Mucci (1983):

$$pK_{cal} = -^{10}\log K_{cal} = 171.9065 + 0.077993\ T - 2839.319 / T - 71.595\ \log T + \\ + (0.77712 - 0.0028426\ T - 178.34 / T) S^{1/2} + \\ + 0.07711\ S - 0.0041249\ S^{3/2} \qquad \textbf{(9.32)}$$

Values are shown in Fig.9.5 as functions of the water temperature for fresh- and seawater and as a function of salinity at 20 °C.

9.4 CARBONIC ACID CONCENTRATIONS

As we have mentioned the difference between the acidity constants for the fresh and seawater are considerable. This greatly effects the distribution of the carbonic acid fractions in natural waters. Examples of this will be shown in the following sections.

The distribution of the dissolved carbonic acid species in pure water can be specified as a fraction of the total dissolved inorganic carbon. From Eqs.9.6, 9.9 and 9.10, respectively, Eqs.9.18, 9.19 and 9.20 we obtain:

$$[H_2CO_3] = K_0 P_{CO_2} \qquad \textbf{(9.33)}$$

$$[H_2CO_3] = \frac{[H^+]}{K_1}[HCO_3^-] \qquad \textbf{(9.34)}$$

$$[CO_3^{2-}] = \frac{K_2}{[H^+]}[HCO_3^-] \qquad \textbf{(9.35)}$$

so that

$$C_T = \left(\frac{[H^+]}{K_1} + 1 + \frac{K_2}{[H^+]}\right)[HCO_3^-] \qquad \textbf{(9.36)}$$

The fractional concentrations can now be given in terms of the total carbon content:

$$[HCO_3^-] = \frac{[H^+]K_1}{[H^+]^2 + [H^+]K_1 + K_1K_2} * C_T \quad (9.37)$$

$$[H_2CO_3] = [CO_2aq] = \frac{[H^+]^2}{[H^+]^2 + [H^+]K_1 + K_1K_2} * C_T \quad (9.38)$$

$$[CO_3^{2-}] = \frac{K_1K_2}{[H^+]^2 + [H^+]K_1 + K_1K_2} * C_T \quad (9.39)$$

and likewise for the apparent acidity constants K' in non-ideal solutions such as seawater.

The relative contributions of $[H_2CO_3]$, $[HCO_3^-]$ and $[CO_3^{2-}]$ to the total carbon content is shown in Fig.9.6 as a function of pH for two different temperatures for freshwater (at ionic strength = 0) and average seawater (S = 35.0‰ or Cl = 19.37°/₀₀).

As was anticipated, the acidity constants of carbonic acid change so rapidly with temperature and with the ionic strength of the solution that it results in a strong dependence of the distribution on both temperature and salinity.

9.5 EXAMPLES FOR OPEN AND CLOSED SYSTEMS

In this section a few examples will be given of how to deal with the above equations. We will refer to *closed systems* in which the dissolved carbonic acid fractions do not exchange, nor with the gaseous system (atmospheric or soil CO_2), neither the solid phase ($CaCO_3$). In an open system the solution exchanges with either the gaseous phase (=open to the gas phase), or the solid (open to $CaCO_3$). We will be dealing with **(i)** a comparison with fresh and seawater, both in equilibrium with atmospheric CO_2, **(ii)** a groundwater sample of which $[H_2CO_3]$ corresponds to a P_{CO2} value far exceeding the atmospheric concentration and which is brought into contact with the atmosphere at a constant temperature, **(iii)** water exposed to the atmosphere in the presence of calcium carbonate rock, and **(iv)** mixing freshwater and seawater (in an estuary) under closed conditions.

9.5.1 COMPARISON OF FRESHWATER AND SEAWATER EXPOSED TO THE ATMOSPHERE

Here we are dealing with an open system to the atmosphere (exchange with atmospheric CO_2) at a constant temperature. The latter is considered to be of infinite dimensions, so that P_{CO2} is constant. The system is closed to $CaCO_3$, so that the carbonate alkalinity (=the concentration of positive metal ions) is constant. The given conditions are shown in Fig.9.7.

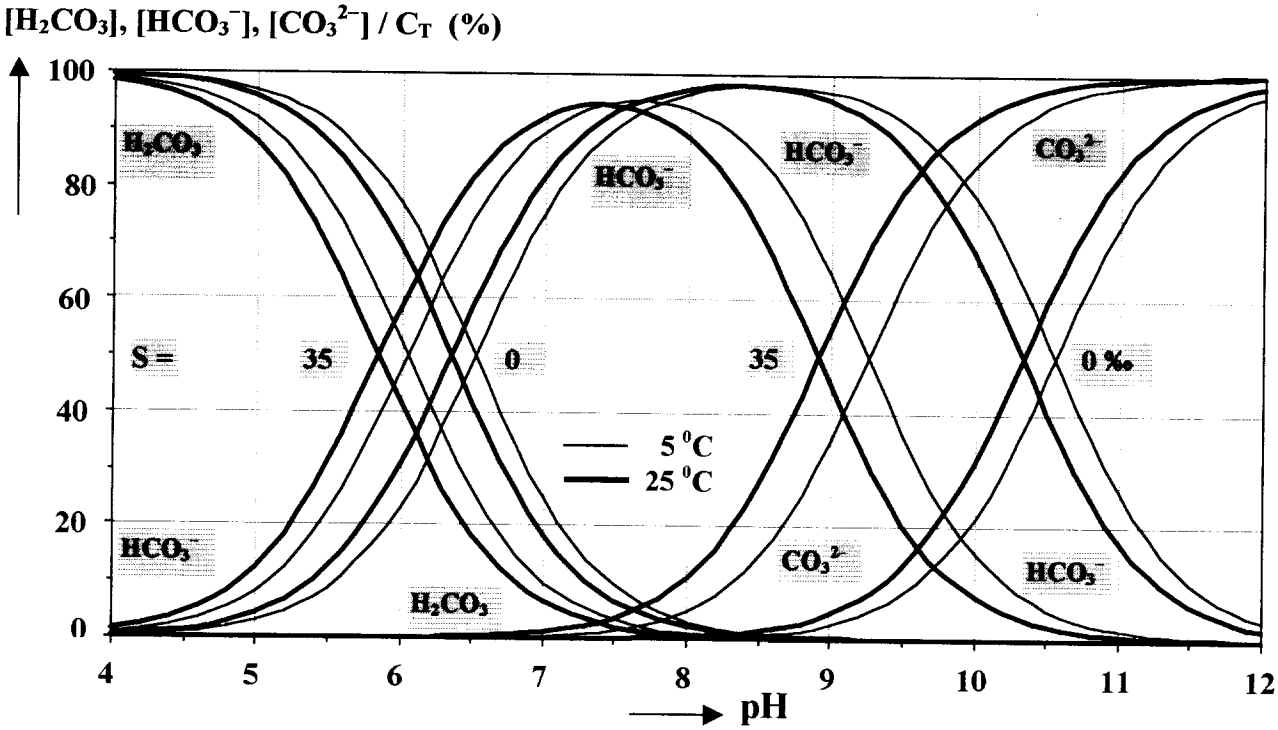

Fig.9.6 Distribution of the carbonic acid fractions as percentages of the total carbon content, C_T. The values are calculated using Eqs.9.37, 9.38, 9.39 for temperatures of 5 and 10 ^{0}C and for salinities of 0 and 35 ‰ as a function of the pH. Seawater has pH values around 8.2. However, the carbon distributions are shown for an (unrealistic) wider range of pH values, to illustrate the dependence of the carbon distribution on salinity.

Here we will use the symbols:

$$a = [H_2CO_3] + [CO_2aq] \qquad b = [HCO_3^-] \qquad c = [CO_3^{2-}]$$

The values of the first and second (apparent) acidity constants are calculated from Eqs.9.22 to 9.28. Furthermore, we apply the Eqs.9.37 to 9.39 for calculating the various dissolved fractions.

Starting with the known value of the atmospheric partial pressure of CO_2, the dissolved CO_2 concentration is obtained, and from that the pH dependent other concentrations.

9.5.1.1 FOR FRESHWATER

$$a = [H_2CO_3] = K_0P_{CO2} = 0.04571(M/L.atm)\times350\times10^{-6}(atm) = 1.600\times10^{-5}\ M/L$$

$$b = [HCO_3^-] = (K_1/[H^+])a = (3.846\times10^{-7}/[H^+])a = 6.154\times10^{-12}/[H^+]$$

$$c = [CO_3^{2-}] = (K_1K_2/[H^+]^2)a = (3.846\times10^{-7}\times3.800\times10^{-11}/[H^+]^2)a = 2.338\times10^{-22}/[H^+]^2$$

The carbonate alkalinity is known:

GIVEN	**S = 0 ‰** **A_C = 2.2 mM/kg** **t = 15 °C** **P_{CO2} = 350×10^{-6} atm**	**S = 35 ‰** **A_C = 2.2 mM/kg** **t = 15 °C** **P_{CO2} = 350×10^{-6} atm**
RESULT	**a = 0.016 mM/kg** **b = 2.143 „** **c = 0.028 „** **C_T = 2.19 „** **pH = 8.542**	**a = 0.013 mM/kg** **b = 1.860 „** **c = 0.170 „** **C_T = 2.04 „** **pH = 8.084**

Fig.9.7 Schematic representation of the conditions of fresh (0‰) and seawater (35‰), both in equilibrium at a constant temperature with the atmosphere with constant CO_2 concentration (partial pressure). The upper part shows the given conditions, the lower part the resulting data.

$$A_C = b + 2c = 6.154\times10^{-12}/[H^+] + 4.677\times10^{-22}/[H^+]^2 = 2.2\times10^{-3}\ M/L$$

From this quadratic equation $[H^+]$ and the pH can be obtained, resulting in:

$$[H^+] = 2.871\times10^{-9}\ M/L \quad \text{and pH} = 8.542$$

The total carbon content of the water then is obtained by inserting $[H^+]$ in the above equations:

$$C_T = a + b + c = 0.016 + 2.14 + 0.028 = 2.19\ mM/L$$

9.5.1.2 FOR SEAWATER

$$a = 0.03811(M/kg.atm)\times350\times10^{-6}(atm) = 1.334\times10^{-5}\ M/kg$$

$$b = (11.480\times10^{-7}/[H^+])\times1.334\times10^{-5} = 15.314\times10^{-12}/[H^+]$$

$$c = (11.480\times10^{-7}\times7.516\times10^{-10}/[H^+]^2)\times1.334\times10^{-5} = 1.151\times10^{-20}/[H^+]^2$$

Again the carbonate alkalinity is known:

$$b + 2c = 15.31\times10^{-12}/[H^+] + 2.302\times10^{-20}/[H^+]^2 = 2.2\times10^{-3}\ M/kg$$

Solving this quadratic equation results in:

$$[H^+] = 8.232\times10^{-9}\ M/kg \quad \text{and} \quad \text{pH} = 8.084$$

The total carbon content is:

$$C_T = 0.013 + 1.86 + 0.170 = 2.04 \text{ mM/kg}$$

Comparison of these results, as shown in Fig.9.7, reveals that in the freshwater the carbonic species consists for 98% of dissolved bicarbonate, while the seawater with a lower pH still contains about 10% of dissolved carbonate ions.

9.5.2 SYSTEM OPEN FOR CO_2 ESCAPE AND $CaCO_3$ FORMATION

The second example describes the chemical changes in a certain given fresh (ground)water from which excess CO_2 escapes to the atmosphere and in which $CaCO_3$ precipitates at saturation. In part (1) we shall indicate how the various carbon concentrations are calculated. In part (2) the solution looses CO_2 to the air (open to the atmosphere) at constant temperature until chemical equilibrium between P_{CO2} and the dissolved CO_2 fraction. Part (3) considers the presence of Ca^{2+} ions and a possible precipitation of calcite (open to the solid phase).

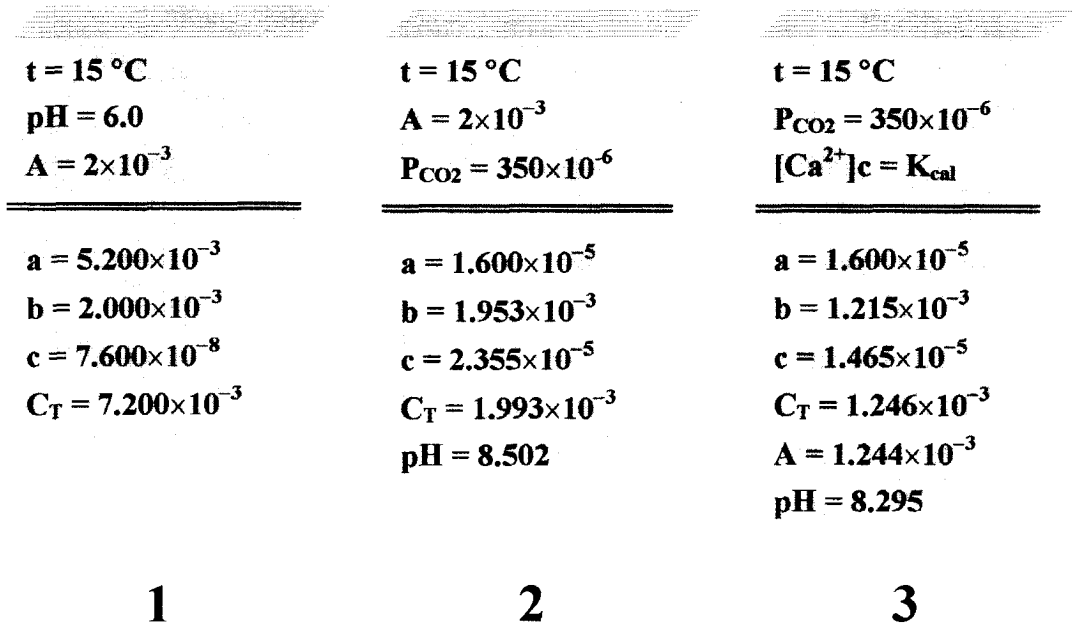

Fig.9.8 Schematic representation of the numerical results from exposing a water sample with given conditions (upper part of 1) to the atmosphere (upper part of 2) and allowing precipitation of calcite (upper part of 3). The lower part of the boxes show the calculated data. All concentrations are in M/kg.

9.5.2.1 STARTING CONDITIONS

We assume that the temperature, pH (resulting in $[H^+]=10^{-pH}$) and the titration alkalinity (A) are known by measurement. The H^+ concentration will be denoted by the symbol h instead of $[H^+]$.

We can use the equations:

$$A = b + 2c + 10^{-14.34}/h - h, \text{ where the latter 2 terms can be neglected}$$

$$b/a = K_1/h$$

$$c/b = K_2/h$$

Multiplication of the latter two relations gives:

$$c / a = K_1K_2 / h^2 \quad \text{or} \quad c = (K_1K_2 / h^2)\, a$$

With

$$A = b + 2c$$

this results in:

$$A = (K_1 / h)\, a + (2K_1K_2 / h^2)\, a$$

so that:

$$a = \frac{h^2}{hK_1 + 2K_1K_2} A \qquad \textbf{(9.40)}$$

$$b = \frac{hK_1}{hK_1 + 2K_1K_2} A = \frac{h}{h + 2K_2} A \qquad \textbf{(9.41)}$$

$$c = \frac{K_1K_2}{hK_1 + 2K_1K_2} A = \frac{K_2}{h + 2K_2} A \qquad \textbf{(9.42)}$$

i.e. 3 equations with 3 unknowns. At a temperature of 15°C, a starting pH value of 6.0 and an alkalinity of 2 mM/L the resulting concentrations are given in Fig.9.8 phase 1.

9.5.2.2 ESCAPE OF CO_2

If the water looses CO_2 in contact with the atmosphere, and in the first instance neglecting the presence of Ca^{2+}, until equilibrium with the atmospheric P_{CO2} (denoted by p) has been reached, we have:

$$\mathbf{a} = K_0 p$$

$$\mathbf{b}^2/(\mathbf{ac}) = K_1/K_2$$

$$A \approx \mathbf{b} + 2\mathbf{c}$$

again 3 equations with 3 unknowns (bald type). With the additional starting values for the atmospheric CO_2 concentration (p), the concentration can be calculated (Fig.9.8, phase 2).

9.5.2.3 PRECIPITATION OF $CaCO_3$

Here we have, apart from the known atmospheric P_{CO2}, the additional complication that calcite precipitates if the product of $[Ca^{2+}]$ and $[CO_3^{2-}]$ exceeds the solubility product given by Eq.9.32 (Fig.9.5), so that CA decreases.

The amount of calcite (or Ca^{2+}) removed from the water, $\Delta[Ca^{2+}]$, equals the amount of carbon removed from the water, ΔC_T. We then have the following equations:

$$a_2 = K_0 p = a_1 = a$$

$$b_2/c_2 = b_1/c_1 = (K_1/K_2)a \quad \text{or} \quad \mathbf{c_2 = (c_1/b_1)b_2}$$

$$A_2 - A_1 = [Ca^{2+}]_2 - [Ca^{2+}]_1 = C_{T2} - C_{T1} \quad \text{or} \quad \mathbf{\Delta[Ca^{2+}] = \Delta C_T}$$

$$[Ca^{2+}]_2\, c_2 = 10^{-pKcal} \quad \text{or} \quad ([Ca^{2+}]_1 + \mathbf{\Delta C_T})\mathbf{c_2} = K_{cal}$$

$$\Delta C_T = (a + b_2 + c_2) - (a + b_1 + c_1) \quad \text{or} \quad \mathbf{\Delta C_T = b_2 + c_2} - (b_1 + c_1)$$

For reasons of simplicity we assume that the alkalinity is balanced by the Ca^{2+} ions alone,

so that $[Ca^{2+}]_1 = 0.5A$

where the subscript (1) refers to the values obtained by step 2, and (2) to the final values after precipitation of $CaCO_3$. These 4 independent equations with 4 unknowns (bald type) can now be solved. The numerical result is shown in Fig.9.8.

Comparison of boxes 1 and 2 shows that:

1) the amount of CO_2 escaped to the atmosphere (= 143 mL STP) is of the order of the amount of dissolved CO_2 present at the start of the experiment
2) the amount of calcite formed is 25.4 mg/L

9.5.3 SYSTEM EXPOSED TO CO_2 IN THE PRESENCE OF $CaCO_3$

In the presence of carbonate rock water may be exposed to a certain CO_2 pressure. The question is how much $CaCO_3$ can be dissolved in equilibrium with the CO_2 atmosphere.

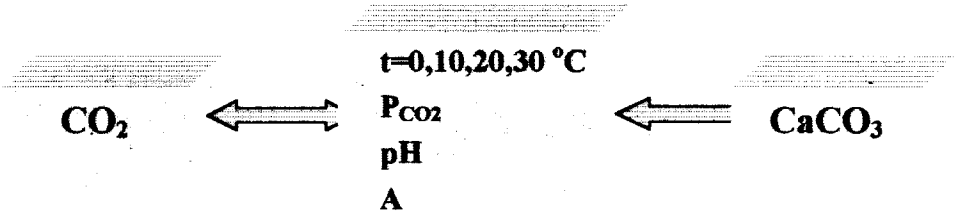

Fig.9.9 Schematic representation of an open system, consisting of a water mass in open contact with a CO_2 atmosphere and with solid $CaCO_3$.

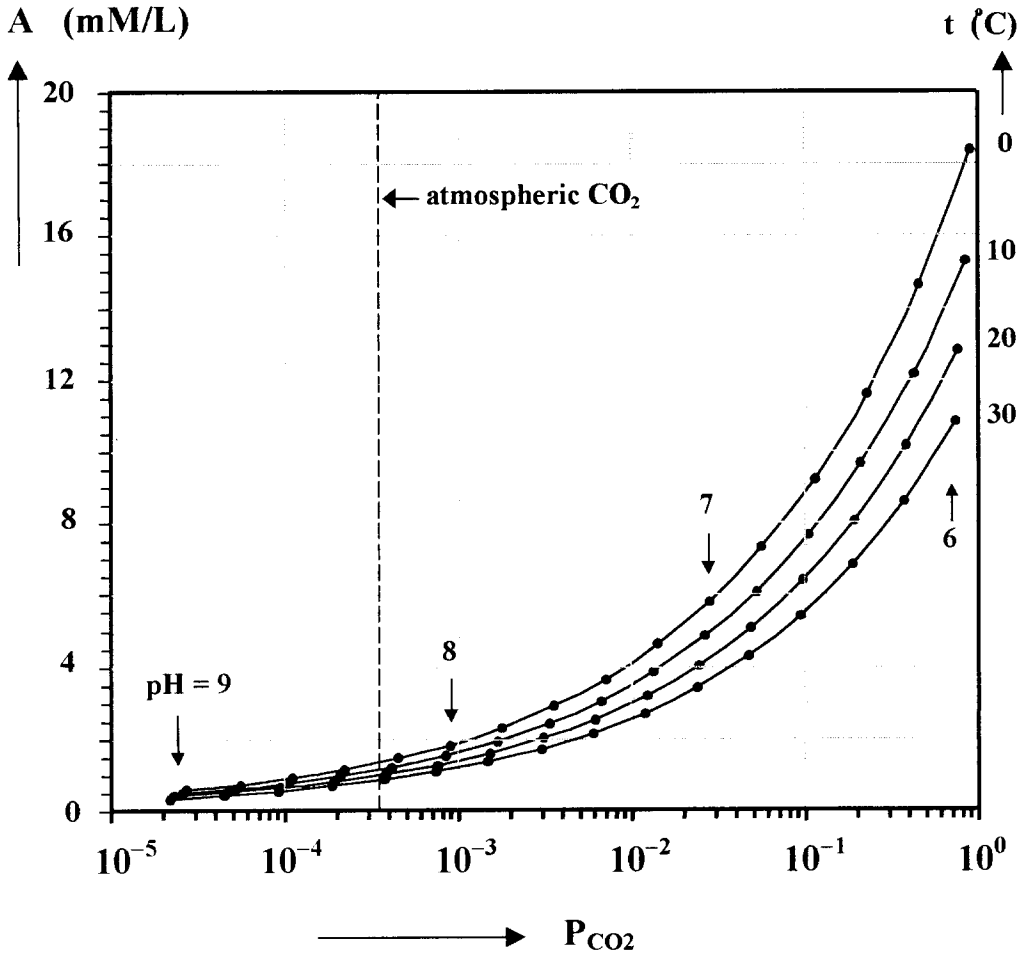

Fig.9.10 Schematic representation of an open system, consisting of a water mass in exchange with an infinite CO_2 reservoir and with carbonate rock. The alkalinities are calculated for 4 different temperatures. The corresponding pH values are indicated in the graph as well as the atmospheric CO_2 partial pressure (P_{CO2}).

Instead of choosing the CO_2 pressure, the calculation procedure is the easiest if we depart from the final pH the water will obtain. The alkalinity is defined by the electroneutrality requirement:

$$A = 2Ca^{2+} + [H^+] = [HCO_3^-] + 2[CO_3^{2-}] + [OH^-] = \frac{2K_{cal}}{c} + h = b + 2c + \frac{K_w}{h} \quad \textbf{(9.44)}$$

Inserting the Eqs.9.33, 9.34 and 9.35 results in the equation:

$$\left(\frac{K_0K_1}{h} + 2\frac{K_0K_1K_2}{h^2}\right)P_{CO_2}^2 + \left(\frac{K_w}{h} - h\right)P_{CO_2} + 2\frac{K_{cal}\,h^2}{K_0K_1K_2} = 0$$

The solution of this equation and the resulting A values for 4 different temperatures are shown in Fig.9.10. Also the corresponding pH values are indicated.

9.5.4 CLOSED SYSTEM, MIXING OF FRESHWATER AND SEAWATER

As an example of a closed system we will discuss the mixing of fresh river water and seawater, such as occurs in an estuary. Calculating $^{13}\delta$ of, for instance, the bicarbonate fraction of the brackish mixture from the $^{13}\delta$ values of bicarbonate in the end members (fresh and seawater) is not straightforward, because the mixing process of the mole fractions of bicarbonate is not conservative, i.e. the dissociation equilibria of carbonic acid shift by the changes pH, and the values of the acidity constants change by the changes in the salinity of

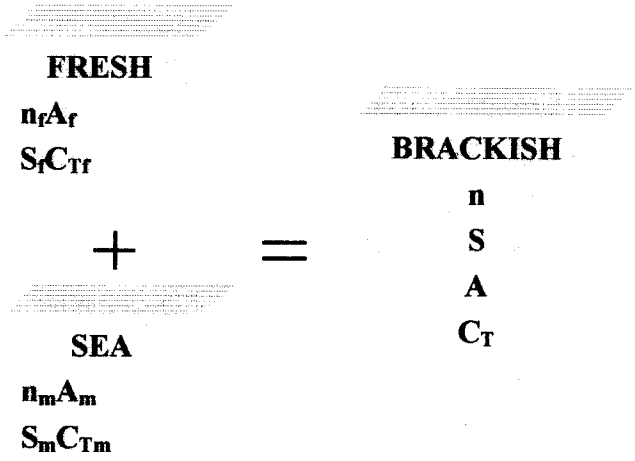

Fig.9.11 Schematic representation of the formation of brackish water as a mixture of fresh (river) and seawater. In the supposedly closed system the parameters shown in the figure are conservative.

the water. The system of the two components together is closed, however, so that, if the end members are denoted by f(resh) and m(arine), the final values for the conservative parameters, i.e. the salinity, the alkalinity and the total carbon content, are:

$$nS = n_fS_f + n_mS_m \qquad \text{or} \qquad S = (n_f/n)S_f + (n_m/n)S_m \qquad \textbf{(9.45)}$$

where $n + m = n$, $S_f \approx 0‰$ and $S_m \approx 35‰$ (Fig.9.11).

Measurement of the salinity of the brackish water results in the (degree of) *brackishness* (X) of the water, here defined as the fraction of seawater (for seawater X =1, for freshwater X ≈ 0):

$$S = \frac{n_f}{n} S_f + \frac{n_m}{n} S_m = \left(1 - \frac{n_m}{n}\right) S_f + \frac{n_m}{n} S_m$$

or

$$X = \frac{n_m}{n} = \frac{S - S_f}{S_m - S_f} \approx \frac{S}{35} \qquad \textbf{(9.46)}$$

Furthermore:

$$nA = n_f A_f + n_m A_m \qquad \text{or} \qquad A = (1 - X)A_f + \mu A_m \qquad \textbf{(9.47)}$$

and

$$C_T = n_f C_{Tf} + n_m C_{Tm} \qquad \text{or} \qquad C_T = (1 - X)C_f + \mu C_m \qquad \textbf{(9.48)}$$

In order to calculate $^{13}\delta_a$ and $^{13}\delta_b$ and $^{13}\delta_c$ the carbonic acid fractions have to be obtained by solving the following 4 equations with 4 unknowns (in bald type):

$$A = \mathbf{b} + 2\mathbf{c} \qquad C_T = \mathbf{a} + \mathbf{b} + \mathbf{c}$$

$$K_1 = \mathbf{hb/a} \qquad K_2 = \mathbf{hc/b}$$

where again $h = [H^+]$, $a = [CO_2]$, $b = [HCO_3^-]$ and $c = [CO_3^{2-}]$. K_1 and K_2 refer to the brackish water values at the proper salinity.

A striking feature of estuaries is the non-linear behaviour of pH as a function of salinity. Examples were shown by Mook and Koene (1975). The position of the pH minimum strongly depends on the carbonate alkalinity ratio of the fresh and marine components (CA_f/CA_m).

The consequence of this non-linear behaviour of the pH, and thus also of the carbonic acid fractions, is that also $^{13}\delta$ of these fractions does not obey conservative mixing (Sect.7.3).

The only possible procedure for determining $^{13}\delta$ values of the dissolved carbonic components in water is by quantitatively converting the DIC into dissolved CO_2 by the addition of acid (such as H_3PO_4) to the water sample and extracting the CO_2 from the water. Consequently only $^{13}\delta_{DIC}$ can be obtained. If $^{13}\delta$ of the constituting fractions (a, b and c) are to be known, these should be calculated from the ^{13}C mass balance (cf. Sect.4.3.1):

$$C_T\, {}^{13}R_{DIC} = a\, {}^{13}R_a + b\, {}^{13}R_b + c\, {}^{13}R_c = a\, {}^{13}\alpha_{a/b}\, {}^{13}R_b + b\, {}^{13}R_b + c\, {}^{13}\alpha_{c/b}\, {}^{13}R_b \qquad \textbf{(9.49)}$$

or with $R/R_{std} = 1 + \delta$:

$$C_T\, {}^{13}\delta_{DIC} = a\, {}^{13}\delta_a + b\, {}^{13}\delta_b + c\, {}^{13}\delta_c = a({}^{13}\delta_b - {}^{13}\varepsilon_{a/b}) + b\, {}^{13}\delta_b + c({}^{13}\delta_c - {}^{13}\varepsilon_{c/b})$$

$$= C_T\,{}^{13}\delta_b - a\,{}^{13}\varepsilon_{a/b} - c\,{}^{13}\varepsilon_{c/b} \quad \textbf{(9.50)}$$

so that

$${}^{13}\delta_{DIC} = {}^{13}\delta_b - (a/C_T){}^{13}\varepsilon_{a/b} - (c/C_T){}^{13}\varepsilon_{c/b} \quad \textbf{(9.51)}$$

and similarly:

$${}^{13}\delta_{DIC} = {}^{13}\delta_a - (b/C_T){}^{13}\varepsilon_{b/a} - (c/C_T){}^{13}\varepsilon_{c/a} \quad \textbf{(9.52)}$$

$${}^{13}\delta_{DIC} = {}^{13}\delta_c - (a/C_T){}^{13}\varepsilon_{a/c} - (b/C_T){}^{13}\varepsilon_{b/c} \quad \textbf{(9.53)}$$

where the ${}^{13}\varepsilon$ values are given in Table 7.2.

10 WATER SAMPLING AND LABORATORY TREATMENT

This chapter on field and specifically on laboratory practice serves to give the hydrologist as well as the beginning laboratory worker an impression of the experimental efforts involved in applying isotope hydrology. A few parts have been taken -and slightly adjusted- from the IAEA Guidelines / Manual for Operation of an Isotope Hydrology Laboratory. Detailed descriptions of the field practice have been given by Clark and Fritz (see Recommended Literature). We have intended to limit the amount of detail on the analytical methods, so that the contents of (parts of) this chapter are valid for any isotope laboratory.

10.1 WATER SAMPLING AND STORAGE

In a successful field sampling programme a volume of water is to be collected and brought or sent to the isotope laboratory that is representative for the water mass under investigation. The main concern during sampling, transport and storage is to avoid isotope fractionation through evaporation or diffusive loss of water vapour, and/or isotope exchange with the surroundings as well as with the bottle material. These effects can be minimised by using appropriate collection methods and bottles. A careful selection and testing of the methods and bottles needs to be made at an early stage. This section provides the background information to help in this selection.

The hydrologist, however, should follow the specific instructions to be given by the laboratory that is intended to analyse the samples.

10.1.1 SAMPLING BOTTLES

The bottle and seal must be made of such a design and appropriate material that any loss by evaporation and diffusion to or exchange of water with the surroundings is prevented. The isotope effect of evaporation can be significant: a 10% loss of sample results in an isotope enrichment of about 10‰ in ^{2}H and 2‰ in ^{18}O. The following conclusions are gained by experience:

- the most secure vessels for storage are glass bottles, allowing storage of at least a decade as long as the seal is not broken
- high-density polyethylene is satisfactory for collection and storage during a few months (water and carbon dioxide easily diffuse through low-density plastics)

- bottles with small necks are the most satisfactory
- caps with positive seals (plastic inserts, neoprene, etc.) are required
- the volume of bottles should normally be 50 mL for the combination of ^{2}H and ^{18}O analyses, 50 L for conventional ^{14}C dating and 250 mL for AMS ^{14}C dating (Chapter 11), and 500 mL for low-level ^{3}H analysis. If the storage may be longer than several months, it is preferable to collect a larger volume and store the samples in glass bottles (the relative influence of evaporation is than minimised). Generally, the dissolved carbon content of large-volume ^{14}C samples are treated in the field (see below).

Further details on sample quantities are also given in Volume IV.

10.1.2 GENERAL FIELD PRACTICE

The following points emphasise good field practice that is applicable to all types of water to be sampled (precipitation, surface water, groundwater):

always use a field note book to record observations and record numbers data on sample collection sheets to be handed over to the laboratory

- determine geographical co-ordinates of sampling points using GPS or national co-ordinate systems, maps, aerial photographs, etc.
- measure altitude, depth to the water table (groundwater), sample depth (depth into groundwater or surface water), well condition, condition of rain gauge, discharge (rivers, artesian wells), lake level, weather conditions, etc.
- it is very important to record other chemical and physical data to aid interpretation such as water temperature, pH, alkalinity, conductivity, and other possible chemical constituents
- fill sample bottles completely, provided the water has no chance of freezing during air transport (in that case fill the bottles two-thirds full)
- mark all bottles individually with waterproof marker (project code, location, date, sample number, collector's name, type of analysis needed); the information has to be cross-referenced with the field notebook and the sample collection sheets.

Specific points of interest will be discussed below.

In the next sections we will discuss sampling of the various types of water.

10.1.3 PRECIPITATION

The sampling strategy for rain and snow is in general dictated by the scientific aim of the programme. For example, the sampling interval may be monthly, weekly, daily, or even each

hour. In all cases it is necessary to record the amount of precipitation so that weighted means of isotopic compositions can be calculated afterwards.

Of course, the maximum information and least risk of evaporation results from short-term collection of precipitation. Samples should be stored individually in bottles. If only monthly mean compositions are required, daily samples can be combined in a larger storage bottle.

For samples that are collected on weekly or monthly basis, the isotopic composition of the sample is likely to be modified by evaporation. This can be minimised by a special construction of the rain gauge, or by placing a small amount of mineral oil (2 mm minimum) in the collection bottle which is floating on the water.

Special care is to be taken when collecting snow. They should be allowed to melt slowly at ambient air temperature, avoiding evaporation.

10.1.4 SURFACE WATER

Generally, the collection method for surface waters pose few problems, when collected in relatively small quantity. Special care has to be taken when collecting water for carbon isotopic analysis. Field measurement of temperature, pH and salinity (especially with marine and brackish water) are needed. The samples are to be stored in glass bottles, in the dark, preferably at low temperature, and should be poisoned by I_2+KI or $HgCl_2$. The poisoning recipes are:

I_2+KI solution: to be prepared by dissolving 15 mg of I_2 and 30 mg of KI per mL of (ultra)pure water; water is poisoned by adding 0.5 mL of this solution per L of sample

$HgCl_2$ solution: to be prepared by dissolving 70 mg $HgCl_2$ per mL of (ultra)pure water; 3 mL of this solution is to be added per L of water sample.

River and stream samples should be taken from mid-stream or a flowing part of the stream. Standing water near stream banks should be avoided as the water may not be well mixed and show effects due to evaporation or pollution.

Samples from lakes and estuaries should be collected from both the surface and from depth. Together with other physical and chemical information, it may be possible to interpret the results in terms of the water-column structure.

Care should be taken when sampling near a confluence. For a considerable distance downstream of a confluence, the river samples may still show variable isotopic compositions due to incomplete mixing between the two different river waters. In large river systems this may amount to a distance of many tens of kilometres.

10.1.5 UNSATURATED ZONE WATER

The isotopic profile of soil moisture can provide information on groundwater recharge. Samples are often taken from the soil as such. The most common methods to extract water

from the soil profile in the laboratory are (i) vacuum distillation, (ii) freeze drying, (iii) squeezing, and (iv) centrifugation.

10.1.6 GROUNDWATER

For all groundwater sampling, it is necessary to characterise as far as possible the hydrogeological situation (geophysical, geochemical, etc.) of the borehole.

Pumped boreholes and production wells present little problem with the sample readily collected from the surface supply. This is specifically true for the large quantity samples for conventional ^{14}C analysis (see Chapter 11). Sampling observation wells and especially very deep aquifers may pose more problems. First one should be aware that standing water in such passive boreholes may not be representative for the water mass in the aquifer, because of evaporation or carbon dioxide exchange with the ambient air. It is usual to pump the borehole until it is purged by approximately twice the well volume, or until steady state chemical conditions (pH, Eh) are obtained. While this is common practice, it should be borne in mind that in certain situations, the cone of depression resulting from pumping may draw in water from other sources.

It may be practically impossible to collect sufficient water from a deep well for routine ^{14}C analysis. In that case one has to turn to the AMS technique for which 250 mL of sample is generally sufficient.

10.1.7 GEOTHERMAL WATER

Both steam and liquid phases should be collected from geothermal fields so that the ratio steam/water can be determined. This is relatively easy in production plants, but difficult in non-developed geothermal regions. The steam is to be condensed, taking care that this procedure operates quantitatively.

Particularly critical for thermal waters is the need to identify the source of the spring and to sample as close to the spring as possible.

10.2 LABORATORY TREATMENT OF WATER SAMPLES

The aim of this section is to offer the hydrologist some insight in the procedures used by the isotope laboratory to determine the isotopic compositions of the water samples he sent/brought to the laboratory. The purpose is not to provide the laboratory detailed recipes for carrying out the analyses. For that the reader is referred to IAEA Guidelines or specific laboratory's operation manuals and literature. The procedures will be discussed on the basis of the various isotopes.

Nearly all isotopic measurement techniques can not be applied to water as such. Therefore, the underlying principle of all methods is that the water or the constituents to be analysed

(such as dissolved carbonic acid) are to be converted into a chemical compound that can be used in the equipment. The specific requirement is that during this conversion no changes are introduced in the isotopic composition, or only changes that are accurately known.

10.2.1 THE $^{18}O/^{16}O$ ANALYSIS OF WATER

10.2.1.1 EQUILIBRATION WITH CO_2 FOR MASS SPECTROMETRIC MEASUREMENT

Since water poses many problems in mass spectrometers –primarily because of the adhesion to metal, causing serious memory effects- the $^{18}O/^{16}O$ ratio of the water sample has to be transferred to a more suitable gas, such as carbon dioxide. The most common sample preparation method for $^{18}\delta$ in water is the $CO_2 - H_2O$ equilibration in which about a millimole amount of CO_2 (10 to 20 mL) is brought into isotopic equilibrium with a few mL of sample water (generally at 25.0 ± 0.2 °C):

$$H_2{}^{18}O + C^{16}O_2 \Leftrightarrow H_2{}^{16}O + C^{18}O^{16}O$$

An aliquot of the equilibrated CO_2 is then transferred to the mass spectrometer for $^{18}O/^{16}O$ measurement. Because the $^{18}O/^{16}O$ ratio in CO_2 and H_2O is different (see Sect.7.2.2 for the value of $^{18}\alpha_{g/l}$) the $^{18}\delta$ value obtained has to be corrected for this fractionation. However. sample and international reference material (see Sect.7.2.3) are treated equally (i.e. equal amounts of water and carbon dioxide and equal temperature), so that the correction is not relevant (Sect.4.3.2):

$$\begin{aligned} {}^{18}\delta(\text{water}) &= \frac{{}^{18}R_{H_2O}}{{}^{18}R_{VSMOW}} - 1 = \frac{{}^{18}\alpha_{g/l}\,{}^{18}R_{H_2O}}{{}^{18}\alpha_{g/l}\,{}^{18}R_{VSMOW}} - 1 \\ &= \frac{{}^{18}R_{CO_2 \text{ in equil.with } H_2O}}{{}^{18}R_{CO_2 \text{ in equil. with VSMOW}}} - 1 = {}^{18}\delta(\text{equilibrated } CO_2) \end{aligned} \qquad \textbf{(10.1)}$$

in other words the $^{18}\delta$ value for CO_2 equilibrated with the water sample is equal to the $^{18}\delta$ value of the water itself, where the $^{18}\delta$ values refer to the international reference VSMOW. We have to emphasise, however, that the δ values do have to be corrected for the water–CO_2 equilibration according to Eq.10.3, because of the additive term in Eq.10.2.

The following experimental details and concerns apply to this method.

- During the isotopic exchange of the oxygen atoms between CO_2 and H_2O the oxygen isotopic composition of the water changes; for this a correction has to be made; from an ^{18}O mass balance consideration we derive:

$$w_0\,{}^{18}R_{w0} + c_0\,{}^{18}R_{c0} = w\,{}^{18}R_w + c\,{}^{18}R_c = w\frac{{}^{18}R_c}{{}^{18}\alpha_{c/w}} + c\,{}^{18}R_c$$

where w_0 and c_0, and w and c are the mole amounts of oxygen atoms in the water and carbon dioxide before and after the equilibration, respectively, and the fractionation factor ${}^{18}\alpha_{c/w}$ is equal to $1 + {}^{18}\varepsilon_{g/l}$ as defined in Table 7.4 (commonly at 25 °C); assuming that $w = w_0$ and $c = c_0$, and writing $\rho = c/w$, the corrected value of the equilibrated CO_2 is:

$${}^{18}\alpha_{c/w}\,{}^{18}R_{w0} = {}^{18}R_c(1 + {}^{18}\alpha_{c/w}\rho) - {}^{18}\alpha_{c/w}\rho\,{}^{18}R_{c0} \qquad \textbf{(10.2)}$$

In terms of δ values this comes to a corrected ${}^{18}\delta$ value of:

$${}^{18}\delta_c' = (1 + {}^{18}\alpha_{c/w}\,\rho)\,{}^{18}\delta_c - {}^{18}\alpha_{c/w}\,\rho\,{}^{18}\delta_{c0} \qquad \textbf{(10.3)}$$

- Automated units can be procured with either an air bath or water bath. The former are easier to operate, but the latter show a better temperature stability and homogeneity throughout the bath.
- A variation in equilibration temperature of 1°C causes an uncertainty in the ${}^{18}\delta_c$ value of 0.2‰. Therefore, the temporal variation of the bath should generally be much less than 0.5°C, preferably no more than 0.2°C.
- The equilibration time depends on the amplitude and frequency of shaking and the amount of sample. Typical equilibration times are in the order of 4 to 8 hours.
- In order to remove oxygen and other gases from the water sample prior to equilibration two ways are being used: (i) freezing the sample and removing the gases by pumping (repeated procedure), (ii) pumping the water sample at ambient temperature through a capillary, so minimising the evaporation (and consequently isotope fractionation) of the sample.
- The pH of the water needs to be in the range of 6 to 7 so that dissolved CO_2 and HCO_3^- are abundant. Otherwise a drop of concentrated H_3PO_4 may be added.
- The equilibration technique determines the oxygen isotopic activity rather than concentration of the sample. Therefore, in saline waters and brines it is required to determine the chemistry of the sample.

10.2.1.2 OTHER METHODS

Equilibrating CO_2 with the water sample is the most common method for measuring ${}^{18}O/{}^{16}O$ in water. There are other methods which are in an experimental stage or specifically applicable to certain problems. These will only briefly be mentioned.

1) Water can be converted quantitatively to O_2 by **fluorination** with bromiumpentafluoride:

$$6H_2O + 2BrF_5 \rightarrow 9HF + 2HBr + 3O_2$$

The oxygen released can be isotopically analysed directly or is reacted with hot graphite to produce CO_2 for mass spectrometric analysis (O'Neil and Epstein, 1966). The advantage of this method is that only 9 mg of water is needed. The disadvantage is that BrF_5 is an extremely dangerous liquid and needs extended laboratory installations and precautions.

2) Water can be reacted in nickel tubes **with graphite** at high temperature to produce CO_2 (Edwards et al., 1993).

3) The $^{18}O/^{16}O$ and $^{17}O/^{16}O$ ratios of water can be determined by analysing O_2 mass spectrometrically that is produced by **electrolysis** of water. The precision obtained is about 0.1‰; the advantage especially concerns the direct measurement of ^{17}O which is problematic in CO_2, as the ^{13}C containing molecule has the same mass and is much more abundant (Meijer and Li, 1998).

4) A promising new method is measuring isotope ratios ($^2H/^1H$, $^{17}O/^{16}O$, $^{18}O/^{16}O$) in water directly by **laser absorption spectroscopy** (Kerstel et al., 1999).

10.2.2 THE $^2H/^1H$ ANALYSIS OF WATER

10.2.2.1 REDUCTION OF WATER TO H_2 FOR MASS SPECTROMETRIC ANALYSIS

Again the introduction of water in the mass spectrometer has to be avoided. Therefore, the $^2H/^1H$ ratio is commonly transferred to a more suitable gas, in casu hydrogen. The production of H_2 gas is generally performed by **reducing** the water at several hundred degrees C with zinc or (depleted) uranium:

$$H_2O + Zn \rightarrow ZnO + H_2 \qquad \text{at } 500^\circ C$$

or $$2H_2O + U \rightarrow UO_2 + 2H_2 \qquad \text{at } 800^\circ C$$

The first method is generally carried out as a batch process in steel tubes. In the second method the evaporated sample is running through a furnace containing uranium turnings. Both options require about 10 µL of water. Although applying uranium has less experimental complications, the disadvantages are that it is poisonous and more difficult to obtain and dispose of.

10.2.2.2 OTHER METHODS

Similar to the equilibration method for $^{18}O/^{16}O$ analysis, the $^2H/^1H$ ratio of a water sample can be transferred to H_2 by **isotopic exchange** (Coplen et al., 1991):

$$^2H^1HO + {}^1H_2 \Leftrightarrow {}^1H_2O + {}^2H^1H$$

As in chemical reactions, the equilibration technique is concerned with the activities rather than concentrations. Consequently, the chemistry of the water sample is to be known. Other disadvantages are that the method needs a relatively large investment and that a very good temperature control is needed, as the isotope fractionation varies considerably with the exchange temperature (6‰ per °C). The advantage is that the procedure is faster than the other techniques.

10.2.3 THE ^{3}H ANALYSIS OF WATER

For measuring the tritium content of water several options exist. The choice is to be determined by the (expected) ^{3}H content of the sample and the precision required. The different treatment procedures are:

1) measuring the ^{3}H activity by *liquid scintillation spectrometry* (LSS)

2) measuring the ^{3}H activity by *proportional gas counting* (PGC)

3) measuring the amount of daughter ^{3}He mass spectrometrically after storing the sampling for a specific time in the laboratory (Sect.12.1.5.2).

Moreover, the possibility exists to increase the original ^{3}H content artificially (i.e. to enrich) by a known amount, usually through *electrolysis*, prior to the ^{3}H measurement. Therefore, the additional options are:

a) treating the sample as it is collected

b) treating the sample after artificial enrichment.

The range of choices is extra broad by the combination of 1), 2), or 3) with either a) or b). The choices to be made will be discussed in Chapter 11. Here we will restrict ourselves to the different chemical/physical procedures.

The LSS technique is being applied to water itself. The sample then has to be mixed with a proper scintillation liquid (Chapter 11). PGC requires a suitable gas, as the stable isotopic analyses.

10.2.3.1 WATER PURIFICATION

Often the water collected contains too many contaminants to allow direct LSS measurement as well as electrolytic enrichment. Especially coloured contaminants hamper a proper liquid scintillation performance. *Purification* of water is carried out by *distillation*. As a matter of fact, most laboratories routinely subject all water samples to distillation. The requirement is that no isotopic change occurs during this treatment. Therefore, the distillation procedure has to be as quantitative as possible, i.e. a yield close to 90%. Also the water sample should hardly be in contact with the ambient air, of which the vapour content may affect the ^{3}H content of the sample through exchange, which is an extremely fast process.

10.2.3.2 ^{3}H ENRICHMENT

Two methods exist for the artificial enrichment of ^{3}H in water:

1) Electrolysis of the water sample

2) Thermal diffusion of H_2 prepared by reduction of water using, for instance, zinc or magnesium. By this method very high enrichment factors can be obtained, but the equipment and sample handling is complicated. It is not in use in common laboratories. The principle of thermal diffusion is that, when a gas mixture is in contact with a cold wall as well as a hot wall, the high-mass (isotopically heavy) component tends to concentrate in the cold and the low-mass (isotopically light) component in the hot region. If this principle is applied to a vertical, double-wall tube structure in which the inner tube is heated and the outer wall is cooled, the heavy component concentrates at the cold wall and then, having a higher density (at low temperature) moves downward and concentrates at the lower end of the tubes. The hot and light component concentrates at the top volume. Consequently, a separation of the (isotopically) heavy and light molecules, in this case $^3H^1H$ and $^1H_2$ respectively, is obtained.

The first method is relatively simple, requires little sample handling and supervision during enrichment, and can be applied simultaneously to a series of samples including reference samples.

During electrolysis the purified sample (sect.10.2.3.1) is provided with Na_2O or ^{3}H-free NaOH to increase the electrical conductivity and subsequently decomposed by an electric current:

$$2H_2O \rightarrow 2H_2 + O_2$$

The hydrogen isotope fractionation is remarkably large (contrary to the oxygen isotope fractionation): about 90% of the ^{3}H content of the original water sample remains in the water (the escaping H_2 gas is very much depleted in ^{3}H). This means that, if a quantity of water is condensated by a factor of 10, the enrichment is about 9.

After electrolysis the enriched sample, now containing a large concentration of NaOH, is again to be distilled to remove the concentrated electrolyte prior to activity measurement.

Depending on the measurement technique to be applied, an amount of water is needed of 5 to 20 mL. If the sample is to be enriched, the desired quantity is 250 mL (see Table 10.2).

10.2.3.3 PREPARATION OF GAS FOR PGC OF ^{3}H

For proportional gas counting (Sect.11.3.1) of ^{3}H a few gases are suitable:

1) **hydrogen**, prepared by

$$H_2O + Zn \text{ or } Mg \rightarrow ZnO + H_2$$

the hydrogen gas prepared has to be mixed with a proper counting gas such as argon

2) **ethane or propane**, prepared by the addition of hydrogen made as under 1) to unsaturated hydrocarbon:

$$C_2H_4 + H_2 \rightarrow C_2H_6 \quad \text{(with Pd catalyst)}$$

$$C_3H_6 + H_2 \rightarrow C_3H_8 \quad \text{(with Pd catalyst)}$$

which are suitable counting gases as such.

The additive reactions given under 2) expire at elevated temperatures in the presence of a suitable catalyst.

10.2.4 THE ^{14}C ANALYSIS OF DISSOLVED INORGANIC CARBON

10.2.4.1 IN THE FIELD

In natural waters the inorganic carbon content plays an important role. As we have seen in preceding chapters, the total *dissolved inorganic carbon* (DIC) consists of varying concentrations of carbonic acid (H_2CO_3 or rather dissolved CO_2), dissolved bicarbonate (HCO_3^-), and dissolved carbonate (CO_3^{2-}). There are two methods in use for obtaining the DIC fraction in water for measuring the ^{14}C content or the $^{13}C/^{12}C$ ratio. Both, however, collect the total amount of DIC (for unravelling the separate $^{13}\delta$ values of the components we have to use the procedures discussed in Chapter 9):

1) addition of acid and extracting the gaseous CO_2 formed:

$$aCO_2(aq) + bHCO_3^- + cCO_3^{2-} + (b + 2c)H^+ \rightarrow (a + b + c)CO_2 + ...H_2O$$

Special, simple to operate, equipment takes care that the escaping CO_2 is dissolved in a small amount of alkaline solution in a plastic bottle and shipped to the laboratory.

2) precipitating DIC as $BaCO_3$ after adding NaOH solution:

$$aCO_2(aq) + bHCO_3^- + cCO_3^{2-} + (2a + b)OH^- \rightarrow (a + b + c)CO_3^{2-} + ...H_2O$$

$$(a + b + c)CO_3^{2-} + BaCl_2 \rightarrow (a + b + c)BaCO_3 + ...Cl^-$$

Also here the equipment (provided by the laboratory) is simple: the precipitate is collected in a small plastic bottle and shipped to the laboratory.

Both procedures are to be carried out in the field, to avoid having to transport a large quantity of water to the laboratory. Depending on the DIC content of the water, for the conventional ^{14}C analysis between 25 and 50 L is required. With the introduction of the AMS technique this problem no longer exists, as for this method only a few mg of carbon is needed. The same is valid for $^{13}C/^{12}C$ analysis. This means that a quantity of 250 mL of water is generally sufficient for both carbon analyses. Additionally, no treatment is required in the field. The ^{13}C sample, however, needs careful storage (sect.10.1.4).

10.2.4.2 IN THE LABORATORY

In principle the procedures for treating the various samples received from collection in the field are analogous: treatment with acid (generally HCl solution) and purification of the escaping CO_2. Subsequently different methods are to be applied, depending on the ^{14}C measurement technique, in chronological order of first application:

1) **activity measurement** in a *proportional gas counter* (PGC) as CO_2, C_2H_2, C_2H_6, or CH_4

   a) if CO_2 is used in the gas counter directly, it has to be extremely pure; this purification is the main effort of the sample treatment by the laboratory

   b) preparing acetylene from CO_2 is performed in 2 steps:

   $2CO_2 + 9Li \rightarrow 4Li_2O + Li_2C_2$ (700 °C)

   $Li_2C_2 + 4LiO_2 + 6H_2O \rightarrow 4Li(OH) + C_2H_2$

   c) preparing ethane from the acetylene prepared as under b)

   $C_2H_2 + 2H_2 \rightarrow C_2H_6$ (with Pd catalyst)

   d) preparing methane from CO_2:

   $CO_2 + 4H_2 \rightarrow 2H_2O + CH_4$ (300 °C + Ru catalyst)

2) **activity measurement** in a *liquid scintillation spectrometer* (LSS) as C_6H_6

   the acetylene gas prepared under 1b) can be condensed to benzene:

   $3C_2H_2 \rightarrow C_6H_6$ (with catalyst)

   the thus formed benzene is to be mixed with a proper scintillation fluid (Chapt.10).

3) **concentration measurement** in an *accelerator mass spectrometer* (AMS) as graphite or CO_2; in the presence of iron catalyst, CO_2 is reduced to graphite:

   $CO_2 + 2H_2 \rightarrow 2H_2O + C$ (at 600 °C with Fe)

   the graphite is directly transferred to the accelerator target (see Chapter 10).

10.2.5 THE $^{13}C/^{12}C$ ANALYSIS OF DISSOLVED INORGANIC CARBON

This procedure has been discussed in sect.10.2.4.2, as it is similar –and in fact it runs parallel- to the ^{14}C procedure. The CO_2 extraction can be carried out by acidifying the water sample and collecting the evading CO_2 during vacuum pumping. The sample can also be flushed with a clean gas, such as nitrogen or argon, and the evading CO_2 likewise condensed in a cold trap.

One concern with these samples is that the water is likely to exchange with the atmosphere, if it is not completely sealed of. $^{13}C/^{12}C$ then changes to ultimately isotopic equilibrium with atmospheric CO_2. Parallel the pH of the water changes to higher values. The sample should therefore be stored in a glass bottle and sealed properly.

The second concern is the ingrowth of organic matter in the water sample. As this has a $^{13}\delta$ value much smaller that the DIC, the latter will increase. In order to avoid this process, the sample is to be stored at low temperature in the dark, preferably after poisoning (sect.10.1.4).

11 MEASURING TECHNIQUES

The aim of this chapter is to give some insight in the various existing techniques for measuring isotope ratios and radioactivities. The potential readers are the hydrologists which apply the isotope techniques and their students assisting in the laboratory on the one hand, and starting laboratory technicians receiving a first glance of their future work, on the other. The review is general in this respect, that it covers the methodological field, although laboratories often do not have all techniques at their disposal. Technical details vary among laboratories and manufacturers. Therefore, we restrict ourselves to the underlying principles.

11.1 MASS SPECTROMETRY FOR STABLE ISOTOPES

11.1.1 PHYSICAL PRINCIPLE

A mass spectrometer is able to separate atoms or rather ions with different mass and measure their relative abundances. This principle is shown in Fig.11.1A where the gas containing different isotopes of an element (^{12}C and ^{13}C in CO_2, for instance) is ionised in the ion source. The positive ions are accelerated by high voltage and subsequently enter a magnetic field perpendicular to the electric field (in fig.11.1A drawn in the surface of this paper). The path of the ions now becomes circular because of the Lorentz force (Fig.11.1B). The circle radius depends on the ion mass: the ions with heavier masses follow the larger circle. In this way the different isotopic ions become separated and can be collected. In these collectors the ions loose their electric charge, causing small electric currents that can be measured (Fig.11.2).

The magnitude of the Lorentz force F is:

$$\vec{F} = \vec{B} \times q\,\vec{v} \qquad \textbf{(11.1)}$$

This force is equal to the centripetal force required for keeping the particle in the circular path:

$$F = \frac{mv^2}{r} = Bqv \qquad \textbf{(11.2)}$$

The velocity of the particle is due to acceleration by the high voltage in the ion source (Fig.11.1B):

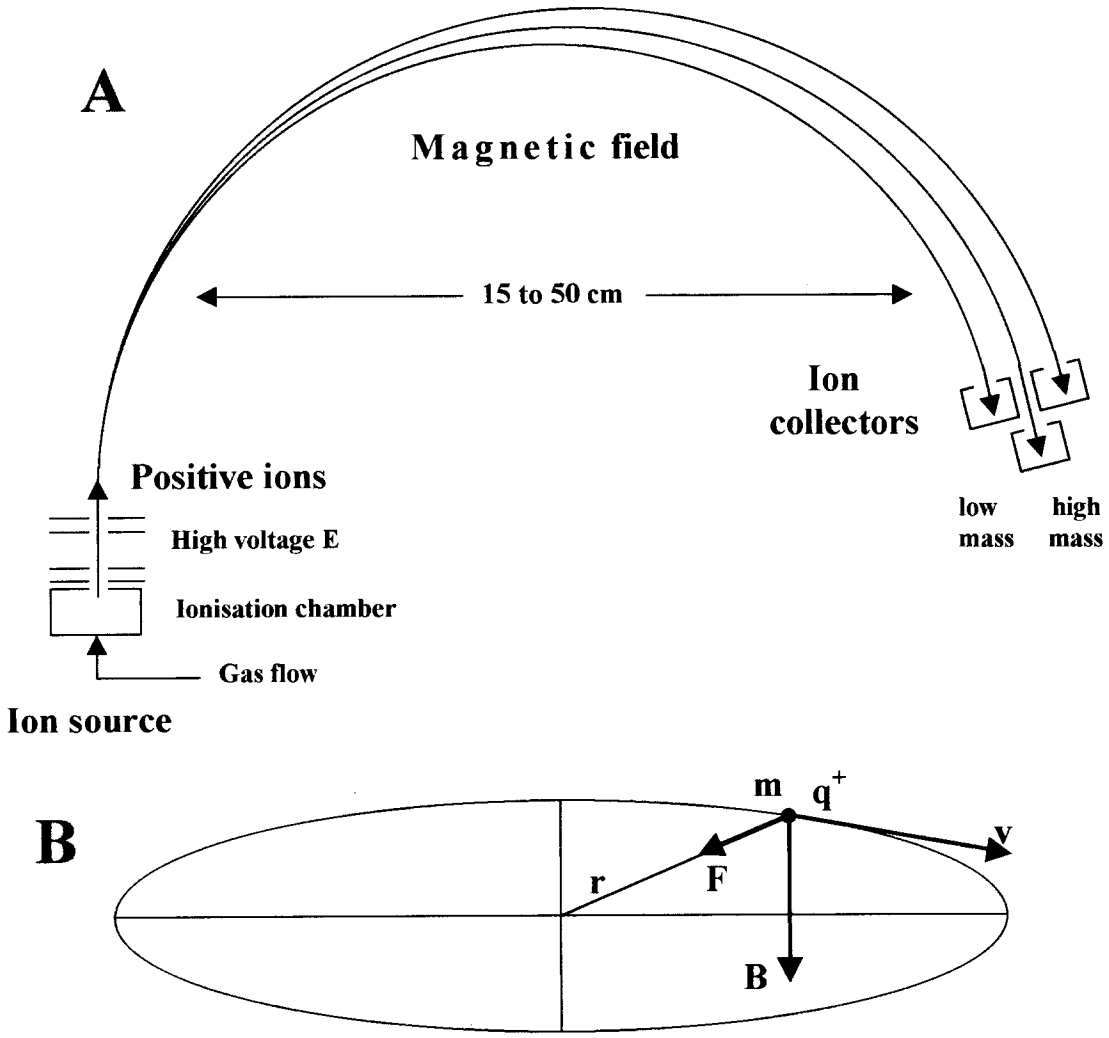

Fig.11.1 Schematic view of mass separation in a mass spectrometer.

A. The gas containing isotopic molecules enters the ion source and is ionised by electron bombardment. The positive ions are extracted from the ionisation chamber and accelerated in the ion source by a high voltage E. In a magnetic field perpendicular to the surface of this paper the isotopically light and heavy ions are separated and collected by collectors. This results in electrical currents that can be measured very precisely.

B. Representation of the Lorentz force: a charged particle with positive electric charge q+ and mass m moves in a flat surface with a speed v in a magnetic field B perpendicular to that surface; the resulting Lorentz force F is perpendicular to B and v and causes the particle to follow a circular path with radius r.

$$E_{kin} = \frac{1}{2}mv^2 = qV \qquad \textbf{(11.3)}$$

From Eq.11.2 and 11.3 follows the radius of the circular path of the different isotopic ions:

$$r = \frac{1}{B}\sqrt{\frac{2mV}{q}} = \left(\frac{\sqrt{2V/q}}{B}\right)\sqrt{m} \qquad \textbf{(11.4)}$$

where q is equal to the electron charge = 1.6 x 10^{-19}C and B and V depend on the instrument settings. During a measurement the electric voltage and the magnetic field are kept constant, so that the radius is proportional to the square root of the ion mass: r (:) $\sqrt{m}$. Differentiation (dr/dm leading to the approximation $\Delta r/\Delta m$) results in:

$$\frac{\Delta r / r}{\Delta m / m} = \left(\frac{\sqrt{2V/q}}{B}\right) \text{ and } m/\Delta m = \left(\frac{\sqrt{2V/q}}{B}\right) r/\Delta r \qquad \textbf{(11.5)}$$

The latter is a measure of the resolution of the mass spectrometer: for Δm = 1, m is the resolution of the instrument if Δr is large enough to allow a clear distinction between the peaks for masses m and m+1 in the mass spectrum.

Isotope Ratio Mass Spectrometers (IRMS) have typically low resolution (in the order of 100), contrary to the "organic" mass spectrometers with resolutions of more than 10^4. The latter, on the other hand, have much lower sensitivity and are therefore not suitable for isotope ratio measurements.

11.2 REPORTING STABLE ISOTOPE ABUNDANCE RATIOS

The ion beams consisting of positive ions of the various isotopic molecules in the gas are focussed in the collectors. Here the electric charge is transferred to the metal collectors, resulting in electric currents (I) in the collector connections (Fig.11.2). From the ratios of these currents the isotopic ratios of the original gases can be determined. Each current is proportional (coefficients c) to the partial pressure of the respective component in the gas.

$$I_2 = c_2[^1H_2^+] \qquad I_{44} = c_{44}[^{12}C^{16}O_2^+]$$

$$I_3 = c_3[^2H^1H^+ + {}^1H_3^+] \qquad I_{45} = c_{45}[^{13}C^{16}O_2^+ + {}^{12}C^{17}O^{16}O^+] \qquad \textbf{(11.6)}$$

$$I_{46} = c_{46}[^{12}C^{18}O^{16}O^+ + {}^{13}C^{17}O^{16}O^+ + {}^{12}C^{17}O_2^+]$$

The isotopic compositions can now be calculated. We restrict ourselves to discussing hydrogen and carbon dioxide, being representative for 2- and 3-atomic gases.

11.2.1 MEASUREMENT OF $^2H/^1H$ IN H_2

The case of hydrogen is complicated by the fact that in the ion source H_2 gas combines with a hydrogen ion to form $^1H_3^+$ which also has mass <3>. The necessary correction is obtained from an extrapolation procedure to ion source gas pressure equal zero where $^1H_3^+$ disappears.

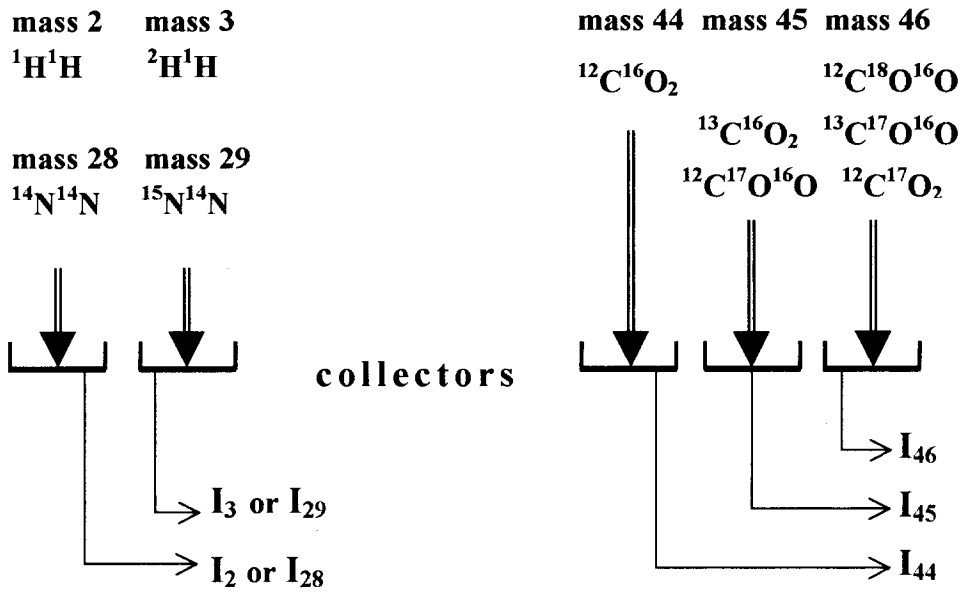

Fig.11.2 The various isotopic ions of hydrogen and carbon dioxide, respectively, are focussed in the collectors (Faraday cups). These collect the electric charges (electrons are picked up by the positive ions) resulting in electric currents for the various isotopic molecules. From the ratios of these the isotopic ratios of H_2 or N_2 (left) and CO_2 (right) can be deduced.

The constants c_2 and c_3 contains the proportionality factors for the ionisation probabilities, the transmission and collection efficiencies of the molecules with masses <2> and <3>. Because these factors are unequal unity, the isotope ratios obtained from the current ratios have to be compared to those of a common (internationally adopted (see Chapter 7)) standard:

$$\frac{(I_3/I_2)_{\text{sample gas}}}{(I_3/I_2)_{\text{reference gas}}} = \frac{(c_3/c_2)\left([^2H^1H + {}^1H_3^+]/[^1H_2]\right)_{\text{sample gas}}}{(c_3/c_2)\left([^2H^1H + {}^1H_3^+]/[^1H_2]\right)_{\text{reference gas}}} \qquad \textbf{(11.7)}$$

After correction for the H_3^+ contribution and inserting the isotopic ratios, the $^2\delta$ value becomes:

$$^2\delta = \frac{(^2H/^1H)_{\text{sample}}}{(^2H/^1H)_{\text{reference}}} - 1 = \frac{(I_3/I_2)^0{}_{\text{sample}}}{(I_3/I_2)^0{}_{\text{reference}}} - 1 \qquad \textbf{(11.8)}$$

where the superscript ^{0} refers to the correction procedure for the H_3^+ contribution to mass <3> ions. Absolute values for the standards (reference samples) are given in Table 11.2.

11.2.2 MEASUREMENT OF $^{15}N/^{14}N$ IN N_2

The mass spectrometric analysis of N_2 for obtaining $^{15}N/^{14}N$ in nitrogen containing materials is equally simple, even more so, since in that case we have not the pressure effect in the ion source that resulted in the formation of $^1H_3^+$ with hydrogen. The measured ion beam ratios are simply translated into isotope ratios:

$$\frac{(I_{29}/I_{28})_{sample}}{(I_{29}/I_{28})_{reference}} = \frac{c_{29}/c_{28}([^{15}N^{14}N]/[^{14}N_2])_{sample}}{c_{29}/c_{28}([^{15}N^{14}N]/[^{14}N_2])_{reference}} =$$

$$= \frac{(^{15}N/^{14}N)_{sample}}{(^{15}N/^{14}N)_{reference}} = {}^{15}\delta + 1 \qquad \textbf{(11.9)}$$

As reference or standard serves air N_2 which shows very little variation:

$$^{15}R(\text{standard air } N_2) = 0.0036765 \qquad \textbf{(11.10)}$$

The mass spectrometric precision obtained is about 0.02 ‰. However, the laboratory samples handling to prepare the N_2 gas as required for the IRMS measurement results in much larger uncertainties, because the chemistry involved is less straightforward.

For a check of the overall chemical and measurement procedures a set of reference materials is available. The values are shown in Table 11.1.

Table 11.1 Reference materials for $^{15}N/^{14}N$ analyses (IAEA, 1995; Böhlke and Coplen, 1995).

Reference sample name	Material	$^{15}\delta$ (‰) rel. to air N_2
IAEA-N1	$(NH_4)_2SO_4$	+ 0.43 ± 0.07
IAEA-N2	$(NH_4)_2SO_4$	+ 20.41 ± 0.12
IAEA-N3	KNO_3	+ 4.72 ± 0.13
USGS-25	$(NH_4)_2SO_4$	− 30.41 ± 0.27
USGS-26	$(NH_4)_2SO_4$	+ 53.75 ± 0.24
USGS-32	KNO_3	+ 180.00
NSVEC	N_2 gas	− 2.78 ± 0.04

11.2.3 MEASUREMENT OF $^{13}C/^{12}C$ AND $^{18}O/^{16}O$ IN CO_2

The measurement of the isotopic composition of CO_2 is complicated by the abundance of molecules with equal mass <45> and <46>, containing different isotopes (Fig.11.2).

From Eq.11.6 we can deduce the following relations for the isotopic ratios:

$$\frac{I_{45}}{I_{44}} = (c_{45}/c_{44})\frac{CO_2 \text{ with mass } 45}{CO_2 \text{ with mass } 44} = (c_{45}/c_{44})\,{}^{45}R^{m}$$

and **(11.11)**

$$\frac{I_{46}}{I_{44}} = (c_{46}/c_{44})\frac{CO_2 \text{ with mass } 46}{CO_2 \text{ with mass } 44} = (c_{46}/c_{44})\,{}^{46}R^{m}$$

The isotopic analysis of CO_2 now proceeds in 3 or 4 steps, described in the next sections.

11.2.3.1 COMPARISON WITH MACHINE REFERENCE

As with hydrogen, the ionisation and transmission efficiencies of the isotopic molecules and ions are not 100%, so that the values of the proportionality factors c in Eq.11.6 can not be replaced by 1. This necessitates comparison of the ion beam ratios with those of a reference.

Routinely laboratories use their own working reference gas (often referred to as the working standard or machine standard, which finally has to be calibrated against the international standard material). Eq.11.11 applies to the sample (s) and the working reference gas (w), we eliminate the efficiency factors c the mass <45> and mass <46> measurements for and other (generally proportional or multiplicative) instrumental errors:

$$\frac{(I_{45}/I_{44})_s}{(I_{45}/I_{44})_r} = \frac{{}^{45}R_S^m}{{}^{45}R_w^m}$$

and **(11.12)**

$$\frac{(I_{46}/I_{44})_s}{(I_{46}/I_{44})_r} = \frac{{}^{46}R_S^m}{{}^{46}R_w^m}$$

11.2.3.2 CALIBRATION

The true isotopic ratios of the working reference, ${}^{45}R_w{}^c$ and ${}^{46}R_w{}^c$, are known from a repeated comparison with the international standards, R_I, (such as VPDB or VSMOW). The values of the latter can be calculated from the ^{13}R, ^{17}R and ^{18}R values given in Table 11.2.

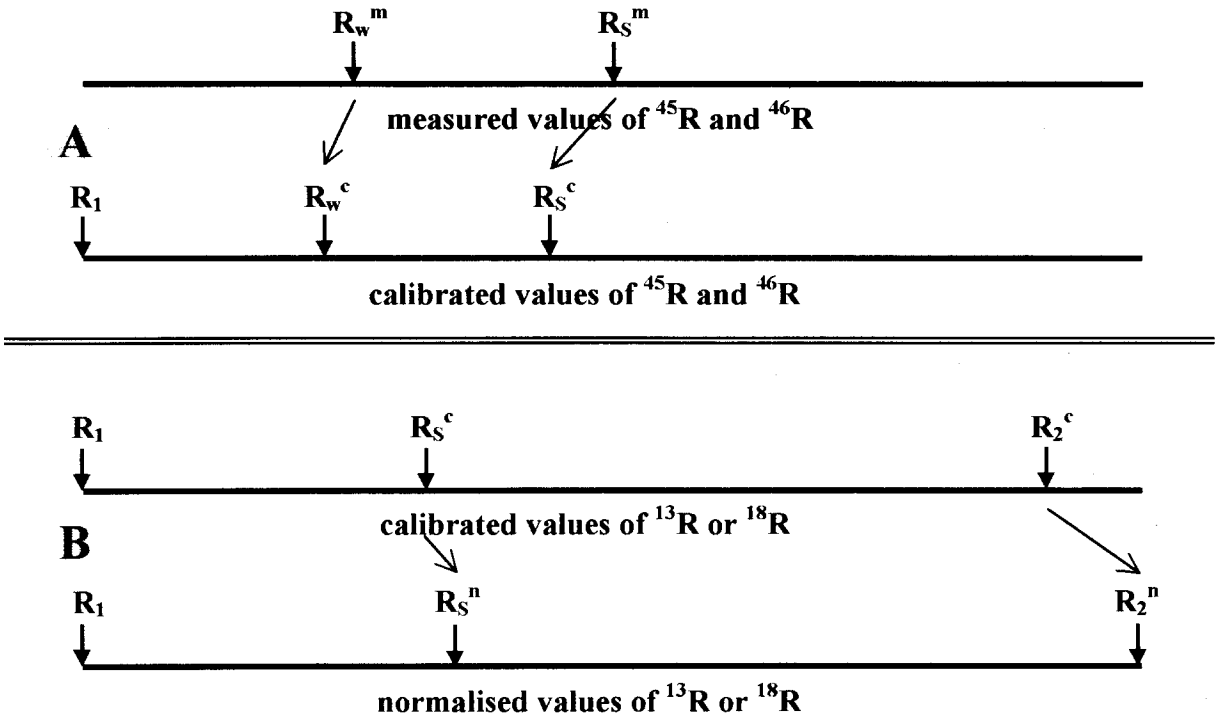

Fig.11.3 Schematic representation of procedures of calibration (**A**) and normalisation (**B**) of isotopic analyses.

A. The measured values of $^{45}R^m$ and $^{46}R^m$ are calibrated (i.e. adjusted to the international standards (R_1) such as VPDB and VSMOW) to give $^{45}R^c$ and $^{46}R^c$; R_w and R_S are corrected proportionally.

B. For normalisation the ^{13}R or ^{18}R scale is stretched in order to reach the established value for a second standard (R_2^n). The corrections to the R_2 and R_S values is again proportional.

^{45}R and ^{46}R calibrated to the proper values of the standards are obtained by a multiplicative correction:

$$\frac{R_S^c}{R_S^m} = \frac{R_w^c}{R_w^m} \qquad \text{or} \qquad {}^{45}R_S^c = \frac{{}^{45}R_w^c}{{}^{45}R_w^m}\,{}^{45}R_S^m$$

and **(11.13)**

$${}^{46}R_S^c = \frac{{}^{46}R_w^c}{{}^{46}R_w^m}\,{}^{46}R_S^m$$

The isotopic ratios, however still applying to the entire CO_2 molecule, are now calibrated.

11.2.3.3 ISOTOPIC CORRECTIONS

As is shown in Fig.11.2, the mass <45> and <46> ion beams contain different isotopic ions:

$$I_{44} = [^{12}C^{16}O^{16}O] \qquad I_{45} = [^{13}C^{16}O^{16}O] + [^{12}C^{17}O^{16}O]$$

$$I_{46} = [^{12}C^{18}O^{16}O] + [^{13}C^{17}O^{16}O] + [^{12}C^{17}O^{17}O]$$

This leads to the isotopic ratios:

$$^{45}R = \frac{I_{45}}{I_{44}} = \frac{[^{13}C^{16}O^{16}O] + [^{12}C^{17}O^{16}O]}{[^{12}C^{16}O^{16}O]} = {}^{13}R + 2\,{}^{17}R \qquad \textbf{(11.14)}$$

$$^{46}R = \frac{I_{46}}{I_{44}} = \frac{[^{12}C^{18}O^{16}O]+[^{13}C^{17}O^{16}O]+[^{12}C^{17}O^{17}O]}{[^{12}C^{16}O^{16}O]} = 2\,{}^{18}R + 2\,{}^{13}R\,{}^{17}R + {}^{17}R^2 \qquad \textbf{(11.15)}$$

In translating ^{45}R and ^{46}R into $^{13}C/^{12}C$, $^{17}O/^{16}O$ and $^{18}O/^{16}O$, we are thus dealing with 3 unknowns. On the other hand we can only determine 2 ratios, viz. ^{45}R and ^{46}R. The third given required is the theoretical relation between the ^{17}O and ^{18}O abundance in natural oxygen (Sect.3.6):

$$\frac{^{17}R_S}{^{17}R_r} = \sqrt{\frac{^{18}R_S}{^{18}R_r}} \qquad \textbf{(11.16)}$$

where s and r refer to a sample and the reference, respectively.

It is the easiest to use an iterative procedure to solve the above equations for sample and standard, starting from the measured and corrected values for ^{45}R and ^{46}R:

1) We apply the approximations $^{17}R = 0$ and thus $^{13}R = {}^{45}R$ (Eq.11.14)

2) With these we calculate ^{18}R from ^{46}R (Eq.11.15)

3) Now the ^{17}R values can be calculated (Eq.11.16)

4) Inserting these in Eq.11.14 results in new and better values for ^{13}R

5) This procedure is repeated until the ^{13}R, ^{17}R and ^{18}R do no longer change.

The values thus obtained for the isotope ratios of the sample $^{13}R_S{}^c$ and $^{18}R_S{}^c$ are automatically adjusted on the VPDB or VSMOW scales for ^{13}C and ^{18}O. The δ values of the sample relative to the international standard can now easily be written as:

Table 11.2 Absolute isotope ratios needed for the calculation procedure of calibrated and normalised isotope ratios. The ^{13}R values are based on the original value of ^{13}R for PDB by Nier (1950) as quoted by Craig (1957). The ^{18}R value are based on the absolute measurement of ^{18}R of VSMOW-water by Baertschi (1976) and known values for the fractionations as given in Fig.6.10. ^{17}R values are based on the absolute measurement by Li et al., 1988) and the square roots of the various ^{18}O fractionations. The values in the shaded box are now obsolete. ^{2}R values are the averages of the reported data.

Reference material	$^{13}R \times 10^2$	$^{17}R \times 10^4$	$^{18}R \times 10^3$	$^{2}R \times 10^6$
PDB-CO_2	1.12372 [1])	3.800	2.0790	
SMOW-CO_2			2.0785	
VPDB-calcite	1.12372000	3.788666	2.0671607	
VPDB-CO_2	1.12372000	3.808033	2.0883491	
NBS19-calcite	1.12591025	3.784496	2.0626129	
NBS19-CO_2	1.12591025	3.803842	2.0837547	
VSMOW-water		3.790	2.0052 [2])	155.76 [3])
VSMOW-CO_2		3.867	2.0878142	
SMOW-CO_2			2.0879186	
SLAP-water		3.683	1.8939104	89.07 [3])
SLAP-CO_2		3.758	1.9719405	

[1]) Craig, 1957

[2]) Baertschi, 1976

[3]) Hageman et al., 1970; De Wit et al., 1980, reasonably well confirmed by Tse et al.(1980).

The values for $^{45}R_1$ and $^{46}R_1$ are obtained from:

$$^{45}R = {}^{13}R + 2{}^{17}R \qquad \textbf{(11.17a)}$$

$$^{46}R = 2{}^{18}R + 2{}^{13}R{}^{17}R + {}^{17}R^2 \qquad \textbf{(11.17b)}$$

$$^{13}\delta_{S/VPDB} = \frac{^{13}R_S^c}{^{13}R_{VPDB}} - 1 \quad \text{and} \quad ^{18}\delta_{S/VPDB} = \frac{^{18}R_S^c}{^{18}R_{VPDB}} - 1 \qquad \textbf{(11.18)}$$

$$^{18}\delta_{S/VSMOW} = \frac{^{18}R_S^c}{^{18}R_{VSMOW}} - 1$$

11.2.3.4 ^{18}O CORRECTION FOR WATER–CO_2 EQUILIBRATION

As was explained in Sect.10.2.1.1, we have to apply a correction for the ^{18}O content of the CO_2 brought in isotopic equilibrium with a water sample. This correction has to be applied at this stage of the calculation procedure. The corrected value for the equilibrated CO_2 is (cf. Sect.4.3.2):

$$^{18}R_c' = {}^{18}\alpha_{c/w}\ {}^{18}R_{w0} = (1 + {}^{18}\alpha_{c/w}\ \rho)\ {}^{18}R_c - {}^{18}\alpha_{c/w}\ \rho\ {}^{18}R_{c0} \qquad \textbf{(11.19)}$$

or as δ values:

$$^{18}\delta_c' = (1 + {}^{18}\alpha_{c/w}\ \rho)\ {}^{18}\delta_c - {}^{18}\alpha_{c/w}\ \rho\ {}^{18}\delta_{c0} \qquad \textbf{(11.20)}$$

11.2.3.5 NORMALISATION

Laboratory intercomparisons have shown a considerable spread in isotopic results from different laboratories on the same materials. It also has been shown that this spread can be reduced by applying two standards instead of one. The R and δ values may in certain circumstances be corrected for the fact that the ratio (for R) or distance (for δ) as measured between R_1 and the second standard R_2 deviates from the true (established) value.

In this procedure of *normalisation* the R or δ scale is so-to-speak stretched proportionally to reach the established ratio or distance for R and δ. This procedure of inter- or extrapolation is represented by Fig.11.3B and is mathematically written as:

$$\frac{R_S^n}{R_S^c} = \frac{R_2^n}{R_2^c} \qquad \textbf{(11.21)}$$

Related to the international standard and written as δ values, the final calibrated as well as normalised isotopic composition of the sample is:

$$\frac{R_S^n}{R_1} = (1+\delta_{S/1}^n) = \frac{R_2^n}{R_2^c}\frac{R_w^c}{R_1}\frac{R_S^m}{R_w^m} = \frac{R_2^n}{R_2^c}(1+\delta_{w/1})(1+\delta_{S/w}^m) \qquad \textbf{(11.22)}$$

The normalisation procedure is often being applied to the ^{18}O and ^{2}H analyses of water, as here two standards relatively wide apart on the VSMOW scale are available. The R_1 and R_2 values are the $^{18}O/^{16}O$ or the $^{2}H/^{1}H$ values of VSMOW and SLAP (Standard Light Antarctic Precipitation) as given in the above table. Normalisation can also be written entirely in terms of δ values and is then approximated by

$$\frac{\delta_{S/VSMOW}^n}{\delta_{SLAP/VSMOW}^n} = \frac{\delta_{S/VSMOW}^m}{\delta_{SLAP/VSMOW}^m} \qquad \textbf{(11.23)}$$

Table 11.3 δ values of isotopic standards, and reference and intercalibration samples measured on CO_2 prepared by (i) combustion of organic compounds, (ii) equilibration of CO_2 with water at 25 °C, or (iii) decomposition of carbonates with orthophosphoric acid (95%). $^{13}\delta$ values are relative to PDB or VPDB, $^{18}\delta$ of CO_2 to VPDB-CO_2, $^{18}\delta$ and $^{2}\delta$ refer to SMOW or VSMOW. Certain reference samples are now obsolete and only quoted for historical interest (data from IAEA, 1995).

Reference	Material	$^{13}\delta$ (‰)	$^{18}\delta$ (‰)	$^{2}\delta$ (‰)	Distributed by
NBS1	water	—	− 7.94	—	exhausted
NBS1A	water	—	−24.33	—	exhausted
NBS16	CO_2	−41.60	−35.98	—	exhausted
NBS17	CO_2	− 4.51	−18.61	—	exhausted
NBS18	carbonatite	− 5.03	−23.00	—	NIST/ IAEA
NBS19	marble	+ 1.95	− 2.20	—	NIST/ IAEA
NBS20	limestone	− 1.06	− 4.14	—	not distributed
NBS21	graphite	−28.16	—	—	exhausted
NBS22	oil	−29.74	—	—	NIST
VSMOW	water	—	0.00	0.00	NIST/IAEA
GISP	water	—	−24.79	−189.7	NIST/IAEA
SLAP	water	—	−55.50	−428.0	NIST/IAEA
IAEA-CO1	marble	+ 2.48	− 2.44	—	NIST/IAEA
IAEA-CO8	calcite	− 5.75	−22.67	—	NIST/IAEA
IAEA-CO9	$BaCO_3$	−47.12	−15.28	—	NIST/IAEA
LSVEC	Li_2CO_3	−46.48	−26.46	—	NIST/IAEA
IAEA-C6	sucrose	−10.43	—	—	IAEA
IAEA-CH7	poly-ethylene	−31.83	—	−100.3	IAEA
USGS-24	graphite	−15.99	—	—	NIST
GS19	CO_2	− 7.50	− 0.19	—	CIO
GS20	CO_2	− 8.62	− 0.99	—	CIO

NIST = National Institute of Standards and Technology, Atmospheric Chemistry Group, B364, Building 222, Gaithersburg, MD 20899, United States of America

IAEA = International Atomic Energy Agency, Analytical Quality Control Services, Agency's Laboratory, Seibersdorf, P.O.Box 100, A-1400 Vienna, Austria, fax +43-1-2060-28222

CIO = Centre for Isotope Research, Nijenborgh 4, 9747 AG Groningen, the Netherlands, tel. +31-50-3634760, fax +31-50-3634738

using the δ^n values:

$$^2\delta_{SLAP/VSMOW} = -428.0\ ‰ \quad \text{or} \quad ^2R_{SLAP} = 0.5720\ ^2R_{SMOW}$$

and

$$^{18}\delta_{SLAP/VSMOW} = -55.50\ ‰ \quad \text{or} \quad ^{18}R_{SLAP} = 0.9445\ ^{18}R_{SMOW}$$

Table 11.3 contains the δ values of the isotopic standards and the available reference intercomparison samples.

11.2.4 MEASUREMENT OF $^{18}O/^{16}O$ AND $^{17}O/^{16}$ IN O_2

This analysis includes, as with CO_2, two measurements, i.e. of the ion beam ratios for masses <34>/<32> and <33./<32>, while the number of unknowns is also two: $^{18}O/^{16}O$ and $^{17}O/^{16}O$. Thus, contrary to CO_2, no assumption has to be made for the relation between the ^{18}O and ^{17}O fractionations. More than that, from these measurements the relation between the two fractionations can be derived.

To calculate the isotope ratios from the measured (superscript m) ion beam ratios a similar procedure is chosen as previously:

$$^{34}R^m = \frac{I_{34}}{I_{32}} = (c_{34}/c_{32})\frac{[^{18}O^{16}O]+[^{17}O_2]}{[^{16}O_2]} = (c_{34}/c_{32})(2\,^{18}R + {}^{17}R^2)$$

and **(11.24)**

$$^{33}R^m = \frac{I_{33}}{I_{32}} = (c_{33}/c_{32})\frac{[^{17}O^{16}O]}{[^{16}O_2]} = (c_{33}/c_{32})(2\,^{17}R)$$

After correction for instrumental errors (specific and probably time-dependent for each instrument), the corresponding δ values are:

$$^{34}\delta = \frac{^{34}R^m_{sample}}{^{34}R^m_{reference}} - 1 = \frac{^{34}R_s}{^{34}R_r} - 1 = \frac{2\,^{18}R_s + {}^{17}R_s^2}{2\,^{18}R + {}^{17}R_r^2} - 1$$

and **(11.25)**

$$^{33}\delta = \frac{^{33}R^m_{sample}}{^{33}R^m_{reference}} - 1 = \frac{^{33}R_s}{^{33}R_r} - 1 = \frac{2\,^{17}R_s}{2\,^{17}R_r} - 1 = \frac{^{17}R_s}{^{17}R_r} - 1$$

Because the $^{17}R_r$ and $^{18}R_r$ values for the reference samples or standards are known, $^{17}R_s$ and $^{18}R_s$, and thus the $^{17}\delta$ and $^{18}\delta$ values can be easily calculated.

11.3 RADIOMETRY FOR RADIOACTIVE ISOTOPES

For measuring radioactivity a number of instruments are available, each with their specific advantages and disadvantages. The main instruments we will discuss are (i) gas counters and (ii) liquid scintillation spectrometers.

With both techniques the radioactive sample is measured as an *internal source*, i.e. it is mixed with, or is an intrinsic part of the counting medium, responsible for the operation of the instrument. This has the following advantages:

1) The β particles from the radioactive decay do not need to penetrate the wall of the instrument; this is especially relevant to detecting β^- particles from ^3H and ^{14}C decay as in both cases the β energy is very small

2) The counting efficiency is nearly 100%, the detection angle is 4π.

11.3.1 GAS COUNTERS

Although the operation of the various gas counter types is different, the basic construction is the same. The principle is shown in Fig.11.4.

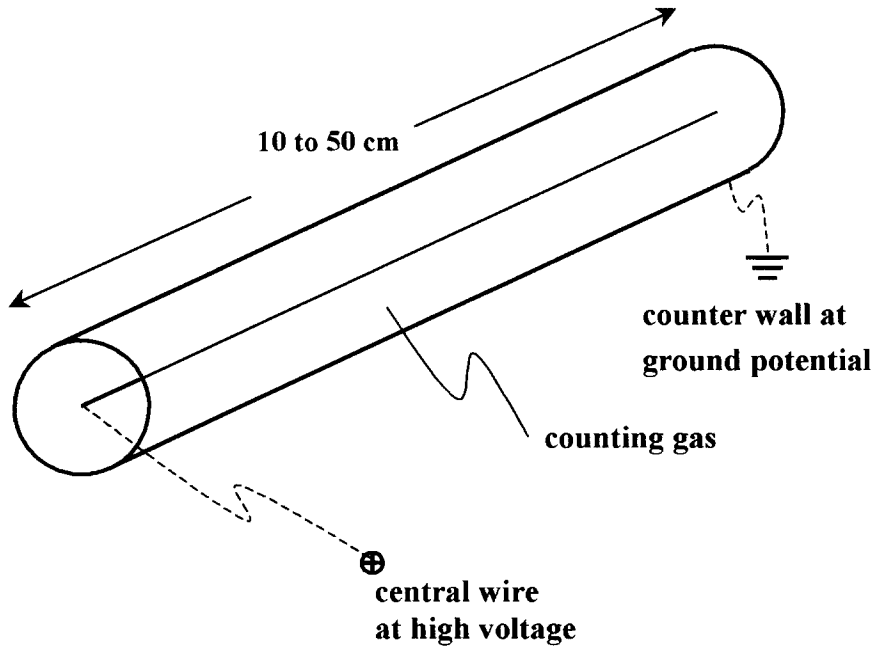

Fig.11.4 Cross section of a gas-filled counter tube for detection of radioactive radiation. The ionisation phenomena in the counter are shown in the cross-section of Fig.11.5.

Basically there are 3 different types of gas counters, depending on the magnitude of the high-voltage applied between the wire and the counter wall:

1) the ionisation chamber

2) the proportional counter

3) the Geiger-Müller counter.

The counters are filled with a counter gas, required to have suitable ionisation characteristics.

11.3.1.1 IONISATION CHAMBER

The incoming radiation, that is, a particle originating from a decay reaction inside or outside the counter tube, looses its energy by collisions with gas molecules in the counter. These events cause the molecules to become ionised. In the electric field inside the tube, the heavy positive ions slowly move towards the wall and become neutral by picking up electrons. The small, negative *primary electrons* set free by the collision become accelerated towards the positive central wire. After being collected by the wire, these electrons are observed as a small electric current or an electric pulse in the wire. In the electronic circuitry, attached to the counter, this pulse is registered and the pulse size measured. This is representative for the number of primary electrons and thus of the energy of the incoming particle. In this way information is obtained about the radioactive decay event.

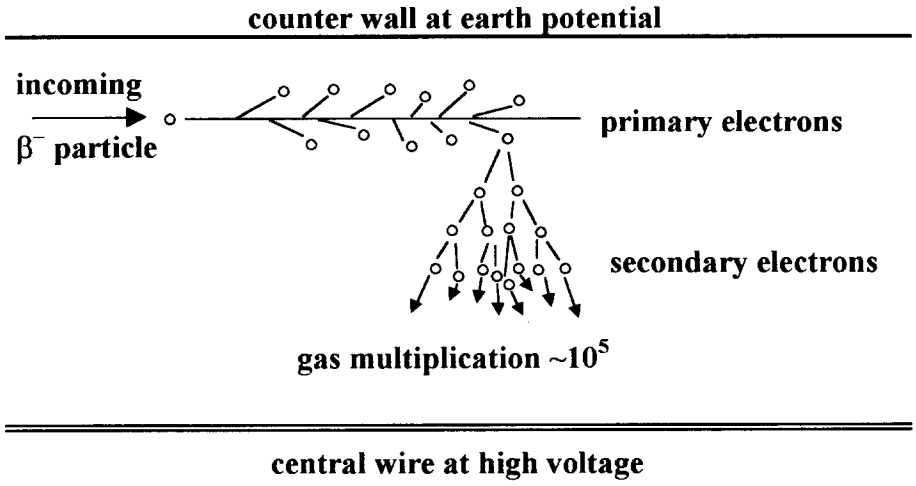

Fig.11.5 Lateral cross section through a gas counter. An incoming β^- particle looses its energy through primary ionisation. At low voltage only these electrons reach the wire resulting in a small electric pulse (ionisation chamber). If the voltage is sufficiently high, the number of primary electrons can be multiplied by a factor of 10^5 (PGC). At very high voltage the secondary ionisation is maximal and the electron avalanche occupies the entire length of the counter: the pulse height is no longer depending on the incoming particle energy or the voltage (GM counter).

11.3.1.2 PROPORTIONAL COUNTER

The primary electrons are accelerated in the electric field between the wire and counter wall. If the voltage on the counter wire is sufficiently high, the primary electrons, accelerated towards the wire, obtain enough velocity and energy to ionise other gas molecules and so create more free electrons. The same is true for these new electrons and so on and so forth. In this way an avalanche of electrons is created moving towards and collected by the wire (Fig.11.5). This phenomenon is called *gas multiplication*. The resulting electric pulse is proportional to this gas multiplication (and thus depending on the high voltage) and is still **proportional to the number of primary electrons and thus to the original energy of the incoming particle** (Proportional Gas Counter, PGC).

11.3.1.3 GEIGER MÜLLER COUNTER

During operation as a proportional counter the secondary electron avalanche is very local. At very high voltage, however, the secondary ionisation process extends over the entire length of the counter tube. The pulse size is maximal and no longer depends on the energy of the incoming particle or the wire voltage: in the GM counter the existence of the particle is registered, but it can not be recognised, as in the case of the proportional counter. This is, however, essential in order to be able to distinguish the particle (for instance, a β^- particle from ^3H or ^{14}C) from strange particles.

Our conclusion, therefore, has to be that the only suitable gas counter for our purpose is the one which operates as a proportional counter. This equipment was the first established for measuring the radioactivities of ^3H and ^{14}C. These atoms have to be brought in a gaseous form suitable for operation in a counter as sample as well as counting gas. This is essential because the β radiation can not penetrate the counter wall, the β energies being extremely low (Fig.8.2). Later another technique came into use, i.e. the liquid scintillation spectrometer.

11.3.1.4 COUNTER OPERATION

At both ends of the proportional gas counter (PGC) the geometry is distorted and thus the electric field. The detection of particles from radioactive decay is, therefore, less efficient. The consequence is that the overall *counter efficiency* is not exactly known: routinely an absolute measurement is not feasible. The solution to this problem is to perform a relative measurement: the sample is to be measured under exactly the same conditions as a reference sample, or, finally, as an international standard (Sect.8.1.2), or the dependence of the detected radioactivity of a sample on the various parameters has to be exactly known. Without going into detail, we mention the essential parameters (Mook and Streurman, 1985).

The amount of gas in the counter; since sample and reference are being measured in the same counter, the counter volume (V) is not relevant, so that measuring the pressure (p) and temperature (T) is sufficient: the amount of gas = V.p/T with T = t + 273.15 K.

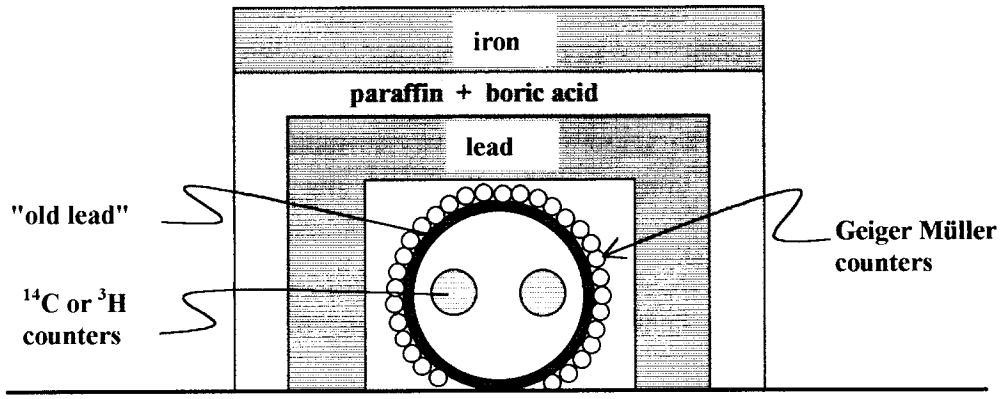

Fig.11.6 Cross section of a typical counter set-up with shielding against radiation from the surroundings, including cosmic radiation. The GM counters operate in "anti-coincidence" with the proportional counters in the middle. The low-mass hydrogen atoms in paraffin are very efficient in reducing the (penetrating) energy (speed) of high-energy neutrons. Boron has a high absorbing capacity for low-energy neutrons. The high-mass lead absorbs γ radiation. "Old lead" has lost the radioactive lead isotope ^{210}Pb (RaD), due to its short half-life (22 a).

The purity of the counting gas; if the gas contains electronegative impurities, i.e. gas molecules with a strong attraction to electrons, part of the primary and secondary electrons are lost, decreasing the pulse size and the counting rate (Brenninkmeijer and Mook, 1979).

The background of the counter, i.e. the counting rate (number of counts per sec.) of the counter without a radioactive source, in our case CO_2 and C_2H_2 or H_2 without ^{14}C or ^{3}H, respectively. This background has to be subtracted from the overall counting rate. In order to minimise the background –which would otherwise be orders of magnitude larger than the actual (net) counting rate we are interested in- the counter is made of low-activity materials and shielded against radiation of the surroundings (see Fig.11.6).

Most counters are made of copper or quartz with sizes ranging between 0.5 and a few litres, although also mini-counters exist. An international compilation was made by Mook (1983).

In principle, the data handling of radiometric equipment is simple. After a certain measuring time t_m a number of N_t disintegrations in the counter have been observed. The statistical uncertainty or *standard deviation* of this number is $\sqrt{N}$. This gross counting rate of N_t/t_m (counts per sec) has to be diminished by the background B (counts /s) to give the net counting rate A' (see Sect.13.3.3):

$$A'(t) = N_t/t_m - B \qquad \textbf{(11.26)}$$

This result has to be standardised, i.e. has to be corrected to a standard amount of sample gas in the counter, simply by applying the Law of Gay-Lussac, in other words by multiplying by the pressure and temperature ratios:

$$A(t) = \frac{T}{T_0}\frac{p_0}{p}A'(t) = \frac{273.15}{t+273.15}\frac{10^5}{p(\text{in Pa})} \qquad \textbf{(11.27)}$$

Now we have obtained the standardised absolute activity: ^3A for ^3H, ^{14}A for ^{14}C (Sect.8.1.2).

The internationally established standard (Oxalic Acid) has to be measured under exactly the same conditions. Then the activity ratio can be calculated as the ratio between these two activities (Eq.8.4).

The standard deviation in the measured activity is (standard in B is negligibly small):

$$\sigma_A \approx \sigma_N = \frac{1}{t_m}\sqrt{\overline{N}} = \sqrt{\frac{\overline{A+B}}{t_m}} \qquad \textbf{(11.28)}$$

11.3.2 LIQUID SCINTILLATION SPECTROMETER

11.3.2.1 PHYSICAL PRINCIPLE

This method is based on the principle that certain materials emit light after their molecules have been excited by collisions with high-energy particles.

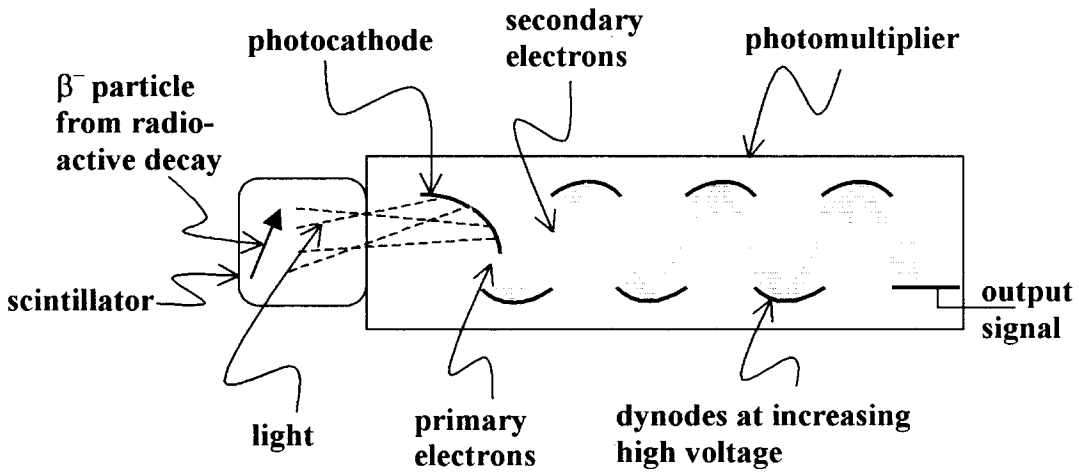

Fig.11.7 Schematic drawing of a (liquid) scintillation counter, the detector part of the LSS. An electron from β^- decay in the scintillating crystal or liquid causes a light flash that is "transformed" into electrons at the photocathode; the number of primary electrons is multiplied by secondary emitting dynodes at increasing high voltage.

This process, called *luminescence*, takes place in a proper solid or liquid. Our interest is focussed on the use of liquids, because there are methods to transfer carbon (including ^{14}C) to benzene which -with some precautions- is suitable as a *scintillator*, whereas water (with ^3H) can be mixed with a scintillating liquid, a commercially available *cocktail* of various

constituents. The requirement of this mixture is that it mixes well with water, transfers the primary electron energies into fluorescent energy, and finally into low-energy fluorescent light within the secondary-emission range of the photo-electrode of the photomultiplier.

In this way we again are dealing with internal radioactive sources, as with the gas counters. For higher-energy β and γ particles solid crystals are available made of organic (anthracene) or inorganic compounds (sodium iodide).

The result is that each incoming particle causes a light flash in the scintillator, which can be "seen" by a light sensitive detector, the *photocathode*. The fact is that certain materials emit electrons when they are hit by a light flash, the so-called *photoelectric effect*. The number of *primary electrons* is very small. Therefore, as with the proportional counter operation, a multiplication process is needed. This is realised in a *photomultiplier tube* (Fig.11.7). Each primary electron is accelerated and able to cause the emission of additional *secondary electrons* in the second electrode plate or *dynode* at a higher positive voltage. This process is repeated several times, so that finally an electric pulse arrives at the last dynode that is easily measurable. Also here the final pulse is proportional to the multiplication factor –a direct function of the voltage- and the energy of the incoming particle. This allows the selective registration of only those particles that originate from the radioactive decay event of interest (such as ^{14}C or ^{3}H).

11.3.2.2 COUNTER OPERATION

In Sect.11.2.4.2 we have mentioned the preparation of benzene from CO_2 via acetylene. Typical quantities being treated are 1 to 10 grams of carbon, resulting in 1.2 to 12 mL of benzene. The scintillation light emitted by excited C_6H_6 does not have the frequency for which the photocathode in the multiplier tube is sensitive. Therefore, certain high-molecular compounds are added in order to shift the frequencies to lower energies.

Generally a large number of samples is arranged in a liquid scintillation spectrometer or counter (LSS), in which the samples are in turn placed in front of the photomultiplier automatically. Also here arrangements have been made to reduce the background radiation as much as possible, primarily by using an anti-coincidence arrangement of other scintillation counters (instead of the use of GM counters with PGC).

The advantage of the LSS is that it can be purchased automated and purchased commercially, while a gas counter set-up has to be made by the laboratory. On the other hand, the operation of a PGC is more "transparent", from a physical point of view.

In principle the same type of calculations lead to the activity of the sample, as shown for the gas counters (Eqs.11.21 and 11.23). Related to the problem of gas purity with the gas counters, liquid scintillation may suffer from impurities in the benzene + scintillator mixture. This results in a decrease of the size of the electric output pulse. For this effect of *quenching* a correction is to be applied.

11.4 MASS SPECTROMETRY FOR LOW-ABUNDANCE ISOTOPES

11.4.1 PRINCIPLE AND APPLICATION OF AMS

Detecting the presence of isotopes with a very low abundance such as the radioactive isotopes, for instance ^{14}C in carbonaceous material, wood, charcoal, peat, bone, shells, groundwater, by detecting the radioactive decay is very inefficient. Of all ^{14}C present in a sample only one thousandth decays in about 8 years, i.e. 3.8×10^{-12} part per sec.

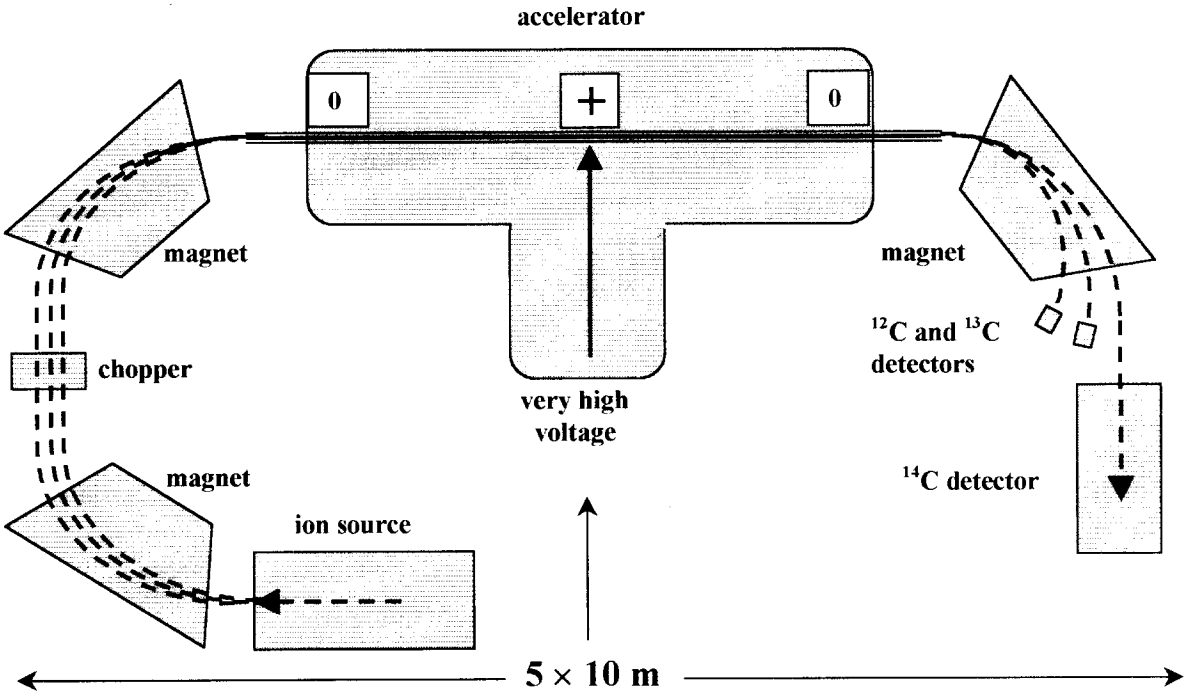

Fig.11.8 Schematic and simplified drawing of an Accelerator Mass Spectrometer (AMS) (Purser, 1992). The ion source produces negative carbon ions. In order to reduce the overwhelming contribution of ^{12}C, the number of C ions are artificially reduced by a factor of 100 in the chopper. The C^- ions are accelerated in the accelerator tube of the left half of the accelerator by an electric field of about 3 MV. In the middle they are stripped of electrons to C^{3+}, so that in the right half, they are further accelerated as positive ions. In the final magnet the ^{12}C, ^{13}C and ^{14}C ion are separated and finally counted.

A much more efficient detection method is mass spectrometry, i.e. measuring the actual concentration of ^{14}C. Nevertheless, only in the late seventies attempts have been successful to detect single ^{14}C particles in carbon and separate these from other foreign elements.

IRMS operates at a few kV and accelerates molecules such as CO_2, which are separated into ion beams of masses 44, 45 and 46. For $^{14}CO_2$ the mass is 46 which signal –due to its

extremely low abundance of $< 10^{-12}$ – is completely lost in the 46 signal from the various stable isotopic combinations in CO_2. It appears that, by making the step to C ions instead of CO_2 ions, the "isobar" problem can be solved. This means accelerating over MV rather than kV.

Under these high-voltage conditions registration becomes possible in a nuclear particle detector. Contrary to IRMS single particles can then be detected, rather than beam currents.

For this purpose existing nuclear accelerators were used, specifically Tandem Van de Graaff Accelerators. Later dedicated machines were constructed and put into operation that are much smaller (Fig.11.8) (Purser, 1992).

The complete set-up of the accelerator with surrounding equipment is called Accelerator Mass Spectrometer (AMS). The essential features of an AMS are the following:

1) In the ion source negative ions are produced. This is necessary because contamination of carbon by nitrogen can not be avoided and a N^+ ion beam would make the detection of ^{14}C practically impossible, ^{14}C having the same position in the ultimate mass spectrum. Negative ions, on the other hand, have the advantage that N^- ions are extremely unstable and loose their charge before entering the accelerator.

2) The negative ions are produced by bombarding graphite –i.e. the sample- with Cs atoms. Presently, only very few CO_2 ion sources are operational for AMS. This would be less aggravating for the chemical preparation procedures, but such a source is a complicated device.

3) Ultimately, positive ions are more easily to detect, so that inside the accelerator the negative electric charge of the carbon ions is removed and replaced by a positive charge by steering the ions through a *stripper gas* (Ar). The stripping process especially destroys molecular isobars with mass 14, such as the beam contaminants ^{13}CH and ^{12}CH. The now positive ions are again accelerated and subsequently mass selected in a magnetic field so that ^{12}C, ^{13}C and ^{14}C can be detected separately.

3) Before entering the accelerator, the ions are mass separated by a magnetic field and the ^{12}C beam is reduced by a factor of 100 by a fast rotating diaphragm (chopper, Fig.11.8). The second magnet recombines the three ion beams.

The special **advantages** of the AMS technique, in comparison with radiometry, are that:

1) only milligram (or smaller) quantities of carbon are needed for one analysis, compared to roughly grams for the radiometric techniques (see Table 11.3) (Mook, 1984),

2) the analysis is considerably faster, i.e. lasts an hour instead of days.

Table 11.4 Survey of specific features of the various isotopic techniques. The ^{3}H and ^{14}C precisions quoted are valid for samples of roughly 10 TU and present-day activities, respectively. The asterisks refer to the cases where larger quantities of sample allow greater precision. For the radiometric techniques we have assumed a counting time of one or two days.

	Rare isotopes	Medium type	Medium quantity	Precision
IRMS	^{2}H, ^{13}C, ^{18}O (^{15}N, ^{34}S)	H_2, CO_2, N_2	few mL gas to few 0.1 mL gas	^{2}H: 0.1 ‰ ^{13}C: 0.01 ‰ ^{18}O: 0.02 ‰ ^{15}N: 0.02 ‰
PGC	^{3}H	H_2, C_2H_6 with enrichment	few mL H_2O few 100 mL H_2O	1 TU (NE) 0.1 TU (E)
	^{14}C	CO_2, C_2H_2, C_3H_8	1 – 50 L CO_2(equiv.)	0.5 – 0.1 % *
LSS	^{3}H	H_2O	few mL H_2O few 100 mL H_2O	few TU (NE) few 0.1 TU (E)
	^{14}C	C_6H_6	few to 15 mL C_6H_6	0.5 – 0.2 % *
AMS	^{14}C	C (graphite) (CO_2)	0.1 – 2 mg C few mL CO_2	0.5 % * ?

* for carbon with ^{14}a = 100%

IRMS = Isotope Ratio Mass Spectrometer
PGC = Proportional Gas Counter
LSS = Liquid scintillation spectrometer
AMS = Accelerator Mass Spectrometer

The **disadvantages** are that:

1) the capital investment is almost 100 times larger,
2) the AMS technique is more complicated from a technical point of view,
3) the precision is not yet as good as the best counters (PGC or LSS) can manage (Table 11.4).

11.5 REPORTING ^{14}C ACTIVITIES AND CONCENTRATIONS

11.5.1 THE CHOICE OF VARIABLES

The following definitions are in use:

The *absolute (specific) ^{14}C activity*, that is the ^{14}C radioactivity (in Bq or, conventionally, in disintegrations per minute (dpm) per gram of carbon) is given the symbol

$$^{14}A \text{ (in dpm/gC)} \qquad \textbf{(11.29)}$$

In general, ^{14}C laboratories are not able to make an absolute measurement, because the measuring efficiency is unknown. Also, in general, the absolute ^{14}C content of a sample is generally not relevant. Therefore, the sample activities are compared with the activity of a reference material, the international standard. In reality, the number of ^{14}C registrations (β registrations from ^{14}C decay in radiometric detectors such as proportional counters and liquid scintillation counters, registrations of ^{14}C concentration in AMS systems) are related to the number of registrations from the reference sample under equal conditions. This results in the introduction of a *^{14}C activity ratio* or *^{14}C concentration ratio*:

$$^{14}a = \frac{\text{measuring efficiency} \times {}^{14}A_{\text{sample}}}{\text{measuring efficiency} \times {}^{14}A_{\text{reference}}} = \frac{{}^{14}A_{\text{sample}}}{{}^{14}A_{\text{reference}}} =$$

$$= \frac{{}^{14}\text{C decay rate in the sample}}{{}^{14}\text{C decay rate in the ref. material}} = \frac{{}^{14}\text{C concentration in the sample}}{{}^{14}\text{C concentration in the ref. material}} \qquad \textbf{(11.30)}$$

Because in the numerator and denominator of the last two fractions, the detection efficiencies are equal for sample and standard,

the use of the ratio ^{14}a is adequate for any type of measuring technique. Henceforth, the symbol ^{14}A will be used for the *^{14}C content*, radioactivity as well as concentration,

whether the analytical technique applied is radiometric or mass spectrometric.

Under natural circumstances the values of ^{14}a are between 0 and 1. In order to avoid a large number of decimals, it is general practice to report these values in % (percent), which is equivalent to $\times 10^{-2}$. Therefore, the factor 10^2 should *not* enter into equations (as $^{14}a/10^2$).

In several cases the differences in ^{14}C content between samples are small. Therefore, the use of relative abundances has been adopted from the stable-isotope field, in casu the *relative ^{14}C content (activity or concentration)*, $^{14}\delta$, defined as the difference between sample and standard ^{14}C content as a fraction of the standard value:

$$^{14}\delta = \frac{{}^{14}A - {}^{14}A_{\text{Ref}}}{{}^{14}A_{\text{Ref}}} = \frac{{}^{14}A}{{}^{14}A_{\text{Ref}}} - 1 = {}^{14}a - 1 \qquad \textbf{(11.31)}$$

The values of δ are small numbers and therefore generally given in ‰ (permil), which is equivalent to $\times 10^{-3}$. Therefore, the factor 10^3 should *not* enter into mathematical equations (as $\delta/10^3$).

A ^{14}C *reference material* or *standard* was chosen to represent as closely as possible the ^{14}C content of carbon in naturally growing plants. The ^{14}C content of the standard material itself does not need to be, in fact is not, equal to the *standard ^{14}C content*. The definition of the standard ^{14}C activity is based on the specific activity of the original NBS oxalic acid (Ox1) (Karlén et al., 1966), as will be discussed in more detail.

11.5.2 THE STANDARDISATION

Before the definition of standards can be completed, two factors have to be discussed that complicate the standardisation of ^{14}C results and the respective symbols.

11.5.2.1 THE QUESTION OF ISOTOPE FRACTIONATION

During the transition of carbon from one compound to another, i.e. the assimilation of CO_2 by plants, the exchange of CO_2 from the air to surface water, etc., isotope fractionation occurs for ^{13}C as well as for ^{14}C. Also the laboratory treatment of sample materials may introduce an isotopic change, for instance by an incomplete chemical reaction. If this fractionation were neglected, samples of different chemical composition (carbonate and plants, C_3 and C_4 plants) but made of the same (age) carbon (determined by atmospheric CO_2) would seem to have different ages.

Therefore, in order to make ^{14}C ages comparable, a correction has to be applied for this fractionation effect. The theoretical relation between ^{14}C and ^{13}C fractionations is written as (Eq.3.43):

$$\frac{^{14}A_N}{^{14}A} = \left(\frac{^{13}R_N}{^{13}R}\right)^{\theta} \qquad \textbf{(11.32)}$$

where ^{14}A and ^{13}R refer to the measured, $^{14}A_N$ to the fractionation-corrected or *normalised* ^{14}C activity, while $^{13}R_N$ (or rather $^{13}\delta_N$) is an internationally adopted standard value. This value is $^{13}\delta_N = -25‰$ versus VPDB (Eq.7.1.3). Also the standard activity has to be normalised in the same way. The only exception is that -for historical reasons- the old Oxalic Acid standard (Ox1) is normalised to its real $^{13}\delta$ value of $-19‰$.

All $^{13}\delta$ values are with respect to the VPDB standard (Gonfiantini, 1984).

For natural processes the value of θ is about 2 (Craig, 1954). Since we have no reliable experimental evidence about the true value of θ, –there are reasons to believe that the true value of θ may be closer to 1.9–, and because this uncertainty is irrelevant compared to the analytical precision of ^{14}C measurements, we will use $\theta = 2$ as a sufficient approximation.

11.5.2.2 THE QUESTION OF RADIOACTIVE DECAY

For radioactive samples a measured activity depends on the time of measurement, t_m:

$$^{14}A(t_m) = {}^{14}A(t_0)e^{-\lambda\Delta t} \qquad \text{or} \qquad {}^{14}A = {}^{14}A^0\, e^{\lambda(t_m - t_0)} \qquad \textbf{(11.33)}$$

which is also valid for the standard material. Therefore, when reporting an absolute ^{14}C content, the year for which the value is valid must be specified. The same is true for the standard. The year of reference was chosen to be AD1950; the superscript ^{0} refers to this "year 0". The standard activity thus is valid for the year 1950. As the ^{14}C content of samples reduces in time simultaneously with the standard material, any comparison between the two results in a ^{14}C content valid for the year 1950 (= t_0).

The consequence is that an absolute ^{14}C content, which is based on a comparison with the Oxalic Acid standard according to standard procedures, is valid for the year 1950, irrespective of the time of measurement.

11.5.2.3 DEFINITION OF THE ^{14}C STANDARD ACTIVITY

We can now define the *standard activity* as 95% of the activity of the specific batch of Oxalic Acid nr.1 (Ox1) in AD 1950:

$$^{14}A^0_{RN} = 0.95\ {}^{14}A^0_{Ox1N} = 13.56 \pm 0.07\ \text{dpm/gC} = 0.226 \pm 0.001\ \text{Bq/gC} \qquad \textbf{(11.34)}$$

where R stands for "Reference", N for "Normalised" for isotope fractionation (to $^{13}\delta = -25‰$, only in the case of Ox1 to $^{13}\delta = -19‰$) and dpm/gC means disintegrations per minute per gram of carbon, while the superscript ^{0} refers to the fact that the definition is valid for the year AD1950 only.

The definition presented by Eq.11.34 is related to time by:

$$^{14}A_{RN} = {}^{14}A^0_{RN}\, e^{-\lambda(t_i - t_0)} = 0.95\ {}^{14}A^0_{Ox1N} e^{-\lambda(t_i - t_0)} = 0.95\ {}^{14}A_{Ox1N} \qquad \textbf{(11.35)}$$

where t_0 and t_i refer to the year 1950 and to the moment of the origin of the sample, respectively.

Because the original supply of oxalic acid has been exhausted, a new batch of oxalic acid (Ox2) is available for distribution by the NIST (formerly US-NBS).

Through careful measurement by a number of laboratories (Mann, 1983), the ^{14}C activity has become related to that of the original Ox1 by:

$$^{14}A^0_{Ox2N} = (1.2736 \pm 0.0004)\ {}^{14}A^0_{Ox1N} \qquad \textbf{(11.36)}$$

Contrary to the Old Oxalic acid (with a true $^{13}\delta$ value of −19.2 ‰, H.Craig, pers.comm., Mann, 1983), the New Oxalic acid (with $^{13}\delta_{Ox2} = -17.6‰$) has to be normalised (= corrected for isotope fractionation) to $^{13}\delta = -25‰$, while both activities refer to AD1950.

Consequently the standard activity is:

$$^{14}A^0_{RN} = \frac{0.95}{1.2736} = 0.7459\ ^{14}A^0_{Ox2N} \qquad \text{or} \qquad ^{14}A_{RN} = 0.7459\ ^{14}A_{Ox2N} \qquad \textbf{(11.37)}$$

where the $^{14}A^0$ values for Ox1 and Ox2 refer to the activity of the material in 1950, irrespective of the time of measurement.

11.5.3 FINAL DEFINITIONS

We can now more carefully specify the ^{14}C content of a sample in terms of the *activity ratio* or *concentration ratio* as the ratio between the measured ^{14}C content and the value of the standard (which always has to be normalised for $^{13}\delta$), with both terms referring to the time of measurement:

$$^{14}a = \frac{^{14}A}{^{14}A_{RN}} = \frac{^{14}A^0 e^{-\lambda(t_m - t_0)}}{^{14}A^0_{RN} e^{-\lambda(t_m - t_0)}} = \frac{^{14}A^0}{^{14}A^0_{RN}} = {}^{14}a^0 \qquad \textbf{(11.38)}$$

where t_0 refers to the year 1950, ^{14}A is the activity of the sample measured at time t_m, and $^{14}A_{RN}$ (= $0.95 \times {}^{14}A_{Ox1}$ with $^{13}\delta_N = -19‰$ or $0.746 \times {}^{14}A_{Ox2}$ with $^{13}\delta_N = -25‰$) is the value of the standard determined with the same detection efficiency, at about the same time t_m and corrected for isotope fractionation. In this way ^{14}a results from different laboratories become comparable. The decay of sample and standard ^{14}C content from t_0 to t_m is described by Eq.11.33.

The consequence of the relative measurement is that the resulting value of ^{14}a does not depend on the time of measurement is, contrary to the absolute ^{14}A value (see Sect.11.5.2.2); the absolute activity resulting from the relative measurement is valid for the year 1950, if multiplied by 0.226 Bq/gC: $^{14}a \times 0.226 = {}^{14}A^0$ (Bq/gC)

As was anticipated above, certain studies on natural systems are concerned with only small differences in ^{14}C content. In those cases it is conventional to report ^{14}C data as the relative difference between the measured sample activity and that of the reference:

$$^{14}\delta = \frac{^{14}A}{^{14}A_R} - 1 = \frac{^{14}A^0}{^{14}A^0_R} - 1 = {}^{14}a - 1 \qquad \textbf{(11.39)}$$

As mentioned, it has become common practice to normalise ^{14}C results for deviations of the measured $^{13}\delta$ from –25‰. Now the discussion of the normalisation procedure can be completed. Since conventionally $^{13}C/^{12}C$ values are related to the international standard for stable isotopes, Vienna PDB, Eq.11.32 can be rewritten by:

$$\frac{^{14}A_N / {}^{14}A_{RN}}{^{14}A / {}^{14}A_{RN}} = \left[\frac{^{13}R_N / {}^{13}R_{VPDB}}{^{13}R / {}^{13}R_{VPDB}}\right]^2$$

or using Eq.11.38, with $^{13}\delta_N = -25‰$, and consequently $1 + {}^{13}\delta_N = 1 + (-25‰) = 0.975$:

$$^{14}a_N = {}^{14}a\left[\frac{1+{}^{13}\delta_N}{1+{}^{13}\delta}\right]^2 = {}^{14}a\left[\frac{1+(-25‰)}{1+{}^{13}\delta}\right]^2 = {}^{14}a\left[\frac{0.975}{1+{}^{13}\delta}\right]^2 \qquad \textbf{(11.40)}$$

and likewise:

$$^{14}A_N = {}^{14}A\left[\frac{0.975}{1+{}^{13}\delta}\right]^2 \qquad \textbf{(11.41)}$$

while Eq.11.39 transforms into:

$$^{14}\delta_N = {}^{14}a_N - 1 \qquad \textbf{(11.42)}$$

11.5.4 SPECIAL CASES

In general the presentation of ^{14}C results depends on the type of application. For each case an example is given to illustrate the applicable definitions and equations.

11.5.4.1 HYDROLOGY

From a geochemical point of view the use of $^{14}a^S$, the non-normalised ^{14}C content at the time of sampling, is the most meaningful, rather than a δ value. Instead of applying a normalisation correction, the initial ^{14}C content of groundwater is going to be determined by specific geochemical reasoning of the origin of the inorganic carbon content. Furthermore, if we are dealing with groundwater ages, it is irrelevant -from a hydrological point of view- whether ages count back in time from the year of sampling (calculation based on $^{14}a^S$) or from 1950 (calculation based on $^{14}a = {}^{14}a^0$). Moreover, the precision of routine ^{14}C dating is ± 50 years or more anyway. Consequently, we can equally well use the most simple ^{14}a value in % as is obtained in simple laboratory procedures.

Without ^{13}C normalisation, the activity ratio in the year of sampling is:

$$^{14}a^S = {}^{14}a_N \left(\frac{1+{}^{13}\delta}{0.975}\right)^2 e^{-(t_S-1950)/8267} \qquad \textbf{(11.43)}$$

Often these values are given in percent of modern carbon (pMC) or percent modern (pM). In addition pM/100 (= $^{14}a^S$) is sometimes called fraction modern. However, the symbol pM is in use by water chemists and oceanographers as picoMole. Therefore, pmc, pMC, pM, and similar variants should not be used: % is adequate in combination with a well-defined symbol. Nevertheless, the use of pMC has become so established, that this "unit" is difficult to avoid. However, it seems more reasonable to use the symbol **%MC** instead of pMC.

Example: groundwater

The measured and normalised activity or concentration ratio is:

$$^{14}a_N = 0.537 = 53.7\ \%$$

The measured $^{13}\delta$ value of the total carbon content (as is obtained by the extraction procedure) is:

$$^{13}\delta = -13.82\ ‰$$

In groundwater hydrology we are interested in the ^{14}C content of the water sample at the time of sample collection. Therefore, the ^{14}a value has to be de-normalised:

$$^{14}a = {}^{14}a_N\,[(1 + {}^{13}\delta) / 0.975]^2 = 0.549 = 54.9\ \% \qquad \text{[cf. 11.40]}$$

The ^{14}C content in the year of sampling (1998) then is:

$$^{14}a^S = {}^{14}a_N\,[(1 + {}^{13}\delta) / 0.975]^2 \exp[-(1998 - 1950) / 8267] = 0.546 = 54.6\ \%$$

$$(\equiv 54.6\ \text{pMC} = \%\ \text{of modern carbon} = \%\text{MC}) \qquad \text{[cf. 11.43]}$$

Using more or less sophisticated models, the ^{14}C and the ^{13}C data, together with information on the chemical composition of the water sample, can be used to estimate the sample age (i.e. the period of time since the infiltration of the water). A straightforward "water age" as obtained by simply applying Eq.11.52 is not possible.

11.5.4.2 OCEANOGRAPHY AND ATMOSPHERIC RESEARCH

The same equation holds for the oceanographic applications. However, as the spread of the data generally is quite small, it is common practice to report the ^{14}C data as relative numbers, i.e. as decay corrected $^{14}\delta$ values:

$$^{14}\delta^S = {}^{14}a^S - 1 = \frac{{}^{14}A}{{}^{14}A^0_{RN}} - 1 \qquad \textbf{(11.44)}$$

In general results are also corrected for isotope fractionation (= normalised):

$$^{14}\delta_N^S = {}^{14}a_N^S - 1 = {}^{14}a \cdot e^{-(t_s - t_0)/8267} \left(\frac{0.975}{1 + {}^{13}\delta} \right)^2 - 1 \qquad \textbf{(11.45)}$$

These equations are used to express the ^{14}C content of samples of oceanwater as well as of atmospheric CO_2.

11.5.4.2.1 Example: oceanic DIC and atmospheric CO_2

The ^{14}C content resulting from a routine measurement includes normalisation to $^{13}\delta = -25$ ‰:

a) deep-ocean bottom water DIC (=dissolved inorganic carbon):

$^{14}a_N = {}^{14}a_N{}^0 = 0.872 = 87.2$ % [cf. 11.40]

from which: $^{14}\delta_N = {}^{14}a_N - 1 = -0.128 = -128$ ‰ [cf. 11.42]

with $^{13}\delta = +1.55$ ‰

When corrected for the fact that the resulting ^{14}C content is valid for the year 1950 instead of the year of sampling (1990):

$$^{14}\delta_N^S = {}^{14}a_N \exp[-(1990 - 1950)/8267] - 1 = -0.132 = -132 \text{ ‰}$$

b) atmospheric CO_2:

from which: $^{14}\delta_N = {}^{14}a_N - 1 = 0.253 = +253$ ‰ [cf. 11.42]

with $^{13}\delta = -7.96$ ‰

When corrected for the fact that the resulting ^{14}C content is valid for the year 1950 instead of the year of sampling (1985):

$$^{14}\delta_N^S = {}^{14}a_N \exp[-(1985 - 1950)/8267] - 1 = 0.247 = +247 \text{ ‰} \qquad \text{[cf. 11.45]}$$

With atmospheric CO_2 samples it remains problematic whether the ^{13}C correction applied (according to Eq.11.40) is correct. The measured $^{13}\delta$ value may very well be affected by the admixture of biospheric or fossil-fuel CO_2, instead of by isotope fractionation alone, as is the –not necessarily valid– presumption of the correction procedure (Mook, 1980b).

11.5.4.3 GEOCHEMISTRY

In geochemical studies it is often necessary to know the original ^{14}C content of a sample in the year of the sample origin t_i (such as the year a treering was formed), instead of the activity in 1950, as is routinely obtained. As the measured ^{14}C content (activity or concentration) is

valid for the year 1950, it has to be corrected for radioactive decay from the year of origin (t_i) to 1950:

$$^{14}A^i = {}^{14}A^0 \, e^{-(t_i - 1950)/8267} \qquad \textbf{(11.46)}$$

and equally for the normalised values:

$$^{14}A_N^i = {}^{14}A_N^0 \, e^{-(t_i - 1950)/8267} \qquad \textbf{(11.47)}$$

For this correction again the "correct" half-life of ^{14}C (5730a) has to be used with $\lambda = 1/8267a^{-1}$. Furthermore, $^{14}A^0$ and $^{14}a^0$ refer to 1950 and $^{14}A^i$ and $^{14}a^i$ to the year of the origin of the carbon containing sample material.

For the normalised and age corrected values we can now write:

$$^{14}\delta^i = {}^{14}a^i - 1 = \frac{^{14}A^i}{^{14}A_{RN}^0} - 1 =$$

$$= \frac{^{14}A^0 \, e^{-(t_i - 1950)/8267}}{^{14}A_{RN}^0} - 1 = {}^{14}a \cdot e^{-(t_i - 1950)/8267} - 1 \qquad \textbf{(11.48)}$$

(where t_i is the date BC (negative) or AD (positive)) and for the normalised values:

$$^{14}\delta_N^i = {}^{14}a_N^i - 1 = {}^{14}a \cdot e^{-(t_i - 1950)/8267} \left(\frac{0.975}{1 + {}^{13}\delta} \right)^2 - 1 \qquad \textbf{(11.49)}$$

Example: atmospheric ^{14}C content from a known-age sample : wood from a treering

The measured activity ratio i.e. the activity with respect to 0.95 times the measured and normalised oxalic acid activity:

$$^{14}a = {}^{14}a^0 = (^{14}A / {}^{14}A_{RN}) = 0.4235 \quad \text{or} \quad = 42.35\,\% \qquad \text{[cf. 11.38]}$$

The measured $^{13}\delta$ of the sample:

$$^{13}\delta = -22.5\,‰$$

The normalised activity ratio of the sample is:

$$^{14}a_N = {}^{14}a \, [0.975 / (1 - 0.0225)]^2 = 0.4213 \quad \text{or} \quad = 42.13\,\% \qquad \text{[cf. 11.40]}$$

Using the normalised, age corrected ^{14}a value calculated above, the conventional ^{14}C age is:

$$T = -8033 \ln {}^{14}a_N = 6943 \text{ BP} \qquad \text{[cf. 11.50]}$$

The normalised relative activity is:

$$^{14}\delta_N = {}^{14}a_N - 1 = -0.5787 \quad \text{or} \quad -578.7 \text{ ‰} \qquad \text{[cf. 11.42]}$$

Suppose the treering is dated dendrochronologically to 5735 calBC (stands for "calibrated BC = corrected according to the ^{14}C calibration curve, shown in Fig.8.5), i.e. $t_i = -5735$ a.

The age-corrected, i.e. the original ^{14}C content of the sample is then:

$$^{14}\delta_N{}^i = {}^{14}a_N{}^i - 1 = {}^{14}a_N \exp[-(-5735 - 1950) / 8267] - 1$$

$$= 0.0674(5) \quad \text{or} \quad = +67.4(5) \text{ ‰} \qquad \text{[cf. 11.49]}$$

11.5.4.4 ENHANCED ^{14}C RADIOACTIVITY

In studies on the extent of radioactive contamination, for instance by ^{14}C, the absolute radioactivity of the sample is required. In such cases, the result of the routine ^{14}C measurement, in casu the ^{14}a value, has to be converted back to the absolute value by:

$$^{14}A = {}^{14}a \times 13.56 \text{ (dpm/gC)} = {}^{14}a \times 0.226 \text{ (Bq/gC)} \qquad \textbf{(11.50)}$$

The measured activity as such is valid for the year 1950 (Eq.11.38), so it has to be corrected for radioactive decay from 1950 (t_0) to the year of sampling (t_s). Moreover, the activity in this case is not to be normalised. If the laboratory provides only normalised values, $^{14}a_N$, these have to be "de-normalised" (i.e. normalisation removed) by applying Eqs.11.34, 11.38, 11.40 and 11.50:

$$^{14}A^S = {}^{14}a_N^0 \left(\frac{1 + {}^{13}\delta}{0.975}\right)^2 e^{-\lambda(t_S - t_0)} \, {}^{14}A_{RN}^0 =$$

$$= {}^{14}a_N \left(\frac{1 + {}^{13}\delta}{0.975}\right)^2 e^{-(t_S - 1950)/8267} \times 0.226 \text{ (Bq / gC)} \qquad \textbf{(11.51)}$$

where t_0 and $^{14}a^0$ both refer to the year 1950, and t_s and A^S to the year of sampling; λ is based on the true ^{14}C half-life of 5730 year; $^{14}a_N$ is the routinely acquired (i.e. normalised) ^{14}C content of the sample.

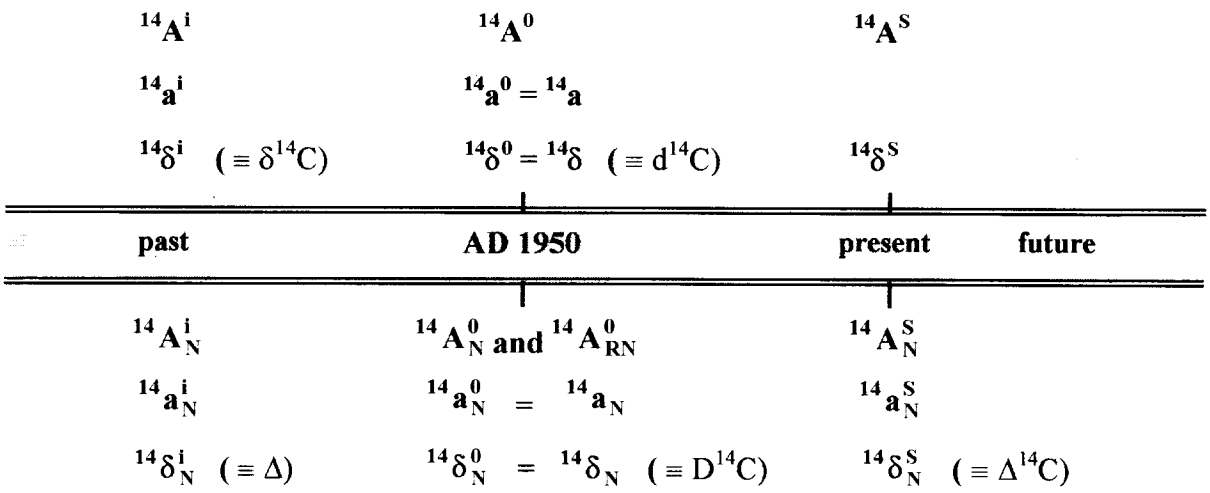

Fig 11.9 Illustration of the definition of symbols for reporting ^{14}C data along the time scale from the past (for the data to be corrected for age/decay), via the year 1950 to the time of sample collection (s) and the future. Above the line are the non-normalised data (not corrected for isotope fractionation), below the normalised values. The bold symbols are defined in this paper, the symbols within brackets were defined by Stuiver and Polach (1977).

Example: fall-out contamination

The AMS measured ^{14}C concentration ratio is:

$$^{14}a_N = 2.200 \quad \text{or} \quad = 220.0\ \%$$

The $^{13}\delta$ analysis obtained in the AMS system resulted in:

$$^{13}\delta = -32.0\ ‰$$

The routinely obtained $^{14}a_N$ value now has to be de-normalised according to:

$$^{14}a = {}^{14}a_N\,[(0.968/\,0.975]^2 = 2.168(5) \quad \text{or} \quad = 216.8(5)\ \% \qquad \text{[cf. 11.40]}$$

The absolute activity in the year 1950 would have been:

$$^{14}A^0 = {}^{14}a^0 \times 0.226 = {}^{14}a \times 0.2260 = 0.4901\ \text{Bq / gC} \qquad \text{[cf. 11.50]}$$

This value has to be corrected for radioactive decay, as the measured value is valid for 1950 instead of the year of sampling $t_s = 1986$:

$$^{14}A^S = {}^{14}A^0\ \exp[-(1986 - 1950) / 8267] = 0.4880\ \text{Bq/gC} \qquad \text{[cf. 11.51]}$$

Table 11.5 Review of the symbols used in reporting ^{14}C activities. The upper symbol is defined in this paper. The symbols in the shaded areas refer to Stuiver and Polach (1977). In the 3rd column the symbols apply to the decay-corrected values, i.e. corrected for decay of the sample activity from 1950 to the year of sampling (Eqs.11.43–44). The symbols in the 6th column refer to Eqs.11.47–49. The superscript 0 assigns the value to the year 1950.

	measured at t_0 (1950); a and δ at any time	normalised	decay corrected till sampling at t_s	decay corrected + normalised	age corrected from origin at t_i	age corrected + normalised
Absolute ^{14}C content of sample	$^{14}A^0$	$^{14}A_N$	$^{14}A^S$	$^{14}A^S_N$	$^{14}A^i$	$^{14}A^i_N$
	A_S	A_{SN}				
Absolute ^{14}C content of standard	$^{14}A^0_R$	$^{14}A_{RN}$		$^{14}A^0_{RN}$		
		A_{ON}		A_{ABS}		
^{14}C abundance ratio	$^{14}a = {}^{14}a^0$	$^{14}a_N$	$^{14}a^S$	$^{14}a^S_N$	$^{14}a^i$	$^{14}a^i_N$
	A_S/A_{ON}	A_{SN}/A_{ON}	A_S/A_{ABS}	A_{SN}/A_{ABS}		
Relative ^{14}C content	$^{14}\delta = {}^{14}\delta^0$	$^{14}\delta_N$	$^{14}\delta^S$	$^{14}\delta^S_N$	$^{14}\delta^i$	$^{14}\delta^i_N$
	$d^{14}C$	$D^{14}C$	$\delta^{14}C$ [1])	$\Delta^{14}C$ [2])	$\delta^{14}C$ [3])	Δ [4])

The upper symbols in each block are defined by their sub- and superscripts.

Symbols stand for:

A = absolute activity or concentration
a = activity/concentration ratio to standard
δ = relative ^{14}C content (i.e. deviation of activity or concentration from standard

Super– and subscripts stand for:

N = normalised
0 = time zero ≡ AD1950
i = initial ≡ time of growth/formation of sampling
s = time

The symbols proposed by Stuiver and Polach (1977) are shown in the shaded areas. They refer to the following fields of study:

[1]) in hydrology the use of the ^{14}a value (or rather $^{14}a^S$) is more common
[2]) in oceanography and atmospheric studies
[3]) in geochemical studies if age correction is possible
[4]) idem, such as past ^{14}C variations from treerings

11.5.4.5 ^{14}C AGES

In geological and archaeological dating, the ages used are the *conventional ^{14}C ages*. is repeated. By international convention, the definition of the conventional ^{14}C age is based on (Sect.8.1.4):

1) the *initial ^{14}C activity* (i.e. the activity of the sample material during "growth" equals the standard activity in AD1950
2) the ^{14}C activities have to be normalised for fractionation (samples to $^{13}\delta = -25‰$, Ox1 to −19 ‰, Ox2 to −25 ‰) (see Chapter 10)
3) the original (Libby) half-life of 5568 has to be used.

The ages are then calculated by applying:

$$\textbf{Conventional age} = -8033 \ln {}^{14}a_N \qquad \textbf{(11.52)}$$

This defines the ^{14}C time scale in years BP (Before Present, i.e. AD1950).

This time scale needs to be calibrated in order to obtain historical (*calibrated*) ages (calAD, calBC, calBP). For the calibration procedures and conventions we refer to the special Calibration Issues, published by Radiocarbon (the most recent edited by Stuiver and Van der Plicht, 1998).

11.5.5 SUMMARY

The interrelation between the various definitions and symbols, especially concerning the validity over the time scale from past to present, is illustrated by Fig.11.9. For comparison, the symbols used by Stuiver and Polach (1977) are given within brackets.

In Table 11.5 all symbols used for reporting ^{14}C data are classified.

Table 11.6 contains the relative and absolute ^{14}C contents of the available ^{14}C reference samples.

The "rational" symbols introduced by Mook and van der Plicht (1999) are based on:

^{14}A = absolute radioactivity (in Bq/gC or in dpm/gC)

^{14}a = activity or concentration ratio between sample and standard (in %)

$^{14}\delta$ = relative difference in activity or concentration (in ‰)

The symbols are prefixing the superscript "^{14}" like in the isotopic symbol ^{14}C. The superscripts "^{i}", "^{0}", and "^{S}" indicate the time to which A, a, or δ are related. The subscript "$_N$" indicates whether the activities and concentrations are normalised.

Table 11.6 ^{14}C content and $^{13}\delta$ values of a number of standards and secondary reference samples, available for distribution. The types of material and the ages represent the range of interest of the radiocarbon laboratories. The values are normalised for their $^{13}\delta$ value (to −25 ‰). As the ^{14}C values presented by ^{14}a (Eq.11.36), the time of measurement is irrelevant. Absolute activities are calculated according to Sect.11.5.4.4, and refer to the year 1950. Full details are reported by Rozanski et al. (1992).

	TYPE OF MATERIAL	$^{14}a_N$ (%)	$^{13}\delta$ (‰)	$^{14}A_N^0$ (Bq/gC)	DISTRIBUTED BY
C-1	Marine carbonate milled Carrara Marble	0.00 ± 0.02	+ 2.42	< 0.0001 [2])	IAEA
C-2	Freshwater carbonate travertine deposit	41.14 ± 0.03	− 8.25	0.0930	IAEA
C-3	Cellulose from 40-yr trees felled 1989	129.41 ± 0.06	− 24.91	0.2925	IAEA / CIO
C-4	Subfossil wood from peat bogs N.Zealand	0.32 ± 0.06	− 23.96	0.00072	IAEA / ANU
C-5	Subfossil wood buried bed forest USA	23.05 ± 0.02	− 25.49	0.05209	IAEA
C-6	Sucrose originally second. standard	150.61 ± 0.11	− 10.40	0.3404	IAEA / ANU
Ox1	Oxalic acid primary ^{14}C standard nr.1	100.00 [1])	− 19.20	0.2260	NIST / IAEA
Ox2	Oxalic acid primary ^{14}C standard nr.2	127.36 ± 0.04	− 17.60	0.2878	NIST/ IAEA

[1]) by definition

NIST = National Institute of Standards and Technology, Atmospheric Chemistry Group, B364, Building 222, Gaithersburg, MD 20899, United States of America

IAEA = International Atomic Energy Agency, Analytical Quality Control Services, Agency's Laboratory, Seibersdorf, P.O.Box 100, A-1400 Vienna, Austria, fax +43-1-2060-28222

CIO = Centre for Isotope Research, Nijenborgh 4, 9747 AG Groningen, the Netherlands, tel. +31-50-3634760, fax +31-50-3634738

12 NATURAL ISOTOPES OF ELEMENTS OTHER THAN H, C, O

In this chapter we are dealing with the less common applications of natural isotopes. Our discussions will be restricted to their origin and isotopic abundances and the main characteristics. Only brief indications are given about possible applications. More details are presented in the other volumes of this series. A few isotopes are mentioned only briefly, as they are of little relevance to water studies.

Based on their half-life, the isotopes concerned can be subdivided:

1) stable isotopes of some elements (He, Li, B, N, S, Cl), of which the abundance variations point to certain geochemical and hydrogeological processes, and which can be applied as tracers in the hydrological systems,
2) radioactive isotopes with half-lives exceeding the age of the universe (^{232}Th, ^{235}U, ^{238}U),
3) radioactive isotopes with shorter half-lives, mainly daughter nuclides of the previous catagory of isotopes,
4) radioactive isotopes with shorter half-lives that are of cosmogenic origin, i.e. that are being produced in the atmosphere by interactions of cosmic radiation particles with atmospheric molecules (^{7}Be, ^{10}Be, ^{26}Al, ^{32}Si, ^{36}Cl, ^{36}Ar, ^{39}Ar, ^{81}Kr, ^{85}Kr, ^{129}I) (Lal and Peters, 1967).

The isotopes can also be distinguished by their chemical characteristics:

1) the isotopes of noble gases (He, Ar, Kr) play an important role, because of their solubility in water and because of their chemically inert and thus conservative character. Table 12.1 gives the solubility values in water (data from Benson and Krause, 1976;. The table also contains the atmospheric concentrations (Andrews, 1992: error in his Eq.4, where $T_i/(T-1)$ should read $(T_i/T)-1$);
2) another category consists of the isotopes of elements that are only slightly soluble and have very low concentrations in water under moderate conditions (Be, Al). These are primarily used for sediment studies and for dating ice sheets;
3) two elements (N, S) have isotopic abundances revealing information on bio(geo)chemical processes in soils and associated waters;
4) three nuclides are cosmogenically produced isotopes from elements that occur as solutes in aqueous systems (Si, Cl, I) and are used for water dating;

5) the decay series of uranium and thorium contain several isotopes of which the relations between the parent/daughter activities are useful pre-eminently.

In the tables at the introduction of each section some relevant physical information is given about abundance and decay to finally a stable daughter nuclide.

This chapter mainly serves to review the physical and chemical characteristics of the isotopes. Only a brief indication is being given of the possibilities of application for studying the water cycle. A thorough discussion is to be found in the other volumes of this series.

Table 12.1 Solubilities of noble gases in water at various temperatures, the atmospheric concentrations and the concentration of the noble gases dissolved in water in equilibrium with the atmosphere at 10°C (Bensen and Krause, 1976; Andrews, 1992).

	Solubility in mL(STP)/L H_2O				Atmosph.	Diss.conc.
	0°C	10°C	20°C	30°C	concentr.	mL/L (10°C)
Helium	9.53	9.07	8.82	8.74	5.24×10^{-6}	4.75×10^{-5}
Neon	12.6	11.4	10.5	10.0	1.82×10^{-5}	2.07×10^{-4}
Argon	53.5	41.7	34.1	29.0	9.34×10^{-3}	3.89×10^{-1}
Krypton	111.2	81.2	62.8	50.9	1.14×10^{-6}	9.26×10^{-5}
Xenon	226	154	112.5	86.7	8.60×10^{-8}	1.32×10^{-5}
Radon	510					

12.1 HELIUM

Table 12.2 Natural isotopes of helium.

	$^{3}_{2}He$	$^{4}_{2}He$
Stability	Stable	Stable
Natural abundance fraction	1.3×10^{-6}	100 %
Natural abundance in air [1]	6.8×10^{-12}	5.24×10^{-6}
Natural abundance in groundwater [2]	10^{-10} to 10^{-13}	10^{-3} to 10^{-5}

[1]) mL gas /mL of air

[2]) mL gas /mL of water

12.1.1 ORIGIN AND CHARACTERISTICS

The radioactive isotope of hydrogen, formed in the atmosphere by a nuclear reaction of nitrogen atoms with neutrons in cosmic radiation (Sect.8.3), decays through β decay to ^{3}He:

$$^3H \rightarrow {}^3He + \beta^- \qquad \textbf{(12.1)}$$

The maximum β energy of ^{3}H is 18 keV and the half-life is 12.43 a (Fig.8.2). The daughter product ^{3}He is stable and chemically inert. ^{3}He is also formed in the earth's crust (primarily in crystal rock) by the reaction:

$$^6Li + n \rightarrow {}^3He + {}^4He \quad \text{or} \quad {}^6Li\,(n,\alpha)\,{}^3He \qquad \textbf{(12.2)}$$

The underground neutrons originate from spontaneous fission of uranium or thorium isotopes or by (α,n) reactions in which the α particles are from decays within the uranium and thorium decay series.

^{4}He originates primarily from the natural decay of ^{235}U, ^{238}U and ^{232}Th in the earth (Sect.12.13).

12.1.2 EXPERIMENTAL AND TECHNICAL ASPECTS

In groundwater concentrations of helium are observed in the range of 10^{-5} to 10^{-2} mL(STP) of He/mL of water. With ^{3}He/^{4}He ratios of 10^{-8} to 10^{-7} this means that the ^{3}He concentrations can be as low as 10^{-13} mL/mL of water. To measure these amounts of gas, specialised mass spectrometers are needed. This is even more true for the measurement of extremely low ^{3}H contents (down to 10^{-2} TU) through ^{3}He accumulation (Sect.12.1.5.2).

In general, water samples are collected of 5 to 500 mL -depending on the laboratory's equipment- and thoroughly sealed before being shipped to the laboratory.

12.1.3 SOURCES OF ^{3}He

The main complication is that the principle of ^{3}H/^{3}He dating is based on the assumption that all ^{3}He in the water sample is tritiogenic (coming from decay of ^{3}H). However, part of the ^{3}He may be of terrigenic origin (from in situ production according to Eq.12.2), part from the original equilibration of the water with the atmospheric gases. The latter contribution can be estimated from the Ne concentration, which can not be of terrigenic origin. A possible terrigenic contribution is to be estimated from the concentration of ^{4}He (also corrected for the atmospheric component (Schlosser et al., 1998). These processes are summarised by:

$$^3He_{tot} = {}^3He_{atm} + {}^3He_{terr} + {}^3He_{trit} \qquad \textbf{(12.3a)}$$

$$^4He_{tot} = {}^4He_{atm} + {}^4He_{terr} \qquad \textbf{(12.3b)}$$

$$Ne_{tot} = Ne_{atm} \qquad \textbf{(12.3c)}$$

where the atmospheric concentration ratio $He_{atm}/Ne_{atm} = 0.288$.

12.1.4 NATURAL ABUNDANCE

The $^3He/^4He$ ratio in atmospheric helium is about 1.3×10^{-6}, with a helium concentration of about 5 ppmv (partial pressure of 5×10^{-6} atm.). The relative constancy of this concentration is due to the state of equilibrium between the loss of helium from the crust to the atmosphere and the loss from the atmosphere to outer space.

Groundwater concentrations are observed of 10^{-3} to 10^{-5} mL(STP)/mL of water, far exceeding the equilibrium value due to relatively high underground helium production. The $^3He/^4He$ ratio in groundwater is still within a narrow range of 5×10^{-8} to 10^{-7}.

Apart from the infiltration of tritium containing water, ^3H can be produced underground in the aquifer, i.e. through *in situ production*:

$$^{14}N + n \rightarrow {}^{12}C + {}^3H \qquad \textbf{(12.4)}$$

The presence of neutrons is due to spontaneous fission of U and Th. Because of its short half-life, ^3H levels will be low, generally below 1 TU. The accumulated ^3He levels will then depend on the degree of isolation of the water, and are thus a measure of that effect.

12.1.5 APPLICATIONS

12.1.5.1 PRINCIPLE OF $^3H/^3He$ DATING

The application of ^3H to obtain underground residence times ("ages") of groundwater was shown to depend on our knowledge of the ^3H input from atmospheric precipitation (Sect.8.4.2). Studying the relation between ^3H and ^3He offers the possibility to determine ages without knowing the tritium input function. If the original ^3H content of the infiltrating precipitation is $^3H_0$, the content after a residence time t, ^3H_t, is presented by:

$$^3H_t = {}^3H_0\, e^{-\lambda t}$$

The amount of ^3He formed during this time is equal to the amount of ^3H lost by decay:

$$^3He_t = {}^3H_0 - {}^3H_t = {}^3H_t(e^{\lambda t} - 1) \qquad \textbf{(12.5)}$$

The $^3H/^3He$ age is then:

$$t = (12.43/\ln 2) \times \ln[{}^3He/{}^3H + 1] \qquad \textbf{(12.6)}$$

Most applications are related to shallow, young groundwater, using the bomb peak of ^3H in the precipitation during the early 1960s. The occurrence of ^3H and ^3He at great depth may be due to fractures, cracks or leaking boreholes, or to in situ production.

12.1.5.2 MASS SPECTROMETRIC MEASUREMENT OF ^3H THROUGH ^3He

Very low ^3H abundances (theoretically down to 0.0005 TU) can be measured by thoroughly degassing and storing 50 to 100 mL of water sample for at least half a year in a tightly sealed

container and subsequently recollecting the decay product of tritium, ^3He. The amount of this inert gas can be quantitatively measured mass spectrometrically. The ^3He produced during this storage time (t) is (Eq.12.5):

$$^3He_t = {}^3H_0 - {}^3H_t = {}^3H_0(1 - e^{-\lambda t})$$

so that the original ^3H content of the sample was:

$$^3H_0 = {}^3He/(1 - e^{-\lambda t}) \qquad (12.7)$$

To give an impression: the amount of ^3He formed during half a year storage of 100 mL of water with a ^3H concentration of 0.5 TU is:

$$^3He_t = 0.5\times10^{-18} \times 2 \times (100/18) \times (1 - e^{-(\ln 2)/12.43) \times 0.5}) \times 22.41\times10^3$$

$$= 3.4\times10^{-15} \text{ mL}$$

12.2 LITHIUM

Table 12.3 Natural isotopes of lithium

	^6_3Li	^7_3Li
Stability	Stable	Stable
Natural abundance fraction	7.5 %	92.5 %

12.2.1 NATURAL ABUNDANCE

In seawater the Li^+ concentration is about 0.18 mg/L. The isotopic composition varies by about 10 ‰.

12.2.2 EXPERIMENTAL AND TECHNICAL ASPECTS

Natural variations in the $^6Li/^7Li$ ratio may be related to a reference sample, available from the IAEA and NIST, referred to as L-SVEC. With respect to L-SVEC, the Li isotopic composition of Li in seawater ($\delta^6Li = (^6Li/^7Li) - 1$) is –32 ‰.

12.2.3 APPLICATIONS

The $^6Li/^7Li$ ratio has been used to study brines and their origin as evaporated (palaeo)seawater. Li isotopes are also being applied to crystalline rocks.

12.3 BERYLLIUM

Table 12.4 Natural isotopes of beryllium

	$^{7}_{4}Be$	$^{9}_{4}Be$	$^{10}_{4}Be$
Stability	radioactive	stable	radioactive
Natural abundance fraction		100 %	
Abundance in air/ice/marine sediment	~5mBq/m^3 air		$10^{7\text{ to }10}$ atoms/kg
Half-life ($T_{1/2}$)	53.3 d		1.5×10^6 a
Decay constant (λ)	1.51×10^{-7} s^{-1}		1.5×10^{-14} s^{-1}
Decay mode / Daughter	EC / ^{7}Li		β^- / ^{10}B

12.3.1 ORIGIN AND CHARACTERISTICS

The origin is cosmogenic, i.e. ^{10}Be (together with short-lived ^{7}Be) is continuously being produced in the atmosphere by the action of the high-energy proton component in cosmic radiation, causing spallation of atmospheric oxygen and nitrogen atoms.

^{10}Be decays according to:

$$^{7}Be + e^{-} \rightarrow {}^{7}Li \qquad \textbf{(12.8)}$$

$$^{10}Be \rightarrow {}^{10}B + \beta^{-} \quad (E_{max} = 560 \text{ keV, no } \gamma \text{ radiation}) \qquad \textbf{(12.9)}$$

12.3.2 EXPERIMENTAL AND TECHNICAL ASPECTS

Although in principle the radioactive decay of ^{10}Be can be measured, the specific activity is so low that this method is not applicable. Detection has become possible by the introduction of the ultrasensitive mass spectrometers (AMS). Therefore, ^{10}Be is only being applied since the 1970s. As usual, ^{10}Be concentrations are compared with (related to) a reference material, SRM 4325, available from the NIST, with a ^{10}Be/^{9}Be ratio of $(2.68 \pm 0.14) \times 10^{-11}$. Be targets are prepared by mixing BeO and Ag.

12.3.3 NATURAL ABUNDANCE

The atmospheric production rate (flux) of ^{10}Be is about 300 atoms m^{-2}s^{-1}. This production rate varies with latitude, altitude and geologic times. It is (together with ^{27}Al) rapidly washed out from the atmosphere by precipitation, and is subsequently incorporated in continental and marine sediments. ^{10}Be concentrations are observed of $(5 \text{ to } 20) \times 10^8$ atoms/g of sediment.

In Antarctic ice concentrations have been observed of 10^7 atoms ^{10}Be/kg of ice (Raisbeck et al., 1978). The concentration in, for instance, the surface water of the ocean largely depends on the residence time of ^{10}Be in the surface layers. Values have been observed of about 7.5×10^5 atoms/L of water (Raisbeck et al., 1979), with Be concentrations of 5 pM/kg (at the surface) to 30 pM/kg of seawater (at depth) (pM = picomol = 10^{-12}mol).

12.3.4 APPLICATIONS

^{10}Be is being applied in particular for dating marine sediments by studying the radioactive decay in the sediment core. The especially useful method of measuring both ^{10}Be and ^{26}Al is mentioned in Sect.12.6.4. With respect to the water cycle is ^{10}Be being used for dating ice.

12.4 BORON

12.4.1 NATURAL ABUNDANCE

In the marine environment the element boron is primarily found as dissolved borate (BO_3^{3-}). An important geochemical characteristic is the easy incorporation of B in marine clays during

Table 12.5 Natural isotopes of boron

	$^{10}_{5}$B	$^{11}_{5}$B
Stability	stable	stable
Natural abundance fraction	18.8 %	81.2 %

which the boron isotopes are being fractionated (Gregoire, 1987).

12.4.2 EXPERIMENTAL AND TECHNICAL ASPECTS

Measurement of the abundance ratio ^{10}B/^{11}B ($\approx$0.23) is carried out by Inductively Coupled Plasma Mass Spectrometry (Gregoire, 1987).

12.4.3 APPLICATIONS

Rare applications have been made in the marine system, related to boron isotope fractionation during adsorption processes of seawater and clay. The ^{10}B/^{11}B ratio of brines has been used in combination with ^{6}Li/^{7}Li to study the relation with old seawater.

12.5 NITROGEN

Table 12.6 Natural isotopes of nitrogen

	$^{14}_{7}N$	$^{15}_{7}N$
Stability	Stable	Stable
Natural abundance fraction	99.63 %	0.37 %

12.5.1 EXPERIMENTAL AND TECHNICAL ASPECTS

The measuring technique for nitrogen has been discussed in Sect.11.2.2. About 2 mg of N is needed for a $^{15}N/^{14}N$ analysis (and if necessary the combined $^{18}O/^{16}O$ analysis).

12.5.2 NATURAL ABUNDANCE AND ISOTOPE FRACTIONATION

The isotope ratio $^{15}N/^{14}N$ in the largest nitrogen reservoir, atmospheric N_2, is extremely constant, due to the relative inert character of nitrogen. The atmospheric $^{15}N/^{14}N$ value is 0.0036765.

Nearly all fractionation processes involving ^{15}N in nature are kinetic. Only dissolution of N_2 in water (equilibrium fractionation $^{15}\varepsilon_{N2(dissolved)/N2(gas)} = + 0.85$ ‰), and the diffusion of N_2 are non-biological processes. The major components in the nitrogen cycle are NH_4^+ and NO_3^-. Fig.12.1 shows ranges of the most common N-containing compounds.

The relevant biochemical processes in the water phase during which isotope fractionation occurs are:

1) **nitrification**, the oxidation from ammonia to nitrite and nitrate:

$$NH_4^- \rightarrow NO_2^- \rightarrow NO_3^- \qquad \textbf{(12.12)}$$

2) **denitrification**, the reduction of nitrate to molecular nitrogen:

$$NO_3^- \rightarrow NO_2^- \rightarrow (NO) \rightarrow N_2O \rightarrow N_2 \qquad \textbf{(12.13)}$$

3) **nitrogen fixation**, the conversion of dissolved molecular nitrogen to organic compounds:

$$N_2\,(aq) \rightarrow \text{N-organic molecules} \qquad \textbf{(12.14)}$$

These processes are carried out by bacteria. The resulting stable nitrogen isotope fractionation may be considerable, but is hard to predict. Generally, the isotopically light (^{14}N containing) molecules are reacted more easily (Létolle, 1980; Hübner, 1986).

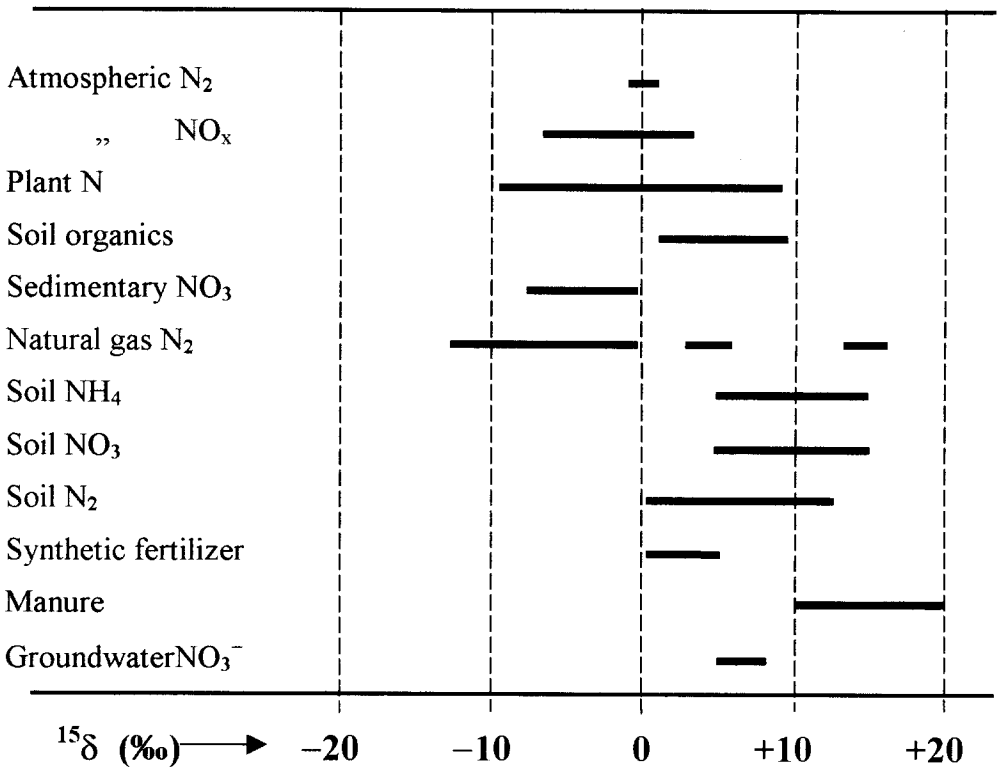

Fig.12.1 Survey of $^{15}\delta$ values of nitrogen containing compounds in nature. The $^{15}\delta$ values are given relative to the isotopic composition of air-N_2.

12.5.3 APPLICATIONS

Strictly hydrological applications are not obvious. ^{15}N primarily serves to study bio(geo)chemical processes in the hydrological environment. However, ^{15}N in dissolved compounds can be applied to tracing water masses underground.

12.5.4 $^{18}O/^{16}O$ IN NITRATE

Information on the origin of nitrate is also obtained from the oxygen isotopic composition of the nitrate ion. It has been shown (quote by Clark and Fritz, 1997; see also Volume IV) that one atom is related to atmospheric O_2 ($^{18}\delta \sim +20$ ‰ relative to VSMOW-water). The other two atoms are derived from the ambient water ($^{18}\delta < 0$ ‰ rel. to VSMOW-water). In synthetic fertilizers the oxygen is mainly coming from air-O_2. Moreover, $^{18}\delta$ appears to be nicely correlated with the denitrification process. In conclusion, the oxygen isotopic composition is certainly a valuable tracer, although the interpretations are not yet unique (Révész et al., 1998).

12.6 ALUMINIUM

Table 12.7 Natural isotopes of aluminium

	$^{26}_{13}Al$	$^{27}_{13}Al$
Stability	radioactive	stable
Natural abundance fraction		100 %
Natural abundance in sediment	~ 10^7 atoms/g quartz	
Half-life ($T_{1/2}$)	7.16×10^5 a	
Decay constant (λ)	3.07×10^{-14} s^{-1}	
Decay mode / Daughter	β^+, EC / ^{26}Mg	

12.6.1 ORIGIN AND CHARACTERISTICS

Like ^{10}Be, ^{26}Al is being formed in the atmosphere by spallation of argon in the air induced by cosmic ray protons:

$$^{40}Ar\ (p,sp)\ ^{26}Al \qquad \textbf{(12.15)}$$

The radioactive decay to ^{26}Mg is through two branches:

$$^{26}Al \rightarrow {}^{26}Mg + \beta^+\ (85\%) \qquad \textbf{(12.16)}$$

$$^{26}Al + e^- \rightarrow {}^{26}Mg\ (15\%) \qquad \textbf{(12.17)}$$

The γ spectrum thus shows the characteristic 511 keV line from annihilation of the β^+ particle.

12.6.2 EXPERIMENTAL AND TECHNICAL ASPECTS

^{26}Al is measured with AMS as Al_2O_3 containing less than 2 mg of Al. This is mixed with silver powder for use as the accelerator target.

12.6.3 NATURAL ABUNDANCE

The atmospheric production rate of ^{26}Al is about 1 atom $m^{-2}s^{-1}$. The production rate, however, varies with latitude, altitude and geologic times. This secular variation is parallel to that of ^{14}C and ^{10}Be.

12.6.4 APPLICATIONS

The natural occurrence of ^{26}Al is primarily being applied to dating ocean sediments. The advantage of a parallel use of ^{26}Al and ^{10}Be -actually the ratio of the two activities- is that the method then is not dependent of the variations in production rate. From:

$$^{26}Al = {}^{26}Al^{0}\, e^{-\lambda(Al)t} \qquad \text{and} \qquad {}^{10}Be = {}^{10}Be^{0}\, e^{-\lambda(Be)t}$$

we calculate the ratio:

$$(^{26}Al/^{10}Be) = (^{26}Al/^{10}Be)^{0}\, e^{-\lambda' t} \tag{12.18}$$

where $\lambda' = \lambda_{Al} - \lambda_{Be} = 0.50 \times 10^{-6}\ a^{-1}$. The ratio decreases in time corresponding to this decay constant. The other application is the dating of polar ice.

12.7 SILICON

Table 12.8 Natural isotopes of silicon

	$^{28}_{14}Si$	$^{29}_{14}Si$	$^{30}_{14}Si$	$^{32}_{14}Si$
Stability	Stable	Stable	Stable	Radioactive
Natural abundance fraction	92.2 %	4.7 %	3.1 %	
Natural abundance rainwater				5×10^{-6} Bq/L
Half-life ($T_{1/2}$)				140 a
Decay constant (λ)				$1.57\times10^{-10}\ s^{-1}$
Decay mode / Daughters				$\beta^- / {}^{32}P$, $\beta^- / {}^{32}S$

12.7.1 ORIGIN AND CHARACTERISTICS

The origin of ^{32}Si is cosmogenic, i.e. it is being produced by bombardment of ^{40}Ar atoms in the atmosphere by neutron from cosmic radiation:

$$^{40}Ar\ (n,sp)\ ^{32}Si \tag{12.19}$$

It decays through β^- emission ($E_{\beta max} = 100$ keV) to the radioactive daughter ^{32}P, which in turn decays through β^- emission to stable ^{32}S with a half-life of 14.3 d:

$$^{32}Si \rightarrow \beta^- + {}^{32}P \rightarrow \beta^+ + {}^{32}S \tag{12.20}$$

Because the activity of ^{32}Si itself is hard to determine, because of the extremely low activity in nature and the complicated decay process. The consequence was that as recent as 1981 the half-life was still believed to be about 650 a. The AMS technique has allowed better (although still somewhat uncertain) measurements, resulting in values of 140 ± 20 a.

12.7.2 NATURAL ABUNDANCE

The cosmogenic ^{32}Si activity is about 5 mB/m^3 of rainwater, again depending on latitude (Dansgaard et al., 1966; Morgenstern et al., 1995). This value decreases more rapidly in the soil, not because of radioactive decay but as a result of adsorption to soil minerals. During the period of nuclear weapons testing in the early 1960s the ^{32}Si activity was about 4 times as high, but the natural level has most probably returned.

12.7.3 EXPERIMENTAL AND TECHNICAL ASPECTS

The original method of measuring a ^{32}Si activity is by chemically separating and purifying the silicon content of the original sample and have the radioactive daughter ^{32}P accumulating in this silicon for some months. This example of a transient equilibrium between a parent and daughter activity was treated in Sect.6.6.1. it was shown in Fig.6.5 that the maximum daughter (in casu ^{32}P) activity is reached in a period of a few daughter half-lives. The ^{32}P activity is relatively easy to detect –apart from the very low intensity- because of the simple decay scheme: only one β^- decay with $E_{\beta max}$ of 1.7 MeV, and no γ radiation. The chemical extraction procedure is laborious since silicate is to be separated from more than a m^3 of water or ice.

Heinemeier et al. (1987) applied the AMS technique to the analysis of ^{32}Si.

12.7.4 APPLICATIONS

Originally ^{32}Si was expected to close the gap in the datable-age range between ^{3}H and ^{14}C in groundwater. However, at present the abundance of ^{32}Si in groundwater is still problematic and ^{32}Si dating is hardly applied. The reason is primarily the occurrence of disturbing geochemical processes in the soil, involving adsorption and exchange of dissolved silicate (including ^{32}Si) with the soil matrix.

12.8 SULPHUR

Studying sulphur in the water cycle especially concerns the behaviour of dissolved sulphate. It is often useful to study the oxygen isotopic composition of the sulphate compounds, in combination with $^{34}S/^{32}S$.

Table 12.9 Natural isotopes of sulphur

	$^{32}_{16}S$	$^{33}_{16}S$	$^{34}_{16}S$	$^{36}_{16}S$
Stability	Stable	Stable	Stable	Stable
Natural abundance fraction	95.02 %	0.75 %	4.21 %	0.02 %

12.8.1 EXPERIMENTAL AND TECHNICAL ASPECTS

Variations in the relative abundance of the sulphur isotopes, ^{32}S and ^{34}S, are reported as $^{34}\delta$, defined as:

$$^{34}\delta = \frac{(^{34}S/^{32}S)_{sample}}{(^{34}S/^{32}S)_{reference}} - 1 \qquad \textbf{(12.21)}$$

As the internationally adopted primary reference or standard has been chosen the Canyon Diablo Troilite (CDT), the FeS phase from an iron meteorite collected around Meteor Crater, Arizona with an absolute $^{34}S/^{32}S$ ratio of 0.045005. However, since a few problems showed up with this material, it was decided to establish a new reference material, of which $^{34}\delta$ is carefully defined relative to CDT. An analogous procedure was followed as for the stable carbon and oxygen isotopes: the new "standard", NZ1, a homogeneous Ag_2S powder, has been accepted to define the new V-CDT scale which is very close to the original CDT scale:

$$^{34}\delta(\text{NZ1 vs V-CDT}) = -0.30\ ‰ \qquad \textbf{(12.22)}$$

From now on all $^{34}\delta$ values are given relative to V-CDT (very close to the original CDT. Furthermore, a series of additional reference samples is in preparation by the care of the IAEA.

Mass spectrometric measurements are carried out on gaseous SO_2 or SF_6. The disadvantage of the first is that, measuring the ion beam ratio [66]/[64] = $[^{34}S^{16}O_2]/[^{32}S^{16}O_2]$ a correction is needed for the presence of $[^{32}S^{18}O^{16}O]$ in the mass<66> ion beam. SO_2 is prepared by oxidation of Ag_2S made of original compounds such as SO_4^{2-} (dissolved or crystalline), gaseous H_2S, or solid sulphides. A disadvantage of the use of SF_6 is that handling fluorineneeds extremely strict safety precautions.

For a $^{34}S/^{32}S$ analysis about 100 mg of S is needed, at the same time sufficient for a $^{18}O/^{16}O$ analysis of the oxygen content of sulphate.

12.8.2 NATURAL ABUNDANCE

Variations in the natural abundance are caused by chemical and biological isotope fractionation processes in the sulphur cycle. Isotopic exchange between dissolved SO_4^{2-} and HS^- (for S isotopes) and between SO_4^{2-} and H_2O are extremely slow processes and can under surface conditions not been observed.

On the other hand, biological (bacterial) processes cause kinetic isotope fractionation. In general, ^{34}S is enriched in sulphate –such as dissolved in the oceans- and depleted in sulphide. This effect is observed during *sulphate reduction*, where S^{6+} is reduced to S^{2-}. The isotope fractionation involved is:

$$^{34}\varepsilon(\ SO_4^{2-} \rightarrow HS^-\ ) = {}^{34}R(HS^-) / {}^{34}(SO_4^{2-}) = -\ 22\ ‰ \qquad \textbf{(12.23)}$$

Oceanic sulphate and the evaporative minerals derived thereof have $^{34}\delta$ values of + 20‰. The $^{18}\delta$ value of oceanic dissolved SO_4^{2-} is + 9.6‰. Rainfall sulphate, originating from oxidation of $(CH_3)S(CH_3)$, dimethylsulphide, a product from decomposition of marine plankton, has $^{34}\delta$ values of about + 5‰.

12.8.3 APPLICATIONS

A general problem with sulphur isotopes is that isotopic values of certain compounds may vary greatly, even if the compounds that have in principle the same type of origin.

Despite that, many exchange processes between S (and O) containing compounds mutually, and between these and water is that in the aqueous environment the isotopes can often be used to identify their sources. Furthermore, $^{34}S/^{32}S$ –occasionally in combination with $^{18}O/^{16}O$– is applied to observe special biochemical processes in surface- and groundwater (Pearson et al., 1980; Krouse, 1980).

12.9 CHLORINE

12.9.1 RADIOACTIVE ^{36}Cl

12.9.1.1 ORIGIN AND CHARACTERISTICS

Production **in the atmosphere** goes through the action of cosmic protons or neutrons:

1) $^{40}Ar\ (p,sp)\ ^{36}Cl$ **(12.24)**

2) $^{36}Ar\ (n,p)\ ^{36}Cl$ **(12.25)**

The cosmic-ray produced ^{36}Cl fall-out rate from the atmosphere is estimated to be 26 atoms $m^{-2}\ s^{-1}$.

Underground ^{36}Cl is being formed near the surface by the action of thermal (= low-energy) neutrons or cosmic-ray muons:

3) $^{35}Cl\ (n,\gamma)\ ^{36}Cl$ and $^{39}K\ (n \text{ or } \mu,\alpha)\ ^{36}K$ **(12.26)**

or at large depth by:

4) $^{35}Cl\ (n,\gamma)\ ^{36}Cl$ **(12.27)**

This production rate largely depends on the concentration of uranium and thorium in the aquifer rock or sediment.

Thermonuclear tests, especially in the Southern Pacific ocean, have temporarily produced large amounts of ^{36}Cl by neutron activation of chloride:

5) $^{35}Cl\ (n,\gamma)\ ^{36}Cl$ **(12.28)**

Table 12.10 Natural isotopes of chlorine

	$^{35}_{17}Cl$	$^{36}_{17}Cl$	$^{37}_{17}Cl$
Stability	Stable	Radioactive	Stable
Natural abundance fraction	75.5 %	10^{-15} to 10^{-13}	24.5 %
Natural abundance in water		4×10^{5} to 5×10^{8} atoms/L	
Half-life ($T_{1/2}$)		3.01×10^{5} a	
Decay constant (λ)		7.30×10^{-14} s^{-1}	
Decay mode / Daughter		β^- / ^{36}Ar	

12.9.1.2 EXPERIMENTAL AND TECHNICAL ASPECTS

Although ^{36}Cl is radioactive and decays through energetic β^- radiation (β_{max} ~700 keV), quantitative detection is difficult because of the very low specific activity. Measurements of the ^{36}Cl abundance in water have been carried out by liquid scintillation (Roman and Airey, 1981). Most natural ^{36}Cl levels, however, came within reach with the introduction of the AMS technique (Bentley et al., 1986). The detection limit for the $^{36}Cl/Cl$ ratio is about 10^{-15}.

About 10 mg of chlorine is needed for an AMS analysis. It is concentrated from a water sample or leached from a sediment and precipitated as AgCl, which is brought on the target holder.

12.9.1.3 ABUNDANCE IN NATURE

Under natural conditions, $^{36}Cl/Cl$ concentration ratios are observed of 10^{-15} to 10^{-13}. With a chloride concentration of [Cl] mg/L of water, this comes to a concentration of ^{36}Cl atoms of:

$$^{36}N = (6\times10^{23}\times10^{-3}/35.5)\times(^{36}Cl/Cl)\times[Cl] \text{ atoms/L}$$

which is in the order of (10^4 to 10^6) ^{36}Cl atoms / L of water per mg/L chloride concentration.

In order to estimate the recharge rate of ^{36}Cl (^{36}N) in atoms per L of infiltrating water, the amount of precipitation (P in mm/a) and evaporation (E in %) have to be known:

$$^{36}N = 3.2\times10^{7}(\text{sec/year}) \times F / [P \times (100 - E)/100] \text{ atoms/L}$$

(Lehman et al., 1991). With F = 26 atoms m^{-2} s^{-1} this comes in a moderate climate to a range of $(0.6 \text{ to } 3)\times10^6$ atoms/L. In most groundwaters the observed values are considerably larger. This is due to the *in situ*, i.e. underground production of ^{36}Cl.

The nuclear tests produced large amounts of ^{36}Cl in seawater, subsequently in part injected into the stratosphere. During the early 1960s the ^{36}Cl fall-out increased to values in the range of 10^4 atoms $m^{-2}s^{-1}$. This resulted in ^{36}Cl concentrations in water in the order of 7×10^8 atoms/L.

^{36}Cl meanwhile returned to its original natural level, contrary to ^{14}C and ^{3}H. The temporarily increased levels can thus be used to trace infiltrated soil moisture during recent decades.

12.9.1.4 APPLICATIONS

12.9.1.4.1 Dating old water

Due to its long half-life, ^{36}Cl is suitable to date old groundwater, i.e. water in excess of 50 000 years old. For deep-underground water there are two sources of ^{36}Cl, i.e. (i) the cosmogenic source, depicted by the $^{36}Cl/Cl$ ratio $^{36}R_0$, and (ii) the underground production by neutron activation of ^{35}Cl, depicted by the ratio $^{36}R_{se}$. The actual ratio to be measured in the water sample is then:

$$^{36}R = {}^{36}R_0\, e^{-\lambda t} + {}^{36}R_{se}\,(1 - e^{-\lambda t})$$

containing the production term given in Eq.6.30.

From this the water age is:

$$t = -\frac{1}{{}^{36}\lambda} \ln \frac{{}^{36}R - {}^{36}R_{se}}{{}^{36}R_0 - {}^{36}R_{se}} \qquad \textbf{(11.29)}$$

where $^{36}\lambda = \ln 2 / (3.2\times10^7)s^{-1}$. R_{se} has to be obtained by analysing the $^{36}Cl/Cl$ ratio of the source rock.

12.9.1.4.2 Infiltration of young water

By observing the relatively high ^{36}Cl content of undeep water from the era of nuclear weapons testing, ages of infiltrated water can be determined of up to a few decades, resulting in values for the infiltration rate (Bentley et al., 1982).

12.9.2 STABLE ^{35}Cl AND ^{37}Cl

12.9.2.1 NATURAL ABUNDANCE AND APPLICATIONS

Because the chlorine ion, Cl^-, is very little reactive, the isotopic variations denoted by;

$$^{37}\delta = (^{37}Cl/^{35}Cl)_{sample} / (^{37}Cl/^{35}Cl)_{seawater\ NaCl} - 1 \qquad \textbf{(12.30)}$$

are very small. Attempts have been made to apply chlorine isotopes to study the characteristics of brines (Eggenkamp, 1994) and the degradation and distribution of Cl containing contaminants (Van Warmerdam et al., 1995).

Stable isotope fractionation involved in Cl^- diffusion through sediments is equals the ratio of the diffusion coefficients (Sect.3.5). Since the Cl^- ions are hydrated, i.e. coupled to water molecules, the diffusion constant of the chlorine ion through water is determined by the masses of the hydrated ions (with n H_2O molecules). For the diffusion of molecule M_A through a medium of molecules M_B (* indicates the rare isotope, i.e. ^{37}Cl, the fractionation factor is (Eq.3.34):

$$^{37}\alpha = \sqrt{\frac{M_A(*M_A + M_B)}{*M_A(M_A + M_B)}} = \sqrt{\frac{[35+18n]([37+18n]+18)}{[37+18n]([35+18n]+18)}} \qquad \textbf{(12.31)}$$

For a hydration rate of n = 4 the resulting fractionation factor is 0.9987; for n = 2, $^{37}\alpha$ = 0.9972 (cf. Eggenkamp, 1994).

12.9.2.2 EXPERIMENTAL AND TECHNICAL ASPECTS

AgCl is precipitated from the water sample by adding $AgNO_3$. The resulting AgCl is purified and reacted with CH_3I to methylchloride, CH_3Cl. This gas is suitable for measuring the $^{37}Cl/^{35}Cl$ ratio by normal IRMS.

The reference for chlorine isotopes is Standard Mean Ocean Chloride (SMOC), as the isotopic composition in seawater chloride is very constant. The $^{37}Cl/^{35}Cl$ ratio of this standard is 0.324.

12.10 ARGON

12.10.1 ORIGIN AND CHARACTERISTICS

The short-living radioactive isotope of Ar, ^{37}Ar, is cosmogenic as a spallation product of ^{40}Ar, and is being produced **underground** by neutrons from Th and U fission:

$$^{40}Ca\ (n,\alpha)\ ^{37}Ar \qquad \textbf{(12.32)}$$

Table 12.11 Natural isotopes of argon.

	$^{36}_{18}Ar$	$^{37}_{18}Ar$	$^{38}_{18}Ar$	$^{39}_{18}Ar$	$^{40}_{18}Ar$
Stability	Stable	Radioactive	Stable	Radioactive	Stable
Natural abundance fraction	0.33 %		0.06 %	8.5×10^{-16}	99.6 %
Natural abundance in air	3.15×10^{-5}		5.9×10^{-6}		9.34×10^{-3}
Natural abundance in water		70 atoms/m^3		8500 atoms/L	
Specific activity in air (Bq/L)		$3\times10^{-7\ to\ -9}$		1.68×10^{-5}	
Half-life ($T_{1/2}$)		35.1 d		269 a	
Decay constant (λ)		$2.31\times10^{-7}\ s^{-1}$		$8.17\times10^{-11}\ s^{-1}$	
Decay mode / Daughter		EC / ^{37}Cl		β^- / ^{39}K	

together with the long-living argon isotope, ^{39}Ar:

$$^{38}Ar\ (n,\gamma)\ ^{39}Ar \qquad \textbf{(12.33)}$$

$$^{39}K\ (n,p)\ ^{39}Ar \qquad \textbf{(12.34)}$$

$$^{42}Ca\ (n,\alpha)\ ^{39}Ar \qquad \textbf{(12.35)}$$

The latter is primarily produced **in the atmosphere** by the reaction:

$$^{40}Ar\ (n,2n)\ ^{39}Ar \qquad \textbf{(12.36)}$$

The respective decay modes are:

$$^{37}Ar + e^- \rightarrow {}^{37}Cl \qquad \textbf{(12.37)}$$

in combination with the emission of X rays, and

$$^{39}Ar \rightarrow {}^{39}K + \beta^- \qquad \textbf{(12.38)}$$

with a maximum β^- energy of 565 keV.

12.10.2 EXPERIMENTAL AND TECHNICAL ASPECTS

From a few hundred litres of water sample the noble gases are extracted and argon separated gas chromatographically. The subsequent proportional counting of the ^{39}Ar β^- decay requires at least 2 L of argon extracted from about 15 m^3 of water (Loosli and Oeschger, 1979). This degassing procedure is carried ouit in the field.

12.10.3 NATURAL ABUNDANCE

The natural specific activity of ^{39}Ar in the atmosphere is about 2 mBq/L of Ar and is reported to be constant within 7 % (Forster et al., 1992), corresponding to about 0.5 mBq/m^3 of water. Underground ^{39}Ar is produced in the presence of neutron from spontaneous fission of Th and U (Eq.12.33-35). The ^{37}Ar abundance is much smaller (Table 12.11).

12.10.4 APPLICATIONS

With its half-life of 269 years, ^{39}Ar is suitable to fill the gap in dating range between ^{3}H and ^{14}C. The advantage is that it is chemically inert. However, the subsurface production of ^{39}Ar makes it problematic. On the other hand, the presence of ^{39}Ar is being used to indicate the underground production of radioisotopes.

^{39}Ar has been shown an excellent isotope for dating glacier ice (Oeschger and Loosli, 1977).

^{39}Ar is applied in oceanography to study the large-scale mixing and circulation.

12.11 KRYPTON

12.11.1 ORIGIN AND CHARACTERISTICS

The long-living krypton isotope ^{81}Kr is produced in the atmosphere by cosmic-ray induced spallation of stable krypton (primarily of ^{84}Kr), and by neutron activation according to:

$$^{80}Kr\ (n,\gamma)\ ^{81}Kr \qquad \textbf{(12.39)}$$

The same reaction is responsible for the production during nuclear test explosions, with additionally:

$$^{82}Kr\ (n,2n)\ ^{81}Kr \qquad \textbf{(12.40)}$$

and through fission of uranium. The ^{81}Kr contribution from bomb testing is considerably smaller than the natural atmospheric ^{81}Kr content (Collon et al. 1997).

The underground production of ^{81}Kr is negligibly small.

^{81}Kr decays by electron capture and emitting 13.5 keV X rays according to:

$$^{81}Kr + e^- (K) \rightarrow {}^{81}Br \qquad \textbf{(12.41)}$$

12.11.2 EXPERIMENTAL AND TECHNICAL ASPECTS

^{81}Kr is detected by radiometry or by AMS. The consequence of the low ^{81}Kr activity compared to the present-day ^{85}Kr activity is that it is no longer possible to measure the atmospheric ^{81}Kr content by radiometric means.

For a ^{85}Kr measurement about 20 µL of krypton gas is needed, to be extracted from the water sample.

Table 12.12 Natural isotopes of krypton

	$^{78}_{36}Kr$	$^{80}_{36}Kr$	$^{81}_{36}Kr$	$^{82}_{36}Kr$
Stability	Stable	Stable	Radioactive	Stable
Natural abundance fraction	0.354 %	2.27 %	$\sim 5\times10^{-13}$	11.56 %
Natural abundance in air	4.0×10^{-9}	2.59×10^{-8}		1.317×10^{-7}
Natural abundance in water			1200 atoms/L	
Half-life ($T_{1/2}$)			2.1×10^5 a	
Decay constant (λ)			1.05×10^{-13} s^{-1}	
Decay mode / Daughter			EC / ^{81}Br	
	$^{83}_{36}Kr$	$^{84}_{36}Kr$	$^{85}_{36}Kr$	$^{86}_{36}Kr$
Stability	stable	stable	radioactive	stable
Natural abundance fraction	11.55 %	56.90 %	1.8×10^{-11}	17.37 %
Natural abundance in air	1.316×10^{-7}	6.48×10^{-7}	2.1×10^{-17}	1.98×10^{-7}
Specific activity in air			1.1 mBq/L *)	
Natural abundance in water			2.5×10^{-6} Bq/L	
Half-life ($T_{1/2}$)			10.76 a	
Decay constant (λ)			2.04×10^{-9} s^{-1}	
Decay mode / Daughter			β^- / ^{85}Rb	

*) Valid for the year 1990, steadily increasing by about 0.025 mBq/L per year (Weiss et al., 1992).

^{85}Kr on the other hand can be measured radiometrically as a mixture of a few μL of krypton, condensed from the original sample by various cold traps and a gas chromatographic separation, with a proper counting gas in a proportional counter. A few hundred litres of groundwater are needed for such ^{85}Kr analysis (Loosli and Oeschger, 1978; Ekwurzel et al., 1994).

12.11.3 NATURAL ABUNDANCE

The natural abundance of the noble gas krypton in the atmosphere is 1.14×10^{-6} ppmv. The estimated pre-nuclear concentration ratio of $^{81}Kr/Kr$ is 5.2×10^{-13}, or a specific activity of 1.5 mBq/L of krypton. Under natural conditions ^{85}Kr was much less abundant, with a $^{85}Kr/Kr$ value of about 3×10^{-18}. However, due to the emission of this isotope as a fission product by the nuclear industry (primarily reprocessing of plutonium as a nuclear fuel), the present-day concentration ratio amounts to 1.5×10^{-11}.

The solubility of krypton in water is 9.3×10^{-5} mL(STP)/L. This means that the maximum concentration of ^{81}Kr is 1300 atoms /L of water.

The natural cosmogenic production rate of ^{85}Kr is extremely small, due to the small reaction cross sections. However, ^{85}Kr is an abundant fission product of uranium and plutonium and is as such during stages of nuclear fuel handling released to the atmosphere. From a very low pre-nuclear level, the atmospheric content has steadily increased to a specific activity of about 1Bq/mL (STP) of krypton in 1990, equivalent to a maximum ^{85}Kr activity of about 0.07 Bq/m^3 of water.

12.11.4 APPLICATIONS

Deep groundwater, isolated from the atmosphere more than 50 years ago, does not contain ^{85}Kr. Consequently ^{81}Kr with its large half-life is in principle an ideal tracer for dating water with (isolation) ages of 50 ka to 1Ma. The problem is the complicated experimental handling and measuring procedure. The first AMS attempts have been promising (Collon, 1997).

As mentioned before, the cosmogenic origin of ^{85}Kr is negligibly small. Therefore, this isotope serves to recognise young groundwaters, and to study their infiltration and hydrodynamics in the soil, especially in combination with ^{3}H.

12.12 IODINE

12.12.1 ORIGIN AND CHARACTERISTICS

^{129}I is naturally produced in the atmosphere by a cosmic-ray induced spallation reaction on xenon. It has also been brought into the atmosphere as a fission product of uranium by nuclear bomb testing and the nuclear industry.

It decays according to:

$$^{129}I \rightarrow {}^{129}Xe + \beta^- \ (E_{max} = 150 \text{ keV}) \qquad \textbf{(12.42)}$$

Table 12.13 Natural isotopes of iodine

	$^{127}_{53}I$	$^{129}_{53}I$
Stability	stable	radioactive
Natural abundance fraction	100 %	$\sim 10^{-12}$
Natural abundance in water		5×10^4 atoms/L
Half-life ($T_{1/2}$)		15.7×10^6 a
Decay constant (λ)		1.40×10^{-15} s^{-1}
Decay mode / Daughter		β^- / ^{129}Xe

12.12.2 EXPERIMENTAL AND TECHNICAL ASPECTS

Nowadays by far the best detection technique is AMS, using 1 to 3 mg of AgI, prepared from iodine extracted from the sample and purified by ion exchange procedures (Sharma et al., 1997). The $^{129}I/I$ detection limit at present is in the order of 10^{-15}.

12.12.3 NATURAL ABUNDANCE

The natural abundance ratio $^{129}I/I$ is about 10^{-12}. This level has increased locally by orders of magnitude due to nuclear bomb testing and the release of ^{129}I as a fission product by nuclear reactors and reprocessing plants. In off-coast ocean surface water the $^{129}I/I$ ratio is estimated to be $\leq 10^{-10}$.

12.12.4 APPLICATIONS

Most applications are devoted to analysing the "nuclear-era" levels of ^{129}I. Especially the high levels in rivers and coastal waters near nuclear industries are being used for tracing oceanic mixing processes and the vertical transport of continental water in the ocean. $^{129}I/I$ values are being observed of up to 10^{-9}.

In groundwater the $^{129}I/I$ ratio is mainly determined by the recharge rate, the rate of leaching from the aquifer rock, and the amount of in situ uranium fission. The latter complicates the dating of deep groundwater.

12.13 DECAY SERIES

In Sect.6.6 we discussed the three *radioactive decay series*. Each chain consists of a parent nuclide which has a half-life larger than the age of the universe, a series of successive α and β decays, and finally a stable isotope of Pb. Because the masses of the successive daughters change only by 4 units and β decay hardly changes the mass, we can speak of the *Thorium series*, or the 4n series (^{232}Th to ^{208}Pb), the *Uranium series*, or the 4n+2 series (^{238}U to ^{206}Pb), and *Actinium series*, or the 4n+3 series (^{235}U to ^{207}Pb). The hypothetical 4n+1 series (possibly ^{237}Np to ^{209}Pb) no longer exists because of the relatively small half-life. Several nuclides show branching decay (either α or β^-); the main decay mode is indicated in Fig.12.2, showing the three decay series. The physical information on the decay and abundance of the members of the decay series is given in Table 12.15.

In old, geochemically undisturbed rock the uranium and thorium containing minerals contain all parent and daughter nuclides in a state of equilibrium. This means that, depending on the relation between half-lives, all members of the decay series are directly or indirectly in secular equilibrium with the parent nuclide, ^{238}U, ^{235}U, or ^{232}Th. In the most abundant ^{238}U, for instance, each ^{238}U is accompanied with a decay from each daughter, granddaughter, and so on. This means that for each ^{238}U decay, now and in the past, 7 more α decays take place. The total number of ^{238}U decays is thus equal to the emission of 8α particles of He atoms. The consequence is that, form the amount of helium gas in a "closed-system" rock, the age, i.e. the time elapsed since the rock matrix became "closed", can be determined. The calculation is a variant of the "daughter accumulation" case, treated in Sect.6.7. The amount of helium in L(STP) per kg of rock produced in a period of time T in a rock with an present-day specific ^{238}U activity of ^{238}A kg^{-1} of rock is:

$$V = 8 \times {}^{238}A(e^{\lambda T} - 1)\,(22.4/6\times10^{23})$$

so that the age T of this rock is

$$T = (1/\lambda)\ln\{[6\times10^{23}V/22.4]/[8\times{}^{238}A] + 1\} \qquad \textbf{(12.43)}$$

This method is referred to as the *U-He dating method*. The same holds for the other decay series, for ^{232}Th with (232–208)/4 = 6 He atoms per decay and for ^{235}U (235–207)/4 = 7 He atoms per decay.

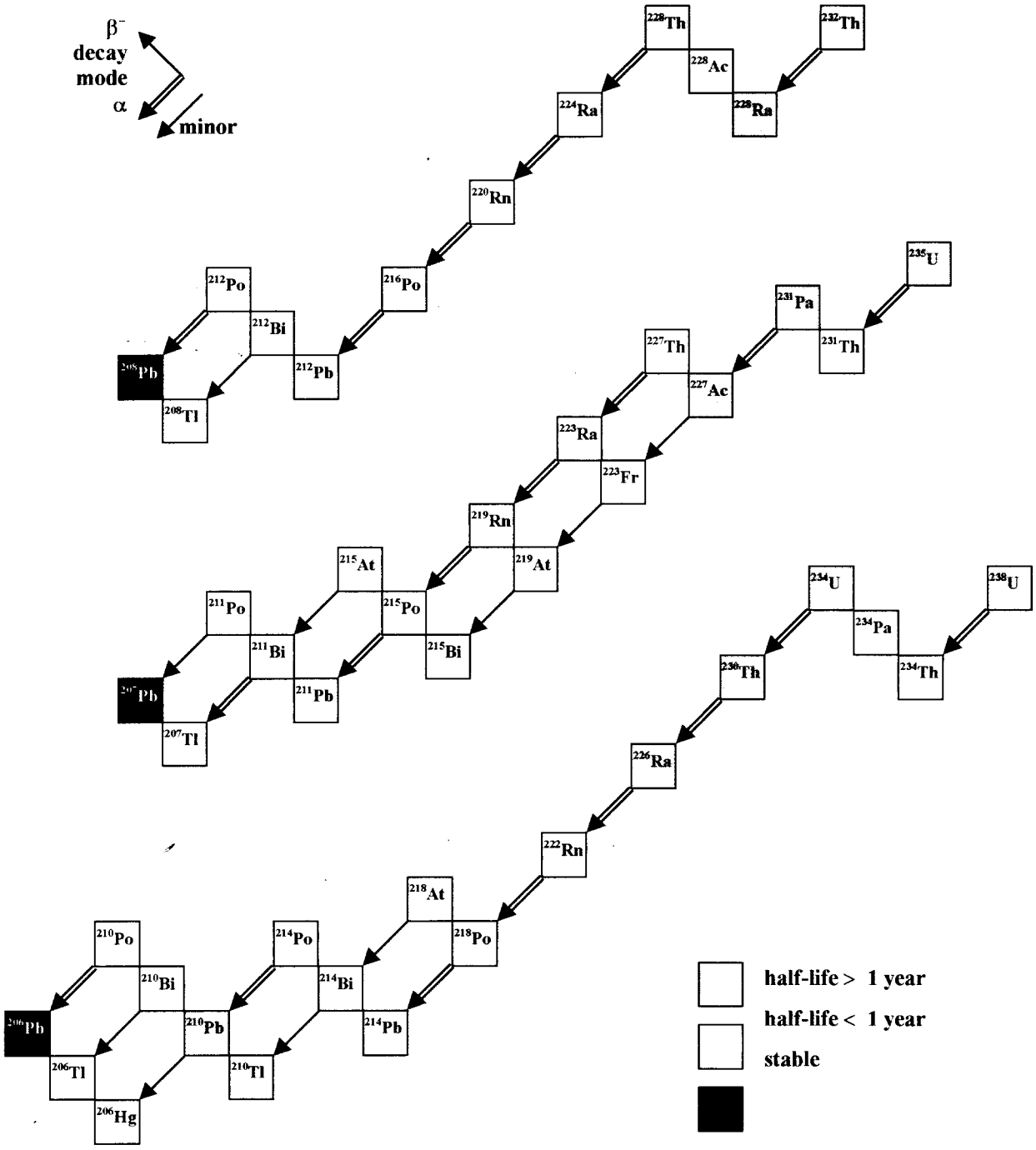

Fig.12.2 The thorium, actinium and uranium decay series according to the Chart of Nuclides (cf. Figs.2.2 and 6.3). The final stable lead isotopes are represented by a black box, the long-living nuclides ($T_{1/2}$ > one year) by a shaded box. The preferential decay modes of branching decay and the resulting decay chain are indicated by a double arrow.

12.14 THE URANIUM SERIES

This decay series is shown as the lower series in Fig.12.2. All physical parameters concerning the radioactive decay are given in Tables 12.14–12.16.

Table 12.14 Natural isotopes of uranium

	$^{234}_{92}U$	$^{235}_{92}U$	$^{238}_{92}U$
Stability	radioactive	radioactive	radioactive
Natural abundance fraction	0.0057 %	0.7200 %	99.2743 %
Half-life ($T_{1/2}$)	2.47×10^5 a	7.038×10^8 a	4.468×10^9 a
Decay constant (λ)	8.892×10^{-14} s^{-1}	3.1208×10^{-17} s^{-1}	4.9156×10^{-18} s^{-1}
Decay mode / Daughter	α / ^{230}Th (decay series→ ^{206}Pb)	α / ^{231}Th (decay series→ ^{207}Pb)	α / ^{234}Th (decay series→ ^{206}Pb)

12.14.1 $^{238}U/^{234}U$

In a state of secular equilibrium (i.e. $^{238}\lambda^{238}N = {}^{234}\lambda^{234}N$) the abundance ratio of $^{234}U/^{238}U$ is inversely proportional to their decay constants or proportional to the half-lives = 5.48×10^{-5}, while the activity ratio $^{234}A/^{238}A = 1$.

The solubility of uranium in water depends on the oxidation state. The U^{6+} state (as UO_2^{2+}) is more soluble that the reduced state U^{4+} (as UO_2^{+}). As ^{234}U and ^{238}U are having the same solubility in water, one would expect the activity ratio in dissolved uranium to be =1. However, this is generally not the case, because ^{234}U is preferentially leached from the rock. As a consequence of the recoil energy given to the ^{234}Th daughter during the ^{238}U decay (Sect.5.3), the bond between ^{234}Th (and the subsequent daughters ^{234}Pa and ^{234}U) and the crystal matrix is broken, so that the ^{234}U atom is more free to enter the solution than the remaining ^{238}U atoms. The actual $^{234}U/^{238}U$ ratio in the water depends on several (geo)chemical conditions within the aquifer. Values of 2 to 3, and up to 10 have been observed. The absence of an equilibrium between the activities is referred to as the *$^{234}U/^{238}U$ disequilibrium*. The growth rate of this ratio in a closed system can be used to study the hydrogeological and geochemical conditions and the transport of groundwater masses (Pearson et al., 1991).

In seawater the $^{234}U/^{238}U$ ratio is also larger than one, due to the effluence of continental freshwater. Commonly values of about 1.4 are being observed.

12.14.2 $^{230}Th - ^{234}U$ DATING

The relation between the activities of ^{234}U and its daughter ^{230}Th is an example of a transient equilibrium (Sect.6.6.2). Because Th is extremely insoluble in water, natural waters contain uranium isotopes in the absence of Th isotopes. This is the basis for a dating method of corals (Bard et al., 1998) and continental sediments like peat (Vogel and Kronfeld, 1980; Van der Wijk, 1988), referred to as *U–Th disequilibrium dating*. ^{234}U is being taken up by the organisms or sediment without the radioactive daughter ^{230}Th. The latter grows into the sample with increasing age. Equations apply discussed in Sect.6.6. Especially the dating of corals has been very successful, because under marine conditions the starting conditions (no Th isotopes, constant ^{234}U activity) are relatively simple.

12.14.3 ^{226}Ra AND ^{222}Rn

Through recoil during the α decay of ^{230}Th, ^{226}Ra can easily be leached from the rock matrix. Radium is present in solution as the divalent alkali-earth cation and behaves chemically like Ca^{2+} and Ba^{2+}. In groundwater specific activities can be observed of up to 5 Bq/L.

The daughter of ^{226}Ra is ^{222}Rn, a radioactive radon isotope with a half-life of 3.8 days. As a noble gas, ^{222}Rn is not being absorbed by solids. Moreover, it is highly soluble in water, contrary to ^{226}Ra. Consequently, ^{222}Rn is likely to accumulate in groundwater. The specific activity can exceed that of its parent ^{226}Ra by orders of magnitude. Because of its short half-life, ^{222}Rn is indicative for young groundwaters. As radon can easily be removed from water, the in-growth of ^{222}Rn in artificially recharged water can be used to estimate residence times.

12.14.4 ^{210}Pb

For the sake of completeness we mention the existence of a relatively long-living member of the uranium series, the radioactive isotope of lead, ^{210}Pb. For hydrological applications this nuclide has little relevance. However, it is extensively used for measuring the accumulation rate of ice or sediments. As an inert gas ^{222}Rn escapes from the soil and subsequently decays in the atmosphere by way of short-living daughters to ^{210}Pb (Fig.12.2). After a short residence time in the air it is deposited either by wet or dry precipitation together with snow (to form ice) or sediment in water. The deposition rate is in the range of 6 to 10 mBq cm^{-1} a^{-1} (Van der Wijk and Mook, 1987). In ice or in aqueous sediments it decays with a half-life of 22.26 a, and can be applied for determining ages up to about 100 years.

12.14.5 EXPERIMENTAL AND TECHNICAL ASPECTS

Originally the α activities were measured by α spectrometry (Van der Wijk, 1987). A few micrograms of uranium is needed for providing a pure metallic, electroplated uranium source for an α detector. The modern mass spectrometric technique (Thermal Ionisation Mass Spectrometry, TIMS) needs less sample and has a lower detection limit, while the results are more precise and obtained faster. The capital investment, however, is a factor of 10 larger.

The α activity of radon isotopes is measured by proportional gas counting.

The activity of ^{210}Pb is measured indirectly by detecting the ingrowth of ^{210}Po in the pure Pb source by α counting. Similarly is the activity of ^{226}Ra measured by ingrowth of ^{222}Rn in the pure radium sample.

12.15 THE ACTINIUM SERIES

The information on decay and abundance is shown in Table 12.14 and Table 12.16. The decay scheme is presented in Fig.12.2.

This series start with the ^{235}U parent and goes through 7 α decays and 4 β decays to stable ^{207}Pb. It is the less abundant isotope of uranium. The concentration ratio has been internationally established as ^{238}U/^{235}U = 137.88.

The daughter element of ^{235}U, protoactinium (^{231}Pa), is equally insoluble in water as thorium. This means that in an aqueous environment the element Pa is rapidly removed from the water. The sediment then contains "unsupported" Pa, i.e. without ^{235}U, so that the decay of ^{231}Pa in the sample is indicative for the age of the sediment. In the next section ^{230}Th will turn out to have the same characteristic (Faure, 1986).

12.16 THE THORIUM SERIES

Table 12.15 Natural isotopes of thorium

	$^{230}_{90}$Th	$^{232}_{90}$Th
Stability	radioactive	radioactive
Natural abundance fraction		100 %
Half-life ($T_{1/2}$)	7.5×10^4 a	1.4010×10^{10} a
Decay constant (λ)	2.93×10^{-13} s^{-1}	1.5678×10^{-18} s^{-1}
Decay mode / Daughter	α / ^{226}Ra (decay series)	α / ^{228}Ra (decay series)

Physical data on the decay and abundance are given in Fig.12.2 and in Tables 12.15-16.

The abundance and the application of the long-living member of the ^{238}U series, ^{230}Th, the daughter of ^{234}U, has been discussed in Sect.12.14.2. Also the combination of the geochemically analogous Pa isotope, ^{231}Pa, both being highly insoluble in water and therefore "unsupportedly" included in a marine sediment, was mentioned earlier. Especially the combination of the two isotopes is valuable, because the decay rates are different. It can be shown that this information cancels the need for knowing both specific activities at the time of sedimentation. The change of the initial ratio of the specific activities in time is indicative for the age.

The couple of parent nuclide ^{232}Th and daughter ^{228}Ra plays a role in studying water-rock interaction. Important is the chemical difference between Th and Ra, the first being much less soluble than the latter. Activity ratios that are expected to be =1 under conditions of decay equilibrium, may be <1 if the rock minerals have lost ^{228}Ra after ^{232}Th recoil or if the sediment is accumulating ^{228}Ra from its parent decay, and > 1 where uptake of ^{228}Ra has taken place from the surrounding water.

Direct hydrological applications of ^{232}Th are unlikely, due to the extremely low solubility of thorium in water.

Table 12.16 Nuclear data on the decay and abundance of the member nuclides of the uranium, actinium and thorium decay series (data from Lederer and Shirley, 1978). The decay of α and β is followed by one or more γ emissions. Where the decay is branching, the least abundant decay mode is given in parenthesis; a = year, d = day, m = minute, s = second

	Half-life	Decay	Abundance
^{238}U	4.468×10^{9} a	α	99.2743%
^{235}U	7.038×10^{8} a	α	0.7200%
^{234}U	2.47×10^{5} a	α	0.0057%
^{234}Pa	1.175 m	β	
^{231}Pa	3.28×10^{4} a	α	
^{234}Th	24.10 d	β	
^{232}Th	1.4010×10^{10} a	α	100%
^{231}Th	25.52 h	β	
^{230}Th	8.0×10^{4} a	α	
^{228}Th	1.913 a	α	
^{227}Th	18.72 d	α	
^{228}Ac	6.13 h	β	
^{227}Ac	21.77 a	(α),β	
^{228}Ra	5.76 a	β	
^{226}Ra	1.60×10^{3} a	α	
^{224}Ra	3.66 d	α	
^{223}Ra	11.44 d	α	
^{223}Fr	21.8 m	(α),β	
^{222}Rn	3.82 d	α	
^{220}Rn	55.6 s	α	
^{219}Rn	3.96 s	α	
^{219}At	0.9 m	α,(β)	
^{218}At	~2 s	α	
^{215}At	0.1 ms	α	
^{218}Po	3.05 m	α,(β)	
^{216}Po	0.15 s	α	
^{215}Po	1.78 ms	α(β)	
^{214}Po	164 μs	α	
^{212}Po	0.30 μs	α	

^{211}**Po**	0.516 s	α	
^{210}**Po**	**138.4 d**	α	
^{215}**Bi**	7.4 m	β	
^{214}**Bi**	**19.7 m**	(α),β	
^{212}**Bi**	**60.6 m**	(α),β	
^{211}**Bi**	**2.15 m**	α,(β)	
^{210}**Bi**	**5.01 d**	(α),β	
^{214}**Pb**	**26.8 m**	β	
^{212}**Pb**	10.64 h	β	
^{211}**Pb**	**36.1 m**	β	
^{210}**Pb**	**22.26 a**	(α),β	
^{208}**Pb**	**stable**	--	**52.3%**
^{207}**Pb**	**stable**	--	**22.1%**
^{206}**Pb**	**stable**	--	**24.1%**
^{210}**Tl**	1.30 m	β	
^{208}**Tl**	3.05 m	β	
^{207}**Tl**	**4.8 m**	β	
^{206}**Tl**	4.2 m	β no γ	
^{206}**Hg**	8.1 m	β	

13 ERRORS, MEANS AND FITS

This chapter contains a choise of essential information on the analysis of measuring uncertainties, and the treatment of large numbers of data. Starting with a discussion on "errors", we arrive at a technique of judging the probability of the truth of a final result.

13.1 ERRORS

In dictionaries the word *error* is defined as the difference between the approximated value –as the result of an observation or measurement, or a calculation- and the true value. The problem is that in general we do not know the "true value", as this is generally the result of a measurement or calculation. Therefore, we have to find a way of estimating the "reliability" of our result.

The name "errors" is not well specified as such. We thus have to become more specific about the definition. Errors can be classified as follows:

1) *Blunders* or *mistakes* in measurement or calculation are usually apparent as being far from expectations. They are to be dealt with by repeating the measurement or calculation.

2) *Systematic errors* are more difficult to detect. They are reproducible discrepancies, often the result of a failure in the instrumentation or a consistent mathematical insufficiency. They are to be found (and corrected for!) by repeating the analysis with different equipment or by recalculation (by a colleague or by different means).

3) *Random errors* are the most common type of errors. They are the result of the unavoidably limited quality of our instrumentation. They can only be partly overcome by refining the instrumentation or the analytical method, and by repeating the measurements (such as reading a temperature or pH) or extending the observation time (for instance, of radioactivity).

13.2 PRECISION AND ACCURACY

13.2.1 DEFINITIONS

It is important to distinguish between precision of and accuracy.

1) The *precision* of a result is a measure of the reproducibility of an observation, of how well the result can be determined, irrespective of how close the result is to the "true" value. The associated "error" is better referred to as the *uncertainty* of a result.

2) The *accuracy* is a measure of the correctness of an observation, of how close the result is to the "true" value.

The two sets of definitions we have given are simply related.

- Precision is a measure of the size of random errors. If we are able to reduce random errors, for instance by better equipment or procedures, the precision of the measurement is better, the result is more precise, and the analysis is more reproducible. Increasing the precision by reducing random errors is a *task of each single laboratory*.
- On the other hand, a systematic error directly effects the accuracy of the measurement; avoiding or eliminating systematic errors makes the result more accurate and trustworthy. Increasing the accuracy of a result is often the goal of *international intercomparisons by a number of laboratories* analysing the same set of samples, and by routinely running standards.

For studying and eventually reducing systematic errors it is important to dispose of data with small random errors, with relatively high precision. On the other hand, it is a waste to spend much effort on increasing the precision, if the systematic error is large. Fig.13.1 illustrates the difference between precision and accuracy.

13.2.2 SIGNIFICANT FIGURES AND DIGITS

When reporting numbers it is a common rule to indicate the uncertainty by the figures and digits of the number given. If a distance is given as 5000 km, it is common sense to trust only the leftmost figure. However, if one is also certain about the next figure (the leftmost 0), it is better to write 5.0×10^3 km. In general, it is preferable to write numbers in the scientific notation, i.e. an argument in decimal notation with a number of digits, multiplied by a power of 10. The rightmost digit contains the uncertainty. As a rule the *precision of the uncertainty* (i.e. the degree of certainty of the uncertainty) is not better than 10% of the uncertainty. For example, if the radioactivity of a sample is determined as 13.56 Bq, it may go with an uncertainty of 13.56±0.12 or 13.56±0.08, but giving an additional digit in the uncertainty like 13.56±0.081 would exaggerate the "certainty of the uncertainty".

The uncertainty also determines the number of digits quoted. For instance, it is right to quote 13.56±0.12 Bq, but it is not consistent to write 13.564±0.12 Bq.

In computer calculations all digits are to be kept; rounding off is done only with the final result. Nevertheless, results written down in the course of a mathematical calculation are to be given with the number of digits that can be justified. The entire calculation itself, however, is to be carried out without intermediate rounding off.

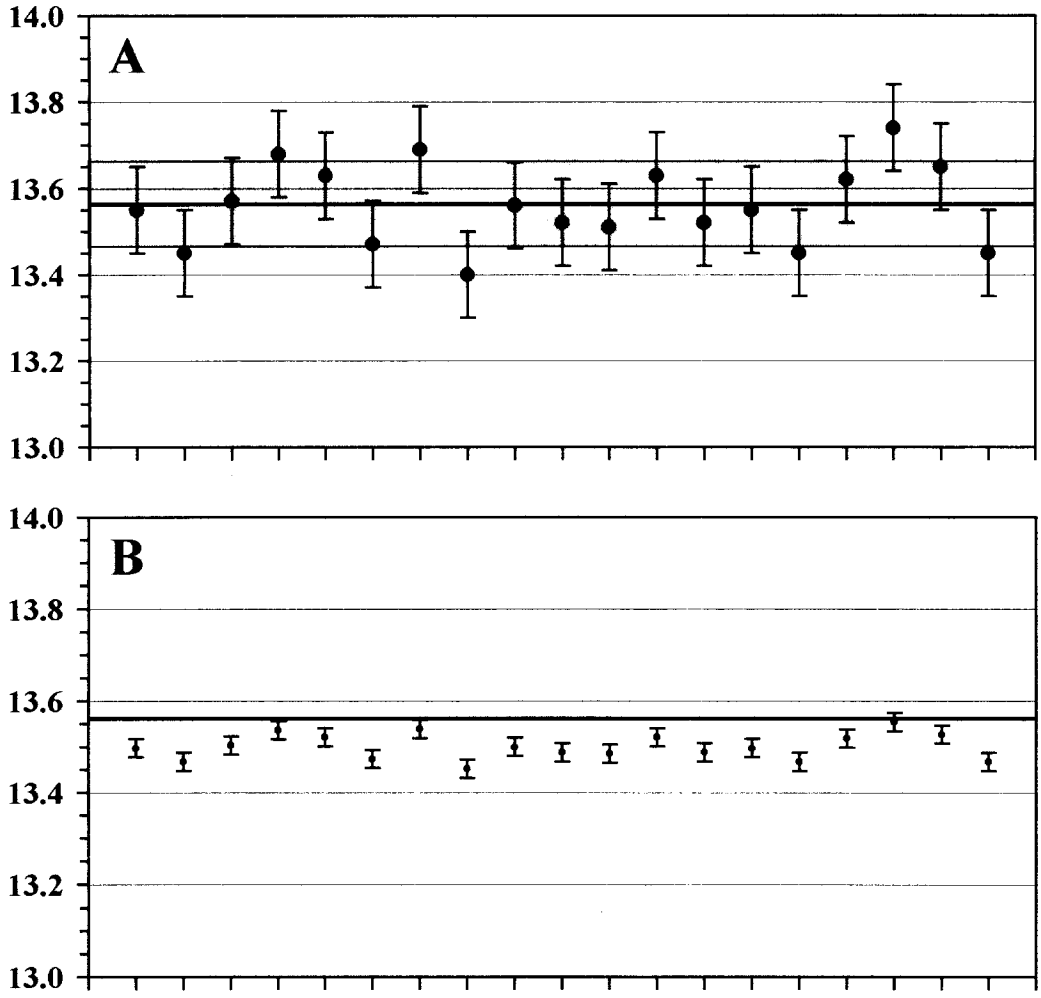

Fig.13.1 Example to illustrate precision and accuracy, showing two series of results from 19 measurements of the same radioactivity.

A. The data are imprecise but accurate, giving the proper average value of 13.56 Bq. The grey area refers to the 1σ confidence level; i.e. 68% of the data should be within this range (example in Sect.13.5.2).

B. The data are precise, but inaccurate probably because of a systematic error, as the average value is now 13.50 Bq, instead of the "true" value of 13.56 Bq.

13.2.3 UNCERTAINTIES

There are two different types of uncertainties.

1) *Instrumental uncertainties*, due to fluctuations in the result of any instrumental observation, whether it concerns measuring the outdoor temperature or weighing your letter on a letter balance, or applying fancy equipment to measure time in the laboratory.

An estimate of the size of the uncertainty can be obtained by an "educated guess", or by repeating the measurement and observe the distribution of the results.

2) *Statistical uncertainties*, due to the fact that certain processes even theoretically show fluctuations. A proper example here is the process of radioactive decay. Even (non-existing) ideal equipment would observe the fluctuation in the activity measurement, or the "statistical spread" in the results. In cases like these procedures exist to determine the uncertainty beyond doubt.

13.3 INSTRUMENTAL UNCERTAINTIES

13.3.1 MEAN VALUES

The *mean* or *average value* of the result of a number of measurements is defined as the sum of the results divided by the number of measurements:

$$\bar{x} \equiv \frac{1}{N}\sum_{i=1}^{N} x_i \equiv (x_1 + x_2 + x_3 + \cdots + x_N)/N \qquad \textbf{(13.1)}$$

N is the number of measurements, i stands for the serial number of an arbitrary measurement and x is the parameter measured. We will often omit N and i = 1, and simply write Σx_i.

The number of measurements is always limited. However, if we would be able to increase this number to infinity, we would end up with a better value of the mean, then defined as

$$\mu \equiv \lim_{N\to\infty} \left(\frac{1}{N}\Sigma x_i\right) \qquad \textbf{(13.2)}$$

The *median* is now defined as the value of the set of data such that the results of half the measurements is smaller, half is larger than the median value. For a symmetrical distribution the mean and the median values are equal. We will later use the deviations of a single result from the mean (or median), $\bar{x} - x_i$; by definition the average deviation of the results from the mean value equals zero:

$$\overline{x_i - \bar{x}} = \frac{1}{N}\sum_{i=1}^{N}(x_i - \bar{x}) = \frac{1}{N}\Sigma x_i - \frac{1}{N}N\bar{x} = \bar{x} - \bar{x} = 0 \qquad \textbf{(13.3)}$$

13.3.2 DISTRIBUTION OF DATA

Results of a number of measurements can be presented in a *histogram*, a graph showing the number of times (y-axis) certain results indicated along the x-axis were obtained (Fig.13.2). It is obvious that the probability of obtaining results further removed from the most frequent

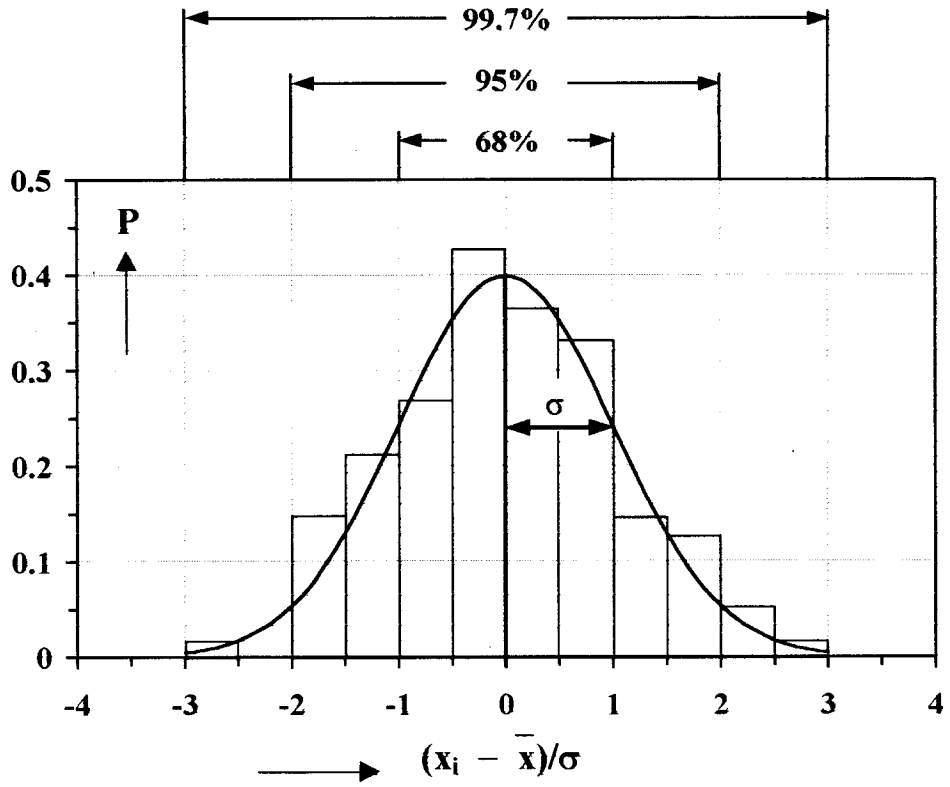

Fig.13.2 Histogram (block-shaped), indicating the irregular distribution of measurement results within a range of $x_{i(\Delta x)}$ i.e. between x_i and $x_i + \Delta x$ around a mean value; the deviations from the mean value ($\bar{x}$) rather than the actual results are given along with the number of observations (y-axis) for values within a certain range. The smooth curve illustrates the Gaussian distribution, which is the hypothetical result of an infinite number of measurements. It also represents the probability distribution (P) of data around the mean value. The deviations from the average value are given in terms of the standard deviation (σ).

On top of the graph the integral or summed probabilities are shown: the probability of observing values between $\bar{x} + \sigma$ and $\bar{x} - \sigma$ is 68 %, between $\bar{x} + 2\sigma$ and $\bar{x} - 2\sigma$ the chance is 95 % and finally between $x + 3\sigma$ and $x - 3\sigma$ 99.7 %.

result is less and less probable. The histogram (or block diagram) consisting of columns representing the number of times (N_i) results $x_{i(\Delta x)}$ within a certain range x_i and $x_i + \Delta x$ have been observed, is referred to as the sample distribution. The mean value is:

$$\bar{x} = \frac{1}{N} \sum_i N_i x_{i(\Delta x)}$$

and **(13.4)**

$$N = \Sigma N_i$$

If in making the histogram Δx or the *class width* is chosen to be too large, nearly all data may be within one column, suggesting a good statistical certainty, but a bad resolution; if Δx is made too small the resolution is increased, but few data fall within one column and the reliability appears to be small (scattering histogram).

The more measurements have been carried out, the better is the impression of the distribution of data around a certain mean value. For an infinite number of results with random errors the sample distribution is represented by a bell-shaped *normal* or *Gaussian distribution*, in which the probability of observing a value of $y = y_i$ at $x = x_i$ is:

$$P_i = \frac{1}{\sigma_i \sqrt{2\pi}} \exp\left\{-\frac{1}{2}\left(\frac{y_i - f(x_i)}{\sigma_i}\right)^2\right\} \qquad \textbf{(13.5)}$$

y_i is the measured value of the dependent variable y, $f(x_i)$ is the y value calculated for the value of the independent variable x_i, σ_i is the standard deviation of y_i, to be defined later. The most probable value to be observed, the *mode*, corresponds to the peak of the distribution, i.e. to the top of the smooth curve. For data with random errors the distribution is symmetrical around the top. Fig.13.2 shows the Gaussian curve together with the histogram resulting from a limited number of measurements.

13.3.3 STANDARD DEVIATION

13.3.3.1 PRECISION OF DATA

It is obvious that if random errors are small, the values of the deviation $(x_i - \bar{x})$ are small and the distribution of the results around the mean is narrower. The average deviation is a measure of the spread of the data around the mean or the so-called *dispersion* of the data set. Eq.13.3 has shown that we can not use the simple average of all deviations, a consequence of the definition of the mean. The average of the absolute values of the deviations, i.e. irrespective of their sign, characterises the dispersion better:

$$\overline{|d|} \equiv \frac{1}{N}\Sigma\, x_i - \bar{x} \qquad \textbf{(13.6)}$$

For mathematical reasons however, using absolute values is not appropriate. Therefore, the squares of the deviations are taken to characterise the distribution. The resulting value is referred to as the *variance*:

$$\sigma^2 \equiv \lim_{N\to\infty}\left[\frac{1}{N}\Sigma(x_i - \mu)\right] = \lim_{N\to\infty}\left(\frac{1}{N}\Sigma x_i^2\right) - \mu^2 \qquad \textbf{(13.7)}$$

The variance is thus the average of the squares minus the square of the averages. The quantitative measure of the size of the random errors, i.e. of the *statistical spread* of the data around the mean, or in other words of the precision is now given by the *standard deviation* σ, which is the square root of the variance. The smaller the standard deviation, the better the precision, the narrower the Gaussian curve.

If we now consider the real set of measurements, the standard deviation of the set is:

$$\sigma \equiv \sqrt{\frac{1}{N-1}\sum(x_i - \bar{x})^2} \qquad \textbf{(13.8)}$$

The fact that N–1 instead of N is inserted in the denominator is discussed in standard texts on statistical analysis. The necessity can be appreciated by considering the extreme case of only one measurement. A single measurement can give no idea on the precision of the measurement. Therefore, the fraction may not be a real number.

The possibility of calculating $\bar{x}$ and σ is included in modern pocket calculators.

In Fig.13.2 various *confidence levels* are indicated. The probability that a random result of a measurement lies between $\bar{x} + \sigma$ and $\bar{x} - \sigma$ is calculated to be 68%. This means that a repeated measurement will result in a new result within $\pm\sigma$ of the mean: the standard deviation is the 68% confidence level, 2σ is the 95% confidence level, and 99.7% is the 3σ confidence level.

13.3.3.2 PRECISION OF THE MEAN

In the preceding discussion we have been dealing with the precision of data, as characterised by the standard deviation. It is equally important to report the uncertainty in the final outcome of a number of measurements. Therefore, we have to calculate the precision of the mean value or, more specifically, the standard deviation of the mean.

Below we will briefly discuss the propagation of errors; i.e. the overall uncertainty obtained from a number results, each with its own uncertainty. The conclusion is that the variance of a mean is the variance of the data set divided by the number of measurements:

$$\sigma_{\bar{x}}^2 = \frac{\sigma_{x_i}^2}{N} = \frac{1}{N(N-1)}\sum(x_i - \bar{x})^2 \qquad \textbf{(13.9)}$$

The standard deviation of the mean is then:

$$\sigma_{\bar{x}} = \frac{\sigma_{x_i}}{\sqrt{N}} = \sqrt{\frac{1}{N(N-1)}\sum(x_i - \bar{x})^2} \qquad \textbf{(13.10)}$$

As an example we will calculate the mean and standard deviations of the data shown in Fig.13.1A and Table 13.1. All data are assumed to have the same uncertainty/precision.

Table 13.1 Set of data corresponding to Fig.13.1A.

Nr.	x_i	$x_i - \bar{x}$	Nr.	x_i	$x_i - \bar{x}$	Nr.	x_i	$x_i - \bar{x}$
1	13.55	−0.01	8	13.40	−0.16	15	13.45	−0.11
2	13.45	−0.11	9	13.56	+0.00	16	13.62	+0.06
3	13.57	+0.01	10	13.52	−0.04	17	13.74	+0.18
4	13.68	+0.12	11	13.51	−0.05	18	13.65	+0.09
5	13.63	+0.07	12	13.63	+0.07	19	13.45	−0.11
6	13.47	−0.09	13	13.52	−0.04			
7	13.69	+0.13	14	13.55	−0.01			

Mean $\bar{x}$ = 13.56

Standard deviation $\sigma_x = \sqrt{\{\Sigma(x_i - 13.56)^2\}/18}$ = ±0.095

σ of mean $= \sigma_x/\sqrt{19}$ = ±0.022

13.4 STATISTICAL UNCERTAINTIES

Statistical uncertainties, defined in Sect.13.2.3, arise from the random fluctuations in the number of events, for instance the number of radioactive disintegrations per unit time, rather than from a limited precision of the measuring equipment. For these statistical fluctuations the theory of statistics provide the mathematical technique for describing the data distribution and the standard deviation. The result is that the standard deviation of a number of counts M detected during a time interval t is simply:

$$\sigma = \sqrt{M} \tag{13.11}$$

For the counting rate R, i.e. the number of counts per second, the standard deviation then is:

$$\sigma_R = \frac{1}{t}\sqrt{M} = \frac{1}{t}\sqrt{Rt} = \sqrt{\frac{R}{t}} \tag{13.12}$$

The relative uncertainty of the counting rate is given by:

$$\frac{\sigma_R}{R} = \frac{1}{\sqrt{Rt}} \tag{13.13}$$

It is obvious that the relative precision is better the higher the counting rate and the larger the measuring time.

The matter of confidence levels with observing data with statistical uncertainties is similar to the instrumental uncertainties as discussed in the previous section. The probability that a "true value" observed in an infinite period of time lies between $x_i + \sigma$ and $x_i - \sigma$ of the measured value is 68%: the standard deviation is the 68% confidence level, 2σ is the 95% confidence level, and 99.7% is the 3σ confidence level.

13.5 ERROR PROPAGATION

13.5.1 STANDARD DEVIATION

We often want to determine a quantity A that is a function of one or more variables, each with its own uncertainty. The uncertainty of each of these variables contributes to the overall uncertainty. We will limit ourselves to give the mathematical expressions for σ^2 in various cases. The equations are based on the general relation for the function:

$$A = f(x, y, z)$$

In the case of statistical uncertainties the standard deviation of A depends on the independent variables x, y and z as:

$$\sigma_A^{\,2} = \sigma_x^{\,2}\left(\frac{\partial A}{\partial x}\right)^2 + \sigma_y^{\,2}\left(\frac{\partial A}{\partial y}\right)^2 + \sigma_z^{\,2}\left(\frac{\partial A}{\partial z}\right)^2 \qquad \textbf{(13.14)}$$

If the uncertainties are estimated instrumental uncertainties, similar equations are to be used for calculating the uncertainty in the final result. For the general relation:

$$A = f(x, y, z)$$

with the estimated instrumental uncertainties Δx, Δy and Δz, the uncertainty in A is:

$$\Delta A^2 = \Delta x^2\left(\frac{\partial A}{\partial x}\right)^2 + \Delta y^2\left(\frac{\partial A}{\partial y}\right)^2 + \Delta z^2\left(\frac{\partial A}{\partial z}\right)^2 \qquad \textbf{(13.15)}$$

resulting in the equivalent equations for ΔA as for σ_A in the Eqs.13.16-13.19. In these examples a and b are constant coefficients, x and y are the independent variables, A the dependent variable.

1) $A = ax + by$ and $A = ax - by$ with uncertainties σ_x and σ_y; in both cases:

$$\sigma_A^2 = a^2\sigma_x^2 + b^2\sigma_y^2 \qquad \textbf{(13.16)}$$

2) $A = \pm a\,xy$ and $A = \pm a\,x/y$

$$\frac{\sigma_A^2}{A^2} = \frac{\sigma_x^2}{x^2} + \frac{\sigma_y^2}{y^2} \qquad \textbf{(13.17)}$$

3) $A = a\,e^{\pm bx}$

$$\sigma_A/A = \pm b\sigma_x \qquad \textbf{(13.18)}$$

4) $A = a\,\ln(\pm bx)$

$$\sigma_A = a\,\sigma_x/x \qquad \textbf{(13.19)}$$

13.5.2 WEIGHTED MEAN

Till now, when calculating average values, we have considered all numbers to have the same precision and thus to have the same *weight*. If we assign to each number its own standard deviation, the mean is then to be calculated according to:

$$\bar{x} = \frac{\Sigma \frac{x_i}{\sigma_i^2}}{\Sigma \frac{1}{\sigma_i^2}} \qquad \textbf{(13.20)}$$

while the standard deviation of the mean is obtained from:

$$\frac{1}{\sigma_x^2} = \Sigma\left(\frac{1}{\sigma_i^2}\right)$$

resulting in:

$$\sigma_x = \frac{1}{\sqrt{\Sigma(1/\sigma_i)^2}} \qquad \textbf{(13.21)}$$

The weight of each result is inversely proportional to the square of the standard deviation; $1/\sigma^2$ is referred to as the *weighting factor*.

If the standard deviations σ_i are equal, the expression for σ of the mean reduces to Eq.13.10:

$$\sigma_x^2 = 1 / \Sigma(1/\sigma_i)^2 = 1 / [N(1/\sigma_i)^2] = \sigma_i^2 / N \quad \text{or} \quad \sigma_x = \sigma_i / \sqrt{N}$$

13.6 LEAST-SQUARES FIT

A measured quantity is often related to some other variable, for instance y = f(x). This function may have any form such as linear, quadratic, harmonic, arbitrary, et cetera. The subject of this section is to briefly discuss methods to obtain the most probable graphical and algebraic adjustment of a function to the data. The major interest is the adjustment of a straight line to a number of data, which are expected to be linearly related.

13.6.1 FIT TO A STRAIGHT LINE

. The principle of least-squares fitting is to minimise the sum of the squares of the deviations of the dependent variable (y) (the uncertainty in x is assumed to be negligible) from the straight line with coefficients a and b:

$$y = a + bx \tag{13.22}$$

The deviation from any value of y (y_i) to the straight line is given by

$$\Delta y_i = y_i - f(x_i) = y_i - a - bx_i \tag{13.23}$$

Minimising the sum of these deviations results in:

$$\Sigma \Delta y_i = 0 \tag{13.24}$$

while applying the absolute values of Δy_i does not result into a useful mathematical procedure. Therefore, we are looking for a procedure to find the coefficients a and b, characterising the straight line, by which the sum of the squares of the deviations:

$$\Sigma(\Delta y_i)^2 = \Sigma(y_i - a - bx_i)^2 \tag{13.25}$$

is minimised. The matching conditions are:

$$\frac{\partial}{\partial a} \Sigma(y_i - a - bx_i)^2 = 0$$

and (13.26)

$$\frac{\partial}{\partial b} \Sigma(y_i - a - bx_i)^2 = 0$$

The resulting values of a and b are:

$$a = \frac{1}{\Delta}\left(\Sigma\frac{x_i^2}{\sigma_i^2}\Sigma\frac{y_i}{\sigma_i^2} - \Sigma\frac{x_i}{\sigma_i^2}\Sigma\frac{x_i y_i}{\sigma_i^2} \right) \qquad \textbf{(13.27a)}$$

and

$$b = \frac{1}{\Delta}\left(\Sigma\frac{1}{\sigma_i^2}\Sigma\frac{x_i y_i}{\sigma_i^2} - \Sigma\frac{x_i}{\sigma_i^2}\Sigma\frac{y_i}{\sigma_i^2} \right) \qquad \textbf{(13.27b)}$$

while

$$\Delta = \Sigma\frac{1}{\sigma_i^2}\Sigma\frac{x_i^2}{\sigma_i^2} - \left(\Sigma\frac{x_i}{\sigma_i^2} \right)^2 \qquad \textbf{(13.27c)}$$

If the standard deviations of y are equal, the values of a and b are:

$$a = (\Sigma x_i^2\, \Sigma y_i - \Sigma x_i\, \Sigma x_i y_i) / \Delta \qquad \textbf{(13.28a)}$$

$$b = (N\, \Sigma x_i y_i - \Sigma x_i\, \Sigma y_i) / \Delta \qquad \textbf{(13.28b)}$$

$$\Delta = N\, \Sigma x_i^2 - (\Sigma x_i)^2 \qquad \textbf{(13.28c)}$$

Many modern pocket calculators have the possibility of calculating the least-squares fit to the straight line. An example is shown in Fig.13.3.The standard deviations of the coefficients a and b are:

$$\sigma_a = \sqrt{\frac{1}{\Delta}\Sigma\frac{x_i^2}{\sigma_i^2}} \qquad \textbf{(13.29a)}$$

and

$$\sigma_b = \sqrt{\frac{1}{\Delta}\Sigma\frac{1}{\sigma_i^2}} \qquad \textbf{(13.29b)}$$

13.6.2 FIT TO NON-LINEAR CURVES

The least-squares fit to, for instance, quadratic or second-degree polynomial, harmonic, exponential and arbitrary curves will not be treated quantitatively. These can be calculated analytically, but the normal routine is to apply the proper computer programmes. These also exist for composite curves, consisting of the superposition of more than one curve. Even through data points, which are not theoretically related to the independent variable, curves can be fitted. One example is the *cubic spline*. In principle cubic (3rd order) fits through successive group of data are adjusted to each other. The resulting curve can be chosen to fit all data points, as well as chosen to smooth irregularities as much as wanted.

13.7 CHI-SQUARE TEST

The least-squares fit is based on minimising the exponential of the Gaussian probability function of Eq.13.5, i.e. of the sum of the (quadratic) deviations between the observed y values (y_i) and the y values calculated from the relation between y and x: $y = f(x_i)$.

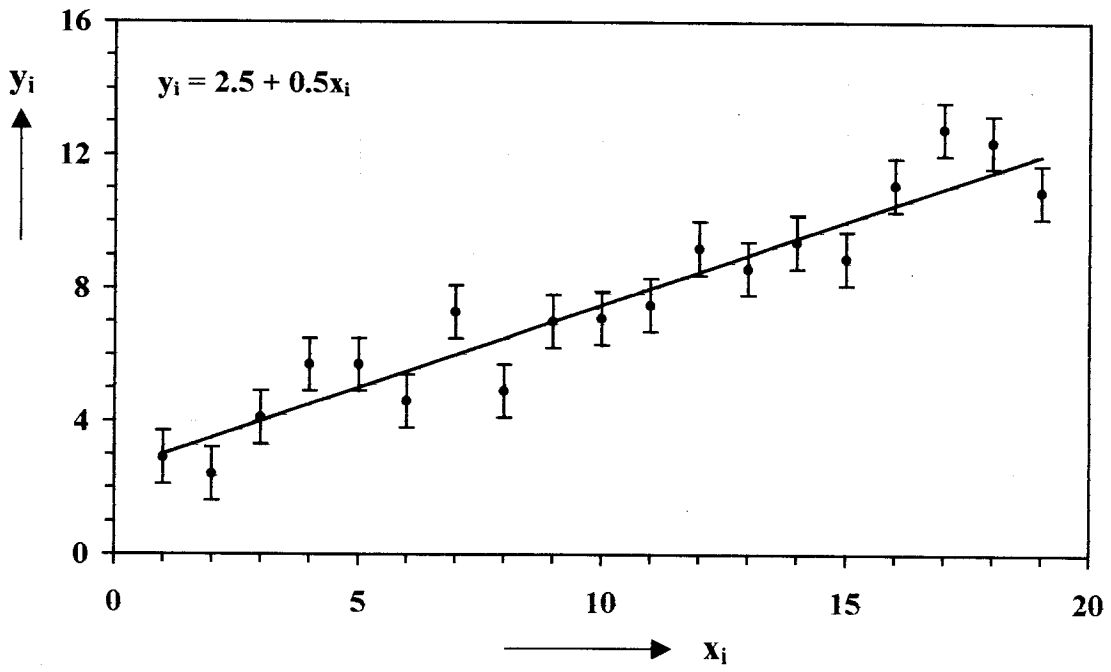

Fig.13.3 Linear least-squares fit through a number of (x,y) data sets, of which the independent and dependent variables are related by the equation y = 2.5 + 0.5x. All y values have the same precision.

For the straight line fit this comes to calculating the coefficients of the linear relation y = a + bx for which the sum $\Sigma(y_i - a - bx_i)^2$ is minimal (Eq.13.25). In view of the definition of the probability, P_i, it logical to take the same sum of the square deviations in relation to the standard deviation as a measure for the *goodness of fit*:

$$\chi^2 = \sum_{i=1}^{N} \left(\frac{y_i - a - bx_i}{\sigma_i} \right)^2 \qquad \textbf{(13.30)}$$

For the set of data in Fig.13.3 and Table 13.2 the χ^2 is calculated.

In summary, the optimum fit to data is that which minimises χ^2. The method by which χ^2 is minimised is the least-squares method. The result of a χ^2 test is reassuring, if the χ^2 divided by the number of data (=19) minus the degrees of freedom (= the number of parameters to be determined, here = 1) is about equal to one (in this case =12/18).

Table 13.2 Series of (x_i, y_i) data sets obeying the relation $y = a + bx$, resulting in a value of χ^2. The graph for these data is shown in Fig.13.3. The optimum fit to the data is that which minimises χ^2.

x	$y_i \pm \sigma$	$y = 2.5 + 0.5x_i$	$[y - f(x_i)]^2/\sigma^2$
1	2.9 ± 0.8	3.0	0.016
2	2.4 ± 0.8	3.5	1.891
3	4.1 ± 0.8	4.0	0.016
4	5.7 ± 0.8	4.5	2.250
5	5.7 ± 0.8	5.0	0.766
6	4.6 ± 0.8	5.5	1.266
7	7.3 ± 0.8	6.0	2.641
8	4.9 ± 0.8	6.5	4.000
9	7.0 ± 0.8	7.0	0.000
10	7.1 ± 0.8	7.5	0.250
11	7.5 ± 0.8	8.0	0.391
12	9.2 ± 0.8	8.5	0.766
13	8.6 ± 0.8	9.0	0.250
14	9.4 ± 0.8	9.5	0.016
15	8.9 ± 0.8	10.0	1.891
16	11.1 ± 0.8	10.5	0.563
17	12.8 ± 0.8	11.0	5.063
18	12.4 ± 0.8	11.5	1.266
19	10.9 ± 0.8	12.0	1.891
χ^2			12.094

REFERENCES

Andrews, J.N., 1992. Mechanisms for noble gas dissolution by groundwaters. In: Isotopes of Noble Gases as Tracers in Environmental Studies, IAEA Symp., Vienna 1989: 87-110.

Baertschi, P., 1952. Die Fraktionierung der Kohlenstoffisotopen bei der Absorption von Kohldioxyd. Helv. Chim. Acta 35: 1030-1036.

Baertschi, P., 1976. Absolute ^{18}O content of Standard Mean Ocean Water. Earth and Planet. Sci. Lett. 31: 341-344.

Bard, E., Arnold, M., Hamelin, B., Tisnerat-Laborde, N. and Cabioch G., 1998. Radiocarbon calibration by means of mass spectrometric $^{230}Th/^{234}U$ and ^{14}C ages of corals. Radiocarbon 40 (3): 1085-1092.

Barry, R.G., 1969a. The world hydrological cycle. In: R.J. Chorley (Editor), Introduction to Physical Hydrology, Methuen, London: 8-25.

Barry, R.G., 1969b. Evaporation and transpiration. In: R.J. Chorley (Editor), Introduction to Physical Hydrology, Methuen, London: 82-98.

Bentley, H.W., Fillips, F.M., Davis, S.N., Gifford, S., Elmore, D., Tubbs, L.E. and Gove H.E., 1982. Thermonuclear ^{36}Cl pulse in natural water. Nature 300: 737-740.

Baumgartner, A. and Reichel E., 1975. The World Water Balance. Elsevier, Amsterdam, pp. 179.

Bentley, H.W., Fillips, F.M. and Davis, S.N., 1986. Chlorine-36 in the terrestrial environment. In: P. Fritz and J. C. Fontes (Editors), Handbook of Environmental Isotope Geochemistry Vol. 2, Elsevier Science Publ. Comp., Amsterdam, New York: 427-480.

Bigeleisen, J., 1952. The effects of isotopic substitutions on the rates of chemical reactions. J. Phys. Chem. 56: 823-828.

Bigeleisen, J. and Wolfsberg, M., 1958. Theoretical and experimental aspects of isotope effects in chemical kinetics. Adv. Chem. Phys. 1: 15-76.

Böhlke, J.K. and Coplen T.B., 1995. Interlaboratory comparison of reference materials for nitrogen-isotope-ratio measurements. IAEA-Tecdoc-825, IAEA Vienna, 1-3 December 1993: 51-66.

Brenninkmeijer, C.A.M.. and Mook, W.G., 1979. The effect of electronegative impurities on CO_2 proportional counting: an on-line purity test counter. Proc. 9th Intern. Radiocarbon Conf., Los Angeles and La Jolla, 1976, Univ. of California Press: 185-196.

Brenninkmeijer, C.A.M., Kraft, P. and Mook, W.G., 1983. Oxygen isotope fractionation between CO_2 and H_2O. Isotope Geoscience 1: 181-190.

Broecker, W.S. and Oversby, V.M., 1971. Chemical equilibria in the earth. McGraw-Hill, New York, London, 318 pp.

Bruijnzeel, L.A., 1996. Predicting the hydrological impacts on land cover transformation in the humid tropics: the need for integrated research. In: J.H.C. Gash, C.A. Nobre, J.M. Roberts and R.L. Victoria (Editors), Amazonian Deforestation and Climate (), Wiley, Chichester: 15-57.

Budyko, M.I., 1978. The heat balance of the Earth. In: J. Gribbin (Editor), Climate Change, Cambridge University Press, London, New York: 85-113.

Chang (Zhang) T.L. and Li, W., 1987. Mass spectrometric determination of the absolute isotopic abundance of carbon in NBS-20. Proc. 2nd Beijing Conf. and Exhib. on Instrum. Analysis: 391-392.

Collon, P., Antaya, T., Davids, B., Fauerbach, M., Harkewicz, R., Hellstrom, M., Kutschera, W., Morrissey, D., Pardo, R., Paul, M., Sherrill, B. and Steiner, M., 1997. Measurement of ^{81}Kr in the atmosphere. Nucl. Instr. and Meth. B 123: 122-127.

Coplen, T.B., Wildman, J. and Chen, J., 1991. Improvement in the gaseous hydrogen – water equilibration technique for hydrogen isotope ratio analysis. Anal. Chem. 63: 910-912.

Craig, H., 1957. Isotopic standards for carbon and oxygen and correction factors for mass-spectrometric analysis of carbon dioxide. Geochim. Cosmochim. Acta 12: 133-149.

Craig, H., 1961a. Standards for reporting concentrations of deuterium and oxygen-18 in natural waters. Science 133: 1833-1834.

Craig, H., 1961b. Isotopic variations in meteoric waters. Science 133: 1702-1703.

Craig, H. and Gordon, L.I., 1965. Deuterium and oxygen-18 variations in the ocean and the marine atmosphere. In: Stable Isotopes in oceanographic studies and Palaeotemperatures, Spoleto: 1-22.

Dansgaard, W., 1964. Stable isotopes in precipitation. Tellus 16: 436-468.

Dansgaard, W., Clausen, H.B. and Aarkog, A., 1966. The Si^{32} fallout in Scandinavia: A new methd for ice dating. Tellus 18: 187-191.

Deines, P., 1980. The isotopic composition of reduced organic carbon. In P.Fritz and J. C. Fontes, (editors), Handbook of Environmental Isotope Geochemistry Vol. I: The Terrestrial Environment, Elsevier, Amsterdam, New York: 329-407.

De Wit, J.C., Van der Straaten, C.M. and Mook, W.G., 1980. Determination of the absolute D/H ratio of VSMOW and SLAP. Geostandards Newslett. 4: 33-36.

Dickson, A.G. and Riley, J.P., 1979. The estimation of acid dissociation constantsin seawater from potentiometric titrations with strond base. I. The ion producy of water-K_w. Marine Chemistry 7: 89-88.

Dickson, A.G. and Millero, F.J., 1987. A comparison of the equilibrium constants for the dissociation of carbonic acid in seawater media. Deep-Sea Research 34: 1733-1743.

Eagleson, P.S., 1986. The emergence of global scale hydrology. Water Resources Res. 22: 6S-14S.

Edwards, T.W.D., Huhay, W.M., Elgood, R.J. and Jiang, H.B., 1993. A modification on the batch process for direct conversion of water and organic oxygen into CO_2 for ^{18}O analysis. In: Isotope techniques in the Study of past and current environmental changes in the hydrosphere and the atmosphere, IAEA Vienna: 574-579.

Eggenkamp, H.G.M., 1994. $\delta^{37}Cl$, the geochemistry of chlorine isotopes. Doct. Thesis, Fac. Earth Sciences, Utrecht Univ., 150 pp.

Ekwurzel, B., Schlosser, P., Smethie, W.M., Plummer, N., Busenberg, E., Weppernig, R.L. and Stute, M., 1994. Dating of shallow groundwater: comparison of the transient tracers $^3H/^3He$, chlorofluorocarbons and ^{85}Kr. Water Resources Research 30: 1693-1708.

Emiliani, C., 1971. The amplitude of pleistocene climatic cycles at low latitudes and the isotopic composition of glacial ice. In: K.K. Turekian (editor), The Late Cenozoic Glacial Ages, Yale University Press, New Haven, London: 183-197.

Emrich, K., Ehhalt, D. and Vogel, J.C., 1970. Carbon isotope fractionation during the precipitation of calcium carbonate. Earth Planet. Sci. Lett. 8: 363-371.

Epstein, S., Buchsbaum, R., Lowenstam, H.A. and Urey, H.C., 1953. Revised carbonate water isotopic temperature scale. Bull. Geol. Soc. Am. 64: 1315-1325.

Epstein, S. and Mayeda, T. 1953. Variations of O^{18} content of waters from natural sources. Geochim. Cosmochim. Acta 4: 213-224.

Epstein, S., 1976. A revised oxygen paleotemperature scale. Geol. Soc. Amer. Bull., pers. comm.

Fontes, J.Ch. and Garnier, J.M., 1979. Determination of the initial activity of the total dissolved carbon, A review of the existing models and a new approach. Water Resour. Res. 12: 399-413.

Forster, M., Maier, P. and Loosli, H.H., 1992. Current techniques for measuring the activity of ^{37}Ar and ^{39}Ar in the environment. Isotopes of Noble Gases as Tracers in Environmental Studies, IAEA, Vienna 1989: 63-72.

Friedman, I., 1953. Deuteriun content of natural water and other substances. Geochim. Cosmochim. Acta 4: 89-103.

Friedman, I. and O'Neil, J.R. 1977. Compilation of stable isotope fractionation factors of geochemical interest. USGS Prof. Paper 440-KK.

Geyer, S., Wolf, M., Wassenaar, L.I., Fritz, P., Buckau, G. and Kim, J.I. 1993. Isotope investigations on fractions of dissolved organic carbon for ^{14}C groundwater dating. In: Isotope Techniques in the Study of Past and Current Environmental Changes in the Hydrosphere and the Atmosphere, IAEA Symp. Vienna 1993: 359-380.

Geyh, M.A. and Wendt, I., 1965. Results of water sample dating by means of the model of Münnich and Vogel. Proc. Int. Conf. on Radiocarbon and Tritium Dating, Pullman, USA:597-603.

Godwin, H., 1962. Half life of radiocarbon. Nature 195: 984.

Gonfiantini, R., 1984. Stable Isotope Reference Samples for Geochemical and Hydrological Investigations. Report Adv. Group Meeting, Vienna, September 1983: 77 pp.

Gregoire, D.C., 1987. Determination of boron isotopic ratios in geological materials by inductively coupled plasma mass spectrometry. Anal. Chemistry 59: 2479-2484.

Hagemann, R., Nief, G. and Roth, E. 1970. Absolute isotopic scale for deuterium analysis of natural waters. Absolute D/H ratio for SMOW. Tellus 22: 712-715.

Harned, H.S. and Scholes, S.R. 1941. The ionisation constant of HCO_3^- from 0° to 50°C. J. Am. Chem. Soc. 63: 1706-1709.

Harned, H.S. and Davis Jr., R., 1943. The ionisation constant of carbonic acid in water and the solubility of carbon dioxide in water and aqueous salt solutions from 0° to 50°C. J. Am. Chem. Soc. 65: 20-2037.

Heinemeier, J., Hornshøj, P., Nielsen, H.L., Rud, N. and Thomsen, M.S., 1987. Accelerator mass spectrometry applied to $^{22,24}Na$, $^{31,32}Si$, and ^{14}C. Nucl. Instr. and Methods B 29: 110-113.

Horita, J. and Wesolowski, D. J., 1994. Liquid-vapor fractionation of oxygen and hydrogen isotopes of water from the freezing to the critical temperature. Geochim. Cosmochim. Acta 58 (16): 3425-3437.

Hübner, H., 1986. Isotope effects of nitrogen in the soil and biosphere. In: P. Fritz and J. Ch. Fontes (eds.), Handbook of Environmental Geochemistry IA, Elsevier Science Publ., Amsterdam, New York: 361-426.

Ingerson, E. and Pearson, F.J.Jr., 1964. Estimating of age and rate of motion for groundwater by the C^{14}-method. In: Recent Researches in the Fields of Hydrosphere, Atmosphere and Nuclear Chemistry. Maruzen Comp., Tokyo:263.

Inoue, H. and Sugimura, Y., 1985. Carbon isotope fractionation during the CO_2 exchange process between air and sea water under equilibrium and kinetic conditions. Geochim. Cosmochim. Acta 44: 2453-2460.

Jones, J.A.A., 1997. Global Hydrology, Longman, Harlow, 399 pp.

Karlén, I., Olsson, I.U., Kållberg, P. and Killiççi, S., 1966. Absolute determination of the activity of two ^{14}C dating standards. Arkiv f. Geofysik 6: 465-471.

Keeling, C.D., 1958. The concentration and isotopic abundances of atmospheric carbon dioxide in rural areas. Geochim. Cosmochim. Acta 13: 322-334.

Kerstel, E.R.Th., van Trigt, R., Dam, N., Reuss, J. and Meijer, H.A.J., 1999. Simultaneous determination of the $^{2}H/^{1}H$, $^{17}O/^{16}O$, and $^{18}O/^{16}O$ isotope abundance ratios in water by means of laser spectrometry. Analytical Chem. 71(23): 5297-5303.

Kotwicki, V., 1991. Water in the universe. Hydrological Sciences Journal 36: 49-66.

Krouse, H.R., 1980. Sulphur isotopes in our environment. In: P. Fritz and J. Ch. Fontes (Editors), Handbook of Environmental Geochemistry I A, Elsevier Science Publ., Amsterdam, New York: 435-471.

Lal, D. and Peters, B. 1967. Cosmic-ray produced radioactivity on the Earth. In: K. Sitte (Editor), Handbuch der Physik 46, Springer Verlag, Berlin: 551-612.

Lamb, H.H., 1982. Climate, History and the Modern World. Methuen, New York, 387 pp.

Lehmann, B. E., H. H. Loosli, W. Balderer, J. Ch. Fontes, J. L. Michelot, and S. Soreau, 1991. Chlorine-36. In: F.J. Pearson et al. (Editors), Applied Isotope Hydrology, Studies in Environmental Science 43, Elsevier Science Publ. Amsterdam, New York: 250-265.

Lerman, J.C., 1972. Carbon-14 dating: origin and correction of isotope fractionation errors in terrestrial living matter. Proc. 8th Int. Conf. Radiocarbon Dating, New Zealand: 612-624.

Létolle, R., 1980. Nitrogen-15 in the natural environment. In: P. Fritz and J. Ch. Fontes (Editors), Handbook of Environmental Geochemistry 1A, Elsevier Science Publ., Amsterdam, 407-434.

Libby, W.F., 1946. Atmospheric helium three and radiocarbon from cosmic radiation. Phys. Rev. 69: 671-672.

Loosli, H.H., and Oeschger, H., 1979. Argon-39, carbon-14 and krypton-85 measurements in groundwater samples. In: Isotope Hydrology II, IAEA Symposium Neuherberg, IAEA Vienna, 1978: 931-997.

Lorius, C. and Oeschger, H., 1994. Palaeo-perspectives: reducing uncertainties in Global Change?. Ambio 23 (1): 30-35.

Lucas, L.L. and Unterweger, M.P., 2000. Comprehensive review and critical evaluation of the half-life of tritium. J. Res. Natl. Inst. Stand. Technol. (to be publ.).

Majoube, M., 1971. Fractionnement en oxygen-18 et en deuterium entre l'eau et sa vapeur. J. Chim. Phys. 68: 1423-1436.

L'Vovich, M.I., 1962. The water balance and its zonal characteristics. Soviet Geography 3: 37-50.

Mann, W.B., 1983. An international reference material for radiocarbon dating. Radiocarbon 25 (2): 519-522.

Mehrbach, C., Culberson, C.H., Hawley, J.E. and Pytkowicz, R.M., 1973. Measurement of the apparent dissociation constants of carbonic acid in seawater at atmospheric pressure. Limnology and Oceanography 18: 897-907.

Meijer, H.A.J. and Li, W.J., 1998. The use of electrolysis for accurate $\delta^{17}O$ and $\delta^{18}O$ isotope measurements in water. Isotopes Environ. Health Stud. 34: 349-369.

Merlivat, L., 1978. Molecular diffusivities of $H_2{}^{16}O$, $HD^{16}O$, and $H_2{}^{18}O$ in gases. J. Chem. Phys. 69: 2864-2871.

Millero, F.J. and Roy, R.N., 1997. A chemical equilibrium model for the carbonate system in natural waters. Croatia Chemica Acta 70: 1-38.

Monteith, J.L., 1965. Evaporation and environment. Proc. Symp. Experimental Biology 19, Cambridge: 205-234.

Mook, W.G. and Vogel, J.C. 1968. Isotopic equilibrium between shells and their environment. Science 159: 874-875.

Mook, W.G., Bommerson, J.C. and Staverman, W.H., 1974. Carbon isotope fractionation between dissolved bicarbonate and gaseous carbon dioxide. Earth Planet. Sci. Lett. 22: 169-176.

Mook, W.G., and Koene, B.K.S., 1975. Chemistry of dissolved inorganic carbon in estuarine and coastal brackish waters. Estuar. Coastal Mar. Science 3: 325-336.

Mook, W.G., 1976. The dissolution-exchange model for dating ground water with ^{14}C. In: Interpretation of Environmental Isotope and Hydrochemical Data in Ground-Water Hydrology. IAEA, Vienna: 213-225.

Mook, W.G., 1980. Carbon-14 in hydrological studies, In: P.Fritz and J.Ch.Fontes (Editors), Handbook of Environmental Isotope Geochemistry 1A, Elsevier Science Publ., Amsterda, New York: 49-74.

Mook, W.G., 1980. The effect of fossil fuel and biogenic CO_2 on the ^{13}C and ^{14}C content of atmospheric carbon dioxide, Radiocarbon 22 (2): 392-397.

Mook, W.G., 1983. International comparison of proportional gas counters for ^{14}C activity measurements. Radiocarbon 25 (2): 475-484.

Mook, W.G., Koopmans, M., Carter, A.F. and Keeling, C.D., 1983. Seasonal latitudinal and secular variations in the abundance and isotopic ratios of atmospheric carbon dioxide I. Results from land stations. J. Geophys. Res. 88: 10.915-10.933.

Mook, W.G. and Streurman, H.J. 1983. Physical and Chemical Aspects of Radiocarbon Dating. PACT Publ.8 on ^{14}C and Archaeology: 31-55.

Mook, W.G., 1984. Archaeological and geological interest in applying ^{14}C AMS to small samples, Proc. 3rd Intern. Symp. on Accelerator Mass Spectrometry, Zürich, Nucl. Instr. Meth. B5, 297-302,

Mook, W.G. and Waterbolk, H.T., 1985. Handbooks for Archaeologists 3: Radiocarbon Dating. European Science Found., Strasbourg,. 65 pp.

Mook, W.G., 1986. ^{13}C in atmospheric CO_2. Neth. J. Sea Res. 20 (2/3): 211-223.

Morgenstern, U., Gellerman, R., Hebert, D., Börner, I., Stolz, W., Vaikmäe, R. and Putnik, H., 1995. ^{32}Si in limestone aquifers. Chemical Geology 120: 127-134.

Mucci, A., 1983. The solubility of calcite and aragonite in seawater at various salinities, temperatures and one atmosphere total pressure. Am. J. of Science 283: 780-799.

Münnich, K.O., 1957. Messung des ^{14}C-Gehaltes von hartem Grundwasser. Naturwiss. 44: 32-39.

Nier, A.O., 1950. A redetermination of the relative abundances of the isotopes of carbon, nitrogen, oxygen, argon and potassium. Phys. Rev. 77: 789-793.

Oeschger, H. and Loosli, H.H., 1977. New developments in sampling and low level counting of natural radioactivity, In: P. Povinec and S. Usacev (Editors), Proc. High Tatras Conf. 1975 on Low Radioactivity Measurements and Applications: 13-22.

Olaussen, E., 1981. On the isotopic composition of Late Cenozoic sea water. Geografiska Annaler 63A: 311-312.

O'Neil, J.R. and Epstein, S., 1966. A method for oxygen isotope analysis of milligram quantities of water and some of its applications. J. Geophys. Res. 71 (20): 4955-4961.

Pearson, F.J.Jr., 1965. Use of C^{13}/C^{12} ratios to correct radiocarbon ages of materials initially diluted by limestone. Proc. Int. Conf. on Radiocarbon and Tritium Dating, Pullman, USA: 357-366.

Pearson, F.J.Jr. and Rightmire, C.T., 1980. Sulphur and oxygen isotopes in aqueous sulphur compounds. In: P. Fritz and J. Ch. Fontes (Editors), Handbook of Environmental Geochemistry vol. 1A, Elsevier Science Publ., Amsterdam: 227-258.

Penman, H.L., 1948. Natural evaporation from open water, bare soil and grass. Proc. Royal Soc. London A 139: 120-145.

Purser, K.H., 1992. A high throughput ^{14}C accelerator mass spectrometer. Radiocarbon 34 (3): 458-457.

Raisbeck, G.M., Yiou, F., Fruneau, M., Lieuvin, M., Loiseaux, J.M., 1978. Measurement of ^{10}Be in 1000- and 5000-year-old Antarctic ice. Nature 275: 731-732.

Raisbeck, G.M., Yiou, F., Fruneau, M., Loiseaux, J.M., Lieuvin, M., 1979. ^{10}Be concentration and residence time in the oceans surface layer. Earth Planet. Sci. Letters 43: 237-240.

Révész, K., Böhlke, J.K. and Yoshinari, T., 1998. $\delta^{18}O$ and $\delta^{15}N$ determination in nitrate. In: Isotope Techniques in the Study of Environmental Change Proc. IAEA Vienna 1997: 851-854.

Richet, P., Bottinga, Y. and Javoy, M., 1977. A review of hydrogen carbon, nitrogen, oxygen, sulphur and chlorine stable isotope fractionation among gaseous molecules. Ann. Rev. Earth Planet. Sci. 5: 65-110.

Roeloffzen, J.C., Mook, W.G. and Keeling, C.D., 1991. Trends and variations in stable carbon isotopes of atmospheric carbon dioxide. Proc. IAEA Conf. on Stable Isotopes in Plant Nutrition, Soil Fertility and Environmental Studies, IAEA ,Vienna: 601-618.

Roether, W., 1967. Estimating the tritium input to ground water from wine samples: ground-water and direct run-off contribution to central European surface waters. Proc. IAEA Conf. on Isotopes in Hydrology, IAEA, Vienna: 73-90.

Roman, D. and Airey, P.L., 1981. The application of environmental chlorine-36 to hydrology I. Liquid scintillation counting. Int. J. Appl. Rad. Isot. 32: 287-290.

Rozanski, K., Stichler, W., Gonfiantini, R., Scott, E.M., Beukens, R.P., Kromer, B. and Van der Plicht, J., 1992. The IAEA ^{14}C intercomparison exercise 1990. Radiocarbon 34 (3): 506-519.

Rubinson, M. and Clayton, R.N., 1969. Carbon-13 fractionation between aragonite and calcite. Geochim. Cosmochim. Acta 33: 997-1002.

Schlosser, P., Shapiro, S.D., Stute, M., Aeschbach-Hertig, W., Plummer, N. and Busenberg, E., 1998. Tritium/^{3}He measurements in young groundwater. Proc. Symp. Isotope Techniques in the Study of Environmental Change, IAEA, Vienna: 165-189.

Sharma, P., Elmore, D., Miller, T. and Vogt, S., 1997. The ^{129}I program at PRIME Lab. Nucl. Instr. and Methods B 123: 347-351.

Shiklomanov, I.A., 1993. World freshwater resources. In: P.H. Gleick (Editor), Water in Crisis, Oxford University Press, New York, Oxford, 473 pp.

Siegenthaler, U. and Munnich, K.O., 1981. $^{13}C/^{12}C$ fractionation during CO_2 transfer from air to sea. In: B.Bolin (Editor), SCOPE 16: Carbon Cycle Modelling, John Wiley, New York: 249-257.

Skaron, S. and Wolfsberg, M., 1980. Anomalies in the fractionation by chemical equilibrium of $^{18}O/^{16}O$ relative to $^{17}O/^{16}O$. J. Chem. Phys. 72: 6810-6811.

Stuiver, M. and Polach, H., 1977. Reporting of ^{14}C data. Radiocarbon 19 (3): 355-363.

Stuiver, M. and Van der Plicht, J. (Editors), 1998. Special Calibration Issue. Radiocarbon 40(3): 1041-1164.

Thode, H.G., Shima, M., Rees, C.F. and Krishnamurty, K.V., 1965. Carbon-13 isotope effects in systems containing carbon dioxide, bicarbonate, carbonate and metal ions. Canad. J. Chem. 43: 582-595.

Throughton, J.H., 1972. Carbon isotope fractionation by plants. Proc. 8th Int. Conf. Radiocarbon Dating, New Zealand: 420-438.

Tse, R.S., Wong S.C. and Yuen, C.P., 1980. Determination of deuterium/hydrogen ratios in natural waters by Fourier transform nuclear magnetic resonance spectrometry. Anal.Chem. 52: 2445.

Unterweger, M.P., Coursey, B.M., Schima, F.J. and Mann, WG., 1978. Preparation and calibration of the 1978 National Bureau of Standards tritated-water standards. Intern. J. Appl. Rad. Isot. 31: 611-614.

Urey, H.C., 1947. The thermodynamic properties of isotopic substances. J. Amer. Chem. Soc.: 562-581.

Van der Straaten, C.M. and Mook, W.G., 1983. Stable isotopic composition of precipitation and climatic variability. In: Palaeoclimates and Palaeowaters, Panel Proc. Series, IAEA, Vienna, 1980: 53-64.

Van der Wijk, A., 1987. Radiometric dating by alpha spectrometry on uranium series nuclides. Thesis Groningen University, 145 pp.

Van der Wijk, A. and Mook, W.G., 1987. ^{210}Pb dating in shallow moorland pools. Geol. Mijnb. 66: 43-55.

Van der Wijk, A., Mook, W.G. and Ivanovich, M., 1988. Correction for environmental ^{230}Th in U/Th disequilibrium dating of peat. The Science of the Total Environment 70: 19-40.

Van Warmerdam, E.M., Frape, S.K., Aravena, R., Drimmie, R.J., Flatt, H. and Cherry, J.A., 1995. Stable chlorine and carbon isotope measurements of selected chlorinated organic solvents. Applied Geochemistry 10: 547-552.

Veizer, J. and Hoefs, J., 1976. The nature of O^{18}/O^{16} and C^{12}/C^{13} secular trends in sedimentary carbonate rocks. Geochim. Cosmochim. Acta 40: 1387-1396.

Vogel, J.C. , and D. Ehhalt, The use of carbon isotopes in ground-water studies, Proc. Conf. on Isotopes in Hydrology, IAEA, Vienna, 383-396, 1963.

Vogel, J. C. , Grootes, P.M. and Mook, W.G., 1970. Isotope fractionation between gaseous and dissolved carbon dioxide. Z. Phys. 230: 225-238.

Vogel, J.C. and Kronfeld, J., 1980. A new method for dating peat. S. Afr. J. Sc. 76: 557-558.

Wanninkhof, R., 1985. Kinetic fractionation of the carbon isotopes ^{13}C and ^{12}C during the transfer of CO_2 from air to seawater. Tellus 37B: 128-135.

Weiss, R.F., 1974. Carbon dioxide in water and seawater: the solubility of a non-ideal gas. Marine Chemistry 2: 203-205.

Weiss, W., Sartorius, H. and Stockburger, H., 1992. Global distribution of atmospheric ^{85}Kr, In: Isotopes of Noble Gases as Tracers in Environmental Studies, IAEA Symp. Vienna, 1989: 29-62.

Zhang, Q. and Li, W., 1987. Mass spectrometric determination of the absolute isotopic abundance of carbon in NBS-20. Proc.2nd Beijing Conf. and Exhib. on Instr. Analysis: 391-392.

LITERATURE

H.Moser **W.Rauert**	**Isotopenmethoden in der Hydrologie** (1980) (in German language) ISBN 3-443-01012-1	Gebr. Borntraeger Berlin, Stuttgart
P.Fritz **J.Ch.Fontes**	**Handbook of Environmental Isotope Geochemistry** ISBN 0-444-41781-8 Vol.1. The Terrestrial Environment A (1980) Vol.2. The Terrestrial Environment B (1986) Vol.3. The Marine Environment A (1989)	Elsevier SciencePubl. Amsterdam, Oxford New York, Tokyo ISBN 0-444-41780-X ISBN 0-444-42225-0 ISBN 0-444-42764-3
F.J.Pearson e.a.	**Applied Isotope Hydrogeology**, a case study in Northern Switzerland (1991) ISBN 0-444-88983-3	Elsevier Science Publ. Amsterdam, Oxford, New York, Tokyo
I.Clark **P.Fritz**	**Environmental Isotopes in Hydrogeology** (1997) ISBN 1-56670-249-6	Lewis Publishers Boca Raton, New York
F.Gasse **Ch.Causse**	**Hydrology and Isotope Geochemistry** ISBN 2-7099-1377-1	Editions de l'Orstom Paris
W.Kaess	**Tracing in Hydrogeology** (1998) ISBN 3-443-01013-X	Balkema
C.Kendall **J.J.McDonnell**	**Isotopes in Catchment Hydrology** (1998) ISBN 0-444-50155-X	Elsevier/North Holland Publ.Comp. Amsterdam

E.Mazor	**Chemical and Isotopic Groundwater Hydrology – The applied approach** (1998) ISBN 0-8247-9803-1	Marcel Dekker Inc.
P.G.Cook **A.L.Herczeg** **(ed.)**	**Environmental Tracers in Subsurface Hydrology** (2000) ISBN 0-7923-7707-9	Kluwer Acad. Publ.
G.Friedlander **J.W.Kennedy** **E.S.Macias** **J.M.Miller**	**Nuclear and Radiochemistry** (1981) ISBN 0-471-86255-X	John Wiley & Sons New York, Chichester, Brisbane, Toronto
G.Faure	**Principles of Isotope Geology** (1986)	John Wiley & Sons

IAEA PUBLICATIONS

IAEA CONFERENCE PROCEEDINGS

1963 **Radioisotopes in Hydrology**, Tokyo, 5-9 March 1963, IAEA, Vienna, 459 pp. (STI/PUB/71) (out of print)

1967 **Isotopes in Hydrology**, Vienna, 14-18 November 1966, IAEA, Vienna, (in co-operation with IUGG), 740 pp. (STI/PUB/141) (out of print)

1970 **Isotope Hydrology**, Vienna, 6-13 March 1970, IAEA, Vienna, (in co-operation with UNESCO), 918 pp. (STI/PUB/255) (out of print)

1974 **Isotope Techniques in Groundwater Hydrology**, Vienna, 11-15 March 1974, IAEA, Vienna, 2 volumes: 504 and 500 pp. (STI/PUB/373) (out of print)

1979 **Isotope Hydrology** (in 2 volumes), Neuherberg, Germany, 19-23 June 1978, IAEA, Vienna, (in co-operation with UNESCO), 2 volumes of 984 pp. (STI/PUB/493) ISBN 92-0-040079-5 and ISBN 92-0-040179-1

1983 **Isotope Hydrology**, Vienna, 12-16 September 1983, IAEA, Vienna, (in co-operation with UNESCO), 873 pp. (STI/PUB/650) ISBN 92-0-040084-1

1987 **Isotope Techniques in Water Resources Development**, Vienna, 30 March-3 April 1987, IAEA, Vienna, (in co-operation with UNESCO), 815 pp. (STI/PUB/757) ISBN 92-0-040087-6

1992 **Isotope Techniques in Water Resources Development**, Vienna, 11-15 March 1991, IAEA, Vienna, (in co-operation with UNESCO), 790 pp.(STI/PUB/875) ISBN 92-0-000192-0

1993 **Isotope Techniques in the Study of Past and Current Environmental Changes in the Hydrosphere and the Atmosphere,** Vienna, 19-23 April 1993, IAEA, Vienna, 624 pp. (STI/PUB/908) ISBN 92-0-103293-5

1995 **Isotopes in Water Resources Management** (in 2 volumes), IAEA, Vienna, 20-24 March 1995, IAEA, Vienna, 2 volumes: 530 and 463 pp. (STI/PUB/970) ISBN 92-0-105595-1 and 92-0-100796-5

1998 **Isotope Techniques in the Study of Environmental Change**, Vienna, 14-18 April 1997, IAEA, Vienna, 932 pp. (STI/PUB/1024) ISBN 92-0-100598-9

1999 **Isotope Techniques in Water Resources Development and Management**, 10-14 May 1999, IAEA, Vienna, CDRom (IAEA-CSP-2/C) ISSN 1562-4153

SPECIAL IAEA SYMPOSIA

1967 **Radioactive Dating and Methods in Low-Level Counting,** Monaco, 2-10 March 1967, IAEA, Vienna, 744 pp. (STI/PUB/152) (out of print)

1979 **Behaviour of Tritium in the Environment,** San Fransisco, USA, 16-20 October 1978, 711 pp. (STI/PUB/498) ISBN 92-0-020079-6

1981 **Methods of Low-Level Counting and Spectrometry,** Berlin, Germany, 6-10 April 1981, IAEA, Vienna, 558 pp. (STI/PUB/592) (out of print)

IAEA REPORTS AND TECHNICAL DOCUMENTS (TECDOCS)

Environmental Isotope Data no.1 – no.10: World Survey of Isotope Concentration in Precipitation, Data from network of IAEA and WMO over period 1953-1991, published 1969-1994.

Interpretation of Environmental Isotope and Hydrochemical Data in Groundwater Hydrology, Proc. Adv. Group Meeting, Vienna, 27-31 January 1975, IAEA, Vienna, 1976, 230 pp. (STI/PUB/429) ISBN 92-0-141076-X

Isotopes in Lake Studies, Proc. Adv. Group Meeting, Vienna, 29 August-2 September 1977, IAEA, Vienna, 1979, 290 pp. ISBN 92-0-141179-0 (out of print)

Arid Zone Hydrology: Investigations with Isotope Techniques, Proc. Adv. Group Meeting, Vienna, 6-9 November 1978, IAEA, Vienna, 1980, 265 pp. (STI/PUB/547) ISBN 92-0-141180-4

Stable Isotope Standards and Intercalibration on Hydrology and Geochemistry, (R. Gonfiantini ed.), Report on Consultants' Meeting, Vienna, 8-10 September 1976, IAEA, Vienna, 1977.

Stable Isotope Hydrology Deuterium and Oxygen-18 in the Water Cycle, (J.R.Gat and R.Gonfiantini eds.), Monograph by Working Group, IAEA, Vienna, 1981, 340 pp. (STI/DOC/10/210)

Palaeoclimates and Palaeowaters: A Collection of Environmental Isotope Studies, Proc. Adv. Group Meeting, Vienna, 25-28 November 1980, IAEA, Vienna, 1981, 207 pp. (STI/PUB/621) ISBN 92-0-141083-2

Guidebook on Nuclear Techniques in Hydrology, by Working Group IAEA, Vienna, 1983, 439 pp. (STI/DOC/10/91/2)

Stable Isotope Reference Samples for Geochemical and Hydrological Investigations, (R. Gonfiantini ed.), Report by Advisory Group's Meeting, Vienna, 19-21 September 1983, IAEA, Vienna, 1984.

Stable and Radioactive Isotopes in the Study of the Unsaturated Soil Zone, Proc. Meeting on IAEA/GSF Progr., Vienna, 10-14 September 1984, IAEA, Vienna,1985, 184 pp. (TECDOC-357)

Isotope Techniques in the Study of the Hydrology of Fractured and Fissured Rocks, Proc. Adv. Group Meeting, Vienna, 17-21 November 1986, IAEA, Vienna, 1989, 306 pp. (STI/PUB/790)

Stable Isotope Reference Samples for Geochemical and Hydrological Investigations, Report on Consultants' Meeting, Vienna, 16-18 September 1985, edited by G. Hut, IAEA, Vienna, 1987.

Use of Artificial Tracers in Hydrology, Proc. Adv. Group Meeting, Vienna, 19-22 March 1990, IAEA, Vienna, 1990, 230 pp. (TECDOC-601)

C-14 Reference Materials for Radiocarbon Laboratories, (K. Rozanski, ed), Report on Consultants' Meeting, Vienna, 18-20 February 1981, IAEA, Vienna 1991.

Guidelines for Isotope Hydrology, Manuel for Operation of an Isotope Hydrology Laboratory IAEA, Vienna, 1999 (in prep.)

Isotopes of Noble Gases as Tracers in Environmental Studies, Report by Consultants' Meeting, Vienna, 29 May-2 June, 1989, IAEA, Vienna, 305 pp. (STU/PUB/859) (out of print) ISBN 92-0-100592-X

Statistical Treatment of Data on Environmental Isotopes in Precipitation, IAEA, Vienna, 1992, 781 pp. (STI/DOC/10/331)

Isotope and Geochemical Techniques applied to Geothermal Investigations, Proc. Res. Coord. Meeting, Vienna, 12-15 October 1993, IAEA, Vienna, 1995, 258 pp. (TECDOC-788)

Reference and Intercomparison Materials for Stable Isotopes of Light Elements, Proc. Cons. Meeting, Vienna, 1-3 December 1993, IAEA, Vienna, 1995. (TECDOC-825)

Manual on Mathematical Models in Hydrogeology, IAEA, Vienna, 1996, 107 pp. (TECDOC-910)

CONSTANTS

a	year = 3.1558×10^{7} s
amu	atomic mass unit = $1.660\ 54\times10^{-27}$ kg
c	velocity of light (in vacuum) = $2.997\ 925\times10^{8}$ m·s^{-1}
cal	calorie = 4.184 J
e	elementary/electron/proton charge = $1.602\ 18\times10^{-19}$ C
eV	electronvolt = $1.602\ 18\times10^{-19}$ J
g	acceleration of free fall = 9.806 65 m·s^{-2}
h	Planck constant = $6.626\ 08\times10^{-34}$ J·s
J	Joule = 0.2390 cal
k	Boltzmann constant = $1.380\ 54\times10^{-23}$ J/K
m_e	electron mass = $9.109\ 39\times10^{-31}$ kg
m_n	neutron mass = $1.674\ 93\times10^{-27}$ kg
m_p	proton mass = $1.672\ 62\times10^{-27}$ kg
M/E eq.	mass/energy equivalence: 1 amu ≡ 931.5 MeV
N_A	Avogadro constant = $6.022\ 14\times10^{23}$ mol^{-1}
π	= 3.141 592 6535
R	gas constant = 8.314 51 J·K^{-1}·mol^{-1}
T	thermodynamic temperature = t (^{0}C) + 273.15 K
V_m	molar volume (= 22.41 L·mole^{-1} at STP)

Symbols and Units

a	$[CO_2aq]$ = concentration dissolved CO_2
a	year
^{y}a	activity ratio (^{y} mass number, e.g. ^{14}a)
aq	dissolved
A	(atomic) mass number
A	absolute (radio)activity (e.g. ^{14}A)
AMS	accelerator mass spectrometer
$\alpha_{l/v}$	fractionation factor (l rel. to v)
α_k	kinetic fractionation factor
α	alpha particle
b	$[HCO_3^-]$ = concentration dissolved bicarbonate
B	magnetic field
B	background counting rate
Bq	Becquerel = 1 disintegration$\cdot s^{-1}$
β	beta particle
c	$[CO_3^{2-}]$ = concentration dissolved carbonate ions
^{0}C	degree centigrade
C_T	concentration dissolved inorganic carbon
C_3	Calvin photosynthesis
C_4	Hatch-Slack photosynthesis
CAM	Crassulacean Acid Metabolism
C_i	Curie = 3.7×10^{10} dps
Cl	chlorinity (in g of chloride per kg of water = ‰)
d	deuterium excess of MWL
d	day = 8.6400×10^{5} s
dpm	disintegrations per minute
dps	disintegrations per second
D	diffusion constant/coefficient
DIC	dissolved inorganic carbon
DOC	dissolved organic carbon
$^{x}\delta$	relative isotope ratio (e.g. $^{13}\delta$) (defined from ^{x}R)
$^{y}\delta$	relative activity ratio (e.g. $^{14}\delta$) (defined from ^{y}A or ^{y}a)
E	energy
E_B	binding energy
EC	electron conversion
ε	fractionation (constant) (enrichment/depletion)
ε_k	kinetic fractionation (constant)
f	fraction
F	force
g	gram
GM	Geiger Müller counter
γ	gamma "particle"/radiation
h	relative humidity
h	hour
I	electric current
IAEA	International Atomic Energy Agency
IRMS	isotope ratio mass spectrometer
J	Joule
keV	kiloelectronvolt = 10^3 eV
K	equilibrium/acidity constant
K	degree Kelvin
LSS	liquid scintillation spectrometer
λ	(radioactive) decay constant
m	mass
m	meter
min	minute
mol	symbol for mole
mole	number of grams equal to molar weight
M	molar weight, mole
MeV	millionelectronvolt = 10^6 eV
MS	mass spectrometer
MWL	meteoric water line
μ	reduced mass
n	neutron
N	neutron number
N	amount
NBS	National Bureau of Standards
NIST	National Institute of Standards and Technology, USA
ν	neutrino
ν	frequency
Ox	oxalic acid (^{14}C standard)
p	pressure
p	proton
pH	$= -^{10}\log [H^+]$
pCi	picoCurie = 10^{-12} Ci
pMC	percent Modern Carbon
P	probability
PDB	PeeDee Belemnite
PGC	proportional gas counter
q	partition function
q	electric charge
Q	nuclear reaction energy
r	radius
^{x}R	isotope ratio (^{x} mass number, e.g. ^{13}R)
s	second
s	slope of MWL = 8

sp	spallation
S	salinity (in g of salt per kg of water = ‰)
SLAP	standard light Antarctic precipitation
SMOW	standard mean ocean water
STP	standard temperature and pressure (0°C, 1 atm)
σ	standard deviation
Σ	total inorganic carbon concentration = C_T
t	time
t	temperature (in °C)
T	absolute temperature (in K)
$T_{1/2}$	half-life
TU	tritium unit $\equiv [^3H]/[^1H] = 10^{-18}$ = 0.118 Bq/L
θ	exponent in fractionation factor ratio for $(\Delta M=2)/(\Delta M=1)$
τ	mean life
v	velocity
V	volume
V	volt
VPDB	Vienna-PDB
VSMOW	Vienna-SMOW
Z	atomic number

SUBJECT INDEX

d

e

f

g

h

i

j

k

l

m

n

o

p

q

r

s

t

u

V

W

X

Y